Integro-partial differential equation models for cell-cell adhesion and its application

by

Andreas Buttenschoen

A thesis submitted in partial fulfillment of the requirements for the degree of

Doctor of Philosophy

in

Applied Mathematics

Department of Mathematical and Statistical Sciences
University of Alberta

Abstract

In both health and disease, cells interact with one another through cellular adhesions. Normal development, wound healing, and metastasis all depend on these interactions. These phenomena are commonly studied using continuum models (partial differential equations). However, a mathematical description of cell adhesion in such tissue models had remained a challenge until 2006, when Armstrong et al. proposed the use of an integro-partial differential equation (iPDE) model. The initial success of the model was the replication of the cell-sorting experiments of Steinberg. Since then, this approach has proven popular in applications to embryogenesis, wound healing, and cancer cell invasions.

In this thesis, I present a first systematic derivation of non-local (iPDE) models for adhesive and chemotactic motion. For this purpose, I develop a framework by which non-local models can be derived from a space-jump process. I show how the notions of cell motility and cell polarization can be naturally included. The significance of such a derivation is that, it allows me to take cell-level properties such as cell-size, cell protrusion length or adhesion molecule densities into account. Thus this derivation validates these popular non-local models. I show that particular choices of these properties yield the original Armstrong cell-cell adhesion model. Finally, I extend the cell adhesion model to include volume exclusion, and complex cell adhesion molecule kinetics.

In Chapter 3, I present a first in depth analytical study of the steady-states of the non-local cell adhesion model derived in this thesis. The importance of steady states is that these are the patterns observed in nature and tissues

(e.g. cell-sorting experiments). As a prerequisite to the subsequent analysis, I present an in depth study of the properties of the non-local cell adhesion operator. I present results on its continuity, compactness, and spectral properties. I then combine bifurcation techniques pioneered by Rabinowitz, equivariant bifurcation theory, and the properties of the equation's solution, to obtain the existence of an unbounded bifurcation branch of non-homogeneous solutions. Using the equation's symmetries, I further classify the solution branches by the derivative's number of zeros (i.e., number of extrema remains fixed). Significantly, this parallels the classifications of solutions of nonlinear Sturm-Liouville problems and equivariant nonlinear elliptic equations. I identify the bifurcation type as pitchfork, and show that integration kernel in the non-local term determines whether an immediate switch in the solution's stability takes places. Finally, using numerical techniques, I verify my analysis, and demonstrate the existence of rotating waves of steady states.

In the final chapter, I extend the non-local cell adhesion model to a bounded domain with no-flux boundary conditions. In the past, boundary conditions for non-local equations were avoided, because their construction is subtle. I encounter three challenges: (1) ensure the non-local operator is well-defined near the boundary, (2) ensure that the non-local operator satisfies the no-flux boundary conditions, and (3) the constructed non-local operators are non-unique in the boundary region. I address the first challenge by introducing spatially dependent integration limits. While more complicated, the new non-local operators share many of their mathematical properties with the periodic non-local operator. However, the spatial dependence of the integration limits complicates differentiation. Indeed, the theory of distributions must be used, to

compute the non-local operator's weak derivative. Using the model's derivation, I ensure that the constructed operators satisfy the no-flux boundary conditions. Finally, I classify the constructed non-local operators, by comparing their action to the periodic non-local adhesion operator, into either repellent, neutral, or attractive. It is however, an open problem to match these newly constructed non-local operators to cell behaviour near physical boundaries.

Preface

Chapter 2 of this thesis has been published as A. Buttenschön, T. Hillen, A. Gerisch, and K. Painter, "A space-jump derivation for non-local models of cell-cell adhesion and non-local chemotaxis," *Journal of Mathematical Biology*, online June 2017. I was the lead investigator responsible for the principal ideas, analysis, numerical experiments and write up. T. Hillen was the supervisory author and was involved with concept formation. K. Painter was involved in concept formation. A. Gerisch offered his expertise on numerical methods for nonlocal equations. All co-authors provided me with feedback and suggestions during manuscript composition.

Acknowledgements

I take this opportunity to thank everyone who has helped me along the way in completing this work.

Firstly, I would like to thank my advisor Dr. Thomas Hillen for his guidance during the last five years. His guidance and feedback through this work has been of utmost importance to me. I would also like to thank the members of our Mathematical Biology Journal Club and members of the Centre for Mathematical Biology, who provided invaluable feedback and ideas throughout the years.

Secondly, I would like to thank Dr. Dirk Drasdo and his group for their hospitality during my stay at INRIA (Institut National de Recherche en Informatique et en Automatique) from December 2015 to May 2016. I would like to acknowledge both MITACS Canada and INRIA for financially supporting my stay at INRIA.

I would like to acknowledge that this work was financially supported by an NSERC CGSM award, an Alberta Innovates Technology Futures Graduate Student Scholarship, and a PIMS Graduate Student scholarship.

Last but not least, I want to thank my family and in particular my parents for their invaluable support.

Contents

List of Tables

List of Figures

Chapter 1

Introduction

1.1 The effect of cellular adhesions in tissues

In both normal and diseased tissues, cells interact through adhesions, with each other and the extracellular matrix (ECM), a ubiquitous protein scaffold. At the molecular level, cellular adhesions are facilitated by proteins such as integrins (cell-matrix adhesion protein) or cadherins (cell-cell adhesion protein) [78], which are situated on the cell surface. Today, we recognize that cell adhesions are fundamental in determining outcomes of normal development, wound healing and metastasis [77, 119, 142]. Early in the last century, however, the first biological experimenters had only just begun to uncover the role the cell adhesion molecules play in tissues.

One of the earliest observations was that if a sponge is squeezed through a fine mesh (Wilson, 1907 [160]), it will reform into an again functional sponge. A few years later, Hoftreter observed that different tissues have different associative preferences [160]. To describe his observations, he introduced the concept of "tissue affinities". Further, he repeated the earlier observations that previously dissociated tissues have the ability to regain their function. Today, this phenomenon is referred to as cell-sorting, and we recognize its critical importance in the formation of functional tissues during organism development.

In 1963, Steinberg proposed the first theory of cell-sorting that argued that cell-level properties, namely a cell's adhesion molecules, drive cell-sorting

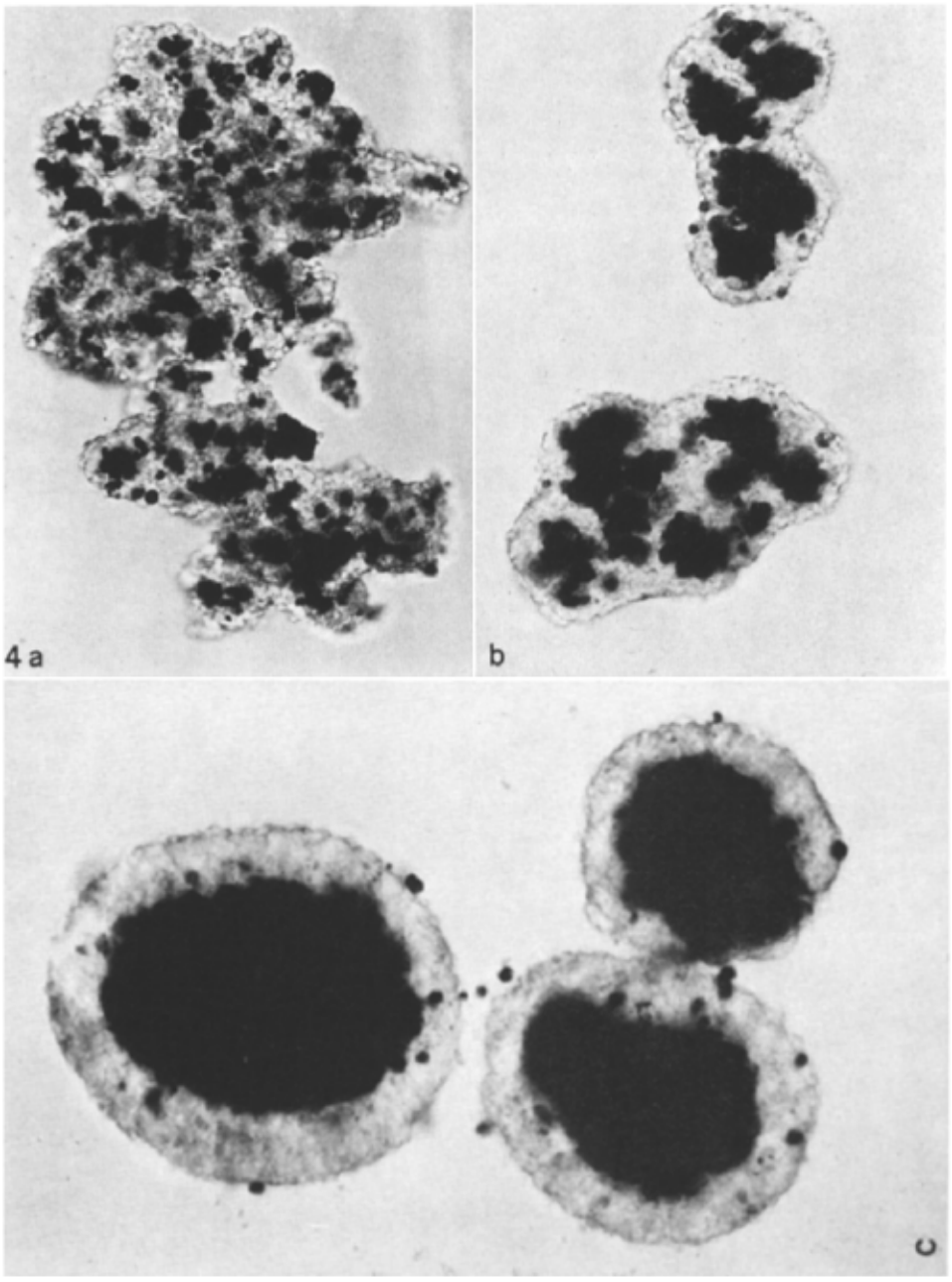

Figure 1.1: Two cell populations with different strength adhesion molecules on their surfaces. Initially (a) the cells are mixed, and then slowly (b) re-sort themselves to the final configuration (c) (For details on the experimental setup and the figure see [12]).

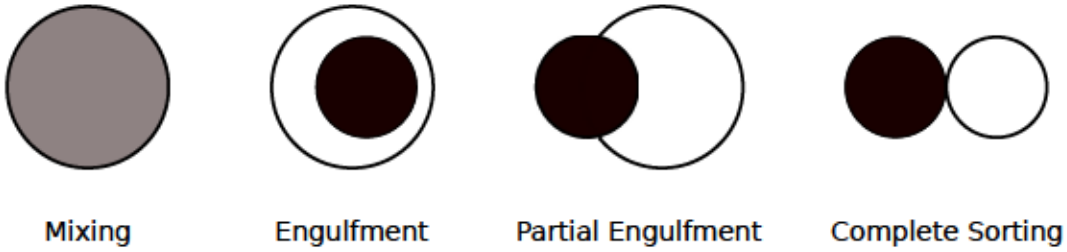

Figure 1.2: The four possible outcomes of cell-sorting with two cell populations. The more cohesive cell population is black. Mixing occurs with preferential cross-adhesion, engulfment with intermediate cross-adhesion, partial engulfment with weak cross-adhesion, and cell-sorting with no cross-adhesion [10, 59].

[160, 161]. His theory, capable of explaining the different cell-sorting patterns is known as the *Differential adhesion hypothesis* (DAH), which argues that cell-sorting is mechanistically equivalent to surface tension driven behaviour in liquids. In other words, cells solely move to maximize their intra-cellular attraction. That is, the DAH asserts that cell-sorting is solely driven by the quantitative differences in the work of adhesion between cell types (e.g. cells with the highest work of adhesion are found at the centre of aggregates). Interesting is that Steinberg referred to adhesion being a "merely close range attraction" [160]. An overview of the experimental verifications can be found in [162].

Harris formulated a first critique of the DAH [82]. The main points of his critique were: (1) cells are living objects, and thus open thermodynamic systems (not closed as assumed by the DAH), (2) cell size and cell membrane protrusions are much larger than individual adhesion bonds, thus making cellular adhesions a non-local process, and (3) the work of adhesion and de-adhesion may be different, as cells can stabilize adhesion bonds after their formation [82]. To resolve these issues, Harris proposed the *differential surface contraction hypothesis*, arguing the contractile strength of a membrane completely describes its surface tension. A model similar to this idea was later implemented in a successful vertex model of cell-sorting in epithelial tissues [20, 21, 30].

In both health and disease, cells interact with one another and their surrounding protein scaffold (the extracellular matrix, ECM), through adhesions. Normal development, wound healing, and metastasis all depend on these in-

teractions [77, 119, 142]. For instance in metastasis, an important question is how changes in cell adhesion affect transitions from epithelia (quiescent) to migratory (mesenchymal) cells (EMT) [77, 129], a hallmark of metastatic cancer [79, 80]. To understand such complex systems, the information gathered from biological experiments and medical data alone is not sufficient, we have to understand this information. Using mathematical models and rigorous mathematics, we can understand in detail the underlying properties driving the observed behaviour.

1.2 Prior modelling efforts on cellular adhesions

The first use of cellular adhesions in a model was a model of cell-sorting in 1992. Graner, Glazier modelled cells as collections of connected lattice sites [71, 74, 75, 76]. Cellular adhesions are implemented by assigning a certain energy value to any interface between two pixels belonging to two different cells. Since a single cell contains many lattice sites, this is a non-local interaction. The evolution of the cells is energy driven i.e. at each step random changes in the lattice configuration are proposed and accepted by a Boltzman like function. This approach is now known as the Cellular Potts model and is widely used in modelling of cell biology. For an overview, see the recent book [156].

In 1996, Byrne, Chaplain studied the growth of avascular tumour spheroids in the presence of an external nutrient [25]. The tumour growth is determined by the balance between proliferative pressure and cell-cell adhesion, which keep the spheroid compact. The Gibbs-Thompson relation is used to relate the tumour spheroid's curvature to the external nutrient concentration. It is assumed that cell-cell adhesions are the forces that maintain this curvature [25]. Later, this model was modified such that the cell's proliferation rate depended on the total pressure acting on the cell (due to adhesion and repulsive forces) [26]. This model was then successfully compared to a cell-based model of tumour spheroid growth [26]. In a similar model, Perumpanani et al. introduced a density dependent diffusion term in a tumour spheroid model, the idea was

that cells in high density areas are slowed down by the presence of adhesion bonds to neighbours [141]. Since then, this approach has been used in more complicated models of tumour growth (see [115, 116]). The adhesive mechanism in these models are purely local. Further, neither of these models was able to reproduce cellular aggregations nor cell sorting commonly linked to adhesive interactions.

Palsson, Othmer used a cell-based model to study collective movements in slugs [140]. Differently to the Cellular Potts model, they used a lattice-free model, resolving the individual physical forces between the cells. This is a non-local description of cell-cell adhesion [139, 140].

In physics-based cell-based models such as that developed by Palsson et al., the adhesive and repulsive forces between individual cells are resolved using the theory of elasticity. Modelling cells as elastic isotropic spheres is the simplest available cell model. The adhesive and repulsion forces between adhering elastic spheres is resolved using a modified Hertz model [153, 154] or the Johnson, Kendall, and Roberts (JKR) model [49, 93, 103]. Since these interactions act over a wide range of cell separations, they are non-local models.

Brodland, Chen used a vertex model (an individual-based model) to model cell-sorting in epithelial tissues [21, 30]. The process was driven by the surface tension at cell-cell interfaces. The surface tension in their model depended on the forces of adhesion, membrane contraction, and circumferential microfilament bundles [21]. They summarized the findings of their numerical studies by formulating the *differential interfacial tension hypothesis* of cell-sorting [20]. Once again this was a non-local description of cell-adhesion.

Turner, Sherratt used a Cellular Potts model to study the effect of adhesion at the invasion front of a tumour [167]. They observed the formation of clusters of invasion, and the formation of "fingering" invasion fronts. In [168], they attempted to scale the Cellular Potts model to a partial differential equation. However, the obtained equations are notoriously difficult even in the simplest settings. This is due to cells occupying several lattice sites (non-local spatial extend) in Cellular Potts models.

Since up to this point all cellular adhesion models capable of explaining aggregations were based on non-local models in cell-based approaches, Ander-

son proposed to combine the continuum and cell-based approach in a hybrid model [9]. The significance of this hybrid approach is that cells are individually represented (adhesion effects can be taken into account) and environmental factors such as diffusing proteins can be modelled using well-established reaction diffusion equations. This approach has been popular in studying the dynamics of tumour spheroids [145, 146].

In 2006, Armstrong, Painter, Sherratt proposed the first continuum model of cellular adhesions capable of explaining adhesion driven cell aggregations [10]. Let $u(x,t)$ denote the density of a cell population at spatial location x and time t. Then its evolution subject to random motility and cell-cell adhesion is given by the following non-local integro-partial differential equations.

$$u_t(x,t) = \underbrace{D\Delta u(x,t)}_{\text{random motility}} \underbrace{-\alpha\nabla\cdot\left(u(x,t)\int_{\mathbb{B}^n(R)} h(u(x+r,t))\Omega(r)\,\mathrm{d}r\right)}_{\text{cell-cell adhesion}}, \quad (1.1)$$

where D is the diffusion coefficient, α the strength of the homotypic adhesion strength, $g(u)$ is a possibly nonlinear function describing the nature of the adhesive force, $\Omega(r)$ an odd function, and R the sensing radius of the cell (for more details on these functions and their biological meaning, see Chapter 2).

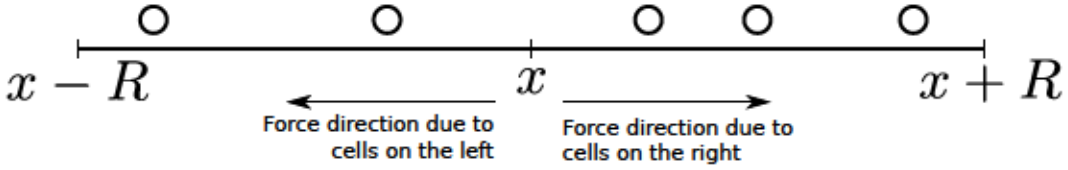

Figure 1.3: An intuitive explanation of the non-local cell-cell adhesion term in equation (1.1). Intuitively the non-local term represents a tug-of-war of the cells on the right and the cells on the left, with the cell at x moving in the direction of largest force. The result of the scenario here would be that the cell at x moves to the right (assuming that $\Omega(r)$ is uniform and $h(u)$ is linear).

The novelty of equation (1.1) is the integral term to model cell-cell adhesion. Intuitively, the integral term can be interpreted as a tug-of-war or in physical terms, cells move in the direction of the largest acting force. The effect is that cells move up "non-local" gradients of cell population and thus arises the possibility for formation of cell aggregates. The two-population version

of equation (1.1) was the first continuum model that correctly replicated cell-sorting experiments [10].

As discussed above, cellular adhesions feature prominently in organism development, wound-healing and cancer invasion (metastasis). Therefore, it is unsurprising that model (1.1) has found extensive use in modelling cancer cell invasion [7, 28, 67, 68, 135, 157], and developmental processes [11]. More recently, spatio-temporal variations of the adhesion strengths [47], and adhesion strength variations due to signalling proteins [16] were considered.

The non-local model (1.1) has also been criticized for oversimplification, namely for its use of a simple diffusion term [123]. Murakawa et al., supported by experimental data, noticed that under certain conditions equation (1.1) gave unrealistic solutions [123]. To address this shortcoming, Murakawa et al. modified the modelling assumption "cells move randomly" to "cells move from high pressure to low pressure regions". For this reason, they introduced a density-dependent diffusion term [123].

Prerequisite for the extensive numerical exploration of the solutions of the non-local equation (1.1) was the development of efficient numerical methods to evaluate its integral term. An efficient method based on the fast Fourier transform was developed in [66]. Using this efficient algorithm, numerical solutions of equation (1.1) are implemented using a spatial finite-volume discretization and the method of lines for the temporal advancement [65].

Existence results for the solutions of the non-local equation (1.1) were developed in [7, 16, 92, 157]. Most significant is the general work by Hillen, Painter, Winkler, who showed local and global existence of classical solutions [92]. For the case of small adhesion strength, travelling wave solutions of equation (1.1) were found and studied in [133].

1.2.1 Non-local partial differential equation models

Having introduced the non-local adhesion model (1.1), we take a look at developments of non-local models in general. Non-local models arise in two different situations: First, one assumes the a priori existence of some non-local interaction, or they arise from local reaction-diffusion equations, upon taking some

limit, or the introduction of a simplification [101, 105]. For example, in a system of four partial differential equations (two cell populations and two diffusing signalling molecules), Knútsdóttir et al. [105] applied a quasi-steady state assumption assuming the signalling molecules diffuse much faster than the cellular populations. The resulting elliptic equations were solved using Green's functions, and thus non-local terms were introduced in the advection terms.

Non-local models have been proposed to describe many different phenomena, such as the fractional Laplacian (Levi random walks). Integro-difference equations, discrete in time, and continuous in space, are popular to study the dispersal of animal populations in ecology [128]. In the continuum time setting, non-local equations arising for birth-jump processes [88] are gaining traction, with applications in cancer stem cell dynamics [18, 44] and fire spotting [117].

The non-local cell-cell adhesion model (1.1) has the non-local term in the advection term. The first non-local equations with the non-local term contained in the advection term were proposed in a series of papers by Nagai et al. in 1983 [124, 125, 126]. Their introduction of the non-local term was driven by a desire to model aggregation processes in ecological systems. For comparison with the non-local adhesion model (1.1), the equations of Nagai et al. looked like this,

$$u_t = \left(u^m\right)_{xx} - \left[\left\{\int_{-\infty}^{\infty} K(x-y)u(y,t)\,\mathrm{d}y\right\}u\right]_x, x \in \mathbb{R}, t > 0, \qquad (1.2)$$

where $m > 1$. Shortly after Alt, studied generalizations of equation (1.2) in [3, 4]. A version of equation (1.2) with finite integration limits and with the special choice of $K(x-y) = \mathrm{sgn}(x-y)$ was studied by Ikeda in [99, 100]. Ikeda established the existence of solutions of equation (1.2) on an unbounded domain and developed spectral results in the special case of $m = 2$, that was used to give a classification of the steady-states of equation (1.2). In 1999, Mogilner et al. used this approach to derive a non-local model describing the evolution of swarms [121]. More recently, such models were used to describe the aggregation of plankton [1], and to model animal populations featuring long-ranged social attractions and short-ranged dispersal [166]. Eftimie et al. used a Lagrangian formulation to obtain non-local hyperbolic models of communicating individu-

als [51, 52]. Since then, equivariant bifurcation theory was used to study the possible steady states of such communication models [23], and very recently they discussed the use of Lyapunov-Schmidt and centre-manifold reduction to study the long-time dynamics of such equations. The non-local adhesion model falls also in this category of equation (1.1) and more recently it was generalized to include both aggregations and repulsive behaviour [136].

A similar type of model was proposed by Othmer, Hillen [132] to replace the chemical gradient in a chemotaxis model by the following non-local term,

$$\mathring{\nabla}_R v(x) := \frac{n}{\omega_D(x) R} \int_{\mathbb{S}_D^{n-1}} \sigma v(x + R\sigma)\, \mathrm{d}\sigma, \tag{1.3}$$

$\mathbb{S}_D^{n-1}(x) = \{\sigma \in \mathbb{S}^{n-1} : x + \sigma R \in D\}$, and $\omega_D(x) = |\mathbb{S}_D^{n-1}(x)|$. It was shown in [91] that this change leads to globally bounded solutions of the non-local chemotaxis equation. Extending the work on steady states of the local chemotaxis equation [151, 170], Xiang used bifurcation techniques to analyse the steady states of the non-local chemotaxis equation in one dimension.

Non-local terms have also been considered in reaction terms, i.e., in equations of the form

$$u_t = u_{xx} + f(x, u, \bar{u}), \tag{1.4}$$

where

$$\bar{u} = \int g(x, u)\, \mathrm{d}x. \tag{1.5}$$

These types of equations were studied in [19, 40, 41, 42, 60, 61, 62]. An application of such a model is for example to Ohmic heating in [110]. A different application considers the growth of phytoplankton in the presence of light and nutrients [178]. Yet another application of such a model is a study on the effect of crop raiding of large bodied mammals [97].

Many of the above mentioned examples are formulated on infinite domains, to avoid subtleties in dealing with boundary conditions, or subtleties in ensuring the non-local term is well-defined. Indeed, even the analysis of local equations such as the viscous Burger equation on bounded domains have remained unaddressed until recently [171].

1.3 Outline of the Main Results

In this thesis I consider non-local models of cell-cell adhesion in the form of integro-partial differential equations (see equation (1.1)). The central problems which we would like to address in this thesis are:

1. Can non-local models be derived from an underlying individual description of cell movement?

2. What are the steady-states of the non-local cell adhesion models (i.e. equation (1.1)) in the absence of boundary effects?

3. How to model and include boundary effects in the non-local term of the cell adhesion models (i.e. equation (1.1))?

In Chapter 2, I develop a framework to derive non-local taxis models from stochastic random walks. The key to the derivation is the extension of the biological concept of a cell's polarization vector to the mathematical world. Intuitively speaking, once a cell has polarized, it will move in that direction. Using this framework, all that remains is a definition of how cells polarize. We develop a cell polarization vector due to the interactions of adhesion molecules, and for non-local chemotaxis. The significance of this work is that it allows us to elucidate in detail how cell level properties such as cell size or density of adhesion molecules affect tissue-level phenomena. Chapter 2 has been published as [24].

In Chapter 3, I investigate the steady states of a single population non-local model of cellular adhesions on a periodic domain. I combine global bifurcation techniques pioneered by Rabinowitz, equivariant bifurcation theory (the equation is $\mathbf{O}(2)$-equivariant), and the mathematical properties of the non-local adhesion term, to obtain the existence of an unbounded global bifurcation branch of non-homogeneous solutions. I further classify the first solution branch by the derivative's number of zeros (i.e. number of extrema remains fixed). The significance of this result is that it parallels the seminal classification of solutions of nonlinear Sturm-Liouville problems (Crandall & Rabinowitz, 1970) and the classification for equivariant nonlinear elliptic equations (Healey & Kielhöfer, 1991).

In Chapter 4, I study the existence of steady states for a non-local model of cellular adhesions on a bounded domain with no-flux boundary conditions. In the past, boundary conditions for non-local equations were avoided, because their construction is subtle and requires biological insight. Using the insights from Chapter 2, I construct a non-local operator, which takes boundary effects into account. The significance is that correct boundary conditions are important to accurate model construction (e.g., boundary dependent organogenesis in zebrafish). Mathematically significant is the construction of the weak derivative (using distributions) for the "no-flux" non-local operator. Using this, I study the effect of no-flux boundary conditions on the steady states of a cell adhesion model.

In Chapter 5, I conclude with a discussion.

Chapter 2

Derivation of a Cell-Cell Adhesion Model Using a Space-Jump Process

Published: A. Buttenschön, T. Hillen, A. Gerisch, and K. Painter, "A space-jump derivation for non-local models of cell-cell adhesion and non-local chemotaxis," *Journal of Mathematical Biology*, online June 2017.

2.1 Introduction

The building blocks of multicelluluar organisms are cells, vessels and protein fibres. These tissue constituents display complex biochemical and physical interactions with cell adhesion and chemotaxis being two such examples. Adhesion is facilitated by transmembrane adhesive complexes, while chemotaxis requires receptors on the surface of the cell membrane. Both chemotaxis and cellular adhesion are instrumental in embryogenesis, cell-sorting and wound healing, along with homoeostasis in multicellular organisms. Misregulation of chemotaxis and cellular adhesion may lead to pathological conditions such as cancer and other degenerative diseases [63, 149]: for instance, reduced cellular adhesion in cancer cells can lead to invasion and metastasis [63]. Both chemotaxis and cellular adhesion have been the focus of intense mathematical modeling efforts, both at

the level of agent-based and continuum models, with the latter typically based on local or non-local partial differential equations [10, 47, 89, 96, 134]. Local models, typically based on the reaction-advection-diffusion framework, have a solid foundation in biased random walks. Non-local models appear to be better suited to describe certain aspects of adhesion, along with non-local chemotaxis, yet as far as we are aware there is no convincing microscopic random walk process that leads to these non-local models. In fact Gerisch et al., [68] have written on page 328 that "A highly desirable objective is to develop continuous models for cellular adhesion as the appropriate limit from an underlying individual model for cell movement". In this chapter we propose to fill this gap and introduce a spatial stochastic random walk that leads, in an appropriate limit, to the non-local adhesion and chemotaxis models. This approach provides a better understanding of the underlying modelling assumptions and allows to modify the continuous model as needed.

2.1.1 Biological Background

This section reviews pertinent biological background on cell adhesion, required for the subsequent derivation. Cellular adhesions are facilitated by cell adhesion molecules, which are proteins present on the cell surface [108]. In layman's terms, they act to stick cells to each other and their surroundings. Through these connections, cells can sense mechanical cues and exert mechanical forces on their environment. It is of note that cellular adhesion is important in both adherent (static) cells and in motile cells [108]. Due to their importance adhesion molecules are ubiquitous in biological organisms and, accordingly, it is not surprising that numerous adhesion molecules are known with integrins and cadherins forming two prominent classes. Integrins are important in both the static and dynamic case [108] and are commonly associated with contacts between cells and the extracellular matrix (ECM) [45]. Cadherins, on the other hand, are more commonly associated with forming stable cell-cell contacts [108]. The density and types of presented adhesion molecules determine the mechanical interaction strength between a cell and its neighbours or the environment. While cell adhesion is important during both homoeostasis and during cell

migration, we will treat the homeostatic case as a special case of migration, in which cells are in a mechanical equilibrium or at a so called steady state.

The motility of cells is fundamental during many biological functions, including embryogenesis and wound healing [43]. In this dynamic setting, cellular adhesion plays an important role in guiding migrating cells. Cells have developed many mechanisms of translocation, with at least four different kinds of membrane protrusions distinguished: lamellipodia, filopodia, blebs and invadopodia [147]. How the directionality of these protrusions is determined varies greatly between cell types, but a unifying feature of migrating cells is the formation of a spatially asymmetric morphology, allowing a clear distinction between front and back [107, 148]. This is the so-called process of cell *polarization* and can result from a wide variety of intrinsic and extrinsic cues, including chemical or mechanical stimuli [39, 64, 148, 165, 173]. Once polarized, membrane protrusions are extended primarily at the cell front [107].

2.1.2 Mathematical Background

Many partial differential equation models for the dynamics of cellular populations are motivated by the conservation of mass equation. Suppose that the population density is given by $u(x,t)$ and its flux by $J(x,t)$. The conservation equation is then given by,

$$u_t(x,t) = -\nabla \cdot J(x,t). \tag{2.1}$$

Different biological phenomena can be described by an appropriate choice for the flux. In many common models the flux is divided into multiple additive parts: for example, a part due to random motion denoted J_d, and a part due to adhesion denoted J_a, that is

$$J(x,t) = J_a(u(x,t)) + J_d\left(u_x(x,t)\right). \tag{2.2}$$

In the following discussion we focus on different choices for J_a and assume Fick's law for the diffusive flux, i.e., $J_d = -Du_x(x,t)$. Armstrong, Painter, Sherratt [10] suggested the following flux term to model movement through

the formation and breaking of cell-cell adhesion between cells. The flux J_a is assumed to be directly proportional to the created force and the population density, and inversely proportional to the cell size, such that

$$J_a = \frac{\phi}{L} u(x,t) F, \tag{2.3}$$

where ϕ is a constant of proportionality, F the total adhesion force and L the typical cell size. This follows from Stokes' law, which gives the frictional force of a spherical body moving at low Reynolds numbers. The total adhesion force is the result of the forces generated within the sensing radius, i.e.,

$$F = \int_{\mathbb{B}^n(R)} h(u(x+r,t))\Omega(r)\,\mathrm{d}r, \tag{2.4}$$

where $h(u(x,t))$ describes the nature of the force and its dependence on the cell density and $\Omega(r)$ describes the force's direction and dependence on the distance r. Substituting the fluxes into the conservation equation we obtain the following integro-partial differential equation:

$$u_t(x,t) = D\Delta u(x,t) - \nabla \cdot \left(u(x,t) K(u(x,t))(x,t)\right), \tag{2.5a}$$

where

$$K(u(\cdot,t))(x) = a \int_{\mathbb{B}^n(R)} h(u(x+r,t))\Omega(r)\,\mathrm{d}r \tag{2.5b}$$

and $a = {}^{\phi}/_{L}$. It is noted that this model was the first continuum model that successfully replicated the patterns observed in Steinberg's classic adhesion-driven cell-sorting experiments [10].

In this chapter we will focus on the modelling of the non-local adhesion process, for this reason we assume in equation (2.5) that the diffusion coefficient is constant. For the modelling of spatial dependent diffusion coefficients we refer the reader to [163] and [27].

The adhesion model (2.5) has since been extended to include both cell-cell and cell-ECM adhesion [67], with this extended version used to study the invasion of cancer cells into the ECM [8, 28, 47, 67, 135, 157]. The adhesion model was also used in a model of neural tube development in vertebrates [11].

In addition to the various biological applications, the mathematical properties of the adhesion model (2.5) have been under intense investigation: conditions for global existence were developed in [28, 50, 92, 157]; travelling wave solutions were found for small parameters a in equation (2.5b) [133]; an efficient and robust numerical scheme for the non-local adhesion model has been developed in [66].

While successful in application it is not yet clear how the microscopic properties of cells, such as cell size, cell protrusions, nature of the adhesion forces or the distribution of adhesion molecules enter the adhesion model (2.5). A derivation of the non-local adhesion model (2.5) from an underlying random walk promises to answer these questions. An early attempt was undertaken by Turner et al. [168], who studied the continuum limit of a Cellular Potts model that included cell-cell adhesion, yet the resulting continuum model was too complicated for significant analysis. Johnston et al. [104] studied the continuum limit they obtained from a stochastic exclusion movement model; under certain parameter regimes, however, the continuum model permits negative diffusion and is unable to replicate the pattern formation observed during cell-sorting. Recently, Middleton et al. [120] showed that an integro partial differential equation (iPDE) model similar to equation (2.5a) can be obtained from the mean field approximation of Langevin equations. There it is shown that this iPDE limit is only effective for weak cell-cell adhesion.

Many commonly used partial differential equation models, such as the chemotaxis equation, have been derived from a space-jump process [89, 131]. This motivates us to derive the adhesion model (2.5) from an underlying stochastic random walk model based on cell-cell mechanics. The challenge is maintaining the finite sensing radius while taking the formal limit of the space-jump model. Through this we offer not only insight into the complicated assumptions on which Armstrong's model (2.5) is based, but also extend it to a more general form. We see that Armstrong's model implicitly assumes (i) point-like cells, (ii) mass action for the adhesion molecule kinetics and (iii) no volume exclusion effects. Our approach allows us to relax these assumptions and extend the model to include large cells, volume exclusion and more complicated adhesion molecule kinetics. In the process we find that our derivation is

general, and hence applicable to other non-local models such as the non-local chemotaxis model in Section 2.4.

2.1.3 Layout of the chapter

The key to a mathematical derivation of a continuum adhesion model lies in the definition of cell polarization. In Section 2.2 the biological notion of a polarization vector is integrated into the framework of a stochastic random walk. This preparatory work will allow us in Section 2.3 to derive the non-local adhesion model from an underlying stochastic random walk and in Section 2.4 to derive the non-local chemotaxis model. In Section 2.5 the proposed stochastic random walk is compared to numerical simulations of the integro-partial differential equation model of adhesion. Finally, in Section 2.6 our results will be discussed and an outlook given on open questions and future work.

2.2 A population model informed by the polarization vector

For the following discussion we let the domain be given by Ω. Here we restrict the domain to $\Omega = \mathbb{R}^n$ in order to focus on modelling cell-cell interactions in the absence of boundary effects. Suppose that a cellular population with population density function $u(x,t)$ is present in Ω. To define precisely the meaning of this population, we make a couple of assumptions. Cells send out membrane protrusions to sample their environment and we assume that these membrane protrusions are much more frequent than translocations of the cell body; the cell body includes the cell nucleus and most of the cell's mass. In modelling cell migration we are most interested in the translocation of the cell body and not the frequent, but temporary, shifts due to cell membrane protrusions. For this reason, we define the population density function $u(x,t)$ as follows,

$$u(x,t) \equiv \text{Density of cells with their cell body centred at } x \text{ at time } t. \quad (2.6)$$

This precise definition of the cell population will become important later in Section 2.3.

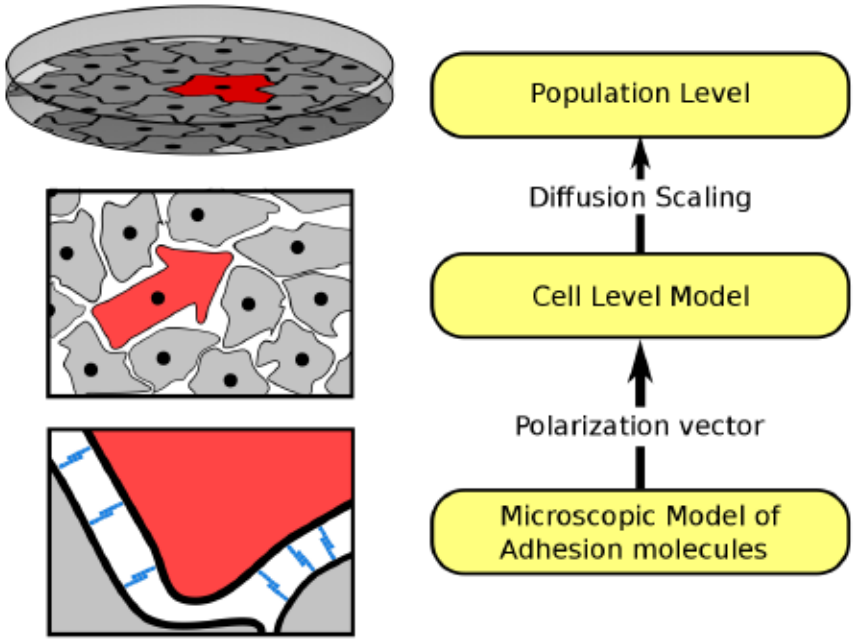

Figure 2.1: Schematic of the bottom-up approach of modelling cell movement due to cell-cell adhesion. Our final goal is to derive an equation describing the evolution of the cell population density. This is called the *population level*. The population level model is derived from a *cell level model*. Finally, the cell level model is informed by the *polarization vector*. The cell depicted in red is given an arrow shape to indicate the polarization vector $\mathbf{p}(x)$. The polarization vector is determined by the formation and breaking of adhesion bonds between the cells. The adhesion bonds are depicted as blue sticks. The polarization vector connects the microscopic and the mesoscopic scale (see Section 2.2.1). The diffusion scaling connects the mesoscopic and the population level (see Section 2.2.3).

We model the evolution of the cell population $u(x,t)$ using a *space-jump* process, using stochastically independent jumpers. In other words, we use a continuous time random walk for which we assume the independence of the waiting time distribution and spatial redistribution. Here the waiting time distribution is taken to be the exponential distribution, with a constant mean waiting time. A possible extension in which the mean waiting time is a function of cell density is briefly motivated in Section 2.6. Let $T(x,y)$ denote the tran-

sition rate for a jump from $y \in \Omega$ to $x \in \Omega$. The evolution of the population density $u(\cdot, t)$ due to these particle jumps is given by the Master equation [131],

$$u_t(x,t) = \lambda \int_D \left[T(x,y)u(y,t) - T(y,x)u(x,t) \right] \mathrm{d}\mu(y), \tag{2.7}$$

where $(D, \mu(y))$ is a measure space with $D \subset \Omega$, and $1/\lambda$ is the mean waiting time. Note that, $T(x,y)$ depends on the population density $u(\cdot,t)$, however we do not explicitly track this to keep the notation managable and within convention see for instance [89]. For more details on the derivation of the master equation see [98, 169].

We make two assumptions about the movement of the cells:

Modelling Assumption 1: We assume that in the absence of spatial or temporal heterogeneity the movement of individual cells can be described by Brownian motion. It has been shown that this is a reasonable assumption for many cell types [15, 122, 152].

Modelling Assumption 2: The cells' polarization may be influenced by spatial or temporal heterogeneity. We denote the polarization vector by $\mathbf{p}(x)$.

In this section we will show how these two assumptions can be naturally included within the *space-jump* framework. We will further discuss the formal limit of equation (2.7) which will lead to macroscopic models describing the spatial-temporal evolution of $u(x,t)$. Figure 2.1 gives an overview of how the polarization vector and the diffusion scaling are used to obtain the final population model.

2.2.1 The polarization vector in a space-jump process

For notational convenience we associate to a jump from $y \in \Omega$ to $x \in \Omega$ the heading $z := x - y$. Using the heading we define $T_y(z) := T(y+z, y) = T(x,y)$. Let D^y denote the set of all possible headings from y. We assume that if $z \in D^y$ then so is $-z \in D^y$. In other words, D^y is a symmetric set. In most cases D^y will be independent of y. We further assume that for every $y \in \Omega$, the function T_y is non-negative as it represents a rate.

Given $y \in \Omega$ we denote the redistribution kernel at this location by $T_y(z)$; we assume that $T_y \in L^1(D^y)$ and that $\|T_y\|_1 = 1$ holds. Note that here we use the measure associated with D^y. This measure can be the standard Lebesgue measure in $\mathbb{R}^n$ if D^y is the ball with radius h in $\mathbb{R}^n$, i.e., $D^y = \mathbb{B}^n(h)$, or it could be the surface Lebesgue measure in $\mathbb{R}^n$ if D^y is the sphere with radius h in $\mathbb{R}^n$, i.e., $D^y = \mathbb{S}^{n-1}(h)$, or it can be a discrete measure if modelling movements on a lattice and $D^y = \{ he_1, -he_1, he_2, \ldots, -he_n \}$, where $e_1, e_2, \ldots, e_n$ are the Cartesian unit vectors. In any case, this normalization makes T_y a probability density function (pdf) on D^y.

Any function which is defined for both z and $-z$ can be decomposed into even and odd components, which are denoted by S_y and A_y respectively. This notation is chosen in imitation of the even/odd notions introduced by Mogilner et al. [121] in a non-local modelling study of swarming behaviour.

Lemma 2.1. *Consider $y \in \Omega$, given $T_y \in L^1(D^y)$, then there exists a decomposition as*

$$T_y(z) = \begin{cases} S_y(z) + A_y(z) \cdot \frac{z}{|z|} & \text{if } z \neq 0 \\ S_y(z) & \text{if } z = 0 \end{cases} \tag{2.8}$$

with $S_y \in L^1(D^y)$ and $A_y \in (L^1(D^y))^n$. The even and odd parts are symmetric such that

$$S_y(z) = S_y(-z) \quad \text{and} \quad A_y(z) = A_y(-z). \tag{2.9}$$

Proof. Given T_y, define

$$\begin{aligned} S_y(z) &= \frac{1}{2} \left(T_y(z) + T_y(-z) \right), \\ A_y(z) &= \frac{1}{2} \left(T_y(z) \frac{z}{|z|} - T_y(-z) \frac{z}{|z|} \right), \quad z \neq 0. \end{aligned}$$

Then the above properties can be checked by direct computation. □

Using this decomposition we define two properties which are analogous to Modelling Assumptions 1 and 2 above. First, we define the motility.

Definition 2.2 (Motility). We define the motility at $y \in \Omega$ as

$$M(y) \coloneqq \int_{D^y \setminus \{0\}} T_y(z)\,\mathrm{d}z = \int_{D^y \setminus \{0\}} S_y(z)\,\mathrm{d}z, \tag{2.10}$$

where the integration is w.r.t. the measure on D^y.

The motility is the probability of leaving y. This probability is 1 if $0 \notin D^y$; it is also 1 if $0 \in D^y$ and T_y is a continuous pdf, and it may be smaller than 1 if $0 \in D^y$ and T_y is a discrete pdf. Here we find that the motility depends solely on the even component S_x, in other words solely on modelling assumption one.

Secondly, we define the polarization vector in a *space-jump* process.

Definition 2.3 (Polarization Vector). The polarization vector at $y \in \Omega$ is defined as,

$$E(y) \coloneqq \frac{\int_{D^y} z\, T_y(z)\,\mathrm{d}z}{\left\|\int_{D^y} z\, T_y(z)\,\mathrm{d}z\right\|} = \frac{\int_{D^y} z\, A_y(z) \cdot \frac{z}{|z|}\,\mathrm{d}z}{\left\|\int_{D^y} z\, A_y(z) \cdot \frac{z}{|z|}\,\mathrm{d}z\right\|}, \tag{2.11}$$

where the integration is w.r.t. measure on D^y.

The first moment of the pdf T_y can be intuitively understood as the expected heading of a jump originating at y. This is in direct correspondence with a polarized cell which, following polarization, moves in the direction of the polarization vector. The expected heading is solely determined by A_y, which therefore plays the role of the polarization vector $\mathbf{p}(y)$ in a space-jump process. This correspondence motivates us to set $A_y = \mathbf{p}(y)$ in the subsequent derivations.

2.2.2 Derivation of macroscopic equations

For the following derivations of the population model, we require the following assumptions.

1: We consider a myopic random walk, i.e.

$$S_x(z) = S_x, \qquad A_x(z) = A_x,$$

then

$$T_x(z) = S_x + A_x \cdot \frac{z}{|z|}.$$

Note that $T_x(z)$ still depends on z and x and the scalar S_x and vector A_x depend on x.

2: We consider small jumps of length h, and write

$$D^x = h\mathbb{S}^{n-1}.$$

Note that D^x is the same for all points in the domain. Elements of $\mathbb{S}^{n-1}$ are denoted by σ with measure $\mathrm{d}\sigma$.

Using Lemma 2.1 and assuming that the set of destinations is uniform across the domain, we can rewrite the Master equation (2.7).

$$\begin{aligned} u_t(x,t) &= \lambda \int_{D^x} T_{x-z}(z)u(x-z,t) - T_x(-z)u(x,t)\,\mathrm{d}\mu(z), \\ &= \lambda \int_{D^x} S_{x-z}(z)u(x-z,t) - S_x(-z)u(x,t)\,\mathrm{d}\mu(z) \\ &\quad + \lambda \int_{D^x} A_{x-z}(z)\frac{z}{|z|}u(x-z,t) + A_x(-z)\frac{z}{|z|}u(x,t)\,\mathrm{d}\mu(z). \end{aligned} \tag{2.12}$$

Using assumptions 1 and 2, and the fact that $\|\sigma\| = 1$, we can rewrite (2.12) as

$$\begin{aligned} u_t(x,t) \;=\; & \lambda h^{n-1} \underbrace{\int_{\mathbb{S}^{n-1}} S_{x-h\sigma}u(x-h\sigma,t) - S_x u(x,t)\,\mathrm{d}\sigma}_{\text{(I)}} \\ & + \lambda h^{n-1} \underbrace{\int_{\mathbb{S}^{n-1}} A_{x-h\sigma}\sigma u(x-h\sigma,t) + A_x\sigma u(x,t)\,\mathrm{d}\sigma}_{\text{(II)}}. \end{aligned} \tag{2.13}$$

Let us consider the integrals (I) and (II) separately.

$$\begin{aligned} \text{(I)} \;&=\; \int_{\mathbb{S}^{n-1}} S_{x-h\sigma}u(x-h\sigma,t) - S_x u(x,t)\,\mathrm{d}\sigma, \\ &=\; \int_{\mathbb{S}^{n-1}} S_x u(x,t) - S_x u(x,t)\,\mathrm{d}\sigma - \int_{\mathbb{S}^{n-1}} h\sigma \cdot \nabla(S_x u(x,t))\,\mathrm{d}\sigma \end{aligned}$$

$$
\begin{aligned}
&+ \int_{\mathbb{S}^{n-1}} \frac{h^2}{2} \sigma\sigma^T : \nabla\nabla^T (S_x u(x,t))\, \mathrm{d}\sigma + \mathcal{O}(h^3), \\
&= h \int_{\mathbb{S}^{n-1}} \sigma \, \mathrm{d}\sigma \cdot \nabla (S_x u(x,t)) + \frac{h^2}{2} \int_{\mathbb{S}^{n-1}} \sigma\sigma^T \, \mathrm{d}\sigma : \nabla\nabla^T (S_x u(x,t)) + \mathcal{O}(h^3) \\
&= \frac{h^2}{2n} |\mathbb{S}^{n-1}| \Delta (S_x u(x,t)) + \mathcal{O}(h^3).
\end{aligned}
$$

The colon notation used above denotes the contraction of two rank-two tensors as

$$
\sigma\sigma^T : \nabla\nabla (Su) = \sum_{ij} \sigma_i \sigma_j \frac{\partial}{\partial x_i} \frac{\partial}{\partial x_j} (Su).
$$

In the last step we used the fact (see for example [87]) that

$$
\int_{\mathbb{S}^{n-1}} \sigma \, \mathrm{d}\sigma = 0, \qquad \int_{\mathbb{S}^{n-1}} \sigma\sigma^T \, \mathrm{d}\sigma = \frac{|\mathbb{S}^{n-1}|}{n} \mathbb{I}, \tag{2.14}
$$

where $\mathbb{I}$ is the $n \times n$ identity matrix. Consider integral (II)

$$
\begin{aligned}
\text{(II)} &= \int_{\mathbb{S}^{n-1}} A_{x-h\sigma} \cdot \sigma u(x - h\sigma, t) + A_x \cdot \sigma u(x,t) \, \mathrm{d}\sigma, \\
&= \int_{\mathbb{S}^{n-1}} A_x \cdot \sigma u(x,t) + A(x) \cdot \sigma u(x,t) \, \mathrm{d}\sigma - \int_{\mathbb{S}^{n-1}} h\sigma\sigma^T : \nabla (A_x u(x,t)) \, \mathrm{d}\sigma \\
&\quad + \int_{\mathbb{S}^{n-1}} \frac{h^2}{2} \sigma\sigma\sigma : \nabla\nabla (A_x u(x,t)) \, \mathrm{d}\sigma + \mathcal{O}(h^3), \\
&= -\frac{h|\mathbb{S}^{n-1}|}{n} \nabla \cdot (A_x u(x,t)) + \mathcal{O}(h^3).
\end{aligned}
$$

Here the colon notation denotes the contraction of two rank-three, tensors as

$$
\sigma\sigma\sigma : \nabla\nabla (Au) = \sum_{ijk} \sigma_i \sigma_j \sigma_k \frac{\partial}{\partial x_i} \frac{\partial}{\partial x_j} (A_k u).
$$

Additionally, we used the above identities (2.14) and the fact that

$$
\int_{\mathbb{S}^{n-1}} \sigma_i \sigma_j \sigma_k \, \mathrm{d}\sigma = 0
$$

for all $i, j, k = 1, \ldots, n$, as shown in [87]. Using the approximate expressions (dropping all $\mathcal{O}(h^3)$ terms) for the integrals (I) and (II) in equation (2.13) we

obtain

$$u_t(x,t) \approx \frac{\lambda h^{n+1}}{2n}|\mathbb{S}^{n-1}|\Delta(S_x u(x,t)) - \frac{\lambda h^n}{n}|\mathbb{S}^{n-1}|\nabla \cdot (A_x u(x,t))\,. \tag{2.15}$$

It is interesting to note that the even part of T enters the diffusion term, while the odd part enters the drift term.

2.2.3 Scaling

We now study the asymptotic behaviour of equation (2.15). In the following $u(\cdot,t)$ will denote a possible non-local dependence on the population density $u(x,t)$. Here we are interested in the limits as the lattice spacing h tends to zero and large time. The large time limit is obtained by letting the rate of steps per unit time λ tend to infinity. Different asymptotic equations are obtained, depending on the asymptotic behaviour of $\lambda(h)$. We consider two cases:

1. **Drift dominated:** In this case we assume that S_x and A_x are of order 1 relative to h and λ, and that space and time scale to the same order. That is, $1/\lambda \sim h^n$, which is a hyperbolic scaling. With these assumptions, we can guarantee that the following limits exist.

$$\lim_{\substack{h\to 0\\ \lambda\to\infty}} \frac{\lambda h^n}{n}|\mathbb{S}^{n-1}|A_x = \alpha(x,u(\cdot,t)) < \infty \tag{2.16a}$$

and it follows that

$$\lim_{\substack{h\to 0\\ \lambda\to\infty}} \frac{\lambda h^{n+1}}{2n}|\mathbb{S}^{n-1}|S_x = 0. \tag{2.16b}$$

Note that in the limits (2.16a) and (2.16b), A_x and S_x respectively may depend on the cell population $u(\cdot,t)$. For this reason, we make the function α depend on $u(\cdot,t)$. The limit equation is then a pure drift equation

$$u_t(x,t) + \nabla \cdot (\alpha(x,u(\cdot,t))u(x,t)) = 0. \tag{2.17}$$

2. **Advection-Diffusion:** In this case we assume that S_x is of order 1 relative to h and λ and A_x is of order h and of order 1 relative to λ. This means, $1/\lambda \sim h^{n+1}$, and that time is scaled with one order of h higher than

space. This is a parabolic scaling. With these assumptions, we ensure the existence of the following limits,

$$\lim_{\substack{h\to 0\\ \lambda\to\infty}} \frac{\lambda h^n}{n}|\mathbb{S}^{n-1}|A_x = \alpha(x, u(\cdot,t)) \tag{2.18a}$$

and

$$\lim_{\substack{h\to 0\\ \lambda\to\infty}} \frac{\lambda h^{n+1}}{2n}|\mathbb{S}^{n-1}|S_x = D(x, u(\cdot,t)). \tag{2.18b}$$

Note that in the limits (2.16a) and (2.16b), A_x and S_x respectively may depend on the cell population $u(\cdot,t)$. For this reason, we make the functions D and α depend on $u(\cdot,t)$. Then we obtain an advection-diffusion equation

$$u_t(x,t) + \nabla\cdot(\alpha(x,u(\cdot,t))u(x,t)) = \Delta(D(x,u(\cdot,t))u(x,t)). \tag{2.19}$$

Note that the spatial diffusion constant appears inside the Laplacian: this is expected for transition rates based on local information only; for more details see [27, 163].

An in depth discussion of the different scalings together with their motivation can be found in [90].

2.3 Derivation of non-local adhesion models

In this section the adhesion model (2.5), as proposed by Armstrong et al. [10], will be derived using the framework developed in Section 2.2. In the first step we will derive an expression for the adhesive polarization vector while in subsequent steps we show how different modelling assumptions give rise to different cell-cell adhesion models. This derivation is carried out on the infinite lattice $h\mathbb{Z}^n$. In addition we choose our time steps sufficiently small such that only a single cell moves in each infinitesimal time interval, while the remaining population effectively remains constant. This non-moving population is referred to as the *background* population in the following (see Fig. 2.2).

2.3.1 Microscopic Model of adhesion molecule interactions

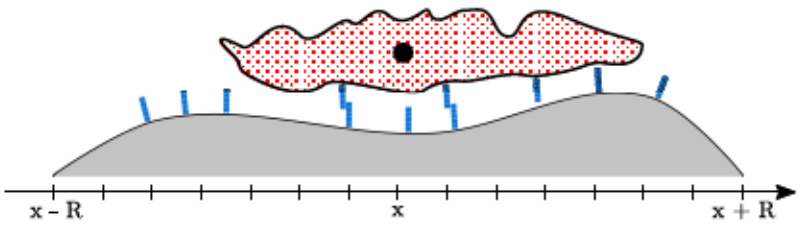

Figure 2.2: The single jumper (white-red checkerboard pattern) with its cell body (black disc) located at x, interacts with the background population (grey) via the adhesion molecules on the respective surfaces, represented as blue sticks.

Consider a cell located at $x \in \Omega$. This cell senses its environment by sending out many membrane protrusions. We now study how a single membrane protrusion interacts with the cell's environment in a test volume $V_h(x+r)$ of side length h, centred at $x+r$. We make four assumptions:

1. The probability of extending a membrane protrusion to V_h depends on the distance $|r|$. Let the proportion of the cell extended into V_h be denoted by $\omega(|r|)$. Since the protrusions are long and thin, the covered volume within the small test volume is proportional to h. Cell protrusions are limited in length by the cell's cytoskeleton, which above a certain threshold will resist further extension [21]. This physical limit is a natural interpretation of the sensing radius R. Consequently, the distribution $\omega(\cdot)$ has compact support i.e. $\operatorname{supp}\omega(r) \subset \mathbb{B}^n(R)$.

2. Cell membrane protrusions are very flexible and are able to fit into very tight spaces. Nevertheless, free space is still required to establish contact. The fraction of available space in $V_h(x+r)$ is denoted by $f(x+r, u(x+r,t))$. This quantity is dimensionless and one choice is discussed in equation (2.32) later.

3. Once a cell protrusion reaches V_h the adhesion molecules on its surface form adhesion bonds with free adhesion molecules of the background

population. If sufficiently many adhesion bonds form the membrane protrusion is stabilized and persists [148]. Otherwise, the protrusion retracts. This retraction is commonly observed as ruffles on the cell surface [2]. We denote the density per unit volume of formed adhesion bonds in V_h by $N_b(x+r)$. We assume that the more adhesion bonds are formed, the stronger the generated adhesion force, and the more likely it is that the protrusion persists. Later we will assume that the number of adhesion bonds in V_h are related to the background cell population i.e. $N_b(x+r, u(\cdot,t))$. Note that this dependence may be non-local as in Section 2.3.5.

4. The direction of the adhesion force is $\frac{r}{|r|}$.

In summary the adhesion strength generated in $V_h(x+r)$ is determined by distance effects, free space and the number of formed adhesion bonds. Detailed functional forms for $f(\cdot)$, $\omega(\cdot)$ and $N_b(\cdot)$ will be discussed in subsequent sections. Let $\boldsymbol{p}_h(x,r)$ denote the adhesion strength generated in V_h. Then, after incorporating the three effects, $\boldsymbol{p}_h(x,r)$ is given by

$$\boldsymbol{p}_h(x,r,u(\cdot,t)) = \beta(x)\ \underbrace{h^n\, N_b(x+r,u(\cdot,t))}_{\#\text{ adhesion bonds}}\ \underbrace{h\,\omega(|r|)}_{\text{amt. of cell in } V_h}\ \underbrace{f(x+r,u(x+r))}_{\text{free space}}, \tag{2.20}$$

where $\beta(x)$ is a factor of proportionality. The factor $\beta(x)$ may include cellular or environmental properties, such as a cell's sensitivity to polarization.

Next we sum over all test volumes present within the sensing radius of the cell. In this step the direction of the adhesive force is important i.e. assumption 4 above. We obtain the cell's polarization vector,

$$\mathbf{p}_{h,\text{net}}(x) = h\beta(x) \sum_{\mathbb{B}^n(R)} h^n\, N_b(x+r,u(\cdot,t))\, f(x+r,u(x+r))\, \omega(|r|)\, \frac{r}{|r|}. \tag{2.21}$$

Now we can make use of our general derivation from Section 2.2. In detail, we let $A_x = \mathbf{p}_{h,\text{net}}(x)$ and take the formal limit as $h \to 0$ and $\lambda \to \infty$. Note that in this case $A_x = \mathcal{O}(h)$, hence limit (2.18a) applies and the final advection term

is

$$\alpha(x, u(\cdot,t)) = \beta(x) \int_{\mathbb{B}^n(R)} N_b(x+r, u(\cdot,t))\, f(x+r, u(x+r))\, \omega(|r|) \frac{r}{|r|}\, \mathrm{d}r. \quad (2.22)$$

The nature of the dependence of N_b on the cell population $u(\cdot,t)$ will be discussed in the following sections. Here we do not specify S_x further, we only require S_x to satisfy the assumptions in Section 2.2. In particular, we will consider the case in which S_x does not depend on $u(\cdot,t)$. The complete model is then,

$$u_t(x,t) = \nabla \cdot [\, \nabla (D(x)u(x,t)) - \alpha(x, u(\cdot,t))u(x,t)\,], \quad (2.23)$$

with $\alpha(x)$ given by (2.22) and $D(x)$ by (2.18b).

2.3.2 The Armstrong Model

To obtain the Armstrong model (2.5) as a special case of (2.23), we assume the following choices.

1. $\omega(r)$ is the uniform distribution on the sensing region $\mathbb{B}^n(R)$. That is,

$$\omega(r) = \frac{1}{|\mathbb{B}^n(R)|}. \quad (2.24)$$

2. There is always free space and spatial constraints do not restrict the adhesion process, so $f(x) \equiv 1$.

3. Mass action kinetics for the reaction between the adhesion molecules of the background population and the extending cell. Specifically, let $N_1(x)$ and $N_2(x)$ denote the density per unit area of adhesion molecules of the walking cell and the background population at x respectively. The binding-unbinding reaction can be written

$$N_1 + N_2 \underset{k_b}{\overset{k_f}{\rightleftharpoons}} N_b\,. \quad (2.25)$$

Using the law of mass action, the kinetics for this reaction are

$$\frac{\mathrm{d}N_b}{\mathrm{d}t} = k_f N_1 N_2 - k_b N_b. \tag{2.26}$$

Assuming that these reactions are fast, the steady state population of N_b may be expressed by

$$N_b = K N_1 N_2, \tag{2.27}$$

where $K = {}^{k_f}/_{k_b}$. The density of adhesion molecules a given cell has on its surface depends on various factors. Here it is assumed that the density of surface adhesion molecules is a given constant. The density of adhesion molecules in the background population $N_2(x)$ is assumed to be directly proportional to the density of the background population at x. Therefore, $N_2(x) \sim u(x)$.

With these choices for the relevant functions, equation (2.23) becomes

$$\begin{aligned} u_t(x,t) = \nabla \cdot \Big[& \nabla \left(D(x) u(x,t) \right) \\ & - a u(x,t) \int_{\mathbb{B}^n(R)} u(x+r,t)\, \omega(|r|) \frac{r}{|r|}\, \mathrm{d}r \Big], \end{aligned} \tag{2.28}$$

where $a = \beta K N_1$ and $\omega(r)$ by (2.24). The one dimensional version of equation (2.28) is the adhesion model proposed by Armstrong et al. [10].

Different choices for $\omega(\cdot)$

The physical limit of cytoskeleton extensions was modelled using $\omega(\cdot)$ where the compact support of $\omega(\cdot)$ introduces the notion of the sensing radius. This is undoubtedly the most important contribution of $\omega(\cdot)$. However, the distribution $\omega(\cdot)$ may vary between different cell phenotypes and we briefly discuss some commonly used distributions. The simplest would be the uniform distribution i.e.

$$\omega(r) = \frac{1}{|\mathbb{B}^n(R)|}. \tag{2.29}$$

Such a uniform distribution may be too unrealistic. The resistance to extension in the cytoskeleton may build up gradually. In such a case a distribution like a

triangle distribution or a Gaussian may be more appropriate. In n-dimensions the triangle distribution generalizes to a cone shaped distribution,

$$\omega(r) = \frac{n+1}{|\mathbb{B}^n(R)|R} \max\left(R - \|r\|_2, 0\right), \tag{2.30}$$

where the prefactor normalizes the distribution. For a discussion of the use of the Laplace or Gaussian distributions see [136]. Mathematically, we may choose any distribution $\omega(\cdot)$ which satisfies $\omega(\cdot) \geq 0$ and $\omega(\cdot) \in L^1(\cdot)$. Note that these are the only required conditions on $\omega(\cdot)$ to guarantee the existence of solution to (2.5) [92].

2.3.3 Volume Filling

In this section two different mechanisms are studied by which volume filling can be included in the adhesion model.

Destination dependent volume filling

First we consider the well known volume filling introduced by Painter et al. [137]. In this work, the transition rates are modified via a decreasing function of the occupancy of the destination site. That is, we modify the transition rates as follows:

$$T_x(z) = q(u(x+z)) \left(S_x(z) + A_x(z) \cdot \frac{z}{|z|} \right). \tag{2.31}$$

The function $q(\cdot)$ denotes the probability of finding space and it is chosen such that $q(U_{\max}) = 0$ and $q(u) \geq 0 \quad \forall\, 0 \leq u \leq U_{\max}$. The effect $q(\cdot)$ has on cell movement is that it reduces the rates of moving to areas with high occupancy. There are many possible choices of $q(\cdot)$. One of the most logical choices is

$$q(u(x,t)) = \left(1 - \frac{u(x,t)}{U_{\max}}\right)^+. \tag{2.32}$$

where $(\cdot)^+ = \max(0, \cdot)$. For this special choice, the term modifying the diffusion term equals one (for details see Painter, Hillen [137]). If such a volume filling

is added, the adhesion model (2.28) becomes,

$$u_t(x,t) = \nabla\cdot\left[\nabla\left(D_u(x)u(x,t)\right) - \beta(x)\left(1-\frac{u(x,t)}{U_{\max}}\right)^+ u(x,t)\int_{\mathbb{B}^n(R)} u(x+r,t)\,\omega(|r|)\frac{r}{|r|}\,\mathrm{d}r\right]. \tag{2.33}$$

This equation describes the situation in which a cell is unable to move if it is fully surrounded by neighbouring cells.

Adhesion molecule volume filling

A second possible form of volume filling is introduced through the free space $f(\cdot)$ term in the polarization of the cell (see equation (2.20)). The free space term in the cell's polarization captures the idea that high occupancy reduces the influence of that location on the cell's polarization: high occupancy is expected to reduce the probability of membrane protrusions that feel out that location. Secondly, a high occupancy could also correlate with a low number of free adhesion molecules. Upon letting the free space term in (2.20) be $f(x) = q(u(x))$, equation (2.23) becomes,

$$u_t(x,t) = \nabla\cdot\left[\nabla\left(D_u(x)u(x,t)\right) - \beta(x)u(x,t)\int_{\mathbb{B}^n(R)} u(x+r,t)\,\left(1-\frac{u(x+r,t)}{U_{\max}}\right)^+\omega(|r|)\frac{r}{|r|}\,\mathrm{d}r\right], \tag{2.34}$$

where $(\cdot)^+ = \max(0,\cdot)$. Equation (2.34) is the same as one of the models presented by Armstrong et al. [10], in which the $h(\cdot)$ function was chosen to be logistic. In this case, areas with high occupancy do not contribute to the adhesion force.

2.3.4 Bell adhesion bond kinetics

Adhesion molecules are confined to the cell surfaces and, for this reason, their binding-unbinding kinetics are different to those of a chemical species moving freely in space. This was recognized by Bell [13], who developed detailed reaction rate constants for this situation. In this section, Bell kinetics replace the mass action kinetics (2.25) used in Section 2.3.2.

Bell kinetics are used in each of the small test volumes V_h, in which a membrane protrusion interacts with the background population (see Section 2.3.1). As in equation (2.25) the densities of adhesion molecules on the membrane protrusion and the background population are denoted by N_1 and N_2, respectively. The density of formed adhesion bonds is denoted by N_b. In contrast to mass action kinetics we distinguish now between free adhesion molecules and formed adhesion bonds. Then the densities of adhesion molecules is split,

$$N_i = N_{if} + N_b \qquad i = 1, 2, \tag{2.35}$$

where N_{if} denotes the unit densities of free adhesion molecules. The kinetic equation governing the evolution of N_b is

$$\frac{\mathrm{d}N_b}{\mathrm{d}t} = k_+^m N_{1f} N_{2f} - k_-^m N_b, \tag{2.36}$$

where k_+^m and k_-^m are the rate constants of bond formation and bond dissociation, respectively. For details on how the reaction rates $k_{+/-}^m$ are determined see Bell [13]. To remove the dependence on N_{if} we use identity (2.35) to obtain,

$$\frac{\mathrm{d}N_b}{\mathrm{d}t} = k_+^m \left(N_1 - N_b\right)\left(N_2 - N_b\right) - k_-^m N_b. \tag{2.37}$$

Following [13, 106] it can be assumed that the number of adhesion molecules in the background population is much larger than the number of adhesion bonds formed, i.e. $N_2 \gg N_b$. This is particularly true, since the number of adhesion molecules on the membrane protrusion is generally expected to be much lower than the background population i.e. $N_1 \ll N_2$. Then equation (2.37)

approximates to

$$\frac{\mathrm{d}N_b}{\mathrm{d}t} = k_+^m N_2 \left(N_1 - N_b\right) - k_-^m N_b. \tag{2.38}$$

The non trivial steady state of this equation is given by

$$N_b = \frac{K N_1 N_2}{1 + K N_2}, \tag{2.39}$$

where $K = {}^{k_+^m}/_{k_-^m}$. Once again it is assumed that N_1 is given by a constant and that $N_2(x) \sim u(x)$. Then using $f(x) \equiv 1$ equation (2.28) becomes

$$\begin{aligned} u_t(x,t) = \nabla \cdot \big[\nabla \left(D(x,t)u(x,t)\right) - \\ a\, u(x,t) \int_{\mathbb{B}^n(R)} \frac{Ku(x+r,t)}{1+Ku(x+r,t)}\, \omega(|r|) \frac{r}{|r|}\, \mathrm{d}r \Big], \end{aligned} \tag{2.40}$$

where $a = \beta N_1$. This describes the situation in which the adhesion force saturates for large cell densities.

2.3.5 Adhesivity of the background population

In the previous sections the adhesion molecules of the background population were assumed to be directly proportional to the background population at that location i.e. $N_2(x) \sim u(x)$. The implicit assumption here, however, is that adhesion molecules of background cells are concentrated at their centres. We

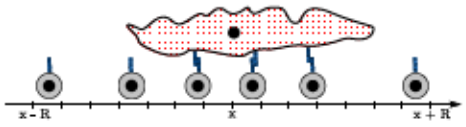

(a) Armstrong model (2.28) assumes that the cells in the background population are point like.

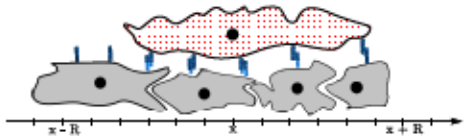

(b) In this case the cells in the background population are assumed to be of similar spatial extent as the single jumper. This means that cells located at x contribute adhesion molecules at locations other than x.

Figure 2.3: In this figure, cells in the background population are shown in grey, while the single jumper is shown with a white-red checkerboard pattern. The adhesion molecules are depicted as blue sticks.

introduce the distribution $\eta(r)$ which describes the distribution of adhesion molecules across the full cell body. Then the sum total of adhesion molecules present at a location x is given by,

$$N_2(x) \coloneqq \int_{\mathbb{B}^n(R)} u(x+r,t)\,\eta(r)\,\mathrm{d}r, \tag{2.41}$$

Note that $\eta(\cdot)$ has no y-dependence, as it is assumed to be equal for all cells. With this definition the adhesion model (2.23) becomes,

$$\begin{aligned} u_t(x,t) = \nabla \cdot \Bigg[& \nabla \left(D(x) u(x,t) \right) \\ & - \beta(x) u(x,t) \int_{\mathbb{B}^n(R)} \int_{\mathbb{B}^n(R)} u(x+y+r,t) \eta(y)\,\mathrm{d}y\, \omega(|r|) \frac{r}{|r|}\,\mathrm{d}r \Bigg]. \end{aligned} \tag{2.42}$$

The double integral formulation of the adhesion model includes all possible adhesion molecules within a small test volume V_h. Therefore, this formulation generalizes the adhesion model (2.28) by treating both the single cell jumper and the background population equal. A pictorial comparison of these two models is shown in Figure 2.3.

Note that, if we assume that $\eta(r) = \delta_0(r)$, then we recover model (2.28). In summary the assumption for Armstrong's model (2.28) are that cells are point-like, have uniform densities of adhesion molecules, and that the adhesion molecules interact via mass action kinetics. At the same time, however, we retain the assumption that cells are able to sense their environment in a non-local fashion.

Centered adhesion molecule distribution

In this section the adhesion molecule distribution $\eta(\cdot)$ is considered, in more detail. The analysis in this section will be carried out in one dimension. The main assumption of the following scaling argument is that most adhesion molecules are concentrated at the cell middle. Hence, the majority contribution to the integral in equation (2.41) originates around $r = 0$. Asymptotic analysis on a small parameter ϵ that controls the width of the distribution $\eta(\cdot)$ is used

to simplify model (2.42). Introduce ϵ to control the width of the distribution $\eta(\cdot)$,

$$\eta^{\epsilon}(r) = \epsilon^{-1}\eta\left(\frac{r}{\epsilon}\right), \tag{2.43}$$

then η^{ϵ} integrates to unity and has compact support.

An asymptotic moment expansion can be obtained for the functional defined in (2.43) [54].

$$\eta\left(\frac{r}{\epsilon}\right) = \sum_{n=0}^{N} \frac{(-1)^n \mu_n \delta^{(n)}(x)}{n!}\epsilon^{n+1} + \mathcal{O}(\epsilon^{N+2}) \tag{2.44}$$

where $\delta^{(n)}$ is the nth derivative of the Dirac delta distribution. The moment μ_n is given by,

$$\mu_n \coloneqq \int_{\mathbb{R}} r^n \eta(r)\,\mathrm{d}r. \tag{2.45}$$

Then η^{ϵ} becomes,

$$\epsilon^{-1}\eta\left(\frac{r}{\epsilon}\right) = \mu_0\delta(x) + \epsilon\mu_1\delta^{(1)}(x) + \frac{1}{2}\epsilon^2\mu_2\delta^{(2)}(x) + \mathcal{O}(\epsilon^3). \tag{2.46}$$

Note that $\mu_0 = 1$ as $\eta(r)$ is a normalized distribution. Upon substitution of (2.46) (dropping all $\mathcal{O}(\epsilon^3)$) into model (2.42) the following is obtained,

$$\begin{aligned} u_t(x,t) = \frac{\partial}{\partial x}\Bigg[(D(x)u(x,t))_x - \beta(x)u(x,t)\int_{-R}^{R}\int_{-R}^{R} u(x+r+y,t)\left(\delta(y)\right. \\ \left. + \epsilon\mu_1\delta^{(1)}(y) + \frac{\mu_2\delta^{(2)}(y)}{2}\epsilon^2\right)\mathrm{d}y\,\omega(|r|)\frac{r}{|r|}\,\mathrm{d}r\Bigg]. \end{aligned} \tag{2.47}$$

Thus resulting in

$$\begin{aligned} u_t(x,t) = \frac{\partial}{\partial x}\Bigg[(D(x)u(x,t))_x - \beta(x)u(x,t)\int_{-R}^{R}\Bigg(u(x+r,t) \\ + \epsilon\mu_1 u'(x+r,t) + \frac{\epsilon^2\mu_2}{2}u''(x+r,t)\Bigg)\omega(|r|)\frac{r}{|r|}\,\mathrm{d}r\Bigg]. \end{aligned} \tag{2.48}$$

This describes the situation in which the adhesion molecule distribution on the cell surface is concentrated at the cell body. In the macroscopic equation

this results in a dependence on higher order derivatives within the non-local term. An open question follows: "In what sense does this equation converge to model (2.28) as $\epsilon \to 0$?".

2.4 Derivation of the non-local chemotaxis model

Chemotaxis defines the directed movement of a biological cell in response to an external chemical gradient. A cell may either move up or down this gradient. Therefore, the directional motion component of the flux is proportional to the chemical gradient. One of the most prominent features of the Keller-Segel chemotaxis model is the formation of blow up solutions [96], although these are not biologically realistic. This has been remediated in many ways, one of which is through the introduction of a non-local chemical gradient by [132] and [91]. The non-local gradient is motivated by the observation that a cell senses the chemical gradient along its cellular surface. In n-dimensions the cell surface is approximated by a sphere of radius R, and the non-local gradient is then defined as,

$$\mathring{\nabla}_R v(x,t) = \frac{n}{R|\mathbb{S}^{n-1}|} \int_{\mathbb{S}^{n-1}} z v(x+Rz,t)\,\mathrm{d}z \tag{2.49}$$

where z is the unit outward normal. Once again the conservation equation (2.1) can be used, by setting the flux $J = J_d + J_c$, where $J_c = \chi u \mathring{\nabla}_R v$. We then obtain,

$$\begin{aligned} u_t &= \nabla \cdot \left(D_u \nabla u - \chi u \mathring{\nabla}_R v \right), \\ v_t &= D_v \Delta v - v + u, \end{aligned} \tag{2.50}$$

where the evolution of the chemical $v(x,t)$ is modelled using a reaction-diffusion equation. It was shown that this model features globally existing solutions [91].

It is well established that cells undergoing chemotaxis polarize in response to the gradient of an external chemical cue [102, 173]. Intracellular mechanisms then amplify, interpret and select the polarization direction [172]. Consequently, it is expected that the cell's polarization vector is proportional to the chemical

gradient that the cell detects.

Following the general derivation in Section 2.2 we let $A_x = \beta(x) \overset{\circ}{\nabla}_R v(x)$. We then obtain two different cases depending on the asymptotic behaviour of A_x.

Taxis dominated migration: Suppose that $A_x \sim \mathcal{O}(1)$. In this case we use limit (2.16a) and limit (2.16b). to obtain,

$$u_t(x,t) + \nabla \cdot \left[\chi(x) u(x,t) \overset{\circ}{\nabla}_R v(x,t) \right] = 0, \tag{2.51}$$

where $\chi(x)$ is determined by the limit (2.16a). Taxis dominated chemotaxis models such as this have been studied in detail in [46].

Advection-Diffusion Limit: Suppose that $A_x \sim \mathcal{O}(h)$. In this case we use limit (2.18a) and limit (2.18b), to obtain

$$u_t(x,t) = \nabla \cdot \left[\nabla \left(D(x) u(x,t) \right) - \chi(x) u(x,t) \overset{\circ}{\nabla}_R v(x,t) \right], \tag{2.52}$$

where $\chi(x)$ is determined by limit (2.18a) and $D(x)$ is determined by limit (2.18b). This equation is the non-local chemotaxis model (2.50) from [89]. The key idea of this *space-jump* derivation of the non-local chemotaxis model was that the sensing radius of the cell remains constant while taking the mesh size h to zero.

2.5 Numerical verification of the derivation

In this section we carry out a numerical verification of the space-jump process presented in Section 2.2 for the adhesion model (2.5). For this purpose we will solve both the stochastic random walk and the partial differential equation (2.5) and compare the results. The stochastic simulation is implemented using the well known Gillespie SSA algorithm [53, 70]. The non-local partial differential equation is solved using a method of lines approach, for details see [66]. Both simulations are carried out on a one dimensional finite domain, with periodic boundary conditions. For the detailed implementation of both simulations see Section 2.5.1 and Section 2.5.2.

2.5.1 Outline of the stochastic simulation

The Gillespie algorithm is originally formulated for the reactions between chemical species [53, 70]. However, it can be applied to spatial phenomena as well. As a foundation for our algorithm we use the stochastic diffusion process from Section 3.2 in [53]. This means, the domain is discretized into uniform intervals i.e. $\Omega = h\mathbb{Z}$. The state vector $Y_i(t)$ denotes the number of cells on lattice site i. Then the reactions between the compartments are,

$$Y_1 \underset{k_{n+2}}{\overset{k_2}{\rightleftharpoons}} Y_2 \underset{k_{n+3}}{\overset{k_3}{\rightleftharpoons}} Y_3 \underset{k_{n+4}}{\overset{k_4}{\rightleftharpoons}} \cdots \underset{k_{2n\ 1}}{\overset{k_{n\ 1}}{\rightleftharpoons}} Y_{n-1} \underset{k_{2n}}{\overset{k_n}{\rightleftharpoons}} Y_n$$

and for the periodic boundary conditions

$$Y_n \underset{k_{n+1}}{\overset{k_1}{\rightleftharpoons}} Y_1$$

Here the reaction rates are non-local spatial functions (see definition of the rates $T(x, y)$ in Section 2.2). The reaction rates for the non-local adhesion models are thus given by,

$$k_i = \begin{cases} d + ch\boldsymbol{p}_{\text{net}}(i) & \text{jump from } i \text{ to } i+1 \\ d - ch\boldsymbol{p}_{\text{net}}(i) & \text{jump from } i \text{ to } i-1 \end{cases} \tag{2.53}$$

where $\boldsymbol{p}_{\text{net}}(x)$ is from equation (2.21). This means that $\boldsymbol{p}_{\text{net}}(i)$ at lattice location i is given by,

$$\boldsymbol{p}_{\text{net}}(i) = \frac{\omega_p}{2R} \sum_{j=-k}^{k} \text{sgn}(j) Y_{i+j}, \tag{2.54}$$

where k is chosen such that $R = kh$. Note that in this case the second factor of h is not required as $Y_i(t)$ already represents a population and not a density. In other words, $hN_b(i) \sim hu(i) = Y_i(t)$. The diffusion coefficient and drift coefficient are transformed into reaction rate constants d and c respectively, via limits (2.18b) and (2.18a). That is,

$$d = \frac{D}{\lambda h^2}, \qquad c = \frac{a}{2\lambda h^2}. \tag{2.55}$$

The Gillespie algorithm is implemented in C++, while the setup, data processing and plotting is written in python. The Mersenne Twister algorithm is used to generated random numbers[1]. All the numerics were carried out on an Intel Core-i7 4790K (Haswell) running Linux. The simulation parameters are given in Table 2.1.

The implemented Gillespie SSA algorithm was verified against two test cases; a constant diffusion simulation, and a constant diffusion with constant advection simulation. The average of 64 stochastic paths generated for both test cases was compared to the solutions of the constant diffusion equation and the constant advection-diffusion equation respectively. The solutions of both test case PDEs were computed using spectral methods. For this the discrete Fourier transform methods from NumPy 1.9[2] were used. In both cases the average of the stochastic paths agreed with the solutions of the PDEs. The verification results are not shown.

2.5.2 Outline of the numerical method for the adhesion model

For the comparison the simple Armstrong adhesion model (2.56) is solved on a one dimensional interval $[0, L]$ with periodic boundary conditions. The equation is solved using a method of lines approach, for more details see Gerisch [66].

The detailed model formulation is,

$$u_t(x,t) = \frac{\partial^2 u(x,t)}{\partial x^2} - a\frac{\partial}{\partial x}\left(u(x,t)\int_{-1}^{1}\frac{r}{|r|}u(x+r,t)\omega(r)\,\mathrm{d}r\right), \qquad (2.56)$$

subject to

$$\begin{cases} u(0,t) = u(L,t) \\ u_x(0,t) = u_x(L,t) \\ u(x,0) = f(x). \end{cases}$$

[1] Implementation from libstc++ gcc 4.9.3 `https://gcc.gnu.org/`

[2] `www.numpy.org`

The function $\omega(\cdot)$ is the uniform distribution over the sensing radius. That is

$$\omega(r) = \frac{\omega_p}{R}. \tag{2.58}$$

Note that the normalization factor in the continuum case $1/R$ is different from the normalization factor in the stochastic simulation $1/2R$ see equation (2.54). The simulation parameters are listed in Table 2.1.

2.5.3 Simulation Parameters

The parameters for both the stochastic and the continuum numerical solutions are listed in Table 2.1. Both the diffusion coefficient and the sensing radius were set to 1.0 to satisfy the non-dimensionalization in [10]. The population density was not rescaled as the stochastic simulation tracked individual particles. The domain size was chosen such that only a single solution peak would form (see Fig. 2.4). The initial cell density was chosen such that it corresponds to a sufficiently large number of particles in the stochastic simulation. The initial density of 4800 cells per unit length, for example, corresponds to approximately 50 cells per lattice site, and a total of approximately 15000 particles. For smaller total cell numbers we observed that the results from the continuum and stochastic simulation deviated for intermediate times, while agreeing for long times. In particular, the time to reach steady state was shortened for the stochastic simulation. The adhesion strength a was chosen such that the constant steady state of equation (2.56) is unstable. Finally, the transition rate scaling λ was chosen and set to 100. Variations of this constant did not affect the simulation outcome.

2.5.4 Results

In Fig. 2.4 we compare the average density of the state vector of 64 stochastic simulations at different time points to the continuum adhesion model (2.56). The relative error between the average density from the stochastic simulations and the numerical differential equation solution is, at maximum, $\approx 2\%$. Thus, under appropriate functional choices, the stochastic model converges to the

Model Parameter	Value
Domain Size L	3.0
Domain subdivisions per unit length	96
Diffusion coefficient D	1.0
Adhesion strength coefficient a	0.003
Sensing radius R	1.0
Transition rate scaling λ	100
Weighting size ω_p	0.82
Initial density u_0	4800.0
Initial conditions (IC)	$u_0(1+\kappa\sin(x))$
Perturbation Size of IC κ	0.09

Table 2.1: Parameters for Adhesion simulations

Armstrong et al. [10] model.

2.5.5 Correction of adhesion paths

Typical sets of paths generated via the Gillespie SSA with the adhesive reaction rates (2.53) are shown in Fig. 2.5a. Studying Fig. 2.5a it is noted that the peaks do not form at the same location between runs. This behaviour is expected, since we have a periodic domain and almost uniform initial data. This disagreement is corrected for by shifting the medians of each individual path to the location at which the PDE forms its peak. This is not a problem because the equation is solved with periodic boundary conditions. For an example of the result of such a correction see Fig. 2.5b. Note that the agreement between the average of stochastic simulation and the continuum solution is much better.

2.6 Discussion

The adhesion model of [10] has been a step forward in the modelling of cohesive cell populations. The model has been used successfully in applications ranging from cell sorting to cancer invasion. Non-local models have been used previously to model cohesion in biological processes, see for example, the work on swarming

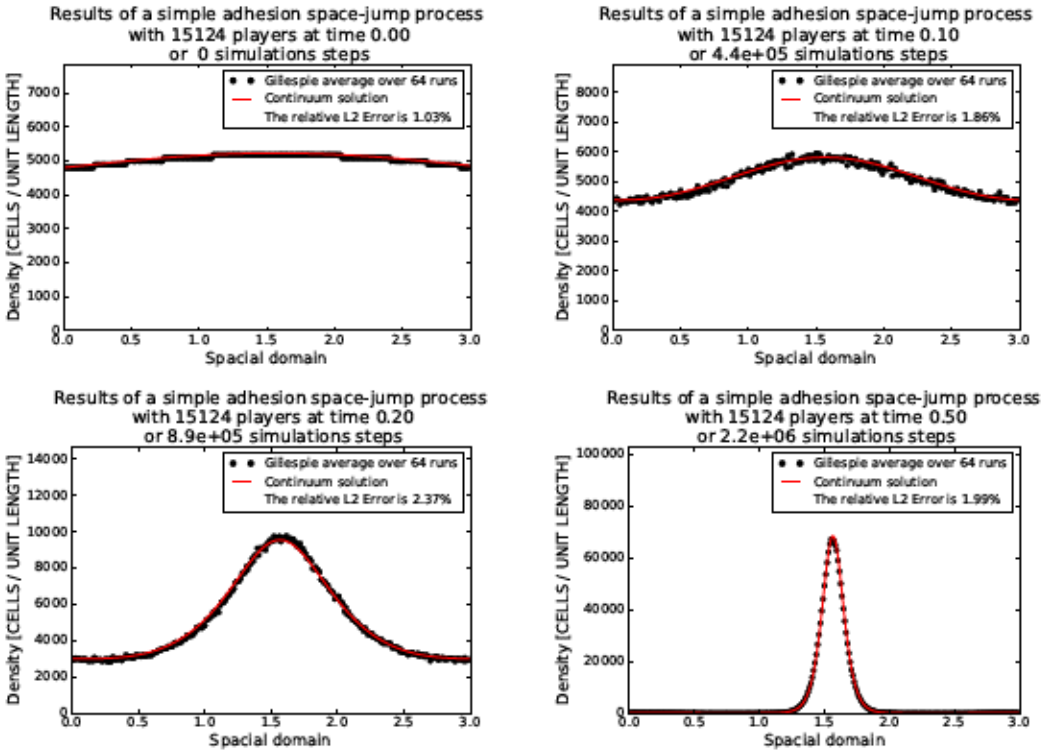

Figure 2.4: The average over 64 stochastic simulations of the state vector is shown as black circles, one for each lattice site. The line (red) represents the solution of equation (2.56). The first image shows the initial condition, then times 0.1, 0.2 and 0.5 are shown. Steady state is reached some time before time point 0.5. The initial condition is given by $f(x) = u_0 + \kappa u_0 \sin(x)$. Note the stochastic paths are shifted by the procedure described in Section 2.5.5. For details on the implementation of the numerical simulations see the appendix. The simulation parameters are listed in Table 2.1.

behaviour by Mogilner et al. [121].

Our derivation from a stochastic random walk perspective allows us to connect the macroscopic quantities of drift and diffusion to microscopic properties of cell behaviour. We analyzed adhesion binding and unbinding dynamics, the availability of free space, the extensions of protrusions and the force balances between adhesion in different directions. We found that the simplest case, in which background cells are local, free space is plenty and adhesive forces are proportional to the cell population, leads to Armstrong's model. However, we also show that more complicated and more realistic assumptions can be included to

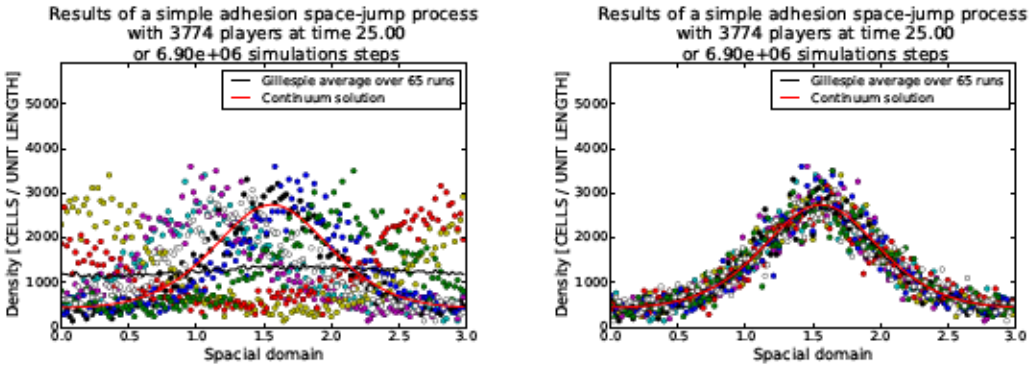

(a) Uncorrected paths **(b)** Corrected paths

Figure 2.5: On the left a typical set of 8 simulation paths generated with the Gillespie SSA algorithm. Each separate path is indicated by a different colour (please see online version for the colour figure). The straight (red) line is the continuum prediction and the black curve the average of the 8 stochastic paths. On the right are the same paths after rotation. Rotation is done as described in the text.

obtain extensions to Armstrong's adhesion model. It is an interesting task for future research to study the properties of volume filling, adhesion saturation and double non-locality.

The key to the presented derivation is the definition of the polarization vector. It is commonly known that cells polarize due to many different gradients [29], including adhesive gradients [130, 148, 165]. Further, during embryo compaction, adhesion between neighbouring cells is established by E-cadherin dependent filopodia, which extend and attach to neighbouring cells. Subsequently, the filopodia remain under tension to bring cell membranes into close contact [175]. This observation fits closely with our definition of the adhesive polarization vector. The definition of the polarization vector allows us to keep our derivation general. This makes it straightforward to derive other taxis models through simply replacing the polarization vector. Here we derived two taxis models: the non-local adhesion model (2.5) and the non-local chemotaxis model (2.50). It is easy to envision similar derivations for other mechanisms of cell polarization.

The polarization of cells is persistent, meaning that even in the absence of an external signal the cells retain their polarization [109]. For instance, amoebae

show a persistence time of approximately 10 min [109]. Li et al. conclude that the motion of amoebae is not a simple random walk, but a process by which left and right successively follow each other to avoid expensive backtracking [109]. During the development of the *Dictyostelium* slug, periodic waves of chemo attractant cAMP are observed [48], which will result in a flipping of the gradient as it passes over the cell. Despite this, the direction of cell migration does not change [48]. Such a persistence mechanism has been studied in other modelling approaches, such as velocity jump processes [86]. It remains, however, an open problem of how to include persistence of cell polarization within the space-jump framework.

A key assumption of our derivation is that the mean waiting time or mean residency time between jumps, is a constant with respect to the population density. An interesting direction of future research would be to weaken this assumption. In the case of cell-cell adhesion, the mean residency time would be expected to increase when strong cell adhesions are made with juxtaposed cells. Therefore, it would be expected that the mean residency time λ is an increasing function of cell density. A good starting point for such an investigation may be the work of [159, 177], who both considered a coupling between the waiting time distribution and jumps.

In this work we have not been concerned with the internal cell dynamics which translate extrinsic or intrinsic cues into cell polarization. For a review discussing internal cell dynamics giving rise to cell polarization see [102]. A common feature of these models is a symmetry breaking process, thus distinguishing the cell front and back. It is an interesting task, to couple such a detailed model of cell polarization to our cell movement model. Such a multi-scale approach would be particularly interesting with respect to the persistence of cell polarization: for example, is it possible to obtain cell polarization by coupling two such models? A further interesting modelling question is whether such a coupling gives rise to models similar to the non-local chemotaxis or non-local adhesion model.

Mathematically, the non-local model (2.5) is very interesting. For the single non-local model existence and uniqueness results are available [28, 92] while the existence of travelling wave solutions has been demonstrated by Ou et al. [133].

The existence of spatially non-homogenous steady states and hence pattern formation has been numerically observed by Armstrong et al. [10]. However, an analytical treatment of the steady states of this model and the conditions under which they form remains a challenge.

The doubly non-local model (2.42) appears to be mathematically new. For this reason, the questions of existence, uniqueness, travelling waves, steady states are all open problems. It is further an open problem to understand the differences of such a doubly non-locality compared to the single non-locality on the form of solutions observed.

Chapter 3

Steady States of a Cell-Cell Adhesion Model on a Periodic Domain

3.1 Introduction

In this chapter, we consider the steady states of the non-local adhesion model introduced in [10]. Let S^1_L denote the L-length circle. Let $u(x,t)$ denote the density of the cell population at location $x \in S^1_L$ at time $t \in \mathbb{R}^+$. The non-local operator modelling cell-cell adhesion interactions is given by

$$\mathcal{K}[u(x,t)](x,t) = \int_{-R}^{R} h(u(x+r,t))\Omega(r)\,\mathrm{d}r. \tag{3.1}$$

The full evolution equation is given by

$$u_t(x,t) = Du_{xx}(x,t) - \alpha\left(u(x,t)\,\mathcal{K}[u(x,t)](x,t)\right)_x. \tag{3.2}$$

In the previous, D is the diffusion coefficient of the cell population, α the strength of the homotypic cellular adhesions, and finally R is the cell's sensing radius. The sensing radius is the distance over which cell's sample their environment using cell membrane protrusions. For more details on this process, see [24]. The initial condition of equation (3.2) is denoted by $u_0(x,t)$. Note that as

we consider the equation on the circle we do not require boundary conditions (or in other words periodic boundary conditions are imposed).

We start off by giving a precise mathematical definition of the non-local term.

Definition 3.1. Let X, Y be Banach spaces of functions, then we define the operator $\mathcal{K}\colon X \to Y$ by

$$\mathcal{K}[u(x)](x) = \int_{-1}^{1} h(u(x+r))\Omega(r)\,\mathrm{d}r. \tag{3.3}$$

The directionality function Ω is assumed to satisfy the following conditions:

(K1) $\Omega(r) = \frac{r}{|r|}\omega(|r|)$,

(K2) $\omega(r) \geq 0$,

(K3) $\omega \in L^1(0,1) \cap L^\infty(0,1)$,

(K4) $\|\omega\|_{L^1(0,1)} = 1/2$.

The function $h(\cdot)$ within the integral describes the nature of the adhesive force and is assumed to satisfy:

(H1) $h \in C^2(\mathbb{R})$,

(H2) $h(u) \geq 0$ for $u \geq 0$,

(H3) $h(u) \leq C\,(1+u)$ for all $u \geq 0$, for some $\mathbb{R} \ni C \geq 0$,

(H4) $h'(\bar{u}) \neq 0$, where $\bar{u}$ is the real number defined in equation (3.10b).

Remark 3.2. Using the assumptions K1 to K4 we can rewrite the non-local function defined in equation (3.3) as

$$\mathcal{K}[u]\colon x \to \int_{0}^{1} \left[\, h(u(x+r)) - h(u(x-r)) \,\right] \omega(r)\,\mathrm{d}r. \tag{3.4}$$

This equivalent formulation will be frequently used in the following.

In the remainder of this chapter, we will work with a non-dimensionalized version of equation (3.2). This is to reduce the complexity of our exposition. For this, we introduce the following non-dimensional variables,

$$x^* = \frac{x}{R}, \qquad t^* = t\frac{D}{R^2}, \qquad u^* = \frac{u}{\hat{u}}, \qquad \alpha^* = \frac{\alpha}{\hat{\alpha}}, \tag{3.5}$$

where $\hat{u}$ depends on the precise choice of the function $h(u)$, and $\hat{\alpha}$ is given by

$$\hat{\alpha} = \frac{D}{R\phi\hat{u}}. \tag{3.6}$$

Finally, $\tilde{L} = {}^{L}/_{R}$. The non-dimensionalization of equation (3.2) is given by

$$u_t(x,t) = u_{xx}(x,t) - \alpha\left(u(x,t)\int_{-1}^{1}\tilde{h}(u(x+r,t))\Omega(r)\,\mathrm{d}r\right)_x. \tag{3.7}$$

In the following, to make our notation simpler we will drop the tildes from L and $h(\cdot)$. For details on this non-dimensionalized, see Appendix A.

3.1.1 Conservation of Mass

As we do not consider any population dynamics (cell production or cell death) in equation (3.2), it is easy to see that mass in the system is conserved.

Lemma 3.3. *Let $u \in \mathcal{C}^1(S^1_L)$ then from [92] we have that equation (3.2) has globally existing solutions. We define the total mass of the population $u(x,t)$ by*

$$\bar{u}(t) \coloneqq \frac{1}{L}\int_0^L u(x,t)\,\mathrm{d}x, \tag{3.8}$$

which is conserved.

Proof. We proceed by computing

$$\begin{aligned} L\frac{\mathrm{d}\bar{u}}{\mathrm{d}t} = \int_0^L u_t(x,t)\,\mathrm{d}x &= \int_0^L \left(u_x - \alpha u\,\mathcal{K}[u]\right)_x\,\mathrm{d}x \\ &= u_x(L) - u_x(0) - \alpha u(0)\left(\mathcal{K}[u](L) - \mathcal{K}[u](0)\right) \\ &= 0. \end{aligned} \tag{3.9}$$

□

3.1.2 The steady-state problem

The steady states of equation (3.7) are solutions of the following non-local equation,

$$u''(x) = \alpha \left(u(x) \mathcal{K}[u(x)](x) \right)' \quad \text{in } S^1_L. \tag{3.10a}$$

Due to the mass conserving property of equation (3.7), we will impose the following integral constraint. Let $\mathbb{R} \ni \bar{u} > 0$, and set

$$\bar{u} = \frac{1}{L} \int_0^L u(x)\, \mathrm{d}x. \tag{3.10b}$$

This constraint will ensure that all solutions that are obtained to the steady state equation of equation (3.7) satisfy its mass conservation property.

3.1.3 Mathematical Background

The success of equation (3.2) is that it can replicate the complicated patterns observed in cell-sorting experiments [10]. In mathematical terms, these patterns are steady states of equation (3.2). Thus understanding the conditions, under which these steady states form and become stable are important. Furthermore, knowing the steady states of this equation is one of the first steps toward understanding the equation's global attractor.

Up to this point, the steady states of equation (3.2) have only been studied numerically and using linear stability analysis [10]. Closely related to equation (3.2) are the local and non-local chemotaxis equation [89, 91, 132]. For both the local and non-local chemotaxis equations a global bifurcation analysis, to understand their steady-states, was carried out [170, 176]. Inspired by their results, we present here a first exploration of the set of non-homogenous steady-states solutions of equation (3.2).

Central to our analysis are the abstract local bifurcation theorem [35] and global bifurcation theorem [144], which originated from work by Crandall, Rabinowitz. Preceding to the formulation of these general theorems, Crandall, Rabinowitz studied the set of solutions of non-linear Sturm-Liouville problems [34, 143]. For linear Sturm-Liouville eigenvalue problems it is well known that

the eigenfunctions can be classified by their number of zeros [32]. Crandall, Rabinowitz showed, that under rather weak assumptions the same classification holds for non-linear eigenvalue problems. In fact, each global solution branch inherited the number of zeros of the eigenfunction at which it originated (bifurcation point). Furthermore they showed, that each global solution branch is unbounded and that branches do not meet (since it is impossible for solutions of Sturm-Liouville problems to have degenerate zeros). In [144], Rabinowitz generalizes the global bifurcation theorem to general non-linear eigenvalue problems. The main theorem gives two alternatives for the behaviour of the global bifurcation branch. It is either bounded, connecting two bifurcation points, or it is unbounded (see Theorem 1.3 in [144]). This is now known as the Rabinowitz-alternative. An extension of the global bifurcation theorem to study so called unilateral (sub-branches in only the positive or negative direction of the eigenfunction at the bifurcation point) branches was originally reported in [144]. The original proof contained holes that were filled in by [111, 113, 158]. Since the original formulation of these bifurcation theorems, similar theorems which apply in more general settings have been developed. Here, we will use bifurcation theorems that are applicable to Fredholm operators [111, 113, 158] (see Section 3.2).

While, both the local and non-local chemotaxis model in [170] and [176] were formulated with no-flux boundary conditions, the formulation of no-flux boundary conditions for equation (3.10) was more challenging due to the complicated non-local structure of $\mathcal{K}[u]$. Thus, to study and analyze the formation of non-homogenous solutions in isolation of boundary considerations, we formulate equation (3.2) on a circle (equivalently periodic boundary conditions). A more detailed discussion on the challenges of construction of no-flux boundary conditions can be found in the next chapter.

At the same time however, formulating our model on a circle gives rise to some additional challenges. The most critical being that eigenvalues of the Laplacian on S^1_L need not be simple. This is a challenge, because bifurcations require eigenvalues of odd multiplicity (the theorems in [113, 158] require simple eigenvalues). This challenge was previously observed by Matano, who studied nonlinear reaction diffusion equations on the circle [118]. The solution

of Matano was to impose symmetry requirements on the non-linear term, so that the equation would be $\mathbf{O}(2)$ equivariant (invariant under translations and reflections see also Section 3.5.1).

Around the same time, Healey extended the Rabinowitz alternative to so called G-reduced problems (G being a symmetry group), which is a nonlinear bifurcation problem formulated on a Banach space whose elements are fix-points of the symmetries defined by G [83]. Thus, showing that certain symmetries persist along global bifurcation branches (similar results are often referred to as the equivariant branching lemma [73]). Subsequently, these ideas were used in a series of papers, which studied the conditions under which solutions of non-linear elliptic equations are classifiable by their number of zeros. The key to these results, was to impose sufficient conditions on the nonlinear terms such that the resulting equation was equivariant under actions of $\mathbf{O}(2) \times \mathbb{Z}_2$ ($\mathbb{Z}_2$ describes the action of the negative identity, i.e., a reflection through the x-axis). [84, 85]. Intuitively, this symmetry requirement ensured that the zeros of solutions were "frozen" (i.e., fixed location), and thus the number of zeros is preserved along the global bifurcation branch. Furthermore, this result easily shows that global solution branches do not meet. Much more recently, Buono et al. used $\mathbf{O}(2)$ equivariance to compare the accessible bifurcations in a non-local hyperbolic model of swarming and the equation's formal parabolic limit [23].

In a similar spirit, we will show that the steady-state equation (3.10) of equation (3.2) is indeed equivariant under actions of $\mathbf{O}(2)$. Using the properties of the non-local term $\mathcal{K}[u]$, we will then show that this leads to "frozen" maxima and minima (equivalently frozen zeros of the derivative u'). Since we consider equation (3.10) on a periodic domain, we can prescribe the location of one maxima (or minima) without restricting possible solutions. This ensures that only simple eigenvalues occur in our subsequent analysis. In the grand finale we prove a global bifurcation result for the steady-state solutions of the non-local cell-cell adhesion equation for the first bifurcation branch. Finally we discuss how this proof could be extended to all bifurcation branches.

This chapter is structured as follows: In Section 3.2 we review the required mathematical background for this chapter. In Section 3.3 we introduce the

required mathematical formulation of equation (3.10) and explore the mathematical properties of the non-local term $\mathcal{K}[u]$. We continue in Section 3.4 with the exploration of steady state properties that are a result of the structure of equation (3.10). In Section 3.5 we carry out the local and global bifurcation analysis, and in Section 3.6 we find conditions that imply a switch of stability at the first bifurcation point. In Section 3.7 we discuss some interesting numerical solutions; and finally in Section 3.8 we discuss our findings and indicate areas that we think merit future exploration.

3.2 Fredholm operators

This section is based on [113], and is meant as a quick introduction to the abstract framework which will be employed in this work.

3.2.1 Notation

In the following document we will use the following notation conventions. Banach spaces and their subspaces will be denoted using capital letters that is X, Y, U, V and so on. Operators between function spaces will be denoted using the calligraphic font for example $\mathcal{L}, \mathcal{F}, \mathcal{K}$. The argument of an operator will be enclosed in square brackets. For instance

$$\mathcal{L}\colon X \to Y, \qquad \mathcal{L}[x] = y. \tag{3.11}$$

This is to distinguish the action of the operator from a family of operators. For example a family of operators may be indexed using a real number λ. Then we have a map from $\mathbb{R} \to \mathfrak{L}(X, Y)$ (space of linear operators from X to Y)

$$\lambda \to \mathcal{L}(\lambda)\colon X \to Y, \tag{3.12}$$

and for each fixed λ we may study $\mathcal{L}(\lambda)[x] = y$. The kernel and range of an operator is denoted $\mathrm{N}[\mathcal{L}]$ and $\mathrm{R}[\mathcal{L}]$.

Spaces of operators are denoted using the fraktur font. The most important is the space of continuous linear operators denoted $\mathfrak{L}$ and the space of compact

operators $\mathfrak{K}$. The space of Fredholm operators is denoted Fred_i where i denotes the index.

Special subspaces such as a continuum of solutions or the solution set of an operator equation are also denoted using the fraktur font. For example, $\mathfrak{C}, \mathfrak{S}$.

3.2.2 Introduction to Nonlinear Analysis

The following sections are based on [113, 114]. Let U, V be two real Banach spaces. We denote the space of bounded linear operators from U to V by $\mathfrak{L}(U,V)$, and by $\mathrm{Fred}_0(U,V)$ the subset of $\mathfrak{L}(U,V)$ containing all Fredholm operators with index 0. The set of all isomorphisms between U and V is denoted $\mathrm{Iso}(U,V)$. The operator $\mathcal{L}$ is said to be Fredholm, whenever

$$\dim \mathrm{N}[\mathcal{L}] < \infty, \qquad \mathrm{codim}\, \mathrm{R}[\mathcal{L}] < \infty. \tag{3.13}$$

Recall that

$$\mathrm{codim}\, \mathrm{R}[\mathcal{L}] = \dim V/\mathrm{R}[\mathcal{L}]. \tag{3.14}$$

The index of a Fredholm operator, is defined by

$$\mathrm{ind}[\mathcal{L}] = \dim \mathrm{N}[\mathcal{L}] - \mathrm{codim}\, \mathrm{R}[\mathcal{L}]. \tag{3.15}$$

Therefore, if $\mathcal{L} \in \mathrm{Fred}_0$ then

$$\dim \mathrm{N}[\mathcal{L}] = \mathrm{codim}\, \mathrm{R}[\mathcal{L}] < \infty. \tag{3.16}$$

Lemma 3.4. *If $\mathrm{Fred}_0(U,V) \neq \emptyset$, then U and V are isomorphic.*

Proof. If $\mathrm{Fred}_0(U,V) \neq \emptyset$, then there it is an isomorphism from its domain to its range. As the map is Fredholm its kernel and co-kernel are finite dimensional. Further, as the map has index zero they have the same dimension, thus are isomorphic. □

The most important example of a Fredholm operator with index zero is the following.

Theorem 3.5 ([72]). *Let $\mathcal{K} \in \mathfrak{K}(U)$ (compact operator), then $\mathcal{F} = \mathcal{I} - \mathcal{K}$ is a Fredholm operator of index zero.*

3.2.3 Operator families and generalized spectrum

This section follows from the abstract setting introduced in [114] that is then used for the formulation of the global bifurcation theorems in [113].

Definition 3.6. Let U, V be two Banach spaces over the field $\mathbb{K}$ and $r \in \mathbb{N}$, then an *operator family* of class $\mathcal{C}^r$ in $\Omega \subset \mathbb{K}$ from U to V is a map

$$\mathcal{L} \in \mathcal{C}^r(\Omega, \mathfrak{L}(U, V)). \tag{3.17}$$

In our case $\Omega \subset \mathbb{R}$ always. We now define the generalized spectrum of an operator family.

Definition 3.7. Let $\mathcal{L} \in \mathcal{C}(\Omega, \mathfrak{L}(U, V))$ be an operator family, then the point $\lambda_0 \in \Omega$ is a *singular value* of $\mathcal{L}$ if

$$\mathcal{L}_0 := \mathcal{L}(\lambda_0) \notin \mathrm{Iso}(U, V), \tag{3.18}$$

and it is a *generalized eigenvalue* of $\mathcal{L}$ if

$$\dim \mathrm{N}[\mathcal{L}_0] \geq 1. \tag{3.19}$$

A generalized eigenvalue λ_0 is simple, whenever

$$\dim \mathrm{N}[\mathcal{L}_0] = 1. \tag{3.20}$$

Definition 3.8. The set of all singular values of the operator family $\mathcal{L}$ is called the *spectrum*, and is defined by

$$\Sigma = \Sigma(\mathcal{L}) = \{\, \lambda \in \Omega \colon \mathcal{L}(\lambda) \notin \mathrm{Iso}(U, V) \,\}. \tag{3.21}$$

Similarly, the set of all generalized eigenvalues of the operator family $\mathcal{L}$, is

defined by

$$\mathrm{Eig}(\mathcal{L}) = \{\, \lambda \in \Omega \colon \dim \mathrm{N}[\mathcal{L}(\lambda)] \geq 1 \,\}\,. \tag{3.22}$$

By the preceding definition it is immediate that $\mathrm{Eig}(\mathcal{L}) \subset \Sigma(\mathcal{L})$.

Definition 3.9. The *resolvent set* of $\mathcal{L}$, is defined by

$$\rho(\mathcal{L}) \coloneqq \Omega \setminus \Sigma. \tag{3.23}$$

Remark 3.10. Since $\mathcal{L} \in \mathcal{C}(\mathbb{R}, \mathfrak{L}(U,V))$ and $\mathrm{Iso}(U,V)$ is an open subset of $\mathfrak{L}(U,V)$ we have that $\rho(\mathcal{L})$ is open and possible empty. Thus $\Sigma(\mathcal{L})$ is closed.

Lemma 3.11. *If* $\mathcal{L}_0 \in \mathrm{Fred}_0(U,V)$ *then* $\lambda_0 \in \Sigma(\mathcal{L})$ *if and only if* $\lambda_0 \in \mathrm{Eig}(\mathcal{L})$.

Proof. We only have to prove one direction. Let $\lambda_0 \in \Sigma(\mathcal{L})$, then $\mathcal{L}_0 \colon U/N[\mathcal{L}_0] \to R[\mathcal{L}_0]$ is an isomorphism by the open mapping theorem. As $\mathcal{L}_0$ is Fredholm with index zero we have that $\dim N[\mathcal{L}_0] < \infty$, hence $\lambda_0 \in \mathrm{Eig}(\mathcal{L})$. □

Hence, if $\mathcal{L}(\Omega) \subset \mathrm{Fred}_0(U,V)$, then $\Sigma(\mathcal{L}) = \mathrm{Eig}(\mathcal{L})$.

Remark 3.12. Note that the concept of a *generalized eigenvalue* of an operator family $\mathcal{L}(\Omega)$, should not be confused with the classical notions of an eigenvalue and spectrum (denote $\sigma(\mathcal{L}(\lambda))$), which is only defined for fixed values of $\lambda \in \Omega$. The classical spectrum is defined as (see for instance [56 Chapter 7])

$$\sigma(T) \coloneqq \{\lambda \in \mathbb{K} \colon \lambda \mathcal{I} - T \text{ is not invertible}\}. \tag{3.24}$$

(Note that $\sigma(T)$ can be decomposed into the point, continuum and residual spectrum depending on the precise way the operator fails to be invertible). It is however, possible to recover these classical notions from this more general definition. Indeed, suppose that $T \in \mathfrak{L}(U,V)$, and consider the operator family

$$\mathcal{L}^T(\lambda) \coloneqq \lambda I_U - T, \tag{3.25}$$

then

$$\sigma(T) = \Sigma(\mathcal{L}^T). \tag{3.26}$$

3.2.4 Abstract Bifurcation Theory

Let U, V be two real Banach spaces, and suppose that we want to analyze the structure of the solution set of the nonlinear operator given by

$$\mathcal{F}(\lambda, u) = 0, \qquad (\lambda, u) \in \mathbb{R} \times U, \tag{3.27}$$

where

$$\mathcal{F}\colon \mathbb{R} \times U \to V, \tag{3.28}$$

is a continuous map satisfying the following requirements:

(F1) For each $\lambda \in \mathbb{R}$, the map $\mathcal{F}(\lambda, \cdot)$ is of class $\mathcal{C}^1(U, V)$ and

$$\mathcal{D}_u \mathcal{F}(\lambda, u) \in \mathrm{Fred}_0(U, V) \quad \text{for all } u \in U. \tag{3.29}$$

(F2) $\mathcal{D}_u \mathcal{F}\colon \mathbb{R} \times U \to \mathfrak{L}(U, V)$ is continous.

(F3) $\mathcal{F}(\lambda, 0) = 0$ for all $\lambda \in \mathbb{R}$.

Definition 3.13. A *component* $\mathfrak{C}$ is a closed and connected subset of the set

$$\mathfrak{S} = \{\, (\alpha, u) \in \mathbb{R} \times U\colon \mathcal{F}(\alpha, u) = 0 \,\} \tag{3.30}$$

that is maximal with respect to inclusion.

Definition 3.14. As $(\lambda, 0)$ is a known zero, it is referred to as the *trivial state*.

Definition 3.15. Given $\lambda_0 \in \mathbb{R}$ it is said that $(\lambda_0, 0)$ is a *bifurcation point* of $\mathcal{F} = 0$ if there exists a sequence $(\lambda_n, u_n) \in \mathcal{F}^{-1}(0)$, with $u_n \neq 0$ for all $n \geq 1$, such that

$$\lim_{n \to \infty} (\lambda_n, u_n) = (\lambda_0, 0). \tag{3.31}$$

For every map $\mathcal{F}$ satisfying F1, F2 and F3, we denote

$$\mathcal{L}(\lambda) = \mathcal{D}_u \mathcal{F}(\lambda, 0), \qquad \lambda \in \mathbb{R}. \tag{3.32}$$

By property F2 we have that $\mathcal{L} \in \mathcal{C}(\mathbb{R}, \mathfrak{L}(U,V))$ and by F1 we have $\mathcal{L}(\lambda) \in \mathrm{Fred}_0(U,V)$, thus

$$\mathcal{L}(\lambda) \in \mathrm{Iso}(U,V) \qquad \text{if and only if} \qquad \dim \mathrm{N}[\mathcal{L}(\lambda)] = 0. \tag{3.33}$$

Lemma 3.16 ([113]). *Suppose $(\lambda_0, 0)$ is a bifurcation point of $\mathcal{F} = 0$. Then, $\lambda_0 \in \Sigma(\mathcal{L})$ ($\mathcal{L} = \mathcal{D}_u \mathcal{F}(\lambda, 0)$).*

Theorem 3.17 (Local Bifurcation [35]). *Let U, V be Banach spaces, W a neighborhood of 0 in U and*

$$\mathcal{F}\colon (-1,1) \times W \to V, \tag{3.34}$$

have the properties:

1. *$\mathcal{F}(\lambda, 0) = 0$ for $|\lambda| < 1$,*
2. *The partial derivatives $\mathcal{F}_\lambda, \mathcal{F}_x, \mathcal{F}_{\lambda x}$ exist and are continuous,*
3. *$\mathrm{N}[\mathcal{F}_x(0,0)]$ and $V/\mathrm{R}[\mathcal{F}_x(0,0)]$ are one-dimensional,*
4. *$\mathcal{F}_{\lambda x}(0,0)[x_0] \notin \mathrm{R}[\mathcal{F}_x(0,0)]$, where*

$$\mathrm{N}[\mathcal{F}_x(0,0)] = \mathrm{span}(x_0). \tag{3.35}$$

If Z is any complement of $\mathrm{N}[\mathcal{F}_x(0,0)]$ in U, then there is a neighbourhood N of $(0,0)$ in $\mathbb{R} \times U$, an interval $(-a,a)$, and continuous functions $\phi\colon (-a,a) \to \mathbb{R}$, $\psi\colon (-a,a) \to Z$ such that $\phi(0) = 0, \psi(0) = 0$ and

$$\mathcal{F}^{-1}(0) \cap N = \{\, (\phi(s), \alpha x_0 + \alpha\psi(s)) : |s| < a \,\} \cup \{\, (\lambda, 0)\colon (\lambda, 0) \in N \,\}. \tag{3.36}$$

If $\mathcal{F}_{xx}$ is continuous then the functions ϕ and ψ are once continuously differentiable.

Theorem 3.18 ([35]). *In addition to the assumptions of Theorem 3.17, let $\mathcal{F}$ be twice differentiable. If ϕ, ψ are the functions of Theorem 3.17, then there is $\delta > 0$ such that $\phi'(s) \neq 0$ and $0 < |s| < \delta$ implies that $\mathcal{F}_x(\phi(s), \alpha x_0 + \alpha\psi(s))$ is an isomorphism of U onto V.*

Theorem 3.19 ([35]). *In addition to the assumptions of Theorem 3.17, suppose $\mathcal{F}$ has n continuous derivatives with respect to (λ, x) and $n+1$ continuous derivatives with respect to x. Then the functions (ϕ, ψ) have n continuous derivatives with respect to s. If*

$$\mathcal{F}_x^{(j)}(0,0)(x_0)^j = 0 \qquad 1 \le j \le n \quad \text{then } \phi^{(j)}(0) = 0, \tag{3.37}$$

and

$$\psi^{(j)}(0) = 0 \qquad \text{for } 1 \le j \le n-1, \tag{3.38}$$

and

$$(1/(n+1))\,\mathcal{F}_x^{(n+1)}(0,0)(x_0)^{n+1} + \mathcal{F}_x(0,0)\psi^{(n)}(0) + \phi^{(n)}(0)\,\mathcal{F}_{\lambda x}(0,0)x_0 = 0. \tag{3.39}$$

Remark 3.20. $\mathcal{F}_x^{(j)}(0,0)(x_0)^j$ means the value of the j-th Fréchet derivative of the map $x \to \mathcal{F}(0,x)$ at $(0,0)$ evaluated at the j-tuple each of whose entries is x_0.

The global version of Theorem 3.17 reads.

Theorem 3.21 ([113]). *Suppose $\mathcal{L} \in \mathcal{C}^1(\mathbb{R}, \mathrm{Fred}_0(U,V))$ and $\lambda_0 \in \mathbb{R}$ is a simple eigenvalue of $\mathcal{L}$, that is*

$$\mathrm{N}[\mathcal{L}(\lambda_0)] = \mathrm{span}[\phi_0], \tag{3.40}$$

and satisfies the following transversality condition

$$\mathcal{L}'(\lambda_0)\phi_0 \notin \mathrm{R}[\mathcal{L}(\lambda_0)]. \tag{3.41}$$

Then, for every continuous function $\mathcal{F}\colon \mathbb{R} \times U \to V$ satisfying (F1), (F2), and (F3) and $\mathcal{D}_u\mathcal{F}(\cdot,0) = \mathcal{L}(\cdot)$, $(\lambda_0, 0)$ is a bifurcation point to a continuum $\mathfrak{C}$ of non-trivial solutions of $\mathcal{F} = 0$. For any of these $\mathcal{F}$'s, let $\mathfrak{C}$ be the component of the set of non-trivial solutions of $\mathcal{F} = 0$ with $(\lambda_0, 0) \in \mathfrak{C}$. Then either,

1. *$\mathfrak{C}$ is not compact; or*
2. *there is another $\Sigma \ni \lambda_1 \neq \lambda_0$ with $(\lambda_1, 0) \in \mathfrak{C}$.*

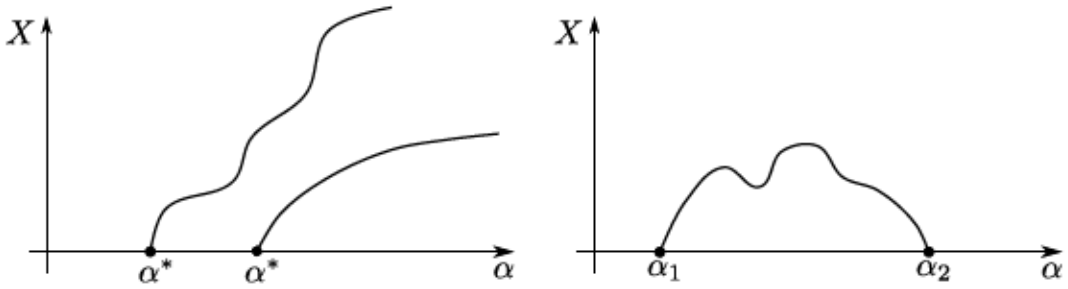

Figure 3.1: Phasespace plot of the two possible alternatives of Theorem 3.21. On the left, the bifurcation branches are unbounded, while on the right, the non-trivial solution branch connects two bifurcation points.

And finally, we have the following unilateral result.

Theorem 3.22 ([113]). *Suppose the injection $U \hookrightarrow V$ is compact, $\mathcal{F}$ satisfies (F1) to (F3), the map*

$$N(\lambda, u) = \mathcal{F}(\lambda, u) - D_u \mathcal{F}(\lambda, 0)u, \qquad (\lambda, u) \in \mathbb{R} \times U \tag{3.42}$$

admits a continuous extension to $\mathbb{R} \times V$, the transversality condition (3.41) *holds, and consider a closed subspace $Y \subset U$ such that*

$$U = \mathrm{N}[\mathcal{L}(\lambda_0)] \oplus Y. \tag{3.43}$$

Let $\mathfrak{C}$ be the component given by Theorem 3.21 and denote by $\mathfrak{C}^+$ and $\mathfrak{C}^-$ the subcomponents of $\mathfrak{C}$ in the directions ϕ_0 and $-\phi_0$ respectively. Then for each $\nu \in \{+, -\}$, $\mathfrak{C}^\nu$ satisfies some of the following alternatives:

1. *$\mathfrak{C}^\nu$ is not compact in $\mathbb{R} \times U$,*
2. *There exists $\lambda_1 \neq \lambda_0$ such that $(\lambda_1, 0) \in \mathfrak{C}^\nu$.*
3. *There exists $(\lambda, y) \in \mathfrak{C}^\nu$ with $y \in Y \setminus \{0\}$.*

In Section 3.5.3, we apply Theorem 3.17 to find local bifurcation branches originating from the trivial steady state solution of the non-local equation (3.10a). In Section 3.5.4, we apply Theorem 3.21 and Theorem 3.22 to obtain a global bifurcation result for the steady states of equation (3.10).

3.3 Mathematical Problem Formulation

In this section, we define the function spaces in which we will look for a solution to equation (3.10a). The search for the appropriate spaces will be guided by the goal of making sure that the Laplacian in equation (3.10a) is invertible.

3.3.1 The Laplace operator with periodic boundary conditions

As we are dealing with functions on S^1_L we implicitly defined periodic boundary conditions. Sometimes it is useful to explicitly use these boundary conditions. For this reason, we define the boundary operator

$$\mathcal{B}[u, u'] \coloneqq (u(0) - u(L), u'(0) - u'(L)), \tag{3.44}$$

which of course has to be equal to zero if we impose periodic boundary conditions.

Definition 3.23. We define the set of test functions

$$\mathcal{C}^\infty_{\text{per}}(0, L) \coloneqq \{\, f \in \mathcal{C}^\infty(0, L) \colon f \text{ is } L \text{ periodic} \,\}. \tag{3.45}$$

Then, for example, $H^1_{\text{per}}(0, L)$ is defined as the completion of $\mathcal{C}^\infty_{\text{per}}(0, L)$ with respect to the H^1 norm.

The abstract formulation in terms of an operator equation will be facilitated by the following operators that we will now define.

Definition 3.24. The averaging operator

$$\mathcal{A} \colon L^p(S^1_L) \to \mathbb{R}, \qquad \mathcal{A}[u] \to \frac{1}{L} \int_0^L u(x) \, \mathrm{d}x. \tag{3.46}$$

It is clear that this operator is continuous and compact.

Definition 3.25. We define the following sub-manifold of $L^2(S^1_L)$

$$L^2_0 \coloneqq \left\{\, u \in L^2(S^1_L) \colon \mathcal{A}[u] = 0 \,\right\}. \tag{3.47}$$

Lemma 3.26. *$L^2_0(S^1_L)$ is closed and hence a Banach space.*

Proof. Note that $L^2_0(S^1_L) = \mathcal{A}^{-1}(0)$, hence it is closed as $\mathcal{A}$ is continuous. Finally, a closed subspace of a Banach space is again a Banach space. □

Lemma 3.27. *The Laplacian operator*

$$\Delta\colon W^{2,2}_{\text{per}}(S^1_L) \to L^2(S^1_L), \qquad \Delta[v] \coloneqq v'', \tag{3.48}$$

is continuous.

Lemma 3.28. *Δ is a Fredholm operator. In particular, we have that*

$$\mathrm{N}[\Delta] = \mathrm{R}[\mathcal{A}] = \left\{ f \in H^2_p(S^1_L)\colon f(x) \equiv c \in \mathbb{R} \right\}, \quad \mathrm{R}[\Delta] = \mathrm{N}[\mathcal{A}] = L^2_0. \tag{3.49}$$

Further, we have that

$$\dim \mathrm{N}[\Delta] = \dim L^2(S^1_L)/\mathrm{R}[\Delta] = 1, \tag{3.50}$$

and thus $\operatorname{ind}\Delta = 0$.

Proof. $u \in H^2_p(S^1_L)$ is an element of $\mathrm{N}[\Delta]$ if and only if it is a solution of

$$\begin{cases} u'' & = 0 \\ \mathcal{B}[u, u'] & = 0 \end{cases}. \tag{3.51}$$

Then, we find that

$$u'(x) = \int_0^x u''(s)\,\mathrm{d}s = 0. \tag{3.52}$$

Hence, $u \equiv c \in \mathbb{R}$. Next suppose that we have $f \in \mathrm{R}[\Delta]$, that is there is $u \in H^2_{\mathcal{B}}$ such that $u'' = f$. Integrating

$$0 = u'(0) - u'(L) = \int_0^L f(s)\,\mathrm{d}s. \tag{3.53}$$

Hence $\mathcal{A}[f] = 0$, and $f \in \mathrm{N}[\mathcal{A}]$. Thus, $\mathrm{R}[\Delta] \subset \mathrm{N}[\mathcal{A}]$. Next suppose that $f \in \mathrm{N}[\mathcal{A}]$. Then, the solution of

$$u'' = f, \tag{3.54}$$

is given by

$$u'(x) = \int_0^x f(s)\,\mathrm{d}s. \tag{3.55}$$

Hence we find that $u'(0) = 0$. Finally, note that $u'(L) = 0$ if and only if $\mathcal{A}[f] = 0$. Thus, we find that $\mathrm{N}[\mathcal{A}] \subset \mathrm{R}[\Delta]$. □

Remark 3.29. Lemma 3.28 shows that $\mathrm{N}[\Delta]$ and $\mathrm{coker}[\Delta] = L^2(S^1_L)/\mathrm{R}[\Delta]$ are finite dimensional. We note that $\mathcal{A}$ can be used as a projection onto both $\mathrm{N}[\Delta]$ and $\mathrm{coker}[\Delta]$.

Lemma 3.30. *The restriction operator* $\Delta_{\mathcal{A}}$

$$\Delta_{\mathcal{A}} \coloneqq \Delta\Big|_{\mathrm{N}[\mathcal{A}]} : \mathrm{N}[\mathcal{A}] \to \mathrm{R}[\Delta], \tag{3.56}$$

is an isomorphism.

Proof. The operator $\Delta_{\mathcal{A}}$ is by definition injective and surjective, and hence by the bounded inverse theorem an isomorphism. □

3.3.2 Estimates for the non-local operator

In this section we discuss the mathematical properties of the non-local operator $\mathcal{K}[u]$ as introduced in Definition 3.1. We begin this section by discussing some common choices for integration kernel $\omega(\cdot)$.

3.3.3 Common choices of functions

For the function $\omega(r)$ there are three commonly used forms (see for instance [136])

(O1) Uniform distribution

$$\omega(r) = \frac{1}{2}. \tag{3.57}$$

(O2) Exponential distribution

$$\omega(r) = \omega_0 \exp\left(-\frac{r}{\xi}\right), \tag{3.58}$$

where ξ is a parameter controlling how quickly $\omega(\cdot)$ goes to zero, and ω_0 is a normalization constant.

(O3) Peak signalling at distance ξ, is given by

$$\omega(r) = \omega_0 \frac{r}{\xi} \exp\left(-\frac{1}{2}\left(\frac{r}{\xi}\right)^2\right), \tag{3.59}$$

where ξ is a parameter controlling how quickly $\omega(\cdot)$ goes to zero, and ω_0 is a normalization constant.

For visual examples of these distributions see Fig. 3.2.

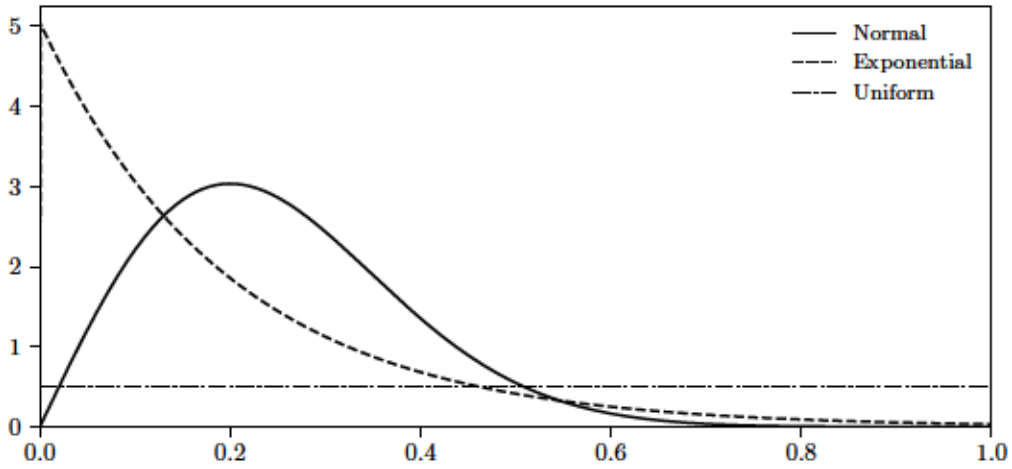

Figure 3.2: The different distributions for $\omega(\cdot)$ with $\xi = 1/4$.

3.3.4 Estimates for the non-local operator

We study the continuity of the function

$$x \to \mathcal{K}[u](x), \tag{3.60}$$

when u is in different function spaces. We start by developing conditions under which the function given in equation (3.60) is continuous.

Lemma 3.31. *Let $u \in \mathcal{C}^0(S^1_L)$ then the function in equation (3.60) is continuous.*

Proof. Let $\epsilon > 0$, let $x_1, x_2 \in S^1_L$ such that $|x_1 - x_2| < \delta$, then consider

$$\begin{aligned} |\mathcal{K}[u](x_1) - \mathcal{K}[u](x_2)| \leq & \int_0^1 |h(u(x_1 + r)) - h(u(x_2 + r))|\omega(r)\,\mathrm{d}r \\ & + \int_0^1 |h(u(x_1 - r)) - h(u(x_2 - r))|\omega(r)\,\mathrm{d}r \\ & \leq C \int_0^1 |u(x_1 + r) - u(x_2 + r)|\omega(r)\,\mathrm{d}r \\ & + C \int_0^1 |u(x_1 - r) - u(x_2 - r)|\omega(r)\,\mathrm{d}r, \end{aligned} \tag{3.61}$$

where in the inequality we used that since $h \in \mathcal{C}^2$ we have that h is Lipschitz continuous. Then $|x_1 \pm r - (x_2 \pm r)| = |x_1 - x_2| < \delta$. Since, by the assumptions of this lemma $u(\cdot)$ is continuous we choose δ sufficiently small such that $|u(x_1 \pm r) - u(x_2 \pm r)| < \epsilon/C$. Finally, using assumption K4 we have that the integral of ω equals $1/2$ and we obtain that,

$$|\mathcal{K}[u](x_1) - \mathcal{K}[u](x_2)| < \epsilon. \tag{3.62}$$

□

Lemma 3.32. *Let $u \in L^p(S^1_L)$ then the function defined in equation (3.60) is continuous.*

Proof. Let $\epsilon > 0$ and let $x_1, x_2 \in S^1_L$ such that $|x_1 - x_2| < \delta$. By the density of $\mathcal{C}^0$ in L^p there is a sequence $(u_n) \subset \mathcal{C}^0$ such that $u_n \to u$ in L^p. This means that $\exists N : \forall n \geq N$ we have that $|u_n - u|_p < \epsilon/3|\omega|_\infty$.

Then, we compute

$$\begin{aligned} |\mathcal{K}[u](x_1) - \mathcal{K}[u](x_2)| \leq & |\mathcal{K}[u](x_2) - \mathcal{K}[u_n](x_2)| + |\mathcal{K}[u_n](x_1) - \mathcal{K}[u](x_1)| + \\ & |\mathcal{K}[u_n](x_2) - \mathcal{K}[u_n](x_1)|. \end{aligned} \tag{3.63}$$

The first two terms are treated equivalently. Let $n > N$, and $i = 1, 2$, then

$$\begin{aligned}
|\mathcal{K}[u](x_i) - \mathcal{K}[u_n](x_i)| &\leq \int_0^1 |h(u(x_i + r)) - h(u_n(x_i + r))|\omega(r)\,\mathrm{d}r \\
&\quad + \int_0^1 |h(u(x_i - r)) - h(u_n(x_i - r))|\omega(r)\,\mathrm{d}r \\
&\leq C \int_0^1 |u(x_i + r) - u_n(x_i + r)|\omega(r)\,\mathrm{d}r \\
&\quad + C \int_0^1 |u(x_i - r) - u_n(x_i - r)|\omega(r)\,\mathrm{d}r \\
&\leq \left(\int_0^L |u(x) - u_n(x)|^p \,\mathrm{d}x \right)^{1/p} \left(\int_0^1 \omega^q(r)\,\mathrm{d}r \right)^{1/q} \\
&\leq |u - u_n|_p |\omega|_\infty < {}^{\epsilon}/_{3}.
\end{aligned} \tag{3.64}$$

The last term can be estimated by Lemma 3.31 such that we have

$$|\mathcal{K}[u_n](x_2) - \mathcal{K}[u_n](x_1)| < {}^{\epsilon}/_{3}. \tag{3.65}$$

Putting everything together, we obtain

$$|\mathcal{K}[u](x_1) - \mathcal{K}[u](x_2)| < \epsilon. \tag{3.66}$$

□

Lemma 3.33 (Non-local Regularity). *Let $p \geq 1$ and $u \in L^p(S^1_L)$. Then the non-local function $\mathcal{K}[u]$ defined in equation (3.60) is in $L^p(S^1_L)$. In particular, the following estimate holds*

$$|\mathcal{K}[u]|_{p,D} < |h(u)|_p, \tag{3.67}$$

and if we use assumption H1, then obtain

$$|\mathcal{K}[u]|_{p,D} < C \left(|u|_p + L \right). \tag{3.68}$$

Proof. By applying Theorem B.1 to equation (3.3), we obtain

$$\begin{aligned}|\mathcal{K}[u](x)|_p &= \left|\int_{-1}^{1} h(u(x+r,t))\Omega(r)\,\mathrm{d}r\right|_p \leq \int_{-1}^{1} |h(u(x+r,t))\Omega(r)|_p\,\mathrm{d}r \\ &= \int_{-1}^{1}\left\{\int_0^L |h(u(x+r,t))|^p\,\mathrm{d}x\right\}^{1/p} |\Omega(r)|\,\mathrm{d}r \leq |h(u)|_p \\ &\leq C\left(|u|_p + L\right).\end{aligned} \tag{3.69}$$

Note that due to assumption K4 we have that $|\Omega|_1 = 1$. □

Next we extend this result to Sobolev spaces.

Lemma 3.34 (Non-local Regularity). *Let $p \geq 1$, and $u \in W^{1,p}(S_L^1)$. Then $\mathcal{K}[u] \in W^{1,p}(S_L^1)$.*

Proof. The first derivative with respect to x of the function defined in equation (3.60) is given by

$$(\mathcal{K}[u](x))' = \int_{-1}^{1} h'(u(x+r))u'(x+r)\Omega(r)\,\mathrm{d}r. \tag{3.70}$$

Its L^p norm can be estimated using equation (3.67) from Lemma 3.33, we then compute

$$\begin{aligned}\|\mathcal{K}[u]\|_{1,p} &= \left(|\mathcal{K}[u]|_p^p + |(\mathcal{K}[u])'|_p^p\right)^{1/p} \leq \left(C^p\left(|u|_p + L\right)^p + |h'(u)u'|_p^p\right)^{1/p} \\ &\leq \left(2^p C^p\left(L^p + |u|_p^p\right) + |h'|_{\mathcal{C}^0}^p |u'|_p^p\right)^{1/p} \\ &\leq 2C|h'|_{\mathcal{C}^0}\left(L^p + |u|_p^p + |u'|_p^p\right)^{1/p}.\end{aligned} \tag{3.71}$$

Then using that $u \in W^{1,p}(S_L^1)$ and assumption H1 all the terms on the right hand side are bounded. □

For the following result we need one higher order of differentiability than obtained in Lemma 3.34.

Lemma 3.35 (Non-local Regularity). *Let $p \geq 1$, and $u \in W^{2,p}(S_L^1)$. Then $\mathcal{K}[u] \in W^{2,p}(S_L^1)$.*

Proof. The second derivative with respect to x of the function defined in equation (3.60) is given by

$$(\mathcal{K}[u](x))'' = \int_{-1}^{1} \left(h'(u(x+r))u''(x+r) + h''(u(x+r))\left(u'(x+r)\right)^2 \right) \Omega(r)\,\mathrm{d}r. \tag{3.72}$$

Its L^p norm can be estimated using equation (3.67) from Lemma 3.33, we then compute

$$\begin{aligned} |\mathcal{K}[u]''|_p &\leq |h'(u)u''|_p + |h''(u)\left(u'\right)^2|_p \\ &\leq |h'|_{\mathcal{C}^0}|u''|_p + |h''|_{\mathcal{C}^0}|u'|_p^2. \end{aligned} \tag{3.73}$$

Then using that $u \in W^{2,p}(S_L^1)$ and assumption H1 all the terms on the right hand side are bounded. Combining this result with the result of Lemma 3.34 we obtain the required result. □

Lemma 3.36. *Let $p \geq 1$, then the map $\mathcal{K}\colon L^p(S_L^1) \to L^p(S_L^1)$ defined in equation (3.3) is $\mathcal{C}^1(L^p(S_L^1), L^p(S_L^1))$, and its Fréchet derivative is given by,*

$$\mathcal{D}_u\left(\mathcal{K}[u(x)]\right)[w(x)](x) = \int_{-1}^{1} h'(u(x+r))w(x+r)\Omega(r)\,\mathrm{d}r. \tag{3.74}$$

Proof. Let's compute

$$\begin{aligned} \mathcal{D}_u\left(\mathcal{K}[u]\right)[w](x) &= \frac{\mathrm{d}}{\mathrm{d}\epsilon}\Big|_{\epsilon=0} \int_{-1}^{1} h(u+\epsilon w)(x+r)\Omega(r)\,\mathrm{d}r \\ &= \int_{-1}^{1} h'(u(x+r))w(x+r)\Omega(r)\,\mathrm{d}r. \end{aligned} \tag{3.75}$$

Then to show that $\mathcal{K}$ is $\mathcal{C}^1$, it suffices to show that the map

$$\begin{aligned} \mathcal{D}_u\mathcal{K}\colon L^p(S_L^1) &\to \mathfrak{L}(L^p(S_L^1), L^p(S_L^1)) \\ u &\to \mathcal{D}_u\left(\mathcal{K}[u]\right)[w], \end{aligned} \tag{3.76}$$

is continuous. Meaning, that we have to show that the operator norm of $\mathcal{D}_u\mathcal{K}$

is bounded. From Lemma 3.33, we have

$$|\mathcal{D}_u\left(\mathcal{K}[u]\right)[w]|_p \leq C\left(|h'|_{C^0}|w|_p + L\right). \tag{3.77}$$

Hence

$$\|\mathcal{D}_u\left(\mathcal{K}[u]\right)[w]\|_{\text{op}} = \sup_{|w|_p=1} |\mathcal{D}_u\left(\mathcal{K}[u]\right)[w]|_p \leq C\left(|h'|_{C^0} + L\right). \tag{3.78}$$

This gives us what was to be proven. □

Lemma 3.37. *Let $u \in \mathcal{C}^2(S^1_L)$ then the function defined in equation* (3.60) *is also in $\mathcal{C}^2(S^1_L)$.*

Proof. Let's compute

$$\begin{aligned}|(\mathcal{K}[u])''| &\leq \int_{-1}^{1} \left[\, |h''(u(x+r))\left(u'(x+r)\right)^2| + |h'(u(x+r))u''(x+r)| \,\right] |\Omega(r)|\,\mathrm{d}r \\ &\leq |h''|_{C^0}|u'|^2_{C^0} + |h'||u''|_{C^0},\end{aligned} \tag{3.79}$$

where we used assumption K4 for $|\Omega|_1 = 1$. Finally, all the terms on the right hand side are bounded by $u \in \mathcal{C}^2(S^1_L)$ and assumption (H1). □

The following lemma will later be used to derive an a priori bound for positive solutions of equation (3.10a).

Lemma 3.38. *Let the operator $\mathcal{K}[u](x)$ be defined as in equation* (3.3)*, and suppose that $u \in L^p(S^1_L)$ such that $u(x) \geq 0$ (this means that $|u|_1 = \mathcal{A}[u] < \infty$). Then, we find that*

$$|\mathcal{K}[u](x)| \leq C|\omega|_\infty\left(\mathcal{A}[u] + L\right). \tag{3.80}$$

Proof. Let $u \in L^p(S^1_L)$ such that $\mathcal{A}[u] < \infty$ and $u(x) \geq 0$. Then, we compute

$$\begin{aligned}\mathcal{K}[u](x) &= \int_{-1}^{1} h(u(x+r))\Omega(r)\,\mathrm{d}r \\ &= \int_0^1 h(u(x+r))\omega(r)\,\mathrm{d}r - \int_{-1}^{0} h(u(x+r))\omega(r)\,\mathrm{d}r.\end{aligned} \tag{3.81}$$

It is easy to see that both integrals on the right hand side are non-negative as $h(u(x)) \geq 0$ whenever $u(x) \geq 0$ (assumption H2) and $\omega(r) \geq 0$. Using assumption H3, it follows that

$$\mathcal{K}[u](x) \leq \int_0^1 h(u(x+r))\omega(r)\,\mathrm{d}r \leq C|\omega|_\infty \left(\mathcal{A}[u] + L\right). \tag{3.82}$$

In the same spirit, we find for

$$\mathcal{K}[u](x) \geq -\int_{-1}^0 h(u(x+r))\omega(r)\,\mathrm{d}r \geq -C|\omega|_\infty \left(\mathcal{A}[u] + L\right). \tag{3.83}$$

□

3.3.5 Continuity and equicontinuity of the non-local operator

The goal in this section is to establish equi-continuity of the non-local operator when applied to bounded subsets of $L^p(S_L^1)$. This will then be used to show compactness of the non-local operator.

Lemma 3.39. *Let the family of bounded functions in $L^p(S_L^1)$ be given by*

$$B_K := \left\{ u \in L^p(S_L^1) \colon |u|_p \leq K \right\}. \tag{3.84}$$

Then $\mathcal{K}[B_K]$ is uniformly equicontinuous.

Proof. For the following, we introduce the function

$$\tilde{\omega}(r) = \begin{cases} \omega(r) & \text{if } r \in [0,1] \\ 0 & \text{else} \end{cases}. \tag{3.85}$$

Let $\epsilon > 0$, choose $\delta < \frac{\epsilon}{4C(L+K)L^{1/q}|\omega|_\infty}$, and let $x_1, x_2 \in S_L^1$ such that $|x_1 - x_2| < \delta$.

Then consider

$$\begin{aligned}\mathcal{K}[u](x_2) - \mathcal{K}[u](x_1) = &\int_0^1 \left[\, h(u(x_2 + r)) - h(u(x_1 + r)) \,\right] \omega(r)\, \mathrm{d}r \\ &- \int_0^1 \left[\, h(u(x_1 - r)) - h(u(x_2 - r)) \,\right] \omega(r)\, \mathrm{d}r.\end{aligned} \tag{3.86}$$

We denote each of the terms by I through IV.

$$\begin{aligned}\mathrm{I} &= \int_0^1 h(u(x_2 + r))\omega(r)\,\mathrm{d}r = \int_{x_2}^{x_2+1} h(u(y))\omega(y - x_2)\,\mathrm{d}y \le \int_0^L h(u(y))\tilde{\omega}(y - x_2)\,\mathrm{d}y, \\ \mathrm{II} &= \int_0^1 h(u(x_1 + r))\omega(r)\,\mathrm{d}r = \int_{x_1}^{x_1+1} h(u(y))\omega(y - x_1)\,\mathrm{d}y \le \int_0^L h(u(y))\tilde{\omega}(y - x_1)\,\mathrm{d}y, \\ \mathrm{III} &= \int_0^1 h(u(x_1 - r))\omega(r)\,\mathrm{d}r = \int_{x_1-1}^{x_1} h(u(y))\omega(x_1 - y)\,\mathrm{d}y \le \int_0^L h(u(y))\tilde{\omega}(x_1 - y)\,\mathrm{d}y, \\ \mathrm{IV} &= \int_0^1 h(u(x_2 - r))\omega(r)\,\mathrm{d}r = \int_{x_2-1}^{x_2} h(u(y))\omega(x_2 - y)\,\mathrm{d}y \le \int_0^L h(u(y))\tilde{\omega}(x_2 - y)\,\mathrm{d}y.\end{aligned}$$

Then, we compute

$$\begin{aligned}\mathrm{I} - \mathrm{II} &= \int_0^L h(u(y)) \left[\, \tilde{\omega}(y - x_2) - \tilde{\omega}(y - x_1) \,\right] \mathrm{d}y \\ &\le C(L + |u|_p) \left(\int_0^L |\tilde{\omega}(y - x_2) - \tilde{\omega}(y - x_1)|^q \,\mathrm{d}y \right)^{1/q}, \\ \mathrm{III} - \mathrm{IV} &= \int_0^L h(u(y)) \left[\, \tilde{\omega}(x_1 - y) - \tilde{\omega}(x_2 - y) \,\right] \mathrm{d}y \\ &\le C(L + |u|_p) \left(\int_0^L |\tilde{\omega}(x_1 - y) - \tilde{\omega}(x_2 - y)|^q \,\mathrm{d}y \right)^{1/q}.\end{aligned}$$

Then for any $y \in S^1_L$ we have that $|x_1 - y - (x_2 - y)| < \delta$ (see Fig. 3.3), and so we find that

$$\left(\int_0^L |\tilde{\omega}(x_1 - y) - \tilde{\omega}(x_2 - y)|^q \right)^{1/q} < 2\delta |\omega|_\infty. \tag{3.87}$$

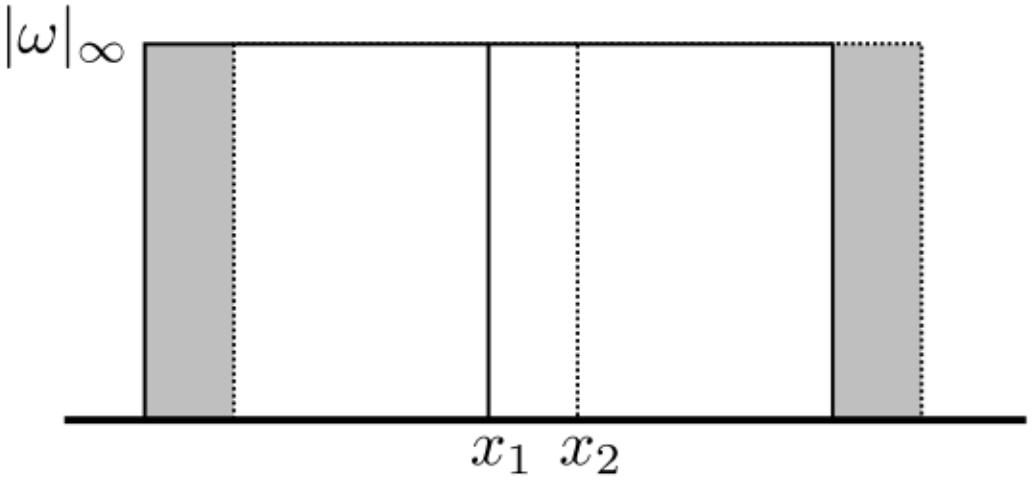

Figure 3.3: Two sensing domains $E(x_1)$ and $E(x_2)$ centred at x_1 and x_2 respectively. This is the situation estimated in equation (3.87). The area contributing to the infinity norm of $\bar{\omega}$ is shaded in grey. Note that the grey area is $E(x_1) \triangle E(x_2)$.

Then using this estimate in equation (3.86), we find that

$$|\mathcal{K}[u](x_2) - \mathcal{K}[u](x_1)| < \epsilon, \tag{3.88}$$

for all $u \in B_K$. □

3.3.6 Compactness of the non-local operator

In this section we continue to study the functions generated by the non-local operator. From Lemma 3.33 we know that $\mathcal{K}[u]$ maps $L^2(S^1_L)$ into $L^2(S^1_L)$.

Lemma 3.40. *Let $\mathcal{K}[u]$ be as defined in equation (3.3) then $\mathcal{K} \in \mathfrak{L}(L^2)$.*

Proof. Follows from Lemma 3.33. □

Lemma 3.41. *The function defined in equation (3.3) is uniformly bounded for $u \in B_K$ (set of bounded functions with norm less than K).*

Proof. Let $u \in B_K$, then

$$\begin{aligned}|\mathcal{K}[u](x)| &\leq \int_0^1 |h(u(x+r)) - h(u(x-r))|\omega(r)\,\mathrm{d}r \\ &\leq \left(\int_0^1 |h(u(x+r)) - h(u(x-r))|^2\,\mathrm{d}r\right)^{1/2} \left(\int_0^1 \omega^2(r)\,\mathrm{d}r\right)^{1/2} \\ &\leq C|u|_2|\omega|_\infty \leq CK|\omega|_\infty.\end{aligned} \tag{3.89}$$

Note that because $u(x+r)$ and $u(x-r)$ do not overlap that integral is bounded by the 2-norm of u. □

Lemma 3.42. *Let $u \in B(L^p)$ (the unit ball of L^p), then $\forall \epsilon > 0, \exists \delta > 0$ such that for $y \in \mathbb{R}$ such that $|y| < \delta$, we have that*

$$\int_0^L |\mathcal{K}[u](x+y) - \mathcal{K}[u](x)|^p\,\mathrm{d}x < \epsilon^p. \tag{3.90}$$

Proof. Let $\epsilon > 0$, by Lemma 3.39 we have that for $x_1, x_2 \in S_L^1$ such that $|x_1 - x_2| < \delta$, and $\forall u \in B(L^p)$ we have that $|\mathcal{K}[u](x_1) - \mathcal{K}[u](x_2)| < \epsilon/L^{1/p}$. From this observation, we easily obtain the required result. □

Lemma 3.43. *The set $\mathcal{K}[B(L^p)]$ is totally bounded.*

Proof. This follows from Theorem B.5, with all the requirements given by Lemma 3.42 and Lemma 3.41. □

Theorem 3.44 (Compactness non-local operator)**.** *The operator $\mathcal{K}\colon L^2(S_L^1) \to L^2(S_L^1)$ is compact.*

Proof. In Lemma 3.43 we have shown that $\mathcal{K}[B(L^2)]$ is totally bounded subset of the complete metric space $L^2(S_L^1)$, hence it is relatively compact. Thus, $\overline{\mathcal{K}[B(L^2)]}$ is compact in $L^2(S_L^1)$ and $\mathcal{K}$ is a compact operator. □

Remark 3.45. This has far reaching consequences, namely it means that $\mathcal{K}[u]$ can never be invertible, as otherwise $\mathcal{I} = \mathcal{K}^{-1}\mathcal{K}$ would be compact. Further a compact operator can never be surjective, and the closed subspaces of its range must be finite dimensional.

3.3.7 Spectral properties of the non-local operators

In this section, we study the spectral properties of the linear non-local operator, that is with $h(u) = u$. That is

$$\mathcal{K}[u] = \int_{-1}^{1} u(x+r)\Omega(r)\,\mathrm{d}r. \tag{3.91}$$

The results of this section will be used in Section 3.5 to study the properties of the linearization of equation (3.10a).

Lemma 3.46. *The operator $\mathcal{K}\colon L^2(S^1_L) \to L^2(S^1_L)$, defined in equation (3.91) is skew-adjoint (that is $\mathcal{K}^* = -\mathcal{K}$).*

Proof. We compute, let $y, t \in L^2(S^1_L)$ (the brackets denote the $L^2(S^1_L)$ inner product)

$$\begin{aligned}(\mathcal{K}[y], z) &= \int_0^L \int_0^1 \left[\, y(x+r) - y(x-r) \,\right] \omega(r)\,\mathrm{d}r\, z(x)\,\mathrm{d}x \\ &= \int_0^1 \int_0^L \left[\, y(x+r) - y(x-r) \,\right] \omega(r) z(x)\,\mathrm{d}x\,\mathrm{d}r.\end{aligned} \tag{3.92}$$

Then applying the change of variable $\chi = x+r$ for the first term, and $\chi = x-r$ for the second term, and using the periodicity of the domain, we obtain after applying Fubini

$$\begin{aligned}(\mathcal{K}[y], z) &= \int_0^L \int_0^1 \left[\, z(\chi - r) - z(\chi + r) \,\right] \omega(r)\,\mathrm{d}r\, y(\chi)\,\mathrm{d}\chi \\ &= (y, \mathcal{K}^*[z]) = (y, -\mathcal{K}[z])\,.\end{aligned} \tag{3.93}$$

Hence we find that $\mathcal{K}^* = -\mathcal{K}$. □

Lemma 3.47. *Let H be a Hilbert space. Let $\mathcal{L} \in \mathfrak{L}(H)$ such that $\mathcal{L}^* = -\mathcal{L}$. Then the quantity $(\mathcal{L}(x), x)$ is purely imaginary and $\mathcal{L}$ has purely imaginary eigenvalues.*

Proof. Let $x \in H$, (the brackets denote the H inner product) then

$$(\mathcal{L}(x), x) = (x, \mathcal{L}^*(x)) = (x, -\mathcal{L}(x)) = -\overline{(\mathcal{L}(x), x)}. \tag{3.94}$$

Then if λ is an eigenvalue of $\mathcal{L}$ with eigenvector x, we find that

$$\lambda = \frac{(\mathcal{L}(x), x)}{(x, x)}. \tag{3.95}$$

Hence, all eigenvalues are purely imaginary. □

Remark 3.48. Note that since any skew-adjoint operator is normal, we have that $\mathcal{K}$ is a normal operator. Thus we have that $\mathcal{K}$ is a compact and normal operator on $L^2(S^1_L)$. This means that it is also a compact, and normal operator on the canonical complexification of $L^2(S^1_L)$ ($H = L^2 + iL^2$) and hence we can apply a spectral theorem [56 Theorem 7.53] to obtain an orthonormal basis of H over which the operator $\mathcal{K}$ is diagonalizable.

Eigenvalue and eigenfunctions of the linear non-local operator

Next we study how the linear non-local operator (3.91) acts on the eigenfunctions of the Laplacian. For this the following integral identities will become useful.

Lemma 3.49. *Let Ω satisfy (K1), (K3) and (K4), then*

$$\int_{-1}^{1} \cos\left(\frac{2\pi n r}{L}\right) \Omega(r)\, \mathrm{d}r = 0, \tag{3.96}$$

and

$$\int_{-1}^{1} \sin\left(\frac{2\pi n r}{L}\right) \Omega(r)\, \mathrm{d}r = 2\int_{0}^{1} \sin\left(\frac{2\pi n r}{L}\right) \omega(r)\, \mathrm{d}r. \tag{3.97}$$

Proof. Both identities follow by integration and the properties of Ω listed in Definition 3.1. □

Lemma 3.50. *The linear non-local operator is bounded.*

Proof. We compute, using Lemma 3.33

$$|\mathcal{K}[u]|_p \leq |u|_p. \tag{3.98}$$

Thus, we find that

$$\|K\| \leq 1. \tag{3.99}$$

□

Lemma 3.51. *Let the non-local operator $\mathcal{K}$ as defined in equation* (3.91)*. Then*

$$\mathcal{K}[1](x) = 0, \tag{3.100}$$

$$\mathcal{K}\left[\sin\left(\frac{2\pi nx}{L}\right)\right](x) = 2M_n(\omega)\cos\left(\frac{2\pi nx}{L}\right), \tag{3.101}$$

$$\mathcal{K}\left[\cos\left(\frac{2\pi nx}{L}\right)\right](x) = -2M_n(\omega)\sin\left(\frac{2\pi nx}{L}\right), \tag{3.102}$$

where

$$M_n(\omega) = \int_0^1 \sin\left(\frac{2\pi nr}{L}\right)\omega(r)\,\mathrm{d}r. \tag{3.103}$$

Proof. Apply the double angle formulas and the integral identities from Lemma 3.49.

□

Remark 3.52. Note that it is easy to see from Lemma 3.51 that the non-local operator $\mathcal{K}[u]$ removes mass, that is $\mathcal{A}[\mathcal{K}[u]] = 0$ always ($\mathcal{A}$ was defined in (3.24)). Hence, for example if $\mathcal{K}\colon L^2(S^1_L) \to L^2(S^1_L)$, then we conclude that $\mathrm{R}[\mathcal{K}] = L^2_0$.

If instead we consider the canonical complexification of $L^2(S^1_L)$ we obtain the following result.

Lemma 3.53. *Let the non-local operator $\mathcal{K}$ as defined in equation* (3.91)*. Then*

$$\mathcal{K}[1](x) = 0, \tag{3.104}$$

$$\mathcal{K}\left[\exp\left(\frac{2\pi nix}{L}\right)\right](x) = 2iM_n(\omega)\exp\left(\frac{2\pi nix}{L}\right). \tag{3.105}$$

Remark 3.54. For the sake of comparison, the eigenvalues corresponding to $\exp\left(\frac{2\pi nix}{L}\right)$ of the derivative operator are,

$$\lambda_n = \frac{2\pi in}{L}. \tag{3.106}$$

Eigenvalues and eigenfunctions of non-local curvature

In this section, we continue to study the functions generated by the linear non-local operator. From Lemma 3.34, we know that $\mathcal{K}[u]'$ maps $H^1(S^1_L)$ into

$H^1(S^1_L)$. Here we study the operator, which we will refer to as the linear non-local curvature,

$$\mathcal{K}[u]' : x \to \left(\int_{-1}^{1} u(x+r)\Omega(r)\,\mathrm{d}r \right)', \tag{3.107}$$

where $(\cdot)'$ denotes the spatial derivative with respect to x. Note that using the properties of Ω, this function can be rewritten as

$$(\mathcal{K}[u])' : x \to \int_{0}^{1} \left(u'(x+r) + u'(x-r)\right)\omega(r)\,\mathrm{d}r. \tag{3.108}$$

Lemma 3.55. *The operator $(\mathcal{K})'$ given above is self-adjoint.*

Proof. Let $y, z \in L^2(S^1_L)$, we then compute using integration by parts and using Lemma 3.46, to obtain

$$\left((\mathcal{K}[y])', z\right) = -\left(\mathcal{K}[y], z'\right) = \left(y, \mathcal{K}[z']\right) = \left(y, (\mathcal{K}[z])'\right). \tag{3.109}$$

□

Lemma 3.56. *Let v_n be an eigenfunction of,*

$$\begin{cases} -v_n'' = \lambda_n v_n, & \text{in } [0, L] \\ \mathcal{B}[v_n, v_n'] = 0. \end{cases} \tag{3.110}$$

The solutions to this problem are given in Lemma B.12. Then the operator $(\mathcal{K})'$ from equation (3.107) has the same set of eigenfunctions satisfying

$$K[v_n]' = \mu_n v_n, \tag{3.111}$$

where

$$\mu_n = -\frac{4\pi n}{L} M_n(\omega), \tag{3.112}$$

where $M_n(\omega)$ is defined in equation (3.103).

Proof. For $n = 0$ we have that $v_0 \sim 1$, then trivially $\mathcal{K}[1] = 0$ and hence $\mu_0 = 0$.

Next consider, $v_n = \sin\left(\frac{2\pi nx}{L}\right)$ then

$$\mathcal{K}[v_n]' = \int_{-1}^{1} \left(\sin\left(\frac{2\pi n(x+r)}{L}\right)\right)' \Omega(r)\,\mathrm{d}r. \tag{3.113}$$

Using both the integral identities from Lemma 3.49, we obtain

$$\mathcal{K}[v_n]' = -\frac{4\pi n}{L}\sin\left(\frac{2\pi nx}{L}\right) M_n(\omega). \tag{3.114}$$

Finally, consider $v_n = \cos\left(\frac{2\pi nx}{L}\right)$, then

$$\mathcal{K}[v_n]' = \int_{-1}^{1} \left(\cos\left(\frac{2\pi n(x+r)}{L}\right)\right)' \Omega(r)\,\mathrm{d}r. \tag{3.115}$$

Once again using the identities in Lemma 3.49, we obtain

$$\mathcal{K}[v_n]' = -\frac{4\pi n}{L}\cos\left(\frac{2\pi nx}{L}\right) M_n(\omega). \tag{3.116}$$

□

Asymptotic behaviour of the non-local eigenvalues

From the definition of $M_n(\omega)$ in equation (3.103) we easily see that $|M_n(\omega)| < {}^1\!/_2$. Here, we want to understand in more detail how $M_n(\omega)$ behaves as $n \to \infty$. For this reason, we introduce the following common definition from Fourier analysis (see for instance [179 Chapter II]).

Definition 3.57. The integral *modulus of continuity* is defined for periodic $f \in L^p(S^1_L)$, $p \geq 1$ by

$$m_p(\delta) = \sup_{0\leq h\leq \delta}\left\{\frac{1}{L}\int_0^L |f(x+h) - f(x)|^p\,\mathrm{d}x\right\}^{1/p}. \tag{3.117}$$

It is obvious that as $\delta \to 0$ we have that $m_p(\delta) \to 0$.

Lemma 3.58. *Let $\omega(r)$ satisfy (K1), (K3), and (K4), then (from equation (3.103))*

$$M_n(\omega) = \int_0^1 \sin\left(\frac{2\pi n r}{L}\right) \omega(r)\, \mathrm{d}r. \tag{3.118}$$

Then, we have that

$$|M_n(\omega)| \leq \frac{L}{2} m_1\left(\frac{L}{2n}\right). \tag{3.119}$$

Proof. First we extend $\omega(r)$ to the whole of $[0, L]$ by defining

$$\tilde{\omega}(r) = \begin{cases} \omega(r) & \text{if } r \leq 1 \\ 0 & \text{otherwise} \end{cases}. \tag{3.120}$$

Then we use an common technique from Fourier theory, (see for instance [179 Chapter II])

$$M_n(\omega) = \int_0^L \sin\left(\frac{2\pi n r}{L}\right) \tilde{\omega}(r)\, \mathrm{d}r = -\int_0^L \sin\left(\frac{2\pi n r}{L}\right) \tilde{\omega}(x + L/2n)\, \mathrm{d}r. \tag{3.121}$$

Taking the average of both integrals, we obtain

$$M_n(\omega) = \frac{1}{2}\int_0^L (\tilde{\omega}(r) - \tilde{\omega}(r + L/2n)) \sin\left(\frac{2\pi n r}{L}\right) \mathrm{d}r. \tag{3.122}$$

Hence, we obtain the conclusion. □

Example 3.59. *Suppose that ω is chosen to be the uniform function i.e. O1 (see Section 3.3.3). Then we can compute $M_n(\omega)$ and find that*

$$M_n(\omega) = \frac{L}{2\pi n} \sin^2\left(\frac{\pi n}{L}\right). \tag{3.123}$$

Hence, $M_n(\omega) \to 0$ as $n \to \infty$, and thus so do the eigenvalues of $\mathcal{K}$ from equation (3.91) *see Lemma 3.51 (since $\mathcal{K}$ is compact this is expected as the only possible accumulation point of the eigenvalues is zero). But the eigenvalues of the non-local curvature* (3.107) *are given by (see Lemma 3.56)*

$$\mu_n = -\frac{4\pi n}{L} M_n(\omega) = -2\sin^2\left(\frac{\pi n}{L}\right). \tag{3.124}$$

Thus, the eigenvalues of the non-local curvature keep oscillating in $(-2, 0)$.

Example 3.60. *Suppose that ω is chosen to be the exponential function i.e. O2. Then we can compute the modulus of continuity by*

$$m_1(\delta) = \left(1 - e^{-\delta}\right) \frac{1 - e^{-L}}{L}. \tag{3.125}$$

Hence, we obtain that

$$|M_n(\omega)| \leq \left(1 - e^{-L/2n}\right) \frac{1 - e^{-L}}{2}. \tag{3.126}$$

Note that for the case of exponential ω it is also possible to find an exact expression for $M_n(\omega)$. Then the eigenvalue of the non-local curvature (3.107) *is given by*

$$|\mu_n| \leq \frac{4\pi n}{L} \left| \left(1 - e^{-L/2n}\right) \frac{1 - e^{-L}}{2} \right|. \tag{3.127}$$

Thus, we find that

$$|\mu_n| \to \pi \left(1 - e^{-L}\right), \text{ as } n \to \infty. \tag{3.128}$$

3.3.8 The non-local operator generalizing the classical derivative

We will explore in what way the linear non-local term $\mathcal{K}$ from equation (3.91) is related to the classical derivative. In particular, we study what happens when the sensing radius R converges to zero. For this section only we consider the R-non-local operator $\mathcal{K}_R$ having a sensing radius $\mathbb{R} \ni R > 0$ instead of 1. That is,

$$\mathcal{K}_R[u] \coloneqq \int_{-R}^{R} u(x + r)\tilde{\Omega}(r)\, \mathrm{d}r, \tag{3.129}$$

where $\tilde{\Omega}$ is defined by

$$\tilde{\Omega} = \frac{r}{|r|}\tilde{\omega}(r), \tag{3.130}$$

where

$$\tilde{\omega}(r) = \frac{\omega(r/R)}{R}. \tag{3.131}$$

With the aim of producing an asymptotic expansion of $\mathcal{K}[\cdot]$ as $R \to 0$, we compute the moments of the distribution $\tilde{\omega}$

$$\begin{aligned}\tilde{\mu}_n = \langle r^n, \tilde{\omega} \rangle &= \int_{-R}^{R} r^n \tilde{\omega}(r)\,\mathrm{d}r \\ &= \int_{-1}^{1} (tR)^n\, \omega(r)\,\mathrm{d}t \\ &= \begin{cases} 0 & \text{if } n \text{ odd} \\ 2R^n \int_0^1 t^n \omega(t)\,\mathrm{d}t & \text{if } n \text{ even} \end{cases}.\end{aligned} \tag{3.132}$$

In other words, we obtain that

$$\tilde{\mu}_n = \begin{cases} 0 & \text{if } n \text{ odd} \\ R^n \mu_n & \text{if } n \text{ even} \end{cases}. \tag{3.133}$$

where μ_n is the n-th moment of ω. Note however, that in the non-local gradient we are dealing with Ω, its moments are defined similarly. We compute

$$\begin{aligned}\mu_n = \langle r^n, \Omega \rangle &= \int_{-R}^{R} r^n \frac{r}{|r|} \tilde{\omega}(r)\,\mathrm{d}r = \int_{-1}^{1} (tR)^n \frac{tR}{|tR|} \omega(t)\,\mathrm{d}t \\ &= R^n \int_0^1 t^n \omega(t)\,\mathrm{d}t - R^n \int_{-1}^{0} t^n \omega(t)\,\mathrm{d}t \\ &= R^n \int_0^1 t^n \omega(t)\,\mathrm{d}t + (-1)^{n+1} R^n \int_0^1 t^n \omega(t)\,\mathrm{d}t \\ &= \begin{cases} 0 & \text{if } n \text{ even} \\ 2R^n \int_0^1 t^n \omega(t)\,\mathrm{d}t & \text{if } n \text{ odd} \end{cases}.\end{aligned} \tag{3.134}$$

Note that we can use a distribution moment expansion for the compactly supported Ω. Hence, we obtain

$$\Omega(r) = \frac{r/R}{|r/R|} \frac{\omega(r/R)}{R} = \sum_{n=0}^{\infty} \frac{(-1)^n \mu_n \delta^{(n)}(r)}{n!} R^n. \tag{3.135}$$

Using the previous equation, in the non-local term $\mathcal{K}_R[u]$ we obtain

$$\begin{aligned}\mathcal{K}_R[u](x) &= \int_{-R}^{R} u(x+r)\left[\sum_{n=0}^{\infty}\frac{(-1)^n\mu_n\delta^{(n)}(r)}{n!}R^n\right]\mathrm{d}r \\ &\approx \mu_1 R u'(x) + \mu_3\frac{R^3}{6}u'''(x) + \mathcal{O}(R^5).\end{aligned} \tag{3.136}$$

If we divide the non-local operator from equation (3.129) by $\mu_1 R$, i.e., consider the operator

$$\mathcal{K}_R[u](x) = \frac{1}{\mu_1 R}\int_{-R}^{R} u(x+r)\Omega(r)\,\mathrm{d}r, \tag{3.137}$$

then we have that $\mathcal{K}_R \to u'$ as $R \to 0$. In that sense, the non-local operator $\mathcal{K}_R[u]$ is a generalization of the classical local derivative. We can obtain a similar asymptotic expansion for the non-local curvature (i.e., the derivative of $\mathcal{K}_R[u]$ as $R \to 0$)

$$\mathcal{K}_R[u](x)' \approx u''(x) + \mathcal{O}(R^4). \tag{3.138}$$

Thus in the same sense as $\mathcal{K}_R[u]$ is a generalization of the classical derivative, this makes $\mathcal{K}_R[u]'$ a generalization of the classical Laplacian.

Example 3.61. *Suppose that*

$$\omega(r) = \begin{cases}\frac{1}{2R} & \text{if } r \in [-R, R] \\ 0 & \text{otherwise.}\end{cases} \tag{3.139}$$

Then the moment of ω (see equation (3.134)) is computed to be $\mu_n(\Omega) = \frac{R^n}{n+1}$. Hence

$$\mathcal{K}_R[u](x) = \frac{2}{R^2}\int_{-R}^{R} u(x+r)\Omega(r)\,\mathrm{d}r. \tag{3.140}$$

The special case of uniform Ω

In this section we assume that the directionality function (Ω) in the non-local operator is uniform, that is $\omega \equiv {}^1/_2$.

Definition 3.62. For any $\mathbb{R} \ni R > 0$, we define the first order non-local

derivative is defined by

$$\nabla_R u(x) = \frac{1}{R}\left(u(x + R/2) - u(x - R/2)\right). \tag{3.141}$$

Definition 3.63. For any $\mathbb{R} \ni R > 0$, we define the second order non-local derivative is defined by

$$\Delta_R u(x) = \frac{1}{R^2}\left(u(x + R) + u(x - R) - 2u(x)\right). \tag{3.142}$$

Remark 3.64. Note that with these definitions we have that $\Delta_R u = \nabla_R \nabla_R u$.

Lemma 3.65. *Let $u \in L^2(S^1_L)$ and suppose that the directionality within the non-local term (see equation (3.140)) is uniform i.e. $\omega \equiv 1/2$, then we have that*

$$(\mathcal{K}_R[u](x))' = \Delta_R u(x). \tag{3.143}$$

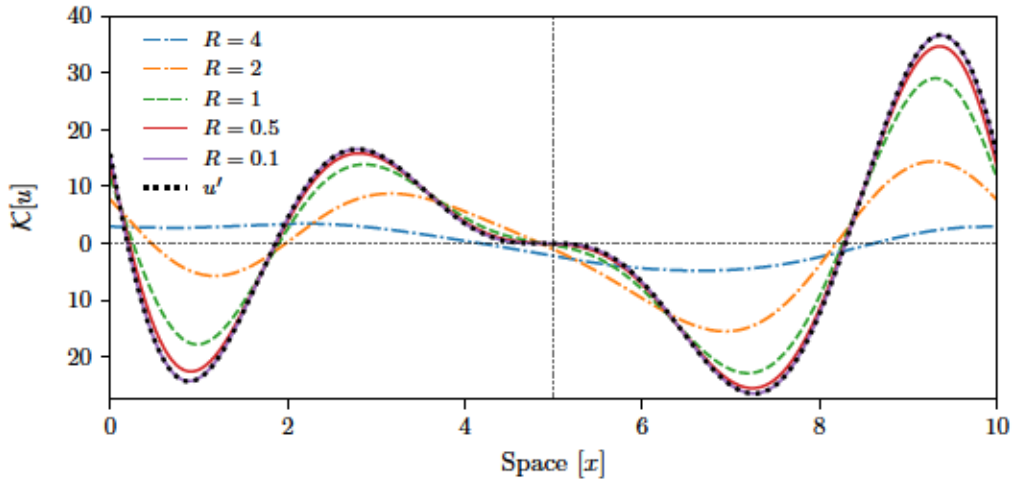

Figure 3.4: Comparison of the non-local term to the first derivative of a function for several values for the sensing radius R.

3.3.9 Summary of mathematical properties of $\mathcal{K}$

In this section, we studied basic mathematical properties of the non-local operator $\mathcal{K}[u]$, such as continuity and growth estimates. The classical chemotaxis

equation is, i.e.,

$$u_t = u_{xx} - \chi \left(u v_x \right)_x . \tag{3.144}$$

In the non-local adhesion model (3.10), the non-local term $\mathcal{K}[u]$ takes the place of the classical derivative v_x. In this section, we have seen that the non-local operator $\mathcal{K}[u]$ can be viewed as a generalization of the local derivative (in the sense that as $R \to 0$, $\mathcal{K}_R[u] \to u'$. In view of this analogy, the estimate ($|\mathcal{K}[u]|_p \leq C(|u|_p + L)$) obtained in Lemma 3.33 can be viewed as a type of reverse Poincaré inequality. Intuitively, this estimate "earns" us an order of differentiability. Similar results for other non-local operators have been obtained in [91, 99, 100].

The linear non-local operator defined in equation (3.91) and its derivative share many mathematical properties with the classical first and second-order derivatives respectively. For the non-local operator $\mathcal{K}[u]$ the shared properties are: skew-adjointness, the eigenfunctions, the zero eigenvalue, the range is contained in the subspace of zero average function, and the null-spaces are all the constant functions. There are however some difference. Most notably is that $\mathcal{K}[u]$ is a compact operator, thus its eigenvalues accumulate at zero (see Example 3.59 and Example 3.60), while the eigenvalues of $(\cdot)'$) diverge.

Similarly, for the non-local curvature $\mathcal{K}[u]'$ which shares the properties self-adjointness, eigenfunctions, and zero eigenvalue with the classical second-order derivative. Differences are that $\mathcal{K}[u]'$ is always a bounded operator, with bounded eigenvalues. Further, in the special case of uniform directionality (Ω) we have that $\mathcal{K}[u]'$ is equivalent to the non-local Laplacian defined in equation (3.142), which also appeared in [99].

3.4 Properties of non-trivial solutions

In this section, we prove several properties of solutions of equation (3.10a). These will be useful later, when we carry out the bifurcation analysis.

Lemma 3.66. *Let $u \in L^2(S^1_L)$ be L-periodic and the nonlinearity within the non-local term is linear i.e. ($h(u) = u$), then $\mathcal{A}[u(x)\,\mathcal{K}[u](x)] = 0$, where $\mathcal{A}[\cdot]$ is the averaging operator defined in Definition 3.24.*

Proof. We proceed by simple calculation, and an application of Fubini's theorem.

$$\begin{aligned}\int_0^L u(x)\,\mathcal{K}[u](x)\,\mathrm{d}x &= \int_0^L u(x)\int_{-1}^1 u(x+r)\Omega(r)\,\mathrm{d}r\,\mathrm{d}x \\ &= \int_0^L u(x)\int_0^1 \left(u(x+r)-u(x-r)\right)\omega(r)\,\mathrm{d}r\,\mathrm{d}x \\ &= \int_0^1\int_0^L u(x)\left(u(x+r)-u(x-r)\right)\,\mathrm{d}x\,\omega(r)\,\mathrm{d}r.\end{aligned} \tag{3.145}$$

Then we claim that

$$\int_0^L u(x)u(x+r)\,\mathrm{d}x = \int_0^L u(x)u(x-r)\,\mathrm{d}x, \tag{3.146}$$

for all $r \in [0,1]$. Using a simple change of variables in the second integral, we note that

$$\int_0^L u(x)u(x-r)\,\mathrm{d}x = \int_{-r}^{L-r} u(x+r)u(x)\,\mathrm{d}x = \int_0^L u(x+r)u(x)\,\mathrm{d}x, \tag{3.147}$$

where the last equality holds due to the periodic domain. Hence, the result follows. □

Note that in the proof of Lemma 3.66, we required that the nonlinearity within the non-local term is the simple linear function ($h(u) = u$). The previous proof does not work for non-linear $h(u)$. We can however recover the result by imposing an additional assumption.

Lemma 3.67. *Let $u \in L^2(S^1_L)$ be L-periodic and $u(x) = u(L-x)$ then $\mathcal{A}[u(x)\,\mathcal{K}[u](x)] = 0$, where $\mathcal{A}[\cdot]$ is the averaging operator defined in Definition 3.24 and $h(\cdot)$ satisfies H1–H4.*

Proof. Due to the fact that $u(x) = u(L-x)$, we obtain that

$$u(x)\,\mathcal{K}[u](x) = -u(L-x)\,\mathcal{K}[u](L-x). \tag{3.148}$$

Hence, upon integration we obtain

$$\begin{aligned}\int_0^L u(x)\,\mathcal{K}[u](x)\,\mathrm{d}x &= \int_0^{L/2} u(x)\,\mathcal{K}[u](x)\,\mathrm{d}x + \int_{L/2}^{L} u(x)\,\mathcal{K}[u](x)\,\mathrm{d}x \\ &= \int_0^{L/2} u(x)\,\mathcal{K}[u](x)\,\mathrm{d}x - \int_0^{L/2} u(x)\,\mathcal{K}[u](x)\,\mathrm{d}x = 0.\end{aligned} \tag{3.149}$$

□

Remark 3.68. Note that if $u \in H^2$, then Lemma 3.66 implies that the flux defined by

$$J(x) = -u'(x) + \alpha u(x)\,\mathcal{K}[u(x)](x), \tag{3.150}$$

satisfies $\mathcal{A}[J] = 0$, and since J is continuous we have that $\exists \hat{x} \in S_L^1 \colon J(\hat{x}) = 0$. Note that the continuity of J follows, since $u \in H^2 \subset\subset \mathcal{C}^1$.

We derive an a priori estimate of positive solutions of equation (3.10a). Prior to being able to prove the estimate we require a few technical results.

Proposition 3.69. *Let $u \in H^2_{\mathcal{B}}$ be a solution of equation* (3.10a)*. Then $u \in \mathcal{C}^3(S_L^1)$.*

Proof. By Sobolev's theorem (Theorem B.4) we have that $u \in \mathcal{C}^{1,1/2}(S_L^1)$. Integrating equation (3.10a) from $\hat{x}$ (the point at which the flux is zero, whose existence is guaranteed by Remark 3.68) we observe that,

$$u'(x) = \alpha u(x)\,\mathcal{K}[u](x). \tag{3.151}$$

Lemma 3.34 implies that whenever $u \in H^2$ we also have that $\mathcal{K}[u] \in H^2$, hence applying the Banach algebra property of H^2 and Sobolev's theorem (Theorem B.4) we have that $u\,\mathcal{K}[u] \in H^2 \subset\subset \mathcal{C}^{1,1/2} \subset \mathcal{C}^1$. Then by equation (3.151) we have that $u' \in \mathcal{C}^1(S_L^1)$ and thus $u \in \mathcal{C}^2(S_L^1)$.

From equation (3.10a) we have that,

$$u''(x) = \alpha \left(u(x)\,\mathcal{K}[u](x)\right)'. \tag{3.152}$$

As $u \in \mathcal{C}^2(S_L^1)$ we apply Lemma 3.37 to find that $\mathcal{K}[u] \in \mathcal{C}^2(S_L^1)$, hence $u\,\mathcal{K}[u] \in \mathcal{C}^2(S_L^1)$. This means, that $u'' \in \mathcal{C}^1(S_L^1)$ and finally we have that $u \in \mathcal{C}^3(S_L^1)$. □

Lemma 3.70. *Let $u \in \mathcal{C}^1(S^1_L)$ be a non-negative solution of equation* (3.10a)*, subject to the integral constraint*

$$\mathcal{A}[u] = \bar{u}, \tag{3.153}$$

where $\bar{u} > 0$. Then we have,

$$\bar{u}e^{-\alpha\mu L} \leq u(x) \leq \bar{u}e^{\alpha\mu L}, \tag{3.154}$$

where $\mu = C(\bar{u} + L)|\omega|_\infty$. Further we have that,

$$|u'(x)| \leq \alpha\mu\bar{u}e^{\alpha\mu L}. \tag{3.155}$$

Then,

$$\|u\|_{\mathcal{C}^1} \leq (1 + \alpha\mu)\,\bar{u}e^{\alpha\mu L} =: K(\alpha, L, \bar{u}, \Omega). \tag{3.156}$$

Proof. Equation (3.10a) is given by,

$$u''(x) = \alpha\left(u(x)\,\mathcal{K}[u](x)\right)'. \tag{3.157}$$

Integrating equation (3.157) from $\hat{x}$ (given in Remark 3.68) to x we obtain,

$$u'(x) = \alpha u(x)\,\mathcal{K}[u](x). \tag{3.158}$$

Thus using Lemma 3.38 we obtain the following differential inequality,

$$u'(x) \leq \alpha C|\omega|_\infty u(x)\,(\bar{u} + L)\,. \tag{3.159}$$

Let's denote $\mu = C(\bar{u} + L)|\omega|_\infty$. Next we note that if $u(x)$ has mass $\bar{u}$ then there is $\tilde{x} \in [0, L]$ such that $u(\tilde{x}) = \bar{u}$. Then, integrating from x to $\tilde{x}$ we obtain,

$$\ln u(\hat{x}) - \ln u(x) \leq \alpha\mu L, \tag{3.160}$$

integrating from $\tilde{x}$ to x we obtain,

$$\ln u(x) - \ln u(\tilde{x}) \leq \alpha\mu L. \tag{3.161}$$

Combining the two inequalities we obtain,

$$-\alpha\mu L \leq \ln u(x) - \ln u(\tilde{x}) \leq \alpha\mu L \tag{3.162}$$

Hence we obtain that,

$$\bar{u}e^{-\alpha\mu L} \leq u(x) \leq \bar{u}e^{\alpha\mu L}. \tag{3.163}$$

The estimate for $u'(x)$ follows from the estimate from $u(x)$. □

Next we show that for steady states $u(x)$ and $\mathcal{K}[u](x)$ have the same maxima and minima and the same inflection points.

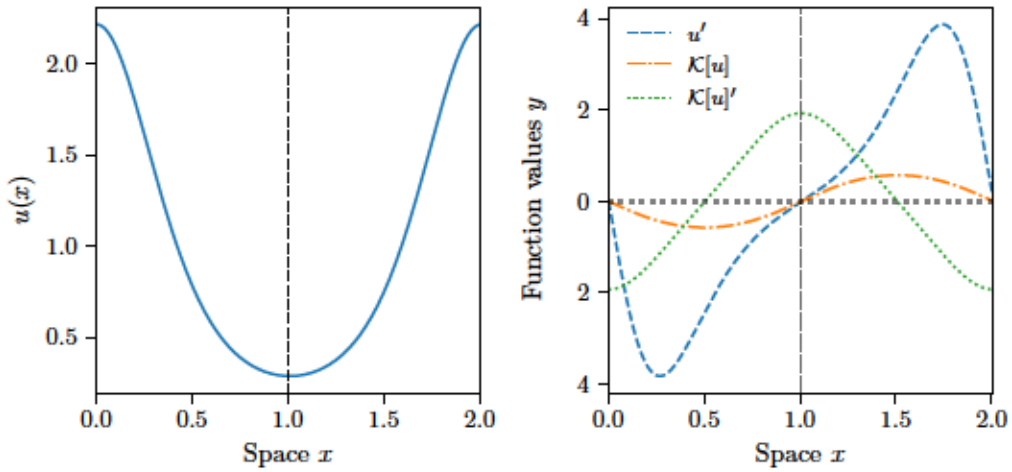

Figure 3.5: Examples of the non-local term $\mathcal{K}[u]$, $\mathcal{K}[u]'$, and u' applied to a positive solution of equation (3.10a). We observe the properties proven in Lemma 3.71 and Lemma 3.72. The dashed black line denotes the locations of the zeros of $\mathcal{K}[u](x)$ and $u'(x)$.

Lemma 3.71. *Suppose $u(x)$ is a solution of equation* (3.10a) *then $u'(\hat{x}) = 0$ if and only if $\mathcal{K}[u](\hat{x}) = 0$ (see Fig. 3.5).*

Proof. Without loss of generality, suppose that at $\hat{x} \in S^1_L$ we have $u'(\hat{x}) = 0$, then equation (3.151) implies that

$$0 = \alpha u(\hat{x})\,\mathcal{K}[u](\hat{x}), \tag{3.164}$$

but both $\alpha \neq 0$ and $u(\hat{x}) \neq 0$, thus $\mathcal{K}[u](\hat{x}) = 0$. □

Lemma 3.72. *Suppose $u(x)$ is a solution of equation* (3.10a)*, then it achieves a non-zero maximum (minimum) at $\hat{x}$ if and only if*

1. $\mathcal{K}[u](\hat{x}) = 0$,
2. $(\mathcal{K}[u](\hat{x}))' \leq (\geq) 0$.

See Fig. 3.5 for an example.

Proof. **(1)** from Lemma 3.71.
(2) Without loss of generality, suppose $u(x)$ achieves a non-zero maximum at $\hat{x}$. This means that $u''(\hat{x}) \leq 0$. Thus from equation (3.10a), we get that

$$0 \geq u''(\hat{x}) = \alpha u(\hat{x}) \left(\mathcal{K}[u](\hat{x})\right)'. \tag{3.165}$$

But both $\alpha \neq 0$, and $u(\hat{x}) \neq 0$ and thus $(\mathcal{K}[u])' \leq 0$. □

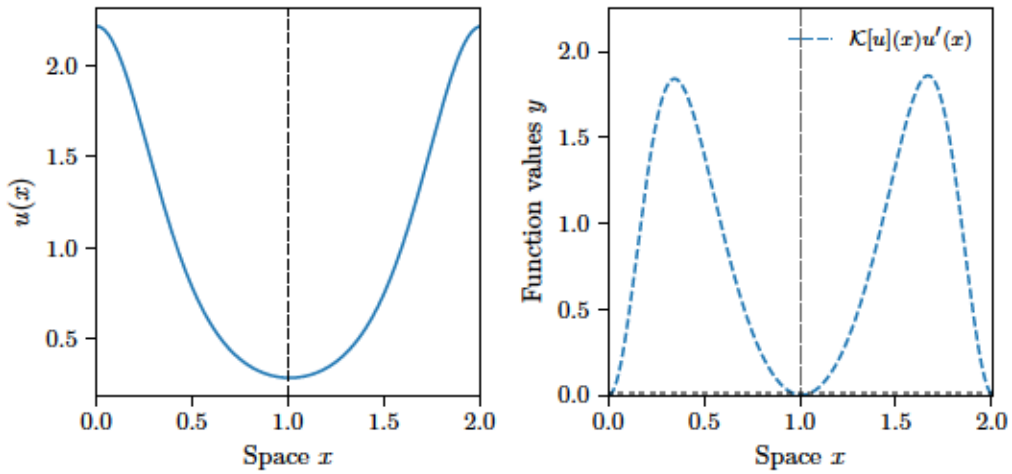

Figure 3.6: Example of the non-local operator $\mathcal{K}[u]$ and u' of a solution of equation (3.10a). It is demonstrated that the sign of both terms is always the same. The dashed black line denotes the locations of the zeros of $\mathcal{K}[u](x)$ and $u'(x)$.

Corollary 3.73. *Suppose $u(x)$ is a non-constant solution of equation* (3.10a) *that achieves non-zero maximum at $\hat{x}$ then there exists $\tilde{x}$ such that $\mathcal{K}[u]'(\tilde{x}) = 0$.*

Proof. If $u(x)$ is a solution, then it is $u \in \mathcal{C}^3(S^1_L)$. Then due to periodicity of the solution, there exists $\bar{x}$ such that $u(x)$ achieves a minimum. Hence, from Lemma 3.72 we have that $(\mathcal{K}[u](\bar{x}))' > 0$ and $(\mathcal{K}[u](\tilde{x}))' < 0$, hence by the Intermediate Value Theorem there exists at least one x_1 such that $(\mathcal{K}[u](x_1))' = 0$. □

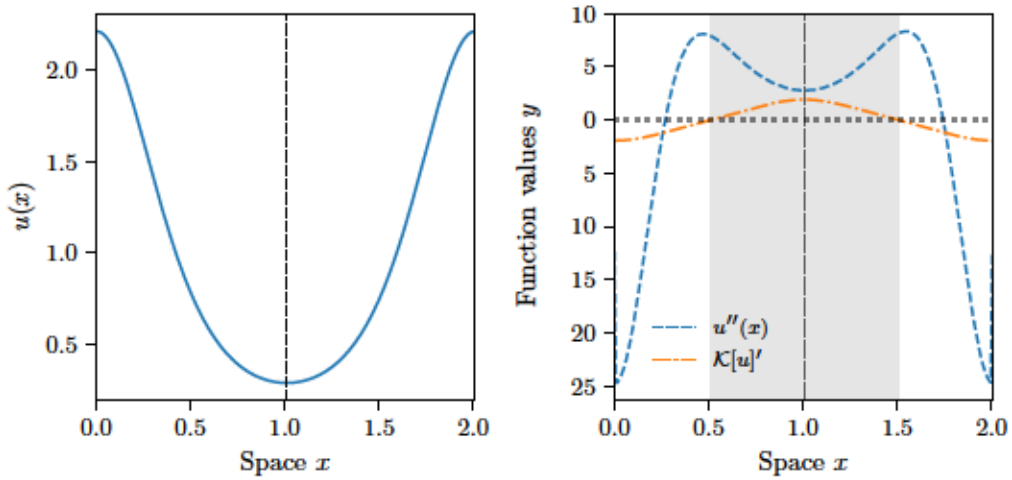

Figure 3.7: A comparision of the second derivative and $\mathcal{K}[u]'$ applied to a solution $u(x)$ of equation (3.10a). This demonstrates the result of Lemma 3.76. The dashed black line denotes the locations of the zeros of $\mathcal{K}[u]$ and u'.

Definition 3.74. Let $u(x)$ be a function, we say that

- it is non-locally convex whenever $(\mathcal{K}[u](x))' \geq 0$,
- it is non-locally concave whenever $(\mathcal{K}[u](x))' \leq 0$.

Lemma 3.75. *Let $u(x)$ be a positive solution of equation* (3.10a) *for $\alpha \geq 0$, then*

$$u'(x)\,\mathcal{K}[u](x) \geq 0. \tag{3.166}$$

For an example, see Fig. 3.6.

Proof. Substituting equation (3.151) into equation (3.10a), we obtain

$$u''(x) = \alpha^2 u(x)\,(\mathcal{K}[u](x))^2 + \alpha u(x)\,(\mathcal{K}[u])', \tag{3.167}$$

note that the first term on the right hand side is positive, and thus we have that

$$u'' \geq \alpha u(x) \left(\mathcal{K}[u]\right)'. \tag{3.168}$$

Then using equation (3.10a) and result (3.168), we obtain that

$$\alpha u'(x)\, \mathcal{K}[u](x) = u''(x) - \alpha u(x) \left(\mathcal{K}[u](x)\right)' \geq 0. \tag{3.169}$$

Since $\alpha > 0$, we obtain the result. □

Lemma 3.76. *Let $u(x)$ be a solution of equation* (3.10a)*, then we have that*

1. *If $u''(x) \leq 0$, then $\left(\mathcal{K}[u](x)\right)' \leq 0$,*
2. *If $\left(\mathcal{K}[u](x)\right)' \geq 0$, then $u''(x) \geq 0$.*

Proof. Proof is by equation (3.168). □

3.5 Bifurcation Analysis

We define the following function space

$$H^2_{\mathcal{B}} \coloneqq \left\{ u \in H^2(S^1_L) \colon \mathcal{B}[u, u'] = 0 \right\}, \tag{3.170}$$

where $\mathcal{B}[\cdot, \cdot]$ was defined in equation (3.44) and we define the following operator

$$\mathcal{F} \colon \mathbb{R} \times H^2_{\mathcal{B}}(S^1_L) \to L^2(S^1_L) \times \mathbb{R}, \tag{3.171a}$$

$$\mathcal{F}[\alpha, u] = \begin{bmatrix} \left(-u' + \alpha u\, \mathcal{K}[u]\right)' \\ \mathcal{A}[u] - \bar{u} \end{bmatrix}. \tag{3.171b}$$

In the following, we will need the Fréchet derivative of $\mathcal{F}$.

Lemma 3.77. *The Fréchet derivative $\mathcal{D}_u \mathcal{F} \colon \mathbb{R} \times H^2_{\mathcal{B}} \to \mathfrak{L}(H^2_{\mathcal{B}}, L^2 \times \mathbb{R})$ of the operator $\mathcal{F}$, is given by*

$$\mathcal{D}_u \mathcal{F}(\alpha, u)[w] = \begin{pmatrix} \left[-w' + \alpha \left(u\, \mathcal{K}_h[w] + w\, \mathcal{K}[u] \right) \right]' \\ \mathcal{A}[w] \end{pmatrix}, \tag{3.172}$$

where

$$\mathcal{K}_h[w] = \int_{-1}^{1} h'(u(x+r))w(x+r)\Omega(r)\,\mathrm{d}r. \tag{3.173}$$

Proof. Let $u, v, w \in H^2_B$, then we compute the first component of $\mathcal{D}_u\mathcal{F}$.

$$\begin{aligned}
&\mathcal{F}(\alpha, u+w) - \mathcal{F}(\alpha, u) - \mathcal{D}_u\mathcal{F}(\alpha, u)[w] \\
&= \alpha \left[\left(\underbrace{u \int_{-1}^{1} \left(h(u+w) - h(w) - h'(u)w\right)\Omega(r)\,\mathrm{d}r}_{\mathrm{I}} \right)' \right. \\
&\qquad \left. + \left(\underbrace{w \int_{-1}^{1} \left(h(u+w) - h(u)\right)\Omega(r)\,\mathrm{d}r}_{\mathrm{II}} \right)' \right].
\end{aligned} \tag{3.174}$$

Note that in the previous we only consider the first component of $\mathcal{F}$, because the second component is trivially zero. Next we require a L^2 estimate of the previous term. For this we consider the two terms separately (we denote them by I and II respectively).

$$|(\mathrm{I})'|_2 \leq \|\mathrm{I}\|_{H^1} \leq \|u\|_{H^1}\|w\|_{H^1} \left\| \frac{h(u+w) - h(u) - h'(u)w}{w} \right\|_{H^1}. \tag{3.175}$$

Now by H1 $h(\cdot) \in \mathcal{C}^2$, hence we have that

$$\lim_{\|w\|\to 0} \left\| \frac{h(u+w) - h(u) - h'(u)w}{w} \right\|_{H^1} = 0. \tag{3.176}$$

For the second term, we proceed similarly

$$|(\mathrm{II})'|_2 \leq \|\mathrm{II}\|_{H^1} \leq \|w\|_{H^1}\|h(u+w) - h(u)\|_{H^1} \leq C\|w\|^2_{H^1}, \tag{3.177}$$

where for the second last inequality, we used the Banach algebra property of H^1 and Lemma 3.33. Finally, for the last inequality we used the properties of $h(u)$ (H3).

Thus, we find that

$$\begin{aligned}&\frac{|\mathcal{F}(\alpha,u+w)-\mathcal{F}(\alpha,u)-\mathcal{D}_u\mathcal{F}(\alpha,u)[w]|_2}{\|w\|_{H^2}}\\&\leq \|u\|_{H^1}\left\|\frac{h(u+w)-h(u)-h'(u)w}{w}\right\|_{H^1}+\|w\|_{H^2},\end{aligned}\tag{3.178}$$

and then, we have that

$$\lim_{\|w\|\to 0}\frac{|\mathcal{F}(\alpha,u+w)-\mathcal{F}(\alpha,u)-\mathcal{D}_u\mathcal{F}(\alpha,u)[w]|_2}{\|w\|_{H^2}}=0.\tag{3.179}$$

Hence $\mathcal{D}_u\mathcal{F}(\alpha,u)$ is the Fréchet derivative of $\mathcal{F}$. □

We then prove a series of properties of $\mathcal{F}$ that allow us to apply the theorems from Section 3.2.

Lemma 3.78. *For each $\mathbb{R}\ni\bar{u}>0$, the operator $\mathcal{F}$ be defined as in equation* (3.171) *has the following properties:*

1. *$\mathcal{F}[\alpha,\bar{u}]=0$ for all $\alpha\in\mathbb{R}$.*
2. *The first component of $\mathcal{F}(\alpha,u)$ maps into $L^2_0(S^1_L)$ (defined in Definition 3.25).*
3. *$\mathcal{D}_u\mathcal{F}(\alpha,u)$ is Fredholm with index 0, for each $\alpha\in\mathbb{R}$.*
4. *$\mathcal{F}[\alpha,u]$ is $\mathcal{C}^1$ smooth.*
5. *$\mathcal{D}_{\alpha u}\mathcal{F}(\alpha,u)$ exists and is continuous.*

Proof.

1. We note that $\mathcal{K}[\bar{u}]=0$, hence the conclusion follows.
2. This is easily seen by integrating the equation, and using the periodic boundary conditions $\mathcal{B}$.
3. The Fréchet derivative of $\mathcal{F}$ with respect to u was found in Lemma 3.77 to be,

$$\mathcal{D}_u\mathcal{F}(\alpha,u)[w]=\begin{pmatrix}\left(-w'+\alpha\left(u\,\mathcal{K}_h[w]+w\,\mathcal{K}[u]\right)\right)'\\ \mathcal{A}[w]\end{pmatrix}.\tag{3.180}$$

We split this operator like,

$$\mathcal{D}_u \mathcal{F}(\alpha, u)[w] = \mathcal{T}_1(\alpha, u)[w] + \mathcal{T}_2(\alpha, u)[w] \tag{3.181}$$

where

$$\mathcal{T}_1(\alpha, u)[w] = \begin{pmatrix} -w'' \\ 0 \end{pmatrix}, \tag{3.182}$$

and

$$\mathcal{T}_2(\alpha, u)[w] = \begin{pmatrix} \alpha \left(u \mathcal{K}_h[w] + w \mathcal{K}[u] \right)' \\ \mathcal{A}[w] \end{pmatrix}. \tag{3.183}$$

$\mathcal{T}_1(\alpha, u)$ is Fredholm with index 0, by Lemma 3.28.

The operator $\mathcal{T}_2(\alpha, u)$ is compact. First, consider the first component of $\mathcal{T}_2$. Now $\mathcal{D}\colon H^1 \to L^2$, $w \to w'$ is continuous. Then let $\mathcal{T}(u)[w] = u \mathcal{K}_h[w] + w \mathcal{K}[u]$, where $u, w \in H^2_{\mathcal{B}}$. Since $h'(u) \in \mathcal{C}^1$ we have that $\mathcal{K}_h[w] \in H^2_{\mathcal{B}}$. Since $H^2_{\mathcal{B}}$ is a Banach algebra we have that $u \mathcal{K}_h[w] \in H^2_{\mathcal{B}}$ and $w \mathcal{K}[u] \in H^2_{\mathcal{B}}$. Since, $H^2 \subset\subset \mathcal{C}^1$, we can conclude that the first component is given by the composition $\mathcal{D} \circ \mathcal{T}(u)$ and hence is compact.

For the second component we let $(w_n) \subset H^2$ be bounded, then $\mathcal{A}[w_n] = \frac{1}{L} \int_0^L w_n(x) \, \mathrm{d}x$, but as $(w_n) \subset L^\infty$, we have that $\mathcal{A}[w_n]$ is a bounded sequence in $\mathbb{R}$ and thus has a convergent subsequence, making $\mathcal{A}$ compact.

Finally, we recall the well known results that the compact perturbation of a Fredholm operator is Fredholm with the same index (see Theorem 3.5). Hence, $\mathcal{D}_u \mathcal{F}(\alpha, u)$ is Fredholm with index 0.

4. For this we have to check that the operator

$$\mathcal{D}_u\colon u \to \mathcal{D}_u \mathcal{F}(\alpha, u), \tag{3.184}$$

is continuous. For this suppose that $u_n \to u$ in H^2 and note that the operator norm in this case for an operator $T \in \mathfrak{L}(H^2, L^2)$ is given by,

$$\|T\| = \sup_{\|w\|_{H^2}=1} |T[w]|_2. \tag{3.185}$$

Thus we have to verify that $|\mathcal{D}_u \mathcal{F}(\alpha, u_n) - \mathcal{D}_u \mathcal{F}(\alpha, u)|_2 \to 0$. We compute

$$\begin{aligned} &|\mathcal{D}_u \mathcal{F}(\alpha, u_n) - \mathcal{D}_u \mathcal{F}(\alpha, u)|_2 \\ &= \alpha \left| \left(\underbrace{w\,(\mathcal{K}[u_n] - \mathcal{K}[u])}_{\mathrm{I}} \right)' + \left(\underbrace{w\,\mathcal{K}[u_n] - w\,\mathcal{K}[u]}_{\mathrm{II}} \right)' \right|_2 . \end{aligned} \tag{3.186}$$

Then, we find that

$$\begin{aligned} |\mathrm{I}'|_2 \leq \|\mathrm{I}\|_{H^1} &\leq \|u_n \int_{-1}^{1} [\,h'(u_n) - h'(u)\,]\, w(x+r)\Omega(r)\,\mathrm{d}r\| \\ &\quad + \|(u_n - u) \int_{-1}^{1} h'(u) w(x+r)\Omega(r)\,\mathrm{d}r\| \\ &\leq M\|u_n - u\|\,(\|u_n\,\mathcal{K}[w]\| + \|\mathcal{K}_h[w]\|)\,, \end{aligned} \tag{3.187}$$

where we used that since h' is differentiable it must also be Lipschitz continuous with constant M. Thus we have that $|(\mathrm{I})'| \to 0$.

$$|\mathrm{II}'|_2 \leq \|\mathrm{I}\|_{H^1} \leq \|w\| \left\| \int_{-1}^{1} [\,h(u_n) - h(u)\,]\, w(x+r)\Omega(r)\,\mathrm{d}r \right\|_{H^1} . \tag{3.188}$$

Then, we have that

$$\left| \int_{-1}^{1} [\,h(u_n) - h(u)\,]\, w(x+r)\Omega(r)\,\mathrm{d}r \right|_p \leq |h(u_n) - h(u)|_p \leq C|u_n - u|_p, \tag{3.189}$$

and

$$\begin{aligned} &\left| \int_{-1}^{1} [\,h'(u_n)u_n - h'(u)u\,]\, w(x+r)\Omega(r)\,\mathrm{d}r \right|_p \\ &\leq |h'(u_n)u_n - h'(u)u|_p \leq C|h'|_{C^0}|u_n - u|_p. \end{aligned} \tag{3.190}$$

Hence, we obtain that $|(\mathrm{II})'| \to 0$, and so we have found that $\mathcal{D}_u \mathcal{F}(\alpha, u)$ is continuous.

5. We simply compute, to find

$$\mathcal{D}_{\alpha u}\mathcal{F}(\alpha,u)=\begin{pmatrix}(u\,\mathcal{K}_h[w]+w\,\mathcal{K}[u])'\\0\end{pmatrix}. \tag{3.191}$$

Its continuity follows from the argument above.

□

Remark 3.79. Note that Lemma 3.78 implies that $\mathcal{F}$ satisfies properties (F1), (F2) and (F3).

3.5.1 Symmetries and equivariant flows

For the following bifurcation analysis we will require a detailed understanding of symmetries of our solutions. We use group theory to describe these symmetries. We obtain the following result.

Lemma 3.80. *The operator $\mathcal{F}$ defined in equation* (3.171b) *is equivariant under the actions of $\mathbf{O}(2)$, i.e.*

$$\mathcal{F}[\alpha,\gamma u]=\gamma\,\mathcal{F}[\alpha,u],\quad\forall\gamma\in\mathbf{O}(2)\,. \tag{3.192}$$

Remark 3.81. The group $\mathbf{O}(2)$ is generated by $\mathbf{SO}(2)$ and a reflection. In more detail, $\mathbf{SO}(2)$ can be represented in $\mathbb{R}^2$ by

$$\sigma_\theta=\begin{pmatrix}\cos\theta&-\sin\theta\\\sin\theta&\cos\theta\end{pmatrix},\quad\theta\in[0,2\pi), \tag{3.193}$$

and the reflection is given by

$$\rho=\begin{pmatrix}1&0\\0&-1\end{pmatrix}. \tag{3.194}$$

It is easy to see, that this group is compact and hence proper. Here we represent

the group by its action on functions on S^1_L by

$$\begin{aligned} \sigma_a u(x) &= u(x-a) \quad \text{translation,} \\ \rho u(x) &= u(L-x) \quad \text{reflection.} \end{aligned} \tag{3.195}$$

In the following, we will denote reflection about $a \in S^1_L$ by

$$\rho_a u(x) = u(2a - x), \tag{3.196}$$

it is easy to see that this operation is in $\mathbf{O}(2)$. For an example, see Fig. 3.8.

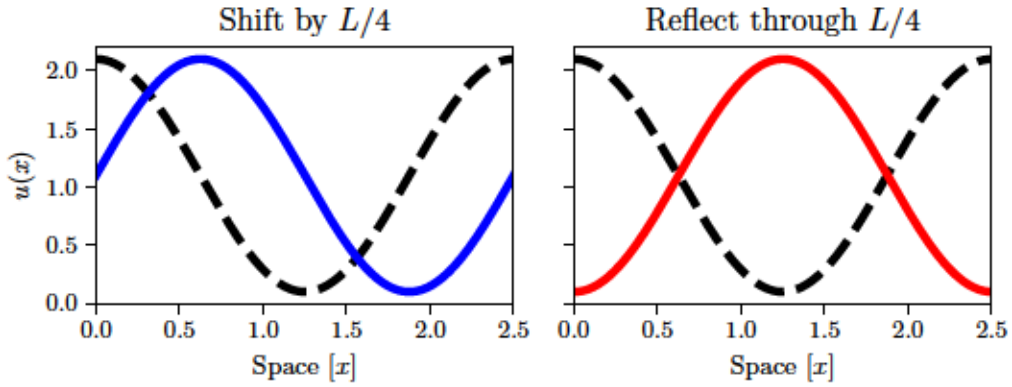

Figure 3.8: Examples of the actions of σ_a (left) and ρ_a and (right). Here $a = {}^{L}/_{4}$. In both subplots, the original function is shown in dashed black, while the shifted and respectively reflected functions are solid.

For the proof of this lemma we require the following lemma describing how the non-local operators behaves under actions of $\mathbf{O}(2)$.

Lemma 3.82. *Let the non-local operator $\mathcal{K}[u]$ be defined as in Definition 3.1, then*

$$\mathcal{K}[\sigma_\theta u] = \sigma_\theta \mathcal{K}[u], \qquad \mathcal{K}[\rho_a u] = -\rho_a \mathcal{K}[u], \tag{3.197}$$

and for the non-local curvature operator, we have that

$$(\mathcal{K}[\sigma_\theta u])' = \sigma_\theta (\mathcal{K}[u])', \qquad (\mathcal{K}[\rho_a u])' = \rho_a (\mathcal{K}[u])'. \tag{3.198}$$

Proof. The results for σ_θ are trivial. For ρ_a, we first deal with $\mathcal{K}[u](x)$. Then,

we find that

$$\begin{aligned}\mathcal{K}[\rho_a u](x) &= \int_0^1 \left[\, h(u(2a-x-r)) - h(u(2a-x+r)) \,\right] \omega(r)\,\mathrm{d}r \\ &= -\mathcal{K}[u](2a-x) = -\rho_a\left(\mathcal{K}[u]\right).\end{aligned} \tag{3.199}$$

Second, we show the same for $\mathcal{K}[u]'$ using a simple change of variables

$$\begin{aligned}\mathcal{K}[\rho_a u]' &= \left(\int_{-1}^1 -h(u(2a-x-r))\Omega(r)\,\mathrm{d}r\right)' \\ &= \left(\int_{-1}^1 -h(u(2a-x+y))\Omega(y)\,\mathrm{d}y\right)' \\ &= -\mathcal{K}[u]'(2a-x) = \rho_a \mathcal{K}[u]'.\end{aligned} \tag{3.200}$$

□

Now we can complete the proof of Lemma 3.80.

Proof of Lemma 3.80. The elements of $\mathbf{SO}(2)$ are given by the translations. Since

$$\frac{\partial}{\partial x} u(x-a) = \frac{\partial}{\partial (x-a)} u(x-a), \tag{3.201}$$

it is trivial to see that $\mathcal{F}$ is equivariant under actions of elements in $\mathbf{SO}(2)$. Note that to obtain all elements in $\mathbf{O}(2)$ we only need the reflection through $a = {}^{L}/_{2}$ as defined in equation (3.195), we find that

$$(\rho v(x))' = (v(2a-x))' = -v'(2a-x) = -(\rho v')(x) \tag{3.202}$$

and hence $(\rho v(x))'' = (\rho v'')(x)$. For the non-local term we apply Lemma 3.82 with $a = {}^{L}/_{2}$. Then substitute these into equation (3.171b) and we obtain the result. □

Note that because we are working on a periodic domain, we know from Lemma B.12 that both $\sin(\cdot)$ and $\cos(\cdot)$ are eigenfunctions of the linearization of equation (3.10a), and hence upon linearization of $\mathcal{F}$ we expect to find eigenspaces spanned by both. For bifurcation we however, require odd-dimensional nullspaces (here one-dimensional). Here, we will exploit the equiv-

ariance with respect to reflection to reduce the dimensionality of the nullspace. We define a new function space

$$H_P^2 \coloneqq \left\{ u \in H_B^2(S_L^1) \colon u(x) = u(L-x) \right\}. \tag{3.203}$$

It is then easy to see that the operator $\mathcal{F}$ now maps $\mathbb{R} \times H_P^2 \to L_P^2 \times \mathbb{R}$, since if $u \in H_P^2$ we find that

$$\mathcal{F}[\alpha, u] = \mathcal{F}[\alpha, \rho u] = \rho \mathcal{F}[\alpha, u]. \tag{3.204}$$

3.5.2 Generalized Eigenvalues of $\mathcal{F}$

Due to Lemma 3.16, we have that possible bifurcation points are those that are generalized eigenvalues of the Fréchet derivative of $\mathcal{F}$ evaluated at the trivial solution $(\alpha, \bar{u})$. To work, with a trivial solution that is $(\alpha, 0)$ we introduce the following change of variables,

$$v(x) \coloneqq u(x) - \bar{u}. \tag{3.205}$$

Under this change of variable, the operator $\mathcal{F}$ becomes

$$\mathcal{F}[\alpha, v] = \begin{bmatrix} (-v' + \alpha(v + \bar{u})\,\mathcal{K}[v])' \\ \mathcal{A}[v] \end{bmatrix}, \tag{3.206}$$

and its Fréchet derivative becomes

$$\mathcal{D}_v \mathcal{F}(\alpha, v)[w] = \begin{pmatrix} (-w' + \alpha\left((v + \bar{u})\,\mathcal{K}_h[w] + w\,\mathcal{K}[v]\right))' \\ \mathcal{A}[w] \end{pmatrix}. \tag{3.207}$$

Note that we treat this now as an operator family indexed by $\alpha \in \mathbb{R}$. In the next two lemmas we characterize the values of α, which lie in the generalized spectrum $\Sigma\left(\mathcal{D}_u \mathcal{F}(\alpha, 0)\right)$.

Lemma 3.83. *Let the operator $\mathcal{F}$ be as defined in* (3.206)*, and let $\alpha > 0$. Its Fréchet derivative has been shown to exist in Lemma 3.78. $M_n(\omega)$ denotes the*

quantity introduced in Lemma 3.51. Then, define

$$\alpha_n \coloneqq \frac{n\pi}{\bar{u}LM_n(\omega)h'(\bar{u})} \quad \text{for } n \in \mathbb{N}. \tag{3.208}$$

Then if $M_n(\omega) > 0$ *we have that*

$$\dim \mathrm{N}[\mathcal{D}_v \mathcal{F}(\alpha_n, \bar{u})] = 1. \tag{3.209}$$

Thus, the spectrum of the linearization is given by

$$\Sigma\left(\mathcal{D}_v \mathcal{F}(\alpha, 0)\right) = \left\{ \alpha_n \colon n \in \mathbb{N} \setminus \{0\} \right\}. \tag{3.210}$$

Remark 3.84. Note that $\alpha = 0$ is not an eigenvalue of $\mathcal{D}_v \mathcal{F}(\alpha, 0)$, since in this case, the only solution of (3.211) is the zero solution.

Remark 3.85. Note that since we assume that $L \geq 2$ we have that $M_1(\omega) > 0$, since then we have that $\sin\left(\frac{2\pi x}{L}\right) > 0$ on $(0,1)$ and $\omega(r) \geq 0$ by assumption. Thus, there is always one such bifurcation point.

Proof. The nullspace of $\mathcal{D}_v \mathcal{F}(\alpha, 0)$ is given by the solution of equation

$$\begin{cases} -w'' + \alpha \bar{u} h'(\bar{u}) \left(\int_{-1}^{1} w(x+r)\Omega(r)\,\mathrm{d}r \right)' = 0 \quad \text{in } [0, L] \\ \mathcal{B}[w, w'] = 0, \quad \mathcal{A}[w] = 0. \end{cases} \tag{3.211}$$

We solve this system using an eigenfunction (see Lemma B.12) ansatz.

$$w(x) = a_0 + \sum_{n=1}^{\infty} a_n \cos\left(\frac{2n\pi x}{L}\right) + \sum_{n=1}^{\infty} b_n \sin\left(\frac{2n\pi x}{L}\right), \tag{3.212}$$

then, because $\mathcal{A}[w] = 0$ we have that $a_0 = 0$ and as $w \in H^2_P$, we have that $b_n = 0, \forall n \in \mathbb{N}$. Hence

$$w(x) = \sum_{n=1}^{\infty} a_n \cos\left(\frac{2n\pi x}{L}\right), \tag{3.213}$$

which is then substituted into equation (3.211) to obtain,

$$\sum_{n=1}^{\infty} a_n \cos\left(\frac{2n\pi x}{L}\right)\left\{2\alpha\bar{u}h'(\bar{u})\int_0^1 \sin\left(\frac{2n\pi x}{L}\right)\omega(r)\,\mathrm{d}r - \frac{2n\pi}{L}\right\} = 0. \tag{3.214}$$

Hence to obtain a non trivial solution we require that,

$$\left\{\alpha\bar{u}h'(\bar{u})\int_0^1 \sin\left(\frac{2n\pi x}{L}\right)\omega(r)\,\mathrm{d}r - \frac{n\pi}{L}\right\} = 0. \tag{3.215}$$

Hence, $\mathcal{D}_v\mathcal{F}(\alpha,0)$ is not an isomorphism, whenever α equals one of the following

$$\alpha_n = \frac{n\pi}{L\bar{u}M_n(\omega)h'(\bar{u})}, \tag{3.216}$$

where $M_n(\omega)$ is defined in equation (3.103). □

Remark 3.86. Note that the values α_n found in Lemma 3.83 are exactly the values at which an eigenvalue λ of the linear operator

$$v'' - \alpha\bar{u}\left(\mathcal{K}[u]\right)' = \lambda v \tag{3.217}$$

crosses through 0.

Lemma 3.87. *Let α_n be a generalized eigenvalue of $\mathcal{D}_v\mathcal{F}(\alpha,0)$ as found in Lemma 3.83. Then we have that,*

$$\mathcal{D}_{\alpha v}\mathcal{F}(\alpha_n,0)[u_n] \notin \mathrm{R}[\mathcal{D}_v\mathcal{F}(\alpha_n,0)]. \tag{3.218}$$

where $u_n(x)$ is the eigenfunction corresponding to α_n from (3.208).

Proof. We proceed by contradiction. We assume that

$$\mathcal{D}_{\alpha v}\mathcal{F}(\alpha_n,0)[u_n] \in \mathrm{R}[\mathcal{D}_v\mathcal{F}(\alpha_n,0)]. \tag{3.219}$$

That means, that there is $y \in \mathrm{R}[\mathcal{D}_v\mathcal{F}(\alpha_n,0)]$ and a $z \in H^2_B$ such that

$$\mathcal{D}_v\mathcal{F}(\alpha_n,0)[z] = y. \tag{3.220}$$

Finally, that y has to be

$$\mathcal{D}_{\alpha v}\mathcal{F}(\alpha_n, 0)[w] = \begin{bmatrix} \bar{u}\mathcal{K}_h[w]' \\ 0 \end{bmatrix}. \tag{3.221}$$

Then equation (3.220) is equivalent to

$$\begin{cases} -z'' + \alpha_n \bar{u} h'(\bar{u}) \left(\int_{-1}^{1} w(x+r)\Omega(r)\,\mathrm{d}r \right)' = \bar{u}\mathcal{K}_h[u_n]' \quad \text{in } [0, L] \\ \mathcal{B}[z, z'] = 0, \quad \mathcal{A}[z] = 0. \end{cases} \tag{3.222}$$

We note that (refer to Lemma 3.56)

$$\mathcal{K}_h[u_n]' = h'(\bar{u}) \left(\frac{4\pi n}{L} \right) \cos\left(\frac{2\pi n x}{L} \right) M_n(\omega). \tag{3.223}$$

Like in the previous lemma, we once again use the ansatz

$$z(x) = \sum_{j=1}^{\infty} t_j \cos\left(\frac{2\pi n x}{L} \right). \tag{3.224}$$

Upon substitution into equation (3.222), we obtain

$$\begin{aligned} &\sum_{j=1}^{\infty} t_j \left(\frac{4\pi j}{L} \right) \cos\left(\frac{2\pi j x}{L} \right) \left\{ M_j(\omega)\alpha_n - \frac{\pi j}{L} \right\} \\ &= \bar{u}h'(\bar{u}) \left(\frac{4\pi n}{L} \right) \cos\left(\frac{2\pi n x}{L} \right) M_n(\omega). \end{aligned} \tag{3.225}$$

Then this equation has a solution if and only if $t_j = 0, \forall j \neq n$ and

$$t_n \left\{ \alpha_n M_n(\omega)\bar{u}h'(\bar{u}) - \frac{\pi n}{L} \right\} = \bar{u}h'(\bar{u})M_n(\omega), \tag{3.226}$$

is satisfied. But $\alpha_n = \frac{\pi n}{\bar{u}h'(\bar{u})M_n(\omega)L}$, hence the term on the left hand side is zero, and we have found a contradiction. □

3.5.3 Local Bifurcation Results

Based on the previous lemmas, we can now formulate the local bifurcation result.

Theorem 3.88. *Let $\mathcal{F}$ be given as in* (3.171). *Then by Lemma 3.78, Lemma 3.83 and Lemma 3.87 all requirements of Theorem 3.17 are satisfied. Then there are continuous functions*

$$(\alpha_k(s), u_k(s))\colon (-\delta_k, \delta_k) \to \mathbb{R} \times H^2_P \tag{3.227}$$

with $\alpha_k(0) = \alpha_k$ such that

$$u_k(x, s) = \bar{u} + s\alpha_k \cos\left(\frac{2\pi k x}{L}\right) + o(s) \tag{3.228}$$

where $(\alpha_k(s), u_k(s))$ is a solution of equation (3.10) *and all non-trivial solutions near the bifurcation point $(\alpha_k, \bar{u})$ lie on the curve $\Gamma_k = (\alpha_k(s), u_k(s))$.*

Proof. To be able to apply Theorem 3.17 we set $U = H^2_P$ and $V = L^2_{0,P} \times \mathbb{R}$ ($L^2_{0,P}$ is the sub-space of functions in L^2 with the symmetry as in equation (3.203) and average zero as in equation (3.25)) and $W = H^2_P$. Then the operator defined in equation (3.206) satisfies all the properties required by Theorem 3.17. These properties are proved by Lemma 3.78, Lemma 3.83 and Lemma 3.87. Finally, we revert the change of variables given in equation (3.205). □

3.5.4 Global Bifurcation

In the above, we found that bifurcations occur at $(\alpha_n, 0)$ and the non-trivial eigenfunctions of $\mathcal{D}_v \mathcal{F}(\alpha_n, 0)$ (see equation (3.172)) are given by

$$u_n(x) = \cos\left(\frac{2\pi n x}{L}\right). \tag{3.229}$$

Following the observations for some PDEs [73, 83, 84, 85], that symmetries of the bifurcating mode u_n are conserved along the bifurcating solution branch, we will show that this is the case here as well. For this we define the so called

isotropy subgroup associated with u_n. The isotropy subgroup contains all the group actions that leave u_n invariant.

$$\Sigma_n \coloneqq \{\, \gamma \in \mathbf{O}(2) \colon \gamma u_n = u_n \,\}. \tag{3.230}$$

It is easy to see, that for the eigenfunction u_n (see equation (3.229)) the isotropy subgroup is given by

$$\Sigma_n \coloneqq \left\{ \sigma_{\frac{mL}{n}}, \rho\sigma_{\frac{mL}{n}} \colon m \in \mathbb{N}, 1 \leq m \leq n \right\} = \mathbf{D}_\mathrm{n}, \tag{3.231}$$

where $\mathbf{D}_\mathrm{n}$ is dihedral group of order $2n$, which is the group of symmetries of regular polygons with n sides. Using the isotropy subgroup, we define the fixed-point subspaces (containing all the functions invariant under actions of the isotropy subgroup).

$$\begin{aligned} H^2_{\Sigma_n} &= \{u \in H^2 \colon \sigma u = u, \forall \sigma \in \Sigma_n\} \\ L^2_{\Sigma n} &= \{u \in L^2 \colon \sigma u = u, \forall \sigma \in \Sigma_n\}. \end{aligned} \tag{3.232}$$

Note that both of the above spaces are again Banach, since both are closed subspaces, which follows from the fact that Σ_n is a topological group and hence the action generated by $\sigma \in \Sigma_n$ is continuous. Then for each $n \in \mathbb{N}$, we obtain a Σ_n reduced problem of $\mathcal{F}$ such that

$$\mathcal{F} \colon \mathbb{R} \times H^2_{\Sigma_n} \to L^2_{\Sigma_n} \times \mathbb{R}, \tag{3.233}$$

since whenever $u \in H^2_{\Sigma_n}$, we have that

$$\mathcal{F}[\alpha, u] = \mathcal{F}[\alpha, \sigma u] = \sigma\, \mathcal{F}[\alpha, u]. \tag{3.234}$$

Then this problem has bifurcation points given in Lemma 3.83 at $\alpha_{kn}, 1 \leq k$.

Lemma 3.89. *Suppose that $u \in H^2_{\Sigma_n}$, then*

$$\mathcal{K}[u]\left(\frac{mL}{2n}\right) = 0, \qquad u'\left(\frac{mL}{2n}\right) = 0. \tag{3.235}$$

Proof. From Lemma 3.82, we have that

$$\mathcal{K}[\rho_a u] = -\rho_a \mathcal{K}[u]. \tag{3.236}$$

Since $u \in H^2_{\Sigma_n}$, we have that $\rho_{\frac{mL}{2n}} u = u$ and so we find that

$$\mathcal{K}[u](x) = \mathcal{K}[\rho_{\frac{mL}{2n}} u] = -\rho_{\frac{mL}{2n}} \mathcal{K}[u](x) = -\mathcal{K}[u]\left(\frac{mL}{n} - x\right), \tag{3.237}$$

where the last equality is simply the application of $\rho_{\frac{mL}{2n}}$ to the function $x \to \mathcal{K}[u](x)$. Letting $x = \frac{mL}{2n}$, we obtain that

$$\mathcal{K}[u]\left(\frac{mL}{2n}\right) = -\mathcal{K}[u]\left(\frac{mL}{2n}\right). \tag{3.238}$$

□

Remark 3.90. Note that if $u(x)$ is a solution of equation (3.10), then the previous Lemma 3.89 fixes the locations of its maxima and minima, since we have that $u'(x) = 0$ if and only if $\mathcal{K}[u](x) = 0$, from Lemma 3.72.

Remark 3.91. Note that the same result as in Lemma 3.89 has to hold for the second derivative of the non-local term $\mathcal{K}[u]''$. That is, we have that

$$\mathcal{K}[u]''\left(\frac{mL}{2n}\right) = -\mathcal{K}[u]''\left(\frac{mL}{2n}\right), \tag{3.239}$$

and thus we must have that $\mathcal{K}[u]''\left(\frac{mL}{2n}\right) = 0$.

The symmetry imposed on Σ_n by the dihedral group motivates the following definition of a *tiling* of the domain S^1_L. Intuitively, the tiling segregates the domain into pieces on which the function $u(x)$ is increasing and decreasing.

Definition 3.92. For $n \in \mathbb{N}$ we define, a *tile* by

$$\Omega_i \coloneqq \left(\frac{iL}{2n}, \frac{(i+1)L}{2n}\right), i = 0, \ldots, 2n-1. \tag{3.240}$$

Then, we have that

$$S_L^1 = \mathrm{cl}\left(\bigcup_{i=0}^{2n-1} \Omega_i\right). \tag{3.241}$$

The points between tiles will be denoted by

$$\partial\Omega = S_L^1 \setminus \bigcup_{i=0}^{2n-1} \Omega_i. \tag{3.242}$$

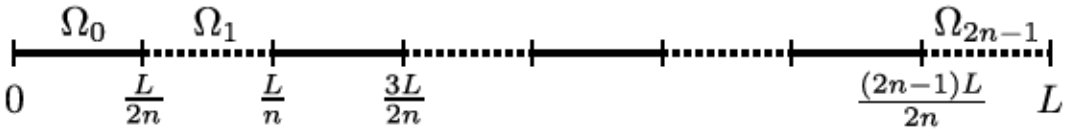

Figure 3.9: A tiling for S_L^1 as defined in Definition 3.92 and where $n \in \mathbb{N}$. The solid components form Ω^1 while the dashed components form Ω^2. $\partial\Omega$ is denoted by the vertical lines.

Using the tiling, we now define function spaces that contain functions with alternating regions of where they are increasing and decreasing. We make this precise in the following definition.

Definition 3.93. Let $n \in \mathbb{N}$, using the tiling from above we define

$$\Omega^1 \coloneqq \bigcup_{i=0}^{n-1} \Omega_{2i}, \qquad \Omega^2 \coloneqq \bigcup_{i=0}^{n-1} \Omega_{2i+1}. \tag{3.243}$$

Then we define the spaces of functions that have n tiles on which they are increasing and n tiles on which they are decreasing. Equivalently, they are the spaces of functions for which u' has $2n$ simple zeros, which are located on $\partial\Omega$ (this is motivated by Lemma 3.89).

$$\mathcal{S}_n^+ = \left\{ u \in C^2 \colon u' > 0 \text{ in } \Omega^1, u' < 0 \text{ in } \Omega^2, u''(x) \neq 0,\ x \in \partial\Omega \right\}, \tag{3.244}$$

and

$$\mathcal{S}_n^- = \left\{ u \in C^2 \colon u' < 0 \text{ in } \Omega^1, u' > 0 \text{ in } \Omega^2, u''(x) \neq 0,\ x \in \partial\Omega \right\}. \tag{3.245}$$

Remark 3.94. It is easy to see that both $S_k^{\pm}$ are nonempty, since $\cos\left(\frac{2\pi kx}{L}\right) \in S_k^-$,

while the negative of this function is an element of S_k^+ (see Fig. 3.10).

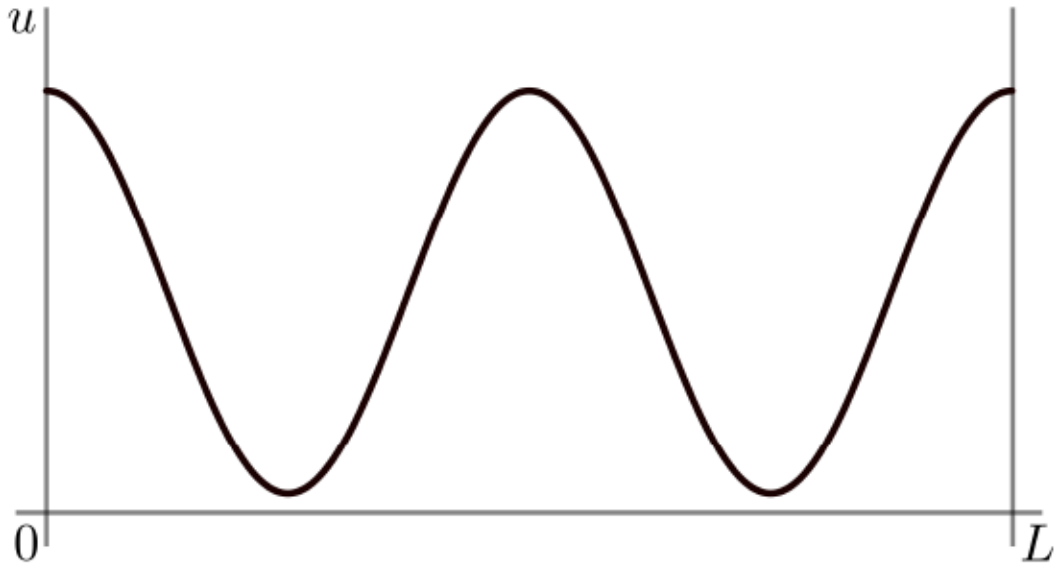

Figure 3.10: An example of a function in $\mathcal{S}_2^-$

Lemma 3.95. *Let $u \in \mathcal{S}_1^{\pm} \cap H^2_{\Sigma_1}$ be non-constant and positive. Further suppose that $h(u) = u$, then $\mathcal{K}[u](x) \neq 0$ for all $x \in \operatorname{int} \Omega^{1,2}$.*

Proof. Without loss of generality, we choose the tiling of the domain to be such that $u' > 0$ on Ω^1 and $u' < 0$ on Ω^2. Pick $\tilde{x} \in \operatorname{int} \Omega^1$, then we denote $\partial\Omega^1 = \{x_l, x_r\}$ and

$$r_L \coloneqq |x_l - \tilde{x}|, \qquad r_R \coloneqq |x_r - \tilde{x}|, \tag{3.246}$$

Then if $r_L, r_R > 1$ then by the monotonicity of u we have that $u(\tilde{x} - r) < u(\tilde{x} + r),\ r \in (0,1)$ and thus $\mathcal{K}[u](\tilde{x}) \neq 0$. If one or both of $r_L, r_R < 1$ then since $L \geq 2$ we have that $|\Omega^1| = {}^{L}/_{2} \geq 1$, thus $r_L + r_R \geq 1$. Since we have Σ_1 symmetry, we use the reflection to map $\tilde{x} \pm r$ back into Ω^1 whenever it hits the boundary $\partial\Omega^1$. For this we require some more notation (also see Fig. 3.11).

$$R^{\pm} \coloneqq \{\tilde{x} \pm r : r \in (0,1)\}. \tag{3.247}$$

It is clear that $R^+ \cap R^- = \emptyset$, since $L \geq 2$. Then the sets that are not in Ω^1,

and have to be reflected back are given by

$$\begin{aligned}\hat{R}^+ &:= \{\tilde{x} + r : r \in (r_R, 1)\} \\ \hat{R}^- &:= \{\tilde{x} - r : r \in (r_L, 1)\}.\end{aligned} \tag{3.248}$$

Following reflection, the subsets of $\hat{R}^{\pm}$ become the following subsets of Ω^1

$$\begin{aligned}\tilde{R}^+ &:= \{x_R - r : r \in (0, 1 - r_R)\}, \\ \tilde{R}^- &:= \{x_L + r : r \in (0, 1 - r_L)\}.\end{aligned} \tag{3.249}$$

Then, we claim that

$$\tilde{x}_L := \sup \tilde{R}^- \leq \inf \tilde{R}^+ =: \tilde{x}_R. \tag{3.250}$$

Indeed, suppose otherwise i.e. $\tilde{x}_L > \tilde{x}_R$. Then, this means that

$$x_L + (1 - r_L) > x_R - (1 - r_R). \tag{3.251}$$

Solving this inequality we obtain that $x_R - x_L < 1$. But this is impossible, since $L \geq 2$.

The proof of the claim implies that $u(\tilde{x} - r) < u(\tilde{x} + r),\ r \in (0, 1)$ and thus $\mathcal{K}[u](\tilde{x}) \neq 0$. □

Remark 3.96. Note that Lemma 3.95 only works for the linear choice of $h(u)$. Generalizing this result to nonlinear functions that satisfies the fairly general assumptions H1–H4 is not straight forward. In Section 3.5.6, we will discuss a more appropriate method, which if successful will make Lemma 3.95 superfluous.

Theorem 3.97. *Let $\mathcal{F}$ be given as in equation* (3.171) *with $h(u) = u$. Then for each $\bar{u} > 0$, the set of solutions of equation* (3.10a) *contains a closed connected set $\mathfrak{C} \subset \mathbb{R} \times H^2_{\Sigma_1}$ such that*

1. *$\mathfrak{C}$ contains $(\alpha_1(s), u_1(x, s))$ for $s \in (-\delta_1, \delta_1)$.*
2. *For any $(\alpha, u) \in \mathfrak{C}$, we have that $\alpha > 0$, $u > 0$.*

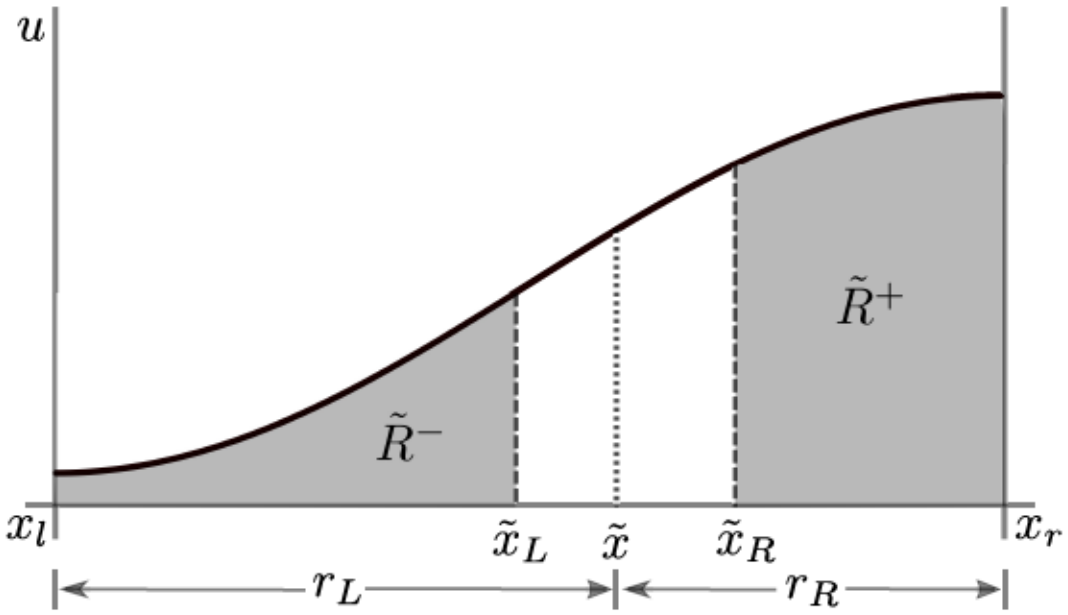

Figure 3.11: The setup for the proof of Lemma 3.95.

3. *Let* $\mathfrak{C} = \mathfrak{C}^+ \cup \mathfrak{C}^-$, *are the subcomponents of* $\mathfrak{C}$ *in the positive and negative direction of the eigenfunction given in* (3.229) *with* $n = 1$. $\mathfrak{C}^\pm$ *are closed and connected subsets of* $\mathfrak{C}$ *such that* $\mathfrak{C}^+ \cap \mathfrak{C}^- = \{(\alpha_1, \bar{u})\}$. *We denote* $\mathfrak{C}_1^\pm := \mathfrak{C}^\pm \backslash \{(\alpha_1, \bar{u})\}$, *and we have* $\mathfrak{C}_1^+ \subset \mathbb{R} \times \mathcal{S}_1^-$, *and that* $\mathfrak{C}_1^- \subset \mathbb{R} \times \mathcal{S}_1^+$, *where* $\mathcal{S}_1^\pm$ *are given by equations* (3.244) *and* (3.245).

4. *The unilateral branches* ($\mathfrak{C}^\pm$) *are unbounded, that is for any* $\alpha \geq \alpha_1$ *there exists* $(\alpha, u) \in \mathfrak{C}^\pm$.

Proof. 1. From Theorem 3.21, it follows that there exists the component $\mathfrak{C}$, which is the maximal, connected and closed subset of the closure of the set of non-trivial solutions,

$$\mathfrak{S} = \left\{ (\alpha, u) \in \mathbb{R} \times H^2_{\Sigma_1} : \mathcal{F}(\alpha, u) = 0, u \neq \bar{u} \right\}. \tag{3.252}$$

containing $(\alpha_1, \bar{u})$, this of course is also a consequence of Theorem 3.88. This proves 1.

2. Since $(\alpha_1, u) \in \mathfrak{C}$, we have $\alpha_1 > 0$. Indeed, if $\alpha \leq 0$, then by the connectedness of $\mathfrak{C}$ there would have to be a point in $\mathfrak{C}$ at which $\alpha = 0$. Thus

suppose that $(0, u) \in \mathfrak{C}$, but then from equation (3.10a) we have that $u \equiv \bar{u}$. Thus $(0, \bar{u})$ is a bifurcation point. But this contradicts Lemma 3.83, which showed that all bifurcation points are non-zero.

We show the positivity of u by considering

$$\mathcal{P} \coloneqq \left\{ u \in H^2_{\mathcal{B}} \colon u > 0 \text{ in } S^1_L \right\}, \tag{3.253}$$

Then we want to show that $\mathfrak{C} \subset \mathbb{R} \times \mathcal{P}$. We first note that $\bar{u} \in \mathcal{P}$ and by Theorem 3.88 we have that the solution component around the bifurcation point is also in $\mathcal{P}$. Since $\mathfrak{C}$ is connected and $\mathcal{P}$ is open, we have that if $\mathfrak{C} \not\subset \mathbb{R} \times \mathcal{P}$, then there exists a $(\alpha, u) \in \mathbb{R} \times \partial\mathcal{P}$ such that $0 \leq u$. First, suppose that there exists $\hat{x} \in S^1_L$ such that $u(\hat{x}) = 0$. Then note that equation (3.10a) can be written as,

$$\begin{cases} -u'' + a(x)u'(x) + b(x)u(x) = 0 \quad \text{in } [0, L] \\ \mathcal{B}[u, u'] = 0, \end{cases} \tag{3.254}$$

where

$$a(x) = \alpha \mathcal{K}[u](x) \qquad b(x) = \alpha \mathcal{K}[u'](x). \tag{3.255}$$

Due to Proposition 3.69, we have that both $a(x), b(x) \in \mathcal{C}^2(S^1_L)$. Then, the maximum principle (Theorem C.2) implies that $u \equiv 0$. However, this contradicts the integral constraint in equation (3.10), which must hold on $\mathfrak{C}$.

Thus we have that, $\mathfrak{C} \subset \mathbb{R} \times \mathcal{P}$.

3. Then consider the decomposition of $\mathfrak{C}$ into subcontina such that $\mathfrak{C}^+ \cap \mathfrak{C}^- = \{(\alpha_1, \bar{u})\}$. We claim that, $\mathfrak{C}^+_1 \subset \mathbb{R} \times \mathcal{S}^-_1$. Since, $\mathfrak{C}^+_1$ is a connected topological space it suffices to show that $\mathfrak{C}^+_1 \cap (\mathbb{R} \times \mathcal{S}^-_1)$ is nonempty, relatively open and relatively closed in $\mathfrak{C}^+_1$. Then we conclude that this space is all of $\mathfrak{C}^+_1$. We split the proof of this claim into three pieces.
(1) To show that $\mathfrak{C}^+_1 \cap (\mathbb{R} \times \mathcal{S}^-_1)$ is **non-empty**, we note that due to the local bifurcation result Theorem 3.88 for small s the solution along the branch is given by equation (3.228) with $n = 1$, thus the solution branch

is in $\mathfrak{C}_1^+ \cap (\mathbb{R} \times \mathcal{S}_1^-)$.

(2) To show that $\mathfrak{C}_1^+ \cap (\mathbb{R} \times \mathcal{S}_1^-)$ is relatively **open** in $\mathfrak{C}_1^+$, we use sequential openness (see Lemma B.11). Let $(\hat{\alpha}, \hat{u}) \in \mathfrak{C}_1^+ \cap (\mathbb{R} \times \mathcal{S}_1^-)$, and consider any sequence $(\alpha_k, u_k) \subset \mathfrak{C}_1^+$ convergent to $(\hat{\alpha}, \hat{u})$. Then we are left with showing that the tail of this sequence is contained in $\mathfrak{C}_1^+ \cap (\mathbb{R} \times \mathcal{S}_1^-)$. Without loss of generality consider $\Omega_0 := [0, L/2]$ (the treatment of Ω_1 is analogous). Since $\hat{u} \in \mathcal{S}_1^-$ we have that $\hat{u}' < 0$ on Ω_0, and that $u'' \neq 0$ on $\partial\Omega_0$. Further, we must have that $\hat{u}'$ is decreasing at the left boundary ($x_l = 0$), and increasing at the right boundary ($x_r = L/2$). Hence, we have that

$$\hat{u}''(x_l) < 0 < \hat{u}''(x_r). \tag{3.256}$$

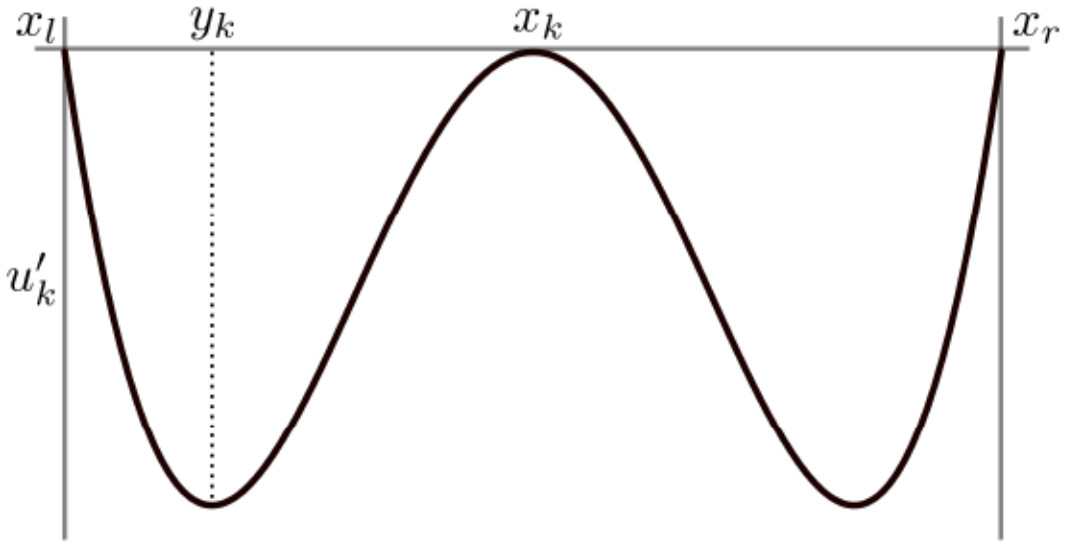

Figure 3.12: Plot of the derivative u'. The point x_k is such that $u'(x_k) = 0$, this implies the existence of point y_k at which $u''(y_k) = 0$.

Since u_k converges to $\hat{u}$, we have that eventually $u_k' \leq 0$ on Ω_0. Suppose that there exist a x_{k_n} (k_n a subsequence of $k \to \infty$) such that $u'(x_{k_n}) = 0$. This implies that there exists y_{k_n} such that $u_k''(y_{k_n}) = 0$ ($y_{k_n} \in (x_l, x_{k_n})$ or $y_{k_n} \in (x_{k_n}, x_r)$). Without loss of generality suppose that $y_{k_n} \in (x_l, x_{k_n})$ (see Fig. 3.12). Since, $\hat{u} \in \mathcal{S}_1^-$ we must have that $x_{k_n} \to x_l$ as $k \to \infty$, which implies that $y_{k_n} \to x_l$. Hence, we have that $u''(y_{k_n}) = 0$ for $y_{k_n} \to x_l$

contradicting (3.256).

(3) To show that $\mathfrak{C}_1^+ \cap (\mathbb{R} \times \mathcal{S}_1^-)$ is relatively **closed**, we consider the sequence $(\alpha_k, u_k) \subset \mathfrak{C}_1^+ \cap (\mathbb{R} \times \mathcal{S}_1^-)$ convergent to $(\hat{\alpha}, \hat{u}) \in \mathfrak{C}_1^+$. Then again consider Ω_0 such that $u_k' < 0, \forall k$. Then we must have that, $\hat{u}' \leq 0$. Suppose that there exists $\tilde{x} \in \Omega_0$ such that $\hat{u}'(\tilde{x}) = 0$. This means, since $\hat{u}' \leq 0$, that that $\hat{u}''(\tilde{x}) = 0$. Evaluating equation (3.10a) and equation (3.158) at $\tilde{x}$ we obtain that

$$\mathcal{K}[\hat{u}](\tilde{x}) = 0, \qquad \mathcal{K}[\hat{u}]'(\tilde{x}) = 0. \tag{3.257}$$

If $\tilde{x} \in \operatorname{int} \Omega_0$ and if $\hat{u}$ is non-constant, then Lemma 3.95 implies that $\mathcal{K}[\hat{u}](\tilde{x}) \neq 0$. Thus we have a contradiction.

If however $\tilde{x} \in \partial\Omega_0$ with $\hat{u}'(\tilde{x}), \hat{u}''(\tilde{x}) = 0$, then evaluating equation (3.10a) at $\tilde{x}$ we again obtain the results as in equation (3.257). If, however $\hat{u}$ is non-constant, then without loss of generality suppose that $\tilde{x} = x_l$. Then we have that $\hat{u}'(x) < 0$ for $x < \tilde{x}$ and $\hat{u}' > 0$ for $x > \tilde{x}$. Since, $L \geq 2$ the domain of the non-local term $\mathcal{K}[u]'$ do not overlap. Then referring to the non-local curvature (3.107) we easily conclude that we must have $\mathcal{K}[u]'(\tilde{x}) > 0$, which is a contradiction to (3.257).

Together, the previous two paragraphs exclude the possibility that $\hat{u}$ is a non-constant function. If on the other hand $\hat{u}$ is constant, then $\hat{u} \equiv \bar{u}$, from the integral constrain in equation (3.10). This means that $(\hat{\alpha}, \bar{u})$ is a bifurcation point. Therefore we must have that $\hat{\alpha} = \alpha_k$ for some $\mathbb{N} \ni k \geq 1$. The case $k = 1$ cannot occur since $\mathfrak{C}_1^+$ does not contain $(\alpha_1, \bar{u})$. For $k \geq 2$ we have from the local bifurcation result (see Theorem 3.88) that in a small neighborhood of $(\alpha_k, \bar{u})$ the solution branch must be given by (3.227). But this means that $u_k' > 0$ and $u_k' < 0$ on Ω_0, which is a contradiction. Thus, $\mathfrak{C}_1^+ \cap (\mathbb{R} \times \mathcal{S}_1^-)$ is closed.

Thus, we have proven that $\mathfrak{C}_1^+ \subset \mathbb{R} \times \mathcal{S}_1^-$. For $\mathfrak{C}_1^-$ we proceed analogously.

4. Theorem 3.22 implies that $\mathfrak{C}^\pm$ each satisfies one of the following alternatives:

   i it is not compact in $\mathbb{R} \times H^2_{\Sigma_1}$,

ii it contains a point $(\hat{\alpha}, \bar{u})$ where $\hat{\alpha} \neq \alpha_1$,

iii it contains a point $(\alpha, \bar{u} + \tilde{u})$ where $\tilde{u} \in Y \setminus \{0\}$,

where

$$Y = \left\{ u \in H^2_{\Sigma_1} \colon \int_0^L u(x) \cos\left(\frac{2\pi x}{L}\right) = 0 \right\}. \tag{3.258}$$

If alternative ii holds, then $\hat{\alpha}$ is a bifurcation point, which is impossible after the proof of 3.

If alternative iii holds, then there is a $(\alpha, \bar{u} + \tilde{u}) \in \mathfrak{C}^{\pm}$ where $\tilde{u} \in Y \setminus \{0\}$. This means the following holds, where we integrate by parts

$$0 = \int_0^L \tilde{u}(x) \cos\left(\frac{2\pi x}{L}\right) \mathrm{d}x = -\frac{L}{2\pi} \int_0^L \tilde{u}'(x) \sin\left(\frac{2\pi x}{L}\right) \mathrm{d}x \tag{3.259}$$

then we note that $\sin\left(\frac{2\pi x}{L}\right)$ and $\tilde{u}'$ have the same zeros and since $\tilde{u}'' \neq 0$ on $\partial\Omega$ we have that $\tilde{u}'$ must change sign at those points. Hence we have two cases. If $\sin\left(\frac{2\pi x}{L}\right) < 0$ whenever $\tilde{u}' < 0$, then we find that

$$\tilde{u}'(x) \sin\left(\frac{2\pi x}{L}\right) > 0, \forall x \tag{3.260}$$

and if $\sin\left(\frac{2\pi x}{L}\right) > 0$, whenever $\tilde{u}' < 0$, we find that

$$\tilde{u}'(x) \sin\left(\frac{2\pi x}{L}\right) < 0, \forall x \tag{3.261}$$

In both cases, we then find that

$$\int_0^L \tilde{u}'(x) \sin\left(\frac{2\pi x}{L}\right) \mathrm{d}x \neq 0 \tag{3.262}$$

which contradicts equation (3.259). Therefore only alternative i holds, and thus $\mathfrak{C}^{\pm}$ are non compact.

Finally, to show 4 we note that since $\mathfrak{C}^{\pm}$ are connected its projection onto the α coordinate are intervals containing α_1. From the a-priori estimate for positive solution derived in Lemma 3.70 we find that for bounded α the solution u is bounded. In particular, uniformly bounded in C^1. From

equation

$$u'' = \alpha u' \mathcal{K}[u] + \alpha u \mathcal{K}[u]', \tag{3.263}$$

we then also have that u'' is bounded, since u and u' are bounded. Iterating this process one more time for u''', we consider equation

$$u''' = \alpha u'' \mathcal{K}[u] + 2\alpha u' \mathcal{K}[u]' + \alpha u \mathcal{K}[u]''. \tag{3.264}$$

The first two terms on the right hand side are bounded, and the second-derivative of $\mathcal{K}[u]$ is also bounded since $u \in \mathcal{C}^3$ and $h(\cdot) \in \mathcal{C}^2$. Hence u is bounded in the norm of $\mathcal{C}^3$ and hence H^3 for bounded α. But $H^3 \subset\subset H^2$, thus $\mathfrak{C}^{\pm}$ are compact in $\mathbb{R} \times H^2$ a contradiction. Thus the α coordinate must be unbounded.

□

Remark 3.98. Note that in part 3 of the proof of Theorem 3.97 we cannot use the symmetry of the function space H^2_P to show that $\mathfrak{C}^+_1 \cap (\mathbb{R} \times \mathcal{S}^-_1)$ is both open and closed. This is because the imposed symmetry only restrict the solution's $(u(x))$ behaviour on the tile boundaries, and not in the interior of a given tile.

Remark 3.99. The most challenging part of the proof of Theorem 3.97 was to show that $\mathfrak{C}^+_1 \cap (\mathbb{R} \times \mathcal{S}^-_1)$ is relatively closed (see part 3 of the proof). There the argument depended on the result of Lemma 3.95. In other words, the mathematical properties of the non-local term $\mathcal{K}[u]$ lead the proof to success. Furthermore, we note that this is step is what limits the result of Theorem 3.97 to only the first bifurcation branch and linear $h(u)$.

If we can generalize the proof that $\mathfrak{C}^+_1 \cap (\mathbb{R} \times \mathcal{S}^-_1)$ is relatively closed, Theorem 3.97 would be valid for all bifurcation branches. This would mean that the results of Theorem 3.97 parallel those obtained by Rabinowitz [143] for nonlinear Sturm-Liouville equations and Healey et al. [84] for nonlinear equivariant elliptic equations.

3.5.5 Degenerate Case

Suppose that $\omega \equiv {}^1/_2$ and that $L = 2kR$ where $k \in \mathbb{N}$. Then we have the following result, indicating a degenerate situation.

Lemma 3.100. *Let $L = 2k$, for $\mathbb{N} \ni k > 0$, and $\omega(r) \equiv 1/2$, then for $n \in \mathbb{N}$ such that $\frac{n}{k}$ is an even integer, we have that*

$$M_n(\omega) = 0. \tag{3.265}$$

The significance of $M_n(\omega)$ being zero is that under those circumstances $(\alpha_n, \bar{u})$ is not a bifurcation point of equation (3.171b). Since we had to assume that $M_n(\omega)$ is positive in the result of Lemma 3.83. Thus under those circumstances it is impossible to obtain steady-state solutions having n-peaks.

Proof of Lemma 3.100. The term $M_n(\omega)$ is introduced in equation (3.103), as

$$M_n(\omega) = \int_0^1 \sin\left(\frac{2\pi n x}{L}\right) \omega(r)\, \mathrm{d}r = \frac{1}{2}\int_0^1 \sin\left(\frac{\pi n x}{k}\right) \mathrm{d}r, \tag{3.266}$$

then this is zero whenever $\frac{n}{k}$ is an even integer. □

3.5.6 Thoughts on generalizing the previous proof

A unresolved challenge in the proof of Theorem 3.97 is to generalize the proof that shows that $\mathfrak{C}_1^+ \cap (\mathbb{R} \times \mathcal{S}_1^-)$ is relatively closed (see part 3 in the proof). This proof would be considerably more general if a maximum principle could be applied (e.g. Theorem C.3). Remark 3.91 suggests that the sign of the second derivative of the non-local term $\mathcal{K}[u]$ changes at the same points as $\mathcal{K}[u]$. This observation motivates the following approach.

Since we have that $u \in \mathcal{C}^3(S_L^1)$ we have that u''' exists and is continuous, thus we can differentiate equation (3.10), to obtain

$$u''' - \alpha u'' \mathcal{K}[u] - 2\alpha u' \mathcal{K}[u]' = \alpha u \mathcal{K}[u]''. \tag{3.267}$$

Now we denote $w = u'$, and

$$a(x) \coloneqq -\alpha\, \mathcal{K}[u](x), \qquad b(x) \coloneqq -2\alpha \mathcal{K}[u]'(x). \tag{3.268}$$

Then, we obtain the following linear non-homogeneous elliptic equation

$$w''(x) + a(x)w'(x) + b(x)w(x) = \alpha u(x)\mathcal{K}[u]''. \tag{3.269}$$

Now suppose that we are on a tiling Ω_i on which $w \geq 0$, and that there exists a point $x \in \operatorname{int}\Omega_i$ such that $w(x) = 0$. Then to apply Theorem C.4, we need that the right hand side of equation (3.269) be non-positive. Indeed, numerical simulations together with Remark 3.91, suggest that

$$u'(x)\mathcal{K}[u]''(x) \leq 0, \tag{3.270}$$

thus if $w \geq 0$, this would imply that $\mathcal{K}[u]'' \leq 0$ (see Fig. 3.13 for a numerical example). Then, since $u > 0$, we have that the right hand side of equation (3.269) is non-positive. Hence, Theorem C.4 can be applied, to obtain that either $w \equiv 0$ or $w > 0$. But if $w \equiv 0$, then $u \equiv \bar{u}$ and hence we must be located at a bifurcation point, which was excluded in the proof of Theorem 3.97. Thus, we find that $w > 0$ contradicting our assumption.

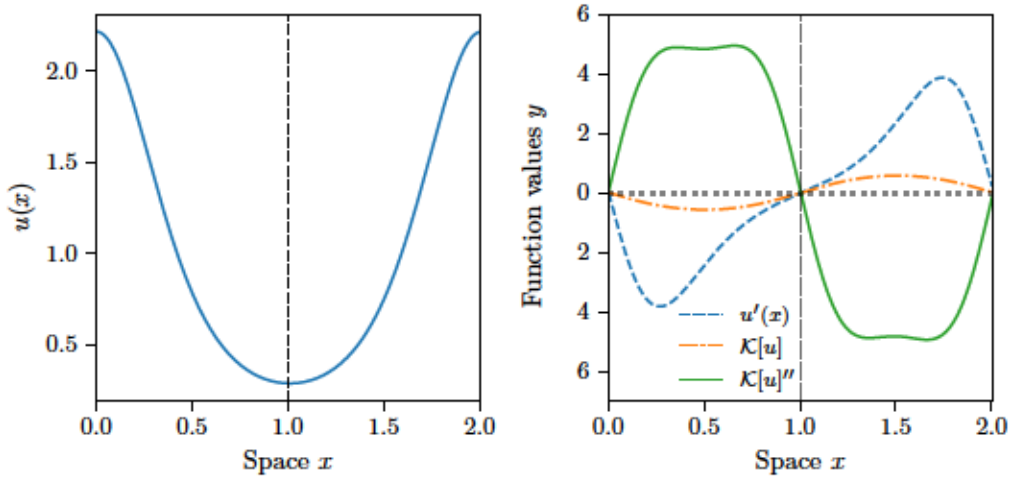

Figure 3.13: A plot demonstrating equation (3.270). On the left, a steady-state solution $u(x)$ of equation (3.10) is shown, for which, on the right, we compute $\mathcal{K}[u]$, $\mathcal{K}[u]''$, and u'. The dashed black line denotes the location of the zeros of $\mathcal{K}[u]$.

Thus it remains to prove that inequality (3.270) is indeed correct. A possible

approach would be to show that $\mathcal{K}[u]$ is mid-point convex (concave); then the continuity of $\mathcal{K}[u]$ would imply convexity (concavity), and we have the result of equation (3.270). Then the proof of Theorem 3.97 will work for any bifurcation branch and any nonlinear function $h(u)$ satisfying assumptions H1–H4.

In this case, the complete separation of the unbounded global bifurcation branches is a result of the "frozen" zeros of the solution's derivative. Critical for the result was the fact that the non-local term $\mathcal{K}[u]$ shares its zeros with the classical derivative.

3.6 Stability of bifurcating branch

We study the stability and the type of the first bifurcating branch. Note that this work is limited to the case $h(u) = u$ as we make heavy use of Lemma 3.51 and Lemma 3.56.

From earlier sections, we can decompose the function space H^2_P into two pieces,

$$H^2_P(S^1_L) = \text{span}\left\{ \cos\left(\frac{2\pi x}{L}\right) \right\} \oplus Y, \tag{3.271}$$

where $\cos\left(\frac{2\pi x}{L}\right)$ spans the nullspace of $\mathcal{D}_v \mathcal{F}(\alpha_1, 0)$, and where

$$Y = \left\{ u \in H^2_p(S^1_L) \colon \int_0^L u(x) \cos\left(\frac{2\pi x}{L}\right) \, \mathrm{d}x = 0 \right\}. \tag{3.272}$$

Theorem 3.101. *Suppose that all the assumptions of Theorem 3.97 are satisfied. Then the first bifurcation branch Γ_1 around $(\alpha_1, \bar{u})$ is locally parameterized by*

$$\begin{bmatrix} u_1(x,s) \\ \alpha_1(s) \end{bmatrix} = \begin{bmatrix} \bar{u} \\ \alpha_1 \end{bmatrix} + s \begin{bmatrix} \alpha_1 \\ 0 \end{bmatrix} \sin\left(\frac{2\pi x}{L}\right) + s^2 \begin{bmatrix} p_1(x) \\ \tilde{\alpha}_3 \end{bmatrix} + o(s^2) \tag{3.273}$$

for $s \in (-\delta, \delta)$, where $p_1(x)$ is determined above. Then the direction of the bifurcation is determined by the sign of $\tilde{\alpha}_3$ and it is a pitchfork type bifurcation as $\alpha_1'(0) = 0$.

The value of $\tilde{\alpha}_3$ can be computed from

$$\tilde{\alpha}_3 = \frac{1}{2}\left(\frac{\pi}{\bar{u}^2 L}\right)^2 \frac{1}{M_1(\omega)(2M_1(\omega) - M_2(\omega))}, \tag{3.274}$$

where $M_n(\omega)$ is defined in Lemma 3.51.

Proof. Then from Theorem 3.19 we have that the bifurcating branches are of class C^3 in particular $(\alpha(s), u(x,s)) \in C^3$ with respect to s. Then we can write an asymptotic expansion of $(u(x,s), \alpha(s))$ for the first bifurcation branch (see Theorem 3.88), that is,

$$\begin{aligned} u(s,x) &= \bar{u} + s\alpha_1 \sin\left(\frac{2\pi x}{L}\right) + s^2 p_1(x) + s^3 p_2(x) + o(s^3) \\ \alpha(s) &= \alpha_1 + s\tilde{\alpha}_2 + s^2\tilde{\alpha}_3 + o(s^3), \end{aligned} \tag{3.275}$$

where $p_i \in Y$. Since $\mathcal{A}[u(s,x)] = Lu^*$, we have that $\mathcal{A}[p_i] = 0$. In the following, we will denote $u_1 = \cos\left(\frac{2\pi x}{L}\right)$. For the following discussion, we will also need fourier expressions for the functions $p_i(x)$. That is, we express both by

$$p_i(x) = \sum_{n=2}^{\infty} b_n^i \cos\left(\frac{2\pi n x}{L}\right). \tag{3.276}$$

Then we substitute the asymptotic expansion into equation (3.10a), and we group the result by associating terms of equal powers of s.

The terms of order s give

$$\alpha_1 u_1'' - \alpha_1^2 \bar{u} K[u_1'] = 0. \tag{3.277}$$

It is straightforward to verify that this equation is satisfied precisely when α_1 is a bifurcation point (see Lemma 3.83). In the following, we use roman numerical (i.e. I) to refer to the projected variants of the terms shown below.

The terms of order s^2 give

$$\underbrace{p_1''(x)}_{\text{I}} - \alpha_1 \underbrace{\bar{u}K[p_1']}_{\text{II}} + \alpha_1^2 \underbrace{(u_1 K[u_1])'}_{\text{III}} - \alpha_1\tilde{\alpha}_2 \underbrace{\bar{u}K[u_1']}_{\text{IV}} = 0. \tag{3.278}$$

First we show that $\tilde{\alpha}_2 = 0$. Indeed, by projecting equation (3.278) onto the nullspace of $\mathcal{D}_v \mathcal{F}(\alpha, 0)$, we will obtain the result. We will show the work term by term in order as they appear in equation (3.278). First,

$$\mathrm{I} = \int_0^L p_1''(x) \cos\left(\frac{2\pi x}{L}\right) \mathrm{d}x = 0 \tag{3.279}$$

by integration by parts. For the second term, we apply the results of Lemma 3.56 to obtain

$$K[p_1'](x) = -2\sum_{n=2}^{\infty} M_n(\omega)\frac{2\pi n}{L} b_n^1 \cos\left(\frac{2\pi n x}{L}\right). \tag{3.280}$$

Then projecting those terms on the nullspace easily shows that

$$\mathrm{II} = 0. \tag{3.281}$$

We proceed similarly for the third term. Using Lemma 3.51, we obtain

$$\begin{aligned} \mathrm{III} &= \int_0^L (u_1 K[u_1])' \cos\left(\frac{2\pi x}{L}\right) \mathrm{d}x = \frac{2\pi}{L}\int_0^L u_1 K[u_1] \sin\left(\frac{2\pi x}{L}\right) \mathrm{d}x \\ &= -\frac{4\pi}{L} M_1(\omega) \int_0^L \sin^2\left(\frac{2\pi x}{L}\right) \cos\left(\frac{2\pi x}{L}\right) \mathrm{d}x = 0. \end{aligned} \tag{3.282}$$

Finally, for the fourth term, using Lemma 3.56, we obtain

$$\mathrm{IV} = -2M_1(\omega)\frac{2\pi}{L}\int_0^L \cos^2\left(\frac{2\pi x}{L}\right) \mathrm{d}x = -2M_1(\omega)\pi. \tag{3.283}$$

Substituting all these results into equation (3.278), we obtain that

$$\tilde{\alpha}_2 = 0. \tag{3.284}$$

The terms of order s^3, with the terms involving $\tilde{\alpha}_3$, are

$$\underbrace{p_2''(x)}_{\mathrm{I}} - \alpha_1 \underbrace{\bar{u} K[p_2']}_{\mathrm{II}} - \alpha_1^2 \underbrace{(u_1 K[p_1])'}_{\mathrm{III}} - \alpha_1^2 \underbrace{(p_1 K[u_1])'}_{\mathrm{IV}} - \alpha_1 \tilde{\alpha}_3 \underbrace{\bar{u} K[u_1']}_{\mathrm{V}} = 0. \tag{3.285}$$

Again we project this equation onto the nullspace of $\mathcal{D}_v \mathcal{F}(\alpha, 0)$ term by term.

The first term is

$$\mathrm{I} = \int_0^L p_2''(x) \cos\left(\frac{2\pi x}{L}\right) \mathrm{d}x = 0. \tag{3.286}$$

The second term, projected onto the nullspace is given by

$$\mathrm{II} = -2 \int_0^L \cos\left(\frac{2\pi x}{L}\right) \sum_{n=2}^{\infty} M_n(\omega) \frac{2\pi n}{L} b_n^2 \cos\left(\frac{2\pi n x}{L}\right). \tag{3.287}$$

Evaluating this, we obtain

$$\mathrm{II} = 0. \tag{3.288}$$

For the third term, we compute

$$\mathrm{III} = \int_0^L (u_1 K[u_1])' \cos\left(\frac{2\pi x}{L}\right) \mathrm{d}x. \tag{3.289}$$

We note that, using Lemma 3.51 we have that

$$(u_1 K[u_1])' = -M_1(\omega) \frac{4\pi}{L} \cos\left(\frac{4\pi x}{L}\right), \tag{3.290}$$

and it is easy to see that III is orthogonal to $\cos\left(\frac{4\pi x}{L}\right)$.

The fourth term is more interesting. Following integration by parts, we obtain

$$\mathrm{IV} = \frac{2\pi}{L} \int_0^L p_1(x) K[u_1] \sin\left(\frac{2\pi x}{L}\right) \mathrm{d}x. \tag{3.291}$$

In this case, following integration by parts we encounter terms of the form

$$\int_0^L \cos\left(\frac{2\pi n x}{L}\right) \sin^2\left(\frac{2\pi x}{L}\right) \mathrm{d}x = \begin{cases} 0 & \text{if } n \neq 2 \\ -L/4 & \text{if } n = 2. \end{cases} \tag{3.292}$$

Then collecting all the terms, we obtain

$$\mathrm{IV} = \pi M_1(\omega) b_2^1. \tag{3.293}$$

Finally, we deal with the last term,

$$\begin{aligned} \mathrm{V} &= \int_0^L K[u_1]' \cos\left(\frac{2\pi x}{L}\right) \mathrm{d}x \\ &= -2M_1(\omega)\frac{2\pi}{L}\int_0^L \cos^2\left(\frac{2\pi x}{L}\right) \mathrm{d}x = -2M_1(\omega)\pi. \end{aligned} \tag{3.294}$$

Hence solving for $\tilde{\alpha}_3$ we obtain

$$\tilde{\alpha}_3 = \frac{\alpha_1}{\bar{u}} \underbrace{\int_0^L p_1(x) \cos\left(\frac{4\pi x}{L}\right) \mathrm{d}x}_{b_2^1}. \tag{3.295}$$

Thus next we will have to find b_2^1.

To find this coefficient, we simply solve the equation of order s^2 for $p_1(x)$, and recalling the result from equation (3.290), we then obtain

$$p_1''(x) - \bar{u}\alpha_1 K[p_1'] = \alpha_1^2 \left(u_1 K[u_1]\right)' = \alpha_1^2 \frac{4\pi}{L} M_1(\omega) \cos\left(\frac{4\pi x}{L}\right). \tag{3.296}$$

Using the Fourier expansion (3.276) of $p_1(x)$ and substituting it into the previous equation and matching modes, we obtain

$$b_2^1 = \frac{\pi}{2\bar{u}^2 L(2M_1(\omega) - M_2(\omega))}, \tag{3.297}$$

which we can substitute into our expression for $\tilde{\alpha}_3$. We find that

$$\tilde{\alpha}_3 = \frac{1}{2}\left(\frac{\pi}{\bar{u}^2 L}\right)^2 \frac{1}{M_1(\omega)(2M_1(\omega) - M_2(\omega))}. \tag{3.298}$$

□

Example 3.102. *Suppose that ω is chosen to be the uniform function i.e. O1, then from Example 3.59 we can compute $M_n(\omega)$. Using this information, we can compute $\tilde{\alpha}_3$. In this case, we find that*

$$\tilde{\alpha}_3 = \left(\frac{\pi}{\bar{u}L}\right)^4 \frac{1}{\sin^6\left(\frac{\pi}{L}\right)}, \tag{3.299}$$

which is always positive.

Then suppose that $L = 2, \bar{u} = 1$, *then we find that*

$$\alpha_1 = \frac{\pi^2}{2}, \qquad \tilde{\alpha}_3 = \left(\frac{\pi}{2}\right)^4. \tag{3.300}$$

A bifurcation diagram for this situation is shown in Fig. 3.14.

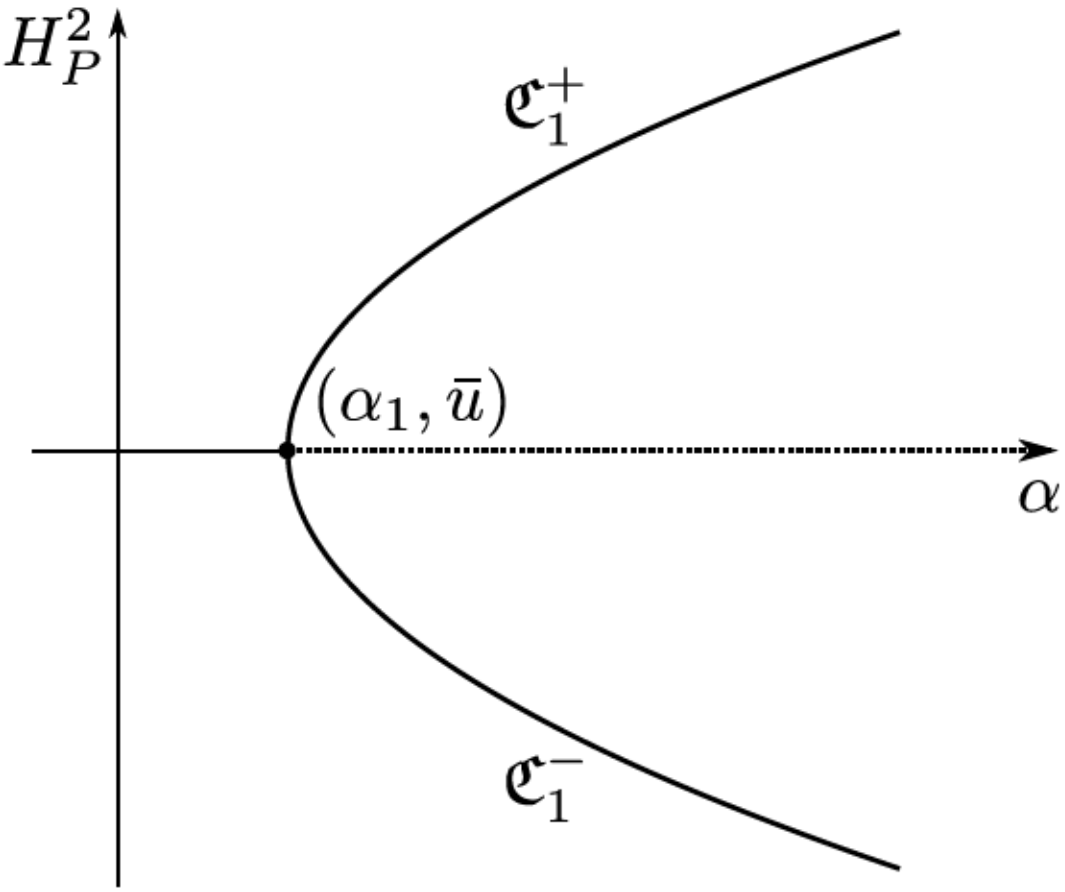

Figure 3.14: Sample bifurcation diagram of the supercritical pitchfork bifurcation, i.e., we have that $\tilde{\alpha}_3 > 0$ and have a switch of stability at the bifurcation point.

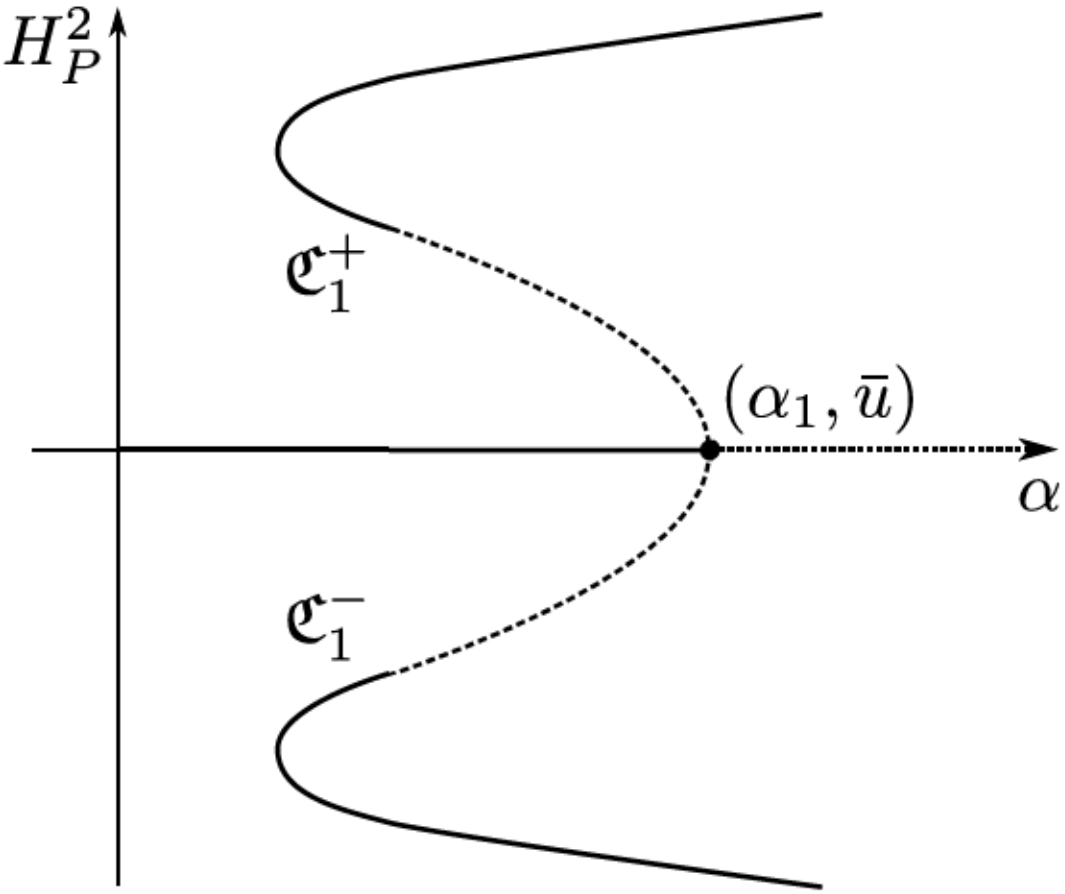

Figure 3.15: Sample bifurcation diagram of the subcritical pitchfork bifurcation, i.e., we have that $\tilde{\alpha}_3 < 0$ and a switch of stability that occurs later.

3.6.1 Stability of solutions

So far we have studied the set of solutions of the equation $\mathcal{F}[\alpha, u] = 0$, which are the steady states of the evolution equation

$$\frac{\mathrm{d}u}{\mathrm{d}t} = \mathcal{F}[\alpha, u]. \tag{3.301}$$

In this section, we are interested in the linear stability of these steady state solutions. The linear stability of such a solution, along a solution branch, is determined by the sign of the eigenvalue of $\mathcal{D}_u \mathcal{F}(\alpha(s), u(s))$. An eigenvalue perturbation result proven in [36], shows that the eigenvalue along the trivial solution branch is related to the eigenvalues along the non-trivial solution

branch near a bifurcation point. An application of the main result of [36] is the goal of this subsection. Again we limit this to the first solution branch. The eigenvalue problem linearized around the bifurcation point $(\alpha_1, \bar{u})$ is given by

$$-w'' + \alpha_1(s)\left(w\,\mathcal{K}[u_1] + u_1\,\mathcal{K}[w]\right)' = \lambda w. \tag{3.302}$$

When $s = 0$, $u_1(0) = \bar{u}$, we have that

$$-w'' + \alpha_1 \bar{u}\left(\mathcal{K}[w]\right)' = \lambda w. \tag{3.303}$$

Lemma 3.103. *The eigenvalues of equation* (3.303) *are given by*

$$\lambda_n = \begin{cases} 0 & \text{if } n = 1 \\ \left(\frac{2\pi}{L}\right)^2 \left(n^2 - \frac{M_n(\omega)}{M_1(\omega)}\right) & \text{if } n > 1 \end{cases}. \tag{3.304}$$

Since $M_n(\omega) \to 0$ as $n \to \infty$, we see that $\lambda_n \to \infty$ as $n \to \infty$, and λ_1 is an isolated eigenvalue.

Proof. Apply Lemma 3.56 and Lemma 3.58. □

Remark 3.104. Let's denote the set of eigenvalue of equation (3.303) by Λ. Then whenever $M_n(\omega)$ is well behaved meaning that $\lambda_n > 0$ for $n \geq 2$, i.e.,

$$\left|\frac{M_n(\omega)}{M_1(\omega)}\right| < n^2. \tag{3.305}$$

Then there exists $\hat{\delta} > 0$ small such that,

$$\Lambda \cap \{\lambda \in \mathbb{C} : \operatorname{Re}\lambda \leq \hat{\delta}\} = \{0\}. \tag{3.306}$$

Note that this does not hold in general as even when $\omega \equiv {}^1/_2$, since we have that $M_1(\omega) \to 0$ as $L \to \infty$.

Example 3.105. *Suppose that ω is chosen to be the uniform function, i.e. O1 (see Section 3.3.3). Then $M_n(\omega)$ was computed in Example 3.59. In this case,*

we find that

$$\frac{M_n(\omega)}{M_1(\omega)} = \frac{1}{n}\frac{\sin^2\left(\frac{\pi n}{L}\right)}{\sin^2\left(\frac{\pi}{L}\right)}. \tag{3.307}$$

If we choose $L = 2$*, we find that*

$$\frac{M_n(\omega)}{M_1(\omega)} = \begin{cases} \frac{(-1)^{n+1}}{n} & \text{if } n \text{ odd} \\ 0 & \text{else} \end{cases}. \tag{3.308}$$

Hence in this case, $M_n(\omega)$ *is well-defined as discussed in Remark 3.104.*

To apply the results of [36] we need to introduce the following definition, and show that our problem satisfies it.

Definition 3.106 (Definition 1.2 [36])**.** Let $\mathcal{T}, \mathcal{M} \in \mathfrak{L}(X, Y)$. Then $\mu \in \mathbb{R}$ is a $\mathcal{M}$-simple eigenvalue of $\mathcal{T}$ if

$$\dim N[\mathcal{T} - \mu\mathcal{M}] = \operatorname{codim} R[\mathcal{T} - \mu\mathcal{M}] = 1, \tag{3.309}$$

and if $N[\mathcal{T} - \mu\mathcal{M}] = \operatorname{span}\{x_0\}$ we have that

$$\mathcal{M}x_0 \notin R[\mathcal{T} - \mu\mathcal{M}]. \tag{3.310}$$

For the purpose here, we define the operator $\mathcal{M}\colon H^2 \to L_0^2 \times \mathbb{R}$ by

$$\mathcal{M}[w] = \begin{pmatrix} w(x) - \frac{1}{L}\int_0^L w(x)\,\mathrm{d}x \\ 0 \end{pmatrix}. \tag{3.311}$$

Lemma 3.107. $\lambda = 0$ *is a* $\mathcal{M}$*-simple eigenvalue of* $\mathcal{D}_u\mathcal{F}(\alpha_1, \bar{u})$.

Proof. Recall that $\mathcal{D}_u\mathcal{F}(\alpha_1, \bar{u})\colon H^2 \to L_0^2 \times \mathbb{R}$ is Fredholm with index 0. Thus, the operator satisfies the first condition in Definition 3.106. We show the second condition by contradiction. Suppose that

$$\mathcal{M}[u_1] \in R[\mathcal{D}_u\mathcal{F}(\alpha, \bar{u})] = \{u \in L^2\colon \int_0^L u(x)\,\mathrm{d}x = 0\}. \tag{3.312}$$

In other words, there exists $w \in H^2$ such that

$$\begin{cases} -w'' + \alpha_1 \bar{u} \mathcal{K}[w]' = \alpha_1 \cos\left(\frac{2\pi x}{L}\right) & \text{in } [0, L] \\ \mathcal{A}(w) = 0. \end{cases} \tag{3.313}$$

We expand $w(x)$ using a Fourier series

$$w(x) = \sum_{n=1}^{\infty} w_n \cos\left(\frac{2\pi n x}{L}\right), \tag{3.314}$$

and substitute that into equation (3.313). We then obtain the equation

$$n\left(\frac{2\pi}{L}\right)^2 \left[n - \frac{M_n(\omega)}{M_1(\omega)}\right] = \begin{cases} 0 & \text{if } n \neq 1 \\ \alpha_1 & \text{if } n = 1, \end{cases} \tag{3.315}$$

which leads to a contradiction when $n = 1$. □

Theorem 3.108. *Let all the assumptions of Theorem 3.97, and of equation* (3.305) *hold. Then for any* $\bar{u} > 0$, *and for* $s \in (-\delta, 0) \cup (0, \delta)$ *the steady state* $u(s, x)$ *given by equation* (3.228) *of* (3.10a) *is asymptotically stable in the class of functions such that* $\int_0^L u(x)\,\mathrm{d}x = \bar{u}$, *whenever* $\tilde{\alpha}_3 > 0$ *and unstable when* $\tilde{\alpha}_3 < 0$.

Proof. Now we are ready to apply [36 Theorem 1.16]. That implies that there are open intervals I, J with $\alpha_1 \in I, 0 \in J$, chosen such that

$$\gamma\colon I \to \mathbb{R} \qquad \mu\colon I \to \mathbb{R}, \tag{3.316}$$

such that

$$\gamma(\alpha_1) = \mu(0) = 0, \tag{3.317}$$

and

$$u\colon J \to H^2 \qquad w\colon J \to H^2 \tag{3.318}$$

such that

$$u(\alpha_1) = u_1 = w(0), \qquad u(\alpha) - u_1 \in Y, \qquad w(s) - u_1 \in Y. \tag{3.319}$$

Then we have two eigenvalue problems

$$\mathcal{D}_u \mathcal{F}[\alpha, \bar{u}](u(\alpha)) = \gamma(\alpha)\mathcal{M}[u(\alpha)] \tag{3.320}$$

$$\mathcal{D}_u \mathcal{F}[\alpha(s), u(s)](w(\alpha)) = \mu(s)\mathcal{M}[w(s)]. \tag{3.321}$$

Whenever $\mu(s) \neq 0$, we have that

$$\lim_{s \to 0, \mu(s) \neq 0} \frac{-s\alpha'(s)\gamma'(\alpha_1)}{\mu(s)} = 1. \tag{3.322}$$

Thus we are left with computing $\gamma'(\alpha_1)$. In the following, we use roman numerical (i.e. I) to refer to the projected variants of the terms shown below. For this reason, we differentiate equation (3.320) with respect to α and then set $\alpha = \alpha_1$ to obtain

$$\underbrace{-\dot{w}''}_{\text{I}} + \underbrace{\bar{u}\mathcal{K}[u_1]'}_{\text{II}} + \underbrace{\alpha_1 \bar{u}\mathcal{K}[\dot{w}]'}_{\text{III}} = \underbrace{\gamma'(\alpha_1)u_1}_{\text{IV}}. \tag{3.323}$$

Then we multiply this equation by u_1 and integrate by parts. We obtain the following results term-wise. The first term gives us

$$\text{I} = \left(\frac{2\pi}{L}\right)^2 \int_0^L \dot{w} \sin\left(\frac{2\pi x}{L}\right) \mathrm{d}x. \tag{3.324}$$

The second term gives us, recalling the result from Lemma 3.56

$$\text{II} = -2\bar{u}\pi M_1(\omega). \tag{3.325}$$

The third term gives us, applying Lemma 3.46 and Lemma 3.51, that

$$\begin{aligned} \text{III} &= \frac{2\pi}{L}\left(\mathcal{K}[\dot{w}], \sin\left(\frac{2\pi x}{L}\right)\right)_{L^2} = -\left(\dot{w}, \mathcal{K}\left[\sin\left(\frac{2\pi x}{L}\right)\right]\right)_{L^2} \\ &= \frac{-4\pi}{L} M_1(\omega) \int_0^L \dot{w} \cos\left(\frac{2\pi x}{L}\right) \mathrm{d}x. \end{aligned} \tag{3.326}$$

Finally, the last term gives

$$\mathrm{IV} = \gamma'(\alpha_1)\frac{L}{2}. \tag{3.327}$$

Combining all the terms we get

$$\underbrace{\left[\left(\frac{2\pi}{L}\right)^2 - \alpha_1\bar{u}\frac{4\pi}{L}M_1(\omega)\right]}_{\mathrm{V}}\int_0^L \dot{w}\cos\left(\frac{2\pi x}{L}\right)\mathrm{d}x - 2\bar{u}\pi M_1(\omega) = \gamma'(\alpha_1)\frac{L}{2}. \tag{3.328}$$

Note that when substituting α_1 into V, we see that this term is zero, and thus we obtain

$$\gamma'(\alpha_1) = -\left(\frac{2\pi}{L}\right)^2\frac{1}{\alpha_1}. \tag{3.329}$$

Then substituting what we found into equation (3.322), we find that

$$\lim_{s\to 0, \mu(s)\neq 0}\frac{2}{\alpha_1}\left(\frac{2\pi s}{L}\right)^2\frac{\tilde{\alpha}_3}{\mu(s)} = 1. \tag{3.330}$$

Thus we conclude, that

$$\operatorname{sgn}\mu(s) = \operatorname{sgn}\tilde{\alpha}_3, \tag{3.331}$$

for $s \in (0,\delta)\cup(-\delta,0)$.

Then whenever $\tilde{\alpha}_3 < 0$, it directly follows that the nearly bifurcated branch is linearly unstable. If $\tilde{\alpha}_3 > 0$, and if condition (3.305) holds, we have that no eigenvalues but the zero eigenvalue are in that set. Hence, by eigenvalue perturbation, the result follows. □

3.6.2 Comparison to dispersion relation

Classically, to determine the instability of the homogeneous steady state one derives the dispersion relation. Let's do the same for equation (3.7). Let $u(x,t) = \bar{u} + v(x,t)$, where $v(x,t)$ is a small perturbation. Upon substitution

of $u(x,t)$ into equation (3.7), and neglecting the nonlinear terms we obtain

$$v_t(x,t) = v_{xx}(x,t) - \alpha\bar{u}\left(\int_{-1}^{1} v(x+r)\Omega(r)\,\mathrm{d}r\right)_x. \tag{3.332}$$

Now let $v \sim e^{ikx+\lambda t}$, where k and λ are the wave number and frequency respectively, then we obtain

$$\lambda(k) = -k^2 - \alpha\bar{u}ik\int_{-1}^{1} e^{ikr}\Omega(r)\,\mathrm{d}r. \tag{3.333}$$

Upon using the evenness of $\omega(r)$ we can simplify the integral term to obtain

$$\lambda(k) = -k^2 + 2\alpha\bar{u}k\int_{0}^{1} \sin(kr)\,\omega(r)\,\mathrm{d}r. \tag{3.334}$$

Then for aggregations to form, we require that $\mathrm{Re}\,\lambda(k) > 0$ for some k. Hence, such a k has to satisfy the inequality

$$k\int_{0}^{1} \sin(kr)\,\omega(r)\,\mathrm{d}r > \frac{k^2}{2\alpha\bar{u}}. \tag{3.335}$$

On the bounded domain $[0, L]$ the accessible wave numbers are $^{2\pi n}/_{L}$. If $M_n(\omega) > 0$, then we can find the critical numbers α_n, which are given by

$$\alpha > \frac{\pi n}{L\bar{u}M_n(\omega)}. \tag{3.336}$$

These coincide exactly with those found in Lemma 3.83.

3.7 Numerical Verification

In this section we demonstrate some typical pattern formation experienced by equation (3.2).

3.7.1 Numerical implementation

The parabolic equation (3.2) is solved using a method of lines approach based on a finite volume method which is described in [65]. The non-local term is efficiently implemented using the fast Fourier transform technique introduced in [68]. As an integrator for the method of lines we use the ROWMAP integrator introduced by [174] and published on their homepage[3]. This integrator was wrapped using `f2py`[4] into a `scipy`[5] class. We then implemented a method of lines on top of the ROWMAP integrator using `NumPy`[6].

Model Parameter	Value
Domain Size L	2.0
Domain subdivisions per unit length	1024
Diffusion coefficient D	1.0
Adhesion strength coefficient α	6.0
Sensing radius R	1.0
Initial conditions (IC)	$1 + \kappa \sin(x)$

Table 3.1: Parameters for long-time cell adhesion simulations to obtain the steady states of equation (3.2).

3.7.2 Results

Example 3.109. *We continue the example with $L = 2$ and uniform ω (see Example 3.59 and Example 3.102). Since in this particular case $M_n(\omega)$ for even n is zero, only $(\alpha_n, \bar{u})$ with odd n are bifurcation points. Thus we only have solutions with odd number of peaks in this case. The steady states arising from the first two bifurcations are shown in Fig. 3.17.*

In Fig. 3.18 we show the short-time evolution of equation (3.2) *that leads to the single peak steady state shown in Fig. 3.16. The long-time evolution is*

[3] `http://www.mathematik.uni-halle.de/wissenschaftliches_rechnen/forschung/software/`

[4] `https://docs.scipy.org/doc/numpy-dev/f2py/`

[5] `https://www.scipy.org/`

[6] `www.numpy.org`

shown in Fig. 3.19, which clearly is a rotating wave. Since we used periodic boundary conditions it is not surprising to observe rotating waves. Indeed they are commonly observed in reaction diffusion equations with periodic boundary conditions [118].

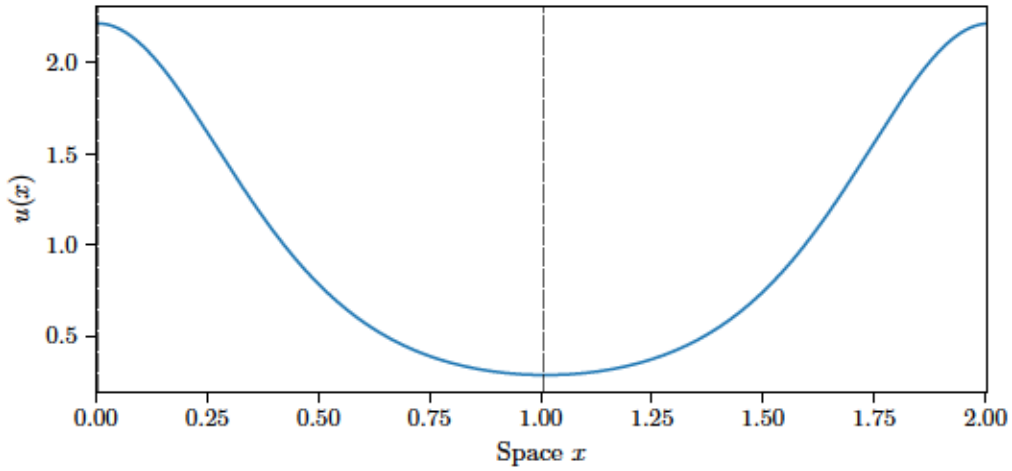

Figure 3.16: The typical single peak steady state equation that is formed for $\alpha = 6$. Thus slightly above the first bifurcation point. The black dashed lines denote the locations of the zeros of $\mathcal{K}[u]$ and $u'(x)$.

3.7.3 Numerical shortcomings

Here we obtained the steady states of equation (3.2) by allowing the time-dependent problem to reach steady states. However, the steady states of many other PDE systems can be solved for directly (i.e. without solving the full time-dependent equation). Commonly numerical schemes developed using the approach of finite difference or finite elements are employed (e.g. Fenics[7]). For nonlinear equations these methods are then combined with an iteration techniques (such as newton-method like operators) to yield solutions. However, using the implementations of these techniques in established numerical frameworks such as Fenics, to solve our nonlinear non-local steady state equation is not straight forward. It may well be that custom solutions are required here.

[7] www.fenics.org

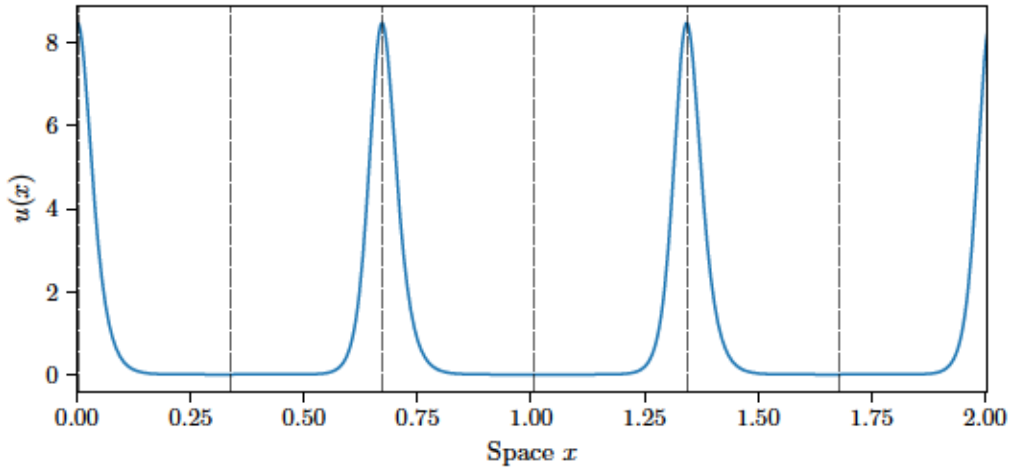

Figure 3.17: The typical triple peak steady state equation that is formed for $\alpha = 150$. Thus slightly above the first bifurcation point. The black dashed lines denote the locations of the zeros of $\mathcal{K}[u]$ and $u'(x)$.

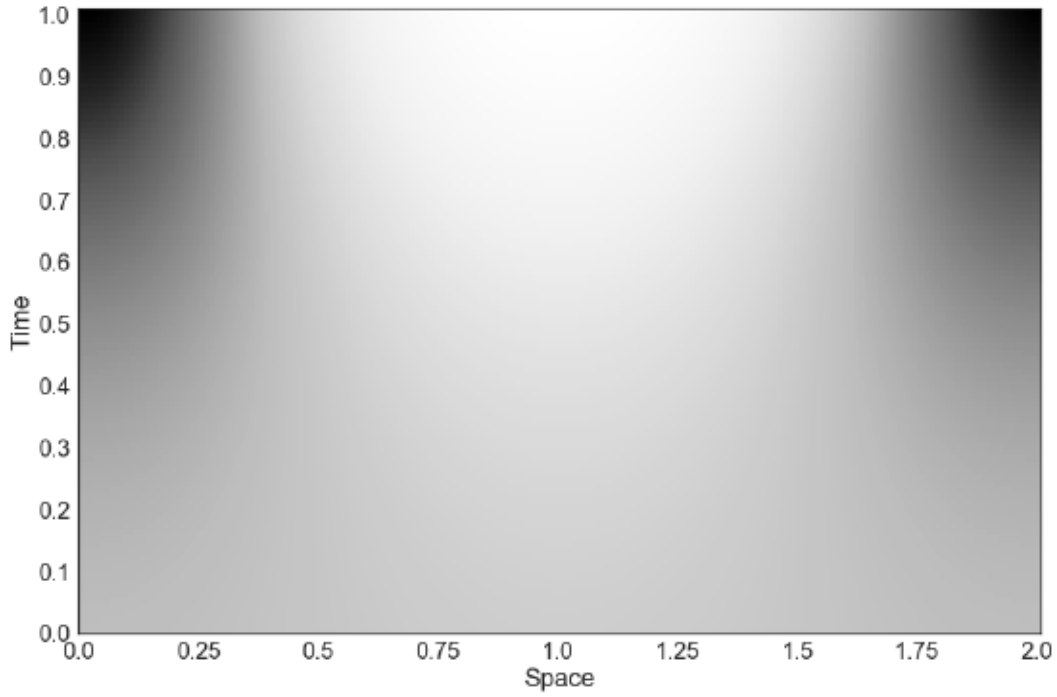

Figure 3.18: Short-time dynamics of equation (3.2) showing the formation of the single peak steady state shown in Fig. 3.16.

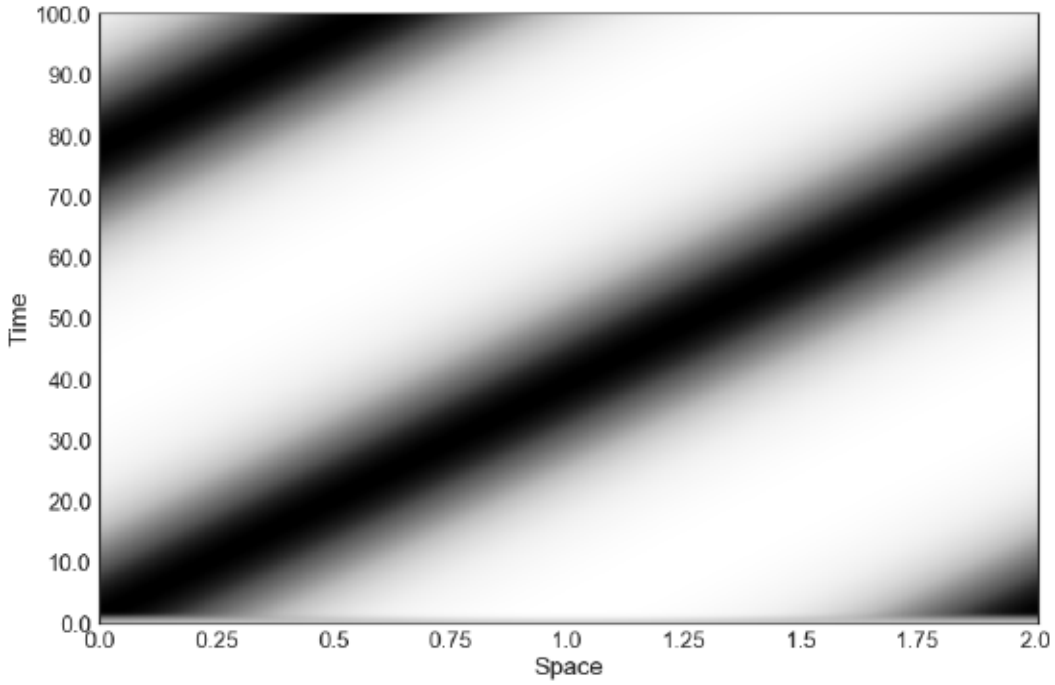

Figure 3.19: Long time numerical solutions of equation (3.2), solved using a finite-volume discretization.

3.8 Discussion

In this chapter, I explored the set of steady-state solutions of the non-local equation of cell-cell adhesion (3.2) on an interval with periodic boundary conditions. The steady states are solutions of equation (3.10), of which the constant function is an obvious solution for all values of α. Using global bifurcation theory pioneered by Crandall and Rabinowitz (outlined in Section 3.5), we identified bifurcation points at which branches of non-trivial solutions split from the branch of trivial solutions. To apply the bifurcation theory outlined in Section 3.5, we cast equation (3.10) as an abstract operator equation $\mathcal{F}[u] = 0$ (see equation (3.171)), whose linearization is shown to be a Fredholm operator with index zero. To ensure that the trivial eigenspaces of the linearization $\mathcal{D}_u \mathcal{F}$ at possible bifurcation points are one-dimensional, we imposed that solutions be reflection symmetric through the domain centre. Since the domain is periodic, this does not reduce the size of $\mathcal{F}^{-1}(0)$. (Indeed, it is equivalent to the well-known decomposition of any periodic function $u \in H^1$ into $u = \bar{u} + v$ where

$v \in H_0^1$). Then, using Fourier series expansions, we establish the existence of the bifurcation points $(\alpha_n, \bar{u})$, whenever the quantity $M_n(\omega) > 0$. This quantity can be interpreted as the n-th Fourier sine coefficient of ω. Then, applying the local bifurcation theorem (Theorem 3.17) of Crandall, Rabinowitz leads to our local bifurcation result Theorem 3.88. While such a local bifurcation analysis is well established in the literature, the true challenge here was the establishment of the required technical properties of the non-local term $\mathcal{K}[u]$ (see Section 3.3.2).

The global bifurcation result for the first solution branch was mathematically more challenging. Indeed, the application of the global version of Rabinowitz's bifurcation theorem is straight forward following the local bifurcation result (see theorem statement Section 3.2). The true challenge lies in discerning which of its two (three) alternatives holds. Using the seminal results of Rabinowitz (nonlinear Sturm-Liouville problems) [144] and Healey, Kielhöfer (equivariant nonlinear elliptic equations) [84] as inspiration, we define function sub-spaces $\mathcal{S}_n^{\pm}$) containing functions whose derivatives have fixed zeros. For nonlinear Sturm-Liouville problems, Rabinowitz used the fact that its solutions cannot have double zeros. Classically, this result is proven by transforming the second-order PDE into a two-dimensional initial value problem (IVP). Initializing this IVP at the double zero will imply that zero is the only solution, which is a contradiction. It is however impossible to transform our non-local steady-state equation into an IVP (not even a delay IVP since our non-local term looks both ahead and behind).

We circumvent this challenge by using the intrinsic symmetries of equation (3.10). Indeed, we show that equation (3.10) is $\mathbf{O}(2)$ equivariant. Employing the ideas of equivariant bifurcation theory [23, 73, 84], we construct, at each bifurcation point, a fixed-point space, which is characterized by the isotropy subgroup at the bifurcation point. In our case, the isotropy subgroup is the dihedral group. Then we are able to apply the global unilateral bifurcation theorem (Theorem 3.22) to the Σ_n reduced problem (see equation (3.233)).

To distinguish between the three possible alternatives of Theorem 3.22, we combine the symmetries of the fixed-point subspace with the symmetry properties of the non-local operator $\mathcal{K}[u]$ (Lemma 3.89), and with the particular

properties of positive steady-states of equation (3.10) (Section 3.4) to find that zeros of the solution's derivative have fixed spatial positions. Using those locations, we introduce our domain tiling Ω_i, on the top of which we construct our nodal sub-spaces $\mathcal{S}_n^{\pm}$. Exploiting the structure of the non-local operator $\mathcal{K}[u]$ one more time (see Lemma 3.95), we are in the position to establish our global bifurcation result (see Theorem 3.97) for the first bifurcation branch.

Unfortunately, the proof of Theorem 3.97 only holds for the first bifurcation branch, i.e., the one in which only a single peak formed. This is because Lemma 3.95 requires that peaks be at minimum separated by two sensing radii. It should be noted however that this is the only shortcoming that hinders the proof of Theorem 3.97 to hold for all bifurcation branches and all nonlinear functions $h(\cdot)$. Further, it seems that an alternative method of proof based on the maximum principle is possible if sign properties of the second derivative of $\mathcal{K}[u]$ can be established. Using the symmetry of the fixed-point subspace, we have shown that this is equivalent to requiring that $\mathcal{K}[u]$ be mid-point convex whenever u is decreasing. Numerical results of steady states suggest that this is indeed the case. Thus it is likely that Theorem 3.97 can soon be extended to cover all bifurcation branches and nonlinear choices of $h(\cdot)$. Such an extension is mathematically significant, since it would parallel the classifications of solutions of nonlinear Sturm-Liouville equations [34, 143] and equivariant nonlinear elliptic equations [84, 85].

It has to be noted that this result does not exclude the possibility of further secondary bifurcations along the solution branches, which may break further symmetries. The analysis of secondary bifurcations has remained a challenge. The only analytical tool available to study secondary bifurcations is the Leray-Schauder degree. More precisely, we are tasked with identifying further changes of the degree along the identified bifurcation branches. This is challenging since no equivalent result to Theorem 3.21 exists for secondary bifurcations. Thus one has to rely on a combination of numerical exploration and mathematical ingenuity in using the equation's structure to identify secondary bifurcations.

The results of Theorem 3.97 could be strengthened if we are in a position to apply the analytic bifurcation theory developed by Dancer [37, 38] (see also [22 Theorem 9.1.1]). This result would give us that the solution branches are

continuous and at each point one has a local re-parameterization [22 Theorem 9.1.1]. Further, the set of possible secondary bifurcations does not have a point of accumulation. For an example of such an application, see [14].

For the case of linear functions within the non-local operator $\mathcal{K}[u]$, we were able to establish that the bifurcation is of pitchfork type. Indeed, both the supercritical and subcritical case are possible depending on the sign of α_3 (see Theorem 3.101) (whose sign is determined by $M_1(\omega)$ and $M_2(\omega)$). Further, using results by Crandall et al. [36], we showed that in the case that $\alpha_3 > 0$ an immediate switch in linear stability of the solution branches takes place at the bifurcation point, while when $\alpha_3 < 0$ the branch of non-trivial solutions initially remains unstable. In this case, numerical results suggest that the switch of stability occurs later.

This abstract bifurcation analysis gives rise to several interesting modelling observations. Most noticeable in our analysis were the mathematical properties of the integral kernel $\Omega(r)$ of the non-local operator $\mathcal{K}[u]$. From the modelling work in Chapter 2, the integral kernel ω describes how likely it is that a cell protrusion reaches a particular target. In our analysis, the properties of Ω enter through the quantity $M_n(\omega)$ at several key moments: (1) the sign of $M_n(\omega)$ determines whether or not we have a bifurcation and (2) it determines whether we immediately observe a switch of stability. Interestingly, the minimum adhesion strength (α_1 in Lemma 3.83) which allows the formation of cell aggregates (non-trivial solutions) is reduced with increasing domain size L, magnitude of $M_n(\omega)$, and size of $h'(\bar{u})$, while no parameter increases α_1. Note that this is solely for the non-dimensionalized equation.

Critical for the development of our classification of solutions was the identification of equation's symmetries. Most important were the symmetrical properties of the non-local term, which models the cell-cell adhesion interactions between cells. Its symmetry properties paralleled those of the classical first-order derivative. Most biological tissues have a high degree of symmetry when viewed under a microscope (e.g., the liver is build up of hexagonal lobules). Even in the experimental results shown in Fig. 1.1, we can almost anticipate the formation of symmetry if only more cells were present. Hence I put forward for future research the questions: To what degree are cellular adhesions (or

non-local forces) responsible for the formation and maintenance of tissues? Does tissue symmetry have functional roles? Could misregulation of cellular adhesions explain the apparent lack of symmetry in cancer tissues?

While the non-local model (3.2) was initially proposed to study cell-sorting, which requires at least two cell populations, there are biological applications with only a single cell population. In zebrafish, for instance, cellular adhesions control the placement of motile progenitor cells during organogenesis [138]. However, the numerical results in Fig. 3.19 suggest that long-time solutions of model (3.2) are rotating waves, which are only observed in equations with periodic boundary conditions (e.g., [118]). Indeed, Paksa et al. [138] reported the physical barriers were critical to the correct placement of the progenitor cells during organogenesis. This highlights the significant modelling challenge of formulating model (3.2) on a bounded domain with no-flux boundary conditions. We address this challenge in Chapter 4.

There are many worthwhile future extensions of this work. The most immediate is an extension to a two-population system to study the possible cell-sorting patterns. Another would be to consider the model extension proposed by Murakawa et al. [123], who added a density dependent diffusion term. An extension to higher spatial dimension would be worthwhile, to more realistically study the formation of tissues. There is a good chance that a tiling could also be found in this situation (see for example the work by Courant who defined tilings in higher dimensions [33]). While the global existence results for solutions of the time-dependent equation (3.2) are known, little is known about their qualitative long-time behaviour. Some questions one may ask are: Do they exhibit coarsening? What is the structure of its global attractor? What are its travelling wave solutions?

Chapter 4

Steady States of an Adhesion Model with a No-Flux Boundary

Let $D \subset \mathbb{R}$ be a bounded subset whose boundary is denoted by ∂D, and let $u(x,t)$ be the density of a cell population at location $x \in D$ and time t. We assume that the population density interacts via cellular adhesions. In 2006, Armstrong et al. [10] proposed the first continuum model of cell-cell adhesion. The Armstrong model is given by the following integro-partial differential equation

$$u_t(x,t) = du_{xx}(x,t) - \alpha \left(u(x,t) \int_{-R}^{R} h(u(x+r,t))\Omega(r)\,\mathrm{d}r \right)_x, \tag{4.1}$$

where d is the diffusion coefficient, R the cell sensing radius and α the strength of the homotypic adhesions, and $h(\cdot)$ is a possibly nonlinear function describing the nature of the adhesive force. For more details on the model parameters, see Chapter 2. The initial condition for equation (4.1) is denoted by $u_0(x)$. Equation (4.1) can be viewed as a conservation equation in which the flux is given by

$$J(x,t) \coloneqq -du_x(x,t) + \alpha u(x,t) \int_{-R}^{R} h(u(x+r,t))\Omega(r)\,\mathrm{d}r. \tag{4.2}$$

In the following, we denote the non-local operator by

$$\mathcal{K}[u](x) \coloneqq \int_{-R}^{R} h(u(x+r,t))\Omega(r)\,\mathrm{d}r. \tag{4.3}$$

Differently to Chapter 3, here the domain D has a boundary. This means that we have to impose boundary conditions and ensure that equation (4.1) is well defined. In particular, the non-local term in equation (4.1) poses a problem, since near the boundary (within one sensing radius R), it is not well-defined. In this chapter, we consider the case of a solid boundary, and want to impose zero-flux boundary conditions. That is, we want to ensure that

$$J(x,t)\cdot\mathbf{n}\Big|_{x\in\partial D} = 0, \tag{4.4}$$

where $\mathbf{n}$ is a unit outward normal vector. Here, we will assume that the diffusion flux and the adhesive flux are independent of each other. That is, to satisfy equation (4.4) we require that

$$\nabla u(x,t)\cdot\mathbf{n}\Big|_{x\in\partial D} = 0, \tag{4.5}$$

and that

$$\mathcal{K}[u](x)\cdot\mathbf{n}\Big|_{x\in\partial D} = 0. \tag{4.6}$$

Condition (4.5) is easily included in the mathematical problem formulation by restricting to the appropriate function space. For instance, define the boundary operator

$$\mathcal{B}[u] = (u'(0), u'(L)), \tag{4.7}$$

and suppose that we have a function space X. Then a space of functions satisfying boundary condition (4.5) is given by

$$X_{\mathcal{B}} \coloneqq X \cap \mathrm{N}[\mathcal{B}]. \tag{4.8}$$

Condition (4.6) is more challenging, and in the subsequent sections we will consider a few approaches to construct $\mathcal{K}[u]$ such that condition (4.6) is satisfied.

Other authors have also considered the problem of well-definedness and

no-flux boundary conditions in equations with non-local operators. Hillen, Painter, Schmeiser [91] considered the global existence of a non-local chemotaxis equations. To correctly define the non-local chemotaxis equation on a bounded domain, they limited the set over which the non-local operator (4.9) integrates, namely

$$\mathring{\nabla}_R v(x) \coloneqq \frac{n}{\omega_D(x) R} \int_{\mathbb{S}_D^{n-1}} \sigma v(x + R\sigma) \, \mathrm{d}\sigma, \tag{4.9}$$

where $\mathbb{S}_D^{n-1}(x) = \{\sigma \in \mathbb{S}^{n-1} : x + \sigma R \in D\}$, and $\omega_D(x) = |\mathbb{S}_D^{n-1}(x)|$. The same approach to ensure well-definedness of the non-local term is briefly discussed in [50]. While the non-local gradient as defined in equation (4.9) ensures that it is well-defined it does not ensure that the no-flux boundary condition (4.7) is satisfied. Xiang who studied global bifurcations of the non-local chemotaxis equation using the global bifurcation analysis by Rabinowitz and Crandall (same approach as in Chapter 3), modified the non-local gradient (4.9) in 1D such that condition (4.6) is satisfied [176]. The construction assumed that two domains are in contact on the boundary, then using a reflection argument through $x = 0, L$. Xiang obtained

$$\mathring{\nabla}_R v(x) \coloneqq \frac{1}{2R} \begin{cases} v(x+R) - v(R-x) & \text{if } 0 \leq x \leq R, \\ v(x+R) - v(x-R) & \text{if } R < x < L - R\,. \\ v(2L-x-R) - v(x-R) & \text{if } L - R \leq x \leq L \end{cases} \tag{4.10}$$

A similar reflection approach is briefly discussed by Topaz, Bertozzi, Lewis [166].

This chapter is structured as follows: In Section 4.1, we use the insights we obtained from the derivation of the non-local cell adhesion model from an underlying random walk (see Chapter 2) to construct a non-local operator that satisfies boundary condition (4.6). In Section 4.2, we study the mathematical properties of this new operator. In Section 4.3, we present some initial findings on the steady states of a non-local cell adhesion model with no-flux boundary conditions. Finally, in Section 4.5, we discuss our findings and indicate areas of future research.

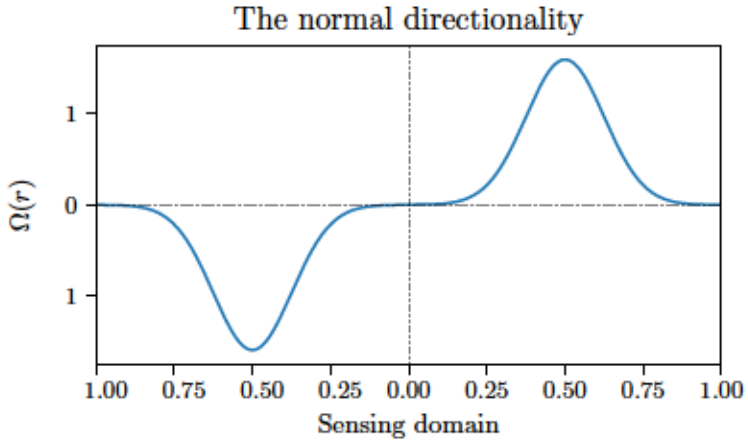

Figure 4.1: A normal directionality function $\Omega(r)$ which has a normal distribution centred at $r = \pm 1/2$ such that $\Omega(\pm 1, 0) = 0$.

4.1 Adhesion model with non-flux boundary conditions.

We begin this section by introducing some notation that will be used throughout this section. In this section, we will assume that the spatial domain is given by, $D = [0, L]$, where $L > 2R$. As in the previous chapter, we explicitly define the non-local term by

$$\mathcal{K}[u(x)](x) \coloneqq \int_V h(u(x+r))\Omega(r)\,\mathrm{d}r, \tag{4.11}$$

where V is the set of all possible headings (see Chapter 2). As discussed in Chapter 2, the set of headings is a symmetric set for example $V = [-R, R]$ or $V = \mathbb{B}^n(R)$ in higher dimensions. Since here we will discuss modifications of the operator in equation (4.11) to satisfy condition (4.6), we introduce a clear distinction between the domain of integration V and the spatial domain D. We introduce the following distinction:

Definition 4.1 (Spatial and Sensing Domains). We call the set D the *spatial domain*, and the set V the *sensing domain* of the non-local gradient $\mathcal{K}[u](x)$, defined in equation (4.11).

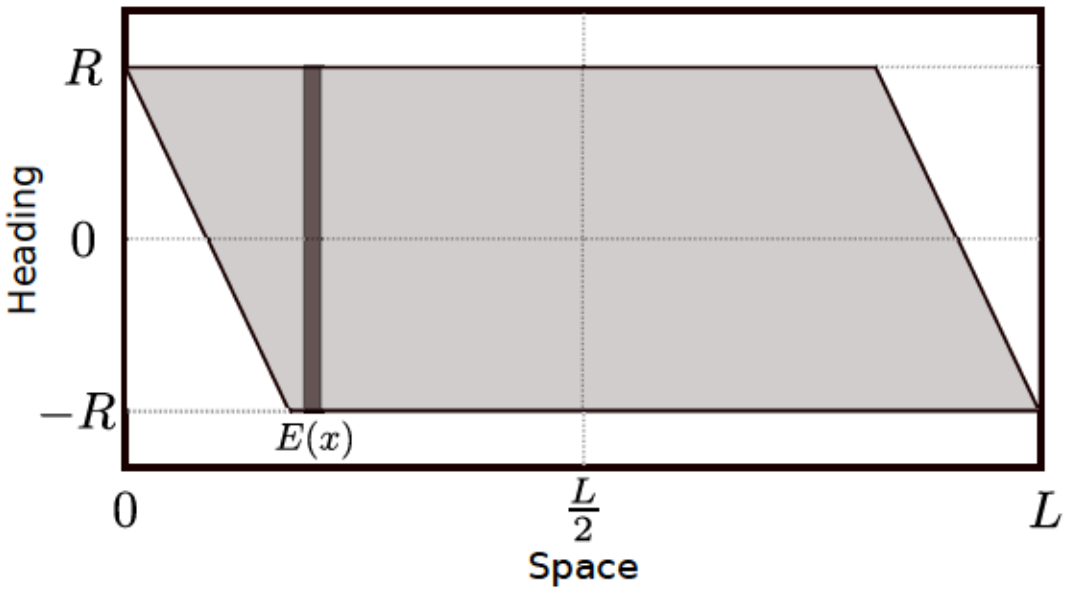

Figure 4.2: An example of the space $D \times V$ with the spatial domain on the x-axis and the sensing domain on the y-axis. A sample sensing slice $E(x)$ of thickness $\mathrm{d}x$ is shown in the darker grey.

Since in this chapter the domain of integration of the non-local operator (4.11) may vary in space, we define a sensing slice contained in the space $D \times V$.

Definition 4.2 (The sensing slice)**.** Let the direct product of the spatial domain D and the sensing domain V be given by the Cartesian product $D \times V$. Then we define *sensing slice* for a fixed $x \in D$ as

$$E(x) = \{\, r \in V : r \in P(x) \,\}, \tag{4.12}$$

where $P(x)$ is a property of r which may depend on the spatial location x, and I will discuss various choices of $P(x)$ later.

The operator $\mathcal{K}$ can be viewed as a function

$$\mathcal{K} : D \times L^p(D) \to \mathbb{R}. \tag{4.13}$$

The definition of appropriate boundary conditions for the non-local operator $\mathcal{K}[u]$ that satisfy condition (4.6) is both a mathematical and modelling problem.

On the one hand we need to ensure that the definition of the non-local operator $\mathcal{K}[u]$ is well-defined near the boundary, on the other hand the precise behaviour of the non-local operator near the boundary is a modelling problem. When a cell encounters a boundary, it might attach to it, be repelled by it, or form a neutral attachment. In either case however the population flux cannot point outside of the domain (i.e. satisfy condition (4.6)). In Section 4.1.1 we will use the number of adhesion bonds $N_b(x)$ and the free space function $f(x)$ near the boundary to define the boundary condition. We are particularly interested in the case that the boundary is neither sticky nor repellent and we will consider a choice where constant solutions are steady states.

We split the development of no-flux boundary conditions of the non-local operator $\mathcal{K}[u]$ into three separate steps. These steps ensure that

1. the non-local operator $\mathcal{K}[u]$ is well-defined near the domain boundary (see Section 4.1.1),

2. the non-local operator $\mathcal{K}[u]$ satisfies the boundary condition (4.6) (see Section 4.1.2),

3. the non-local operator $\mathcal{K}[u]$ describes the required cell behaviour near a physical boundary (see Section 4.1.3).

4.1.1 Naive boundary conditions

Following [50, 91], we can ensure that the non-local operator (4.11) is well-defined near the boundary as follows

$$\mathcal{K}[u](x) \coloneqq \int_{E(x)} h(u(x+r))\Omega(r)\,\mathrm{d}r, \tag{4.14}$$

where $E(x) \coloneqq \{\, r \in V : x + r \in D \,\}$, and $h(\cdot)$ is continuous. Note that $E(x)$ is an example of a sensing slice defined in Definition 4.2. The sensing slice $E(x)$ ensures that the non-local operator in equation (4.14) is well-defined. However, this formulation does not satisfy the no-flux boundary conditions (4.4). This is easily observed when applying the non-local operator (4.14) to the constant

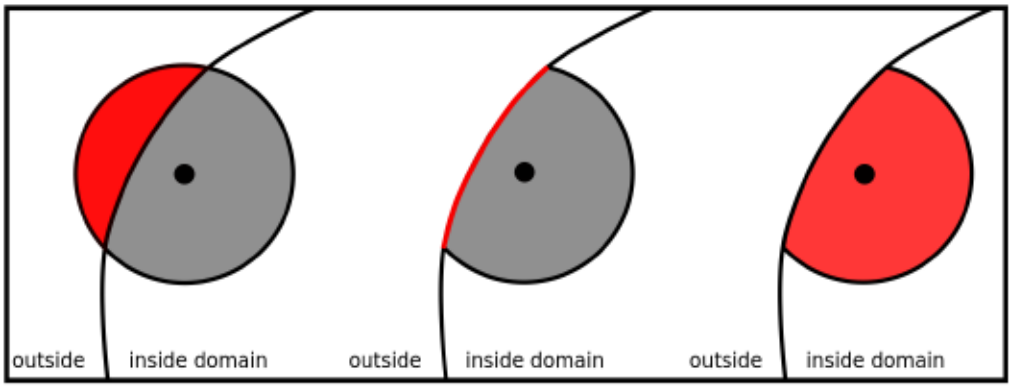

Figure 4.3: The three challenges of non-local operator construction near a domain boundary. The black dot denots the point at which we are computing the non-local term. The sphere denotes a sensing radius of size R. Left: The part of the sensing domain that falls outside the domain, makes the non-local operator not well-defined. Middle: We must ensure that the non-local operator satisfies the no-flux boundary condition on the boundary. Right: The constructed non-local operators are not unique in the region near the boundary.

function. We observe that within a sensing radius R of the boundary $\mathcal{K}[\bar{u}]$ is non-zero, i.e.,

$$\mathcal{K}[\bar{u}] = \int_{E(x)} \Omega(r)\,\mathrm{d}r \neq 0, \quad \text{for } x \in [0, R] \cup [L - R, L]. \tag{4.15}$$

See also Fig. 4.4.

4.1.2 Construction of no-flux boundary conditions

Here we construct the necessary conditions such that the boundary condition (4.6) is satisfied. We use the non-local operator as defined in the derivation of model (4.1) from an underlying random walk (see Chapter 2). In particular, we use the non-local term that is given in terms of the densities of bound adhesion molecules $N_b(x)$, free space $f(x)$, and the distance distribution (see Section 2.3.1). That is,

$$\mathcal{K}[N_b](x) = \int_{-R}^{R} N_b(x + r) f(x + r) \Omega(r)\,\mathrm{d}r. \tag{4.16}$$

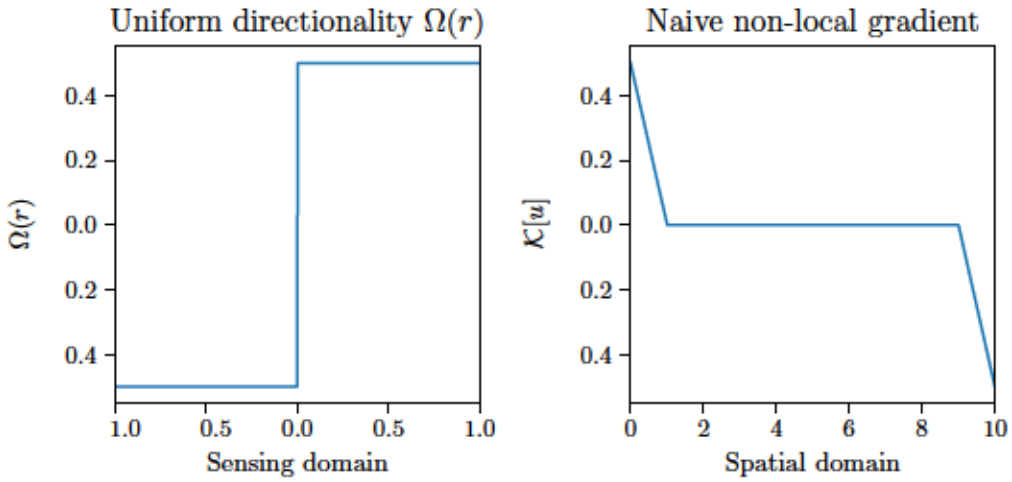

Figure 4.4: Left: The uniform function $\Omega(r)$ plotted with a sensing radius $R = 1$. Right: The naive non-local operator (4.14) with uniform directionality ($\Omega(r)$) applied to a constant function.

To simplify the subsequent discussion, we introduce the following change of variables under the integral,

$$y \coloneqq x + r. \tag{4.17}$$

With this, the non-local term (4.16) becomes

$$\mathcal{K}[N_b](x) = \int_{x-R}^{x+R} N_b(y) f(y) \Omega(y - x) \, \mathrm{d}y. \tag{4.18}$$

The boundary is solid. For this reason, cell protrusions cannot pass through it. Thus, the number of adhesion bonds formed beyond the wall has to be zero. Secondly, the solid wall may have a variety of adhesive properties, such as repulsive or adhesive. Thus, adhesion bonds could be formed on the boundary. These modifications enter the number of adhesion bonds formed as follows,

$$N_b(y) = \begin{cases} \tilde{N}_b(y) & \text{if } y \in \mathrm{int}(D) \\ n_b^0(y)\delta(y) & \text{if } y = 0 \\ n_b^L(y)\delta(y - L) & \text{if } y = L \\ 0 & \text{else} \end{cases}, \tag{4.19}$$

where $n_b^i(x)$ are functions that will be chosen such that the non-local term (4.11) satisfies boundary conditions (4.6). Similarly, we define the free space function as follows

$$f(y) = \begin{cases} \tilde{f}(y) & \text{if } y \in D \\ 0 & \text{else} \end{cases}. \tag{4.20}$$

Since the effect of the free space function and the function describing the formed adhesion bonds are the same, we drop the function $f(\cdot)$ from the subsequent discussion, and focus on $N_b(y)$ defined in equation (4.19).

First consider the non-local term $\mathcal{K}[N_b](x)$ defined in equation (4.18) in the interval $[0, R]$. There, the non-local term (4.18) can be decomposed as follows,

$$\mathcal{K}[N_b](x) = \int_x^{x+R} \tilde{N}_b(y)\Omega(y-x)\,\mathrm{d}y + \int_0^x \tilde{N}_b(y)\Omega(y-x)\,\mathrm{d}y + n_b^0(x)\Omega(-x). \tag{4.21}$$

Then we choose the function $n_b^0(x)$ so that the boundary condition (4.6) is satisfied. That is, for $x = 0$ we set $n_b^0(y)$ to be

$$n_b^0(0) = \frac{-1}{\Omega(0)} \int_0^R \tilde{N}_b(y)\Omega(y-x)\,\mathrm{d}y. \tag{4.22}$$

Similarly, on the interval $[L-R, L]$, we have the following decomposition of the non-local term (4.11)

$$\mathcal{K}[N_b](x) = \int_{x-R}^{x} \tilde{N}_b(y)\Omega(y-x)\,\mathrm{d}y + \int_x^L \tilde{N}_b(y)\Omega(y-x)\,\mathrm{d}y + n_b^L(x)\Omega(L-x). \tag{4.23}$$

To satisfy the no-flux boundary condition (4.6) at $x = L$, we set $n_b^L(y)$ to be

$$n_b^L(L) = \frac{-1}{\Omega(0)} \int_{L-R}^{L} \tilde{N}_b(y)\Omega(y-x)\,\mathrm{d}y. \tag{4.24}$$

To satisfy the boundary condition (4.6), we only have to ensure that the non-local operator is zero at the boundary point. In the region within a single sensing radius of the boundary, however, we can choose the functions $n_b^0(x)$ and $n_b^L(x)$, and hence the behaviour of $\mathcal{K}[u]$ freely.

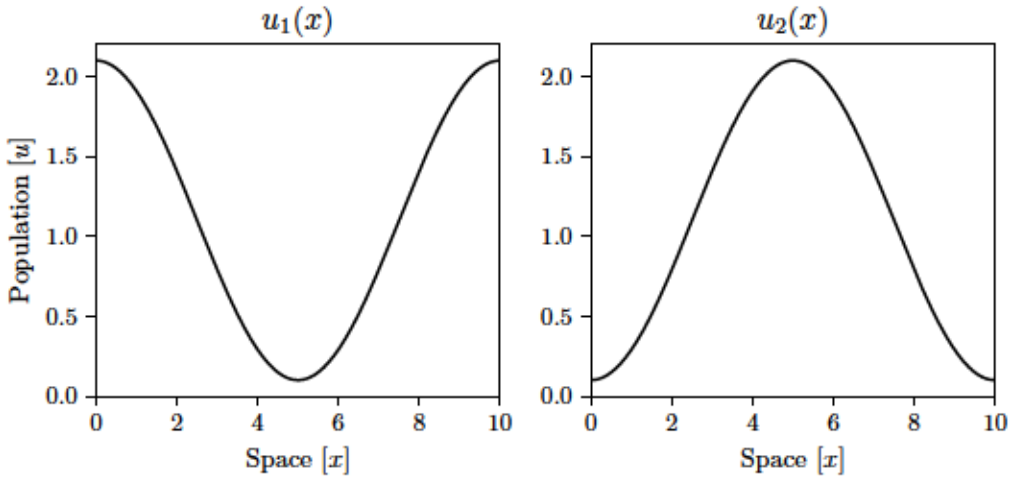

Figure 4.5: The two sample functions $u_1(x)$ (left) and $u_2(x)$ (right) to which we apply the various non-local operators. Important is whether the function has a peak or trough on the boundary. $u_1(x)$ has a peak on the boundary, while $u_2(x)$ features a trough. The average per unit length $\bar{u}_{1,2}$ of both functions is 1.1.

4.1.3 Various behaviours near the boundary

Depending on the adhesive properties of the boundary, a cell may either be attracted, not-affected (neutral), or repelled. In the following, we propose various different behaviours of the non-local term $\mathcal{K}[u]$ within one sensing radius of the boundary.

Example 4.3 (Repellent boundary conditions 1). *Here we choose the function $n_b^0(x)$ such that it satisfies condition (4.22) at $x = 0$ and $n_b^0(R) = 0$ at $x = R$, and is continuous in between. We choose*

$$n_b^0(x) = \frac{1}{\Omega(-x)} \int_0^{R-x} \tilde{N}_b(y)\Omega(y-x)\,\mathrm{d}y. \tag{4.25}$$

Thus resulting in a non-local gradient in $x \in [0, R]$ of

$$\mathcal{K}[N_b](x) = \int_{R-x}^{x+R} \tilde{N}_b(y)\Omega(y-x)\,\mathrm{d}y. \tag{4.26}$$

Similarly, we set $n_b^L(x)$ such that it satisfies condition (4.24) at $x = L$ and

$n_b^L(L-R)=0$. *That is,*

$$n_b^L(x)=\frac{-1}{\Omega(L-x)}\int_{(L-R)-(x-L)}^{L}\tilde{N}_b(y)\Omega(y-x)\,\mathrm{d}y. \tag{4.27}$$

The resulting non-local operator in $[L-R,L]$ *is given by*

$$\mathcal{K}[N_b](x)=\int_{x-R}^{2L-R-x}\tilde{N}_b(y)\Omega(y-x)\,\mathrm{d}y. \tag{4.28}$$

Combining the boundary non-local terms (4.26) *and* (4.28) *with the standard non-local operator* (4.11) *we obtain*

$$\mathcal{K}[N_b](x)=\begin{cases}\displaystyle\int_{R-x}^{x+R}\tilde{N}_b(y)\Omega(y-x)\,\mathrm{d}y & \text{if } x\in[0,R]\\[2ex] \displaystyle\int_{x-R}^{x+R}\tilde{N}_b(y)\Omega(y-x)\,\mathrm{d}y & \text{if } x\in[R,L-R]\\[2ex] \displaystyle\int_{x-R}^{2L-R-x}\tilde{N}_b(y)\Omega(y-x)\,\mathrm{d}y & \text{if } x\in[L-R,L]\end{cases}. \tag{4.29}$$

Note that the $\Omega(\cdot)$ *terms preceding the integrals in equations* (4.25) *and* (4.27) *cancel out.*

Reverting the change of variables (4.17) *we obtain*

$$\mathcal{K}[N_b](x)=\begin{cases}\displaystyle\int_{R-2x}^{R}N_b(x+r)\Omega(r)\,\mathrm{d}r & \text{if } x\in[0,R]\\[2ex] \displaystyle\int_{-R}^{R}N_b(x+r)\Omega(r)\,\mathrm{d}r & \text{if } x\in[R,L-R]\\[2ex] \displaystyle\int_{-R}^{2L-R-2x}N_b(x+r)\Omega(r)\,\mathrm{d}r & \text{if } x\in[L-R,L]\end{cases}. \tag{4.30}$$

In this example we modified the limits of integration so that the operator defined in equation (4.30) *is both well-defined and satisfied the boundary condition* (4.6). *The reason why this is called a repellent operator is demonstrated in Fig. 4.6.*

Example 4.4 (Repellent boundary conditions 2). *In this example, we set*

$$n_b^0(x) = -2n_b^0(0)\int_{x-R}^{0}\Omega(y-x)\,\mathrm{d}y, \tag{4.31}$$

and

$$n_b^L(x) = 2n_b^L(L)\int_{L-x}^{R}\Omega(y-x)\,\mathrm{d}y. \tag{4.32}$$

Then it is easy to see that $n_b^0(x)$ satisfies equation (4.22) and $n_b^L(x)$ satisfies equation (4.24). In the special case that $\omega(r) \equiv 1/2$ this reduces to

$$n_b^0(x) = \frac{x-R}{2R}, \qquad n_b^L(x) = \frac{x-R}{2R}. \tag{4.33}$$

Combining the boundary non-local terms (4.31) and (4.32) with the standard non-local operator (4.11), we obtain

$$\mathcal{K}[N_b](x) = \begin{cases} \displaystyle\int_0^{x+R}\tilde{N}_b(y)\Omega(y-x)\,\mathrm{d}y & \\ \qquad\displaystyle -2n_b^0(0)\int_{x-R}^{0}\Omega(y-x)\,\mathrm{d}y & \text{if } x\in[0,R] \\ \displaystyle\int_{x-R}^{x+R}\tilde{N}_b(y)\Omega(y-x)\,\mathrm{d}y & \text{if } x\in[R,L-R] \\ \displaystyle\int_{x-R}^{L}\tilde{N}_b(y)\Omega(y-x)\,\mathrm{d}y & \\ \qquad\displaystyle +2n_b^L(L)\int_{L-x}^{R}\Omega(y-x)\,\mathrm{d}y. & \text{if } x\in[L-R,L] \end{cases}. \tag{4.34}$$

In this example we continuously reduce the size of the correction terms $n_b^{0,L}$ so that they are zero when the separation to the boundary is above a sensing radius R. This example can be viewed as the naive boundary conditions combined with correction terms $n_b^{0,L}$. This ensures that the non-local operator defined in equation (4.34) is well-defined and zero on the boundary of D. The reason why this is called a repellent operator is demonstrated in Fig. 4.6.

In the following, we will compare the behaviour of the non-local operators which incorporate boundary effects to the behaviour of the periodic non-local

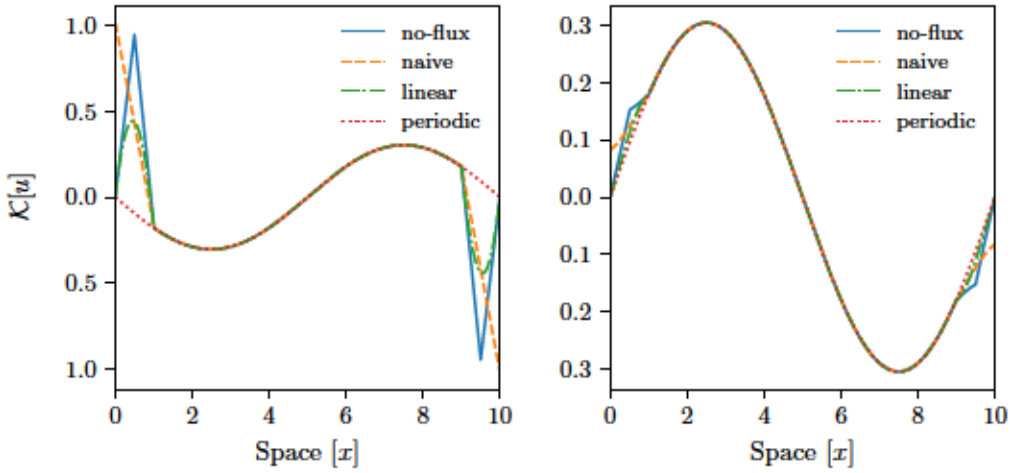

Figure 4.6: A comparison of the various different non-local operators applied to the functions $u_1(x)$ and $u_2(x)$ as shown in Fig. 4.5. The non-flux term (equation (4.30)) applied to $u(x)$ is shown as the sharp solid line, the smooth solid line is the operator defined in Example 4.4 applied to $u(x)$, the periodic operator (defined in Chapter 3) applied to $u(x)$ is shown as a dotted line, and the naive operator (equation (4.14)) is shown as a separated line. Here we used Ω being uniform (see Fig. 4.4).

operator which was used in Chapter 3. In each case, we apply the various non-local operators to two sample functions which are shown in Fig. 4.5.

Comparisons of the repellent non-local operators constructed in this section are presented in Fig. 4.6 with uniform $\Omega(r)$ and in Fig. 4.7 with normal $\Omega(r)$ (see Fig. 4.1 for its functional form). The reason for why these operators are called repellent will become further clear in Section 4.3.2.

We note that the non-local operator constructed in Example 4.3 and Example 4.4 are repellent. In particular, either operator (i.e. (4.30), or (4.34)) is zero when applied to the constant function. Since equation (4.1) conserves mass, we want that the non-local term returns zero when applied to the particular constant $\bar{u}$.

Example 4.5 (Neutral boundary conditions). *We start with the non-local operator constructed in Example 4.3 i.e. equation* (4.30)*, and we add an additional correction function $c(x)$. We require that $c(\hat{x}) = 0$ for $\hat{x} \in \partial D$ such that*

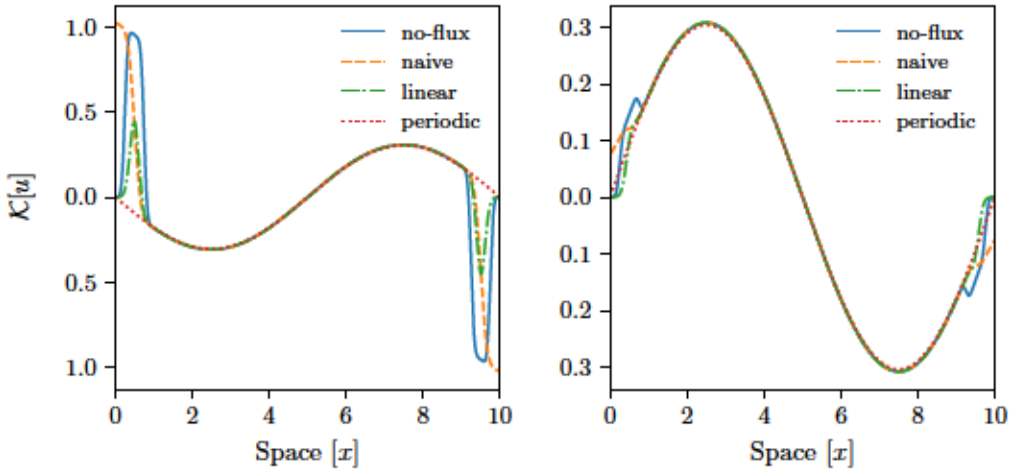

Figure 4.7: A comparison of the various different non-local operators applied to the functions $u_1(x)$ and $u_2(x)$ as shown in Fig. 4.5. Here we used Ω being normal (see Fig. 4.1). The non-flux term (equation (4.30)) applied to $u(x)$ is shown as the sharp solid line, the smooth solid line is the operator defined in Example 4.4 applied to $u(x)$, the periodic operator (defined in Chapter 3) applied to $u(x)$ is shown as a dotted line, and the naive operator (equation (4.14)) is shown as a separated line.

$\mathcal{K}[u]$ still satisfies boundary condition (4.6).

$$\mathcal{K}[u](x) \coloneqq \int_{f_1(x)}^{f_2(x)} u(x+r)\Omega(r)\,\mathrm{d}r - c(x). \tag{4.35}$$

We now want to choose $c(x)$ such that $\mathcal{K}[\bar{u}](x) = 0$ for any $x \in D$. We let $c(x)$ be defined by

$$c(x) \coloneqq \begin{cases} c^0(x) & \text{if } x \in [0, R] \\ 0 & \text{if } x \in [R, L-R]\,, \\ c^L(x) & \text{if } x \in [L-R, L] \end{cases} \tag{4.36}$$

where we will determine $c^0(x)$ and $c^L(x)$ now. For $x \in [0, R/2]$ we have that

$$\begin{aligned} \mathcal{K}[\bar{u}](x) &= \bar{u}\int_{R-2x}^{R} \Omega(r)\,\mathrm{d}r - c^0(x) \\ &= \bar{u}\int_{R-2x}^{R} \omega(r)\,\mathrm{d}r - c^0(x) = 0, \end{aligned} \tag{4.37}$$

and for $x \in [R/2, R]$, *we have that*

$$\begin{aligned}\mathcal{K}[\bar{u}](x) &= \bar{u}\int_{R-2x}^{R} \Omega(r)\,\mathrm{d}r - c^0(x) \\ &= \bar{u}\left[\int_0^R \omega(r)\,\mathrm{d}r - \int_{R-2x}^{0} \omega(r)\,\mathrm{d}r\right] - c^0(x).\end{aligned} \tag{4.38}$$

Thus, we have that

$$c^0(x) \coloneqq \begin{cases} \bar{u}\displaystyle\int_{R-2x}^{R} \omega(r)\,\mathrm{d}r & \text{if } x \in [0, R/2] \\ \\ \bar{u}\displaystyle\int_{2x-R}^{R} \omega(r)\,\mathrm{d}r & \text{if } x \in [R/2, R] \end{cases}. \tag{4.39}$$

We carry out the same operator for the right hand side boundary, i.e., $[\,L-R, L\,]$.

For $x \in [L-R, L-R/2]$, *we have that*

$$\begin{aligned}\mathcal{K}[\bar{u}](x) &= \bar{u}\int_{-R}^{2L-2x-R} \Omega(r)\,\mathrm{d}r - c^L(x) \\ &= \bar{u}\left[\int_0^{2L-2x-R} \omega(r)\,\mathrm{d}r - \int_{-R}^{0} \omega(r)\,\mathrm{d}r\right] - c^L(x),\end{aligned} \tag{4.40}$$

and for $x \in [L-R/2, L]$, *we have*

$$\begin{aligned}\mathcal{K}[\bar{u}](x) &= \bar{u}\int_{-R}^{2L-R-2x} \Omega(r)\,\mathrm{d}r - c^L(x) \\ &= -\bar{u}\int_{-R}^{2L-2x-R} \omega(r)\,\mathrm{d}r - c^L(x) = 0.\end{aligned} \tag{4.41}$$

Thus, we have that

$$c^L(x) \coloneqq \begin{cases} -\bar{u}\displaystyle\int_{2L-2x-R}^{R} \omega(r)\,\mathrm{d}r & \text{if } x \in [L-R, L-R/2] \\ \\ -\bar{u}\displaystyle\int_{-R}^{2L-2x-R} \omega(r)\,\mathrm{d}r & \text{if } x \in [L-R/2, L]. \end{cases} \tag{4.42}$$

With that definition of the function $c(x)$, *we can rewrite the non-local op-*

erator $\mathcal{K}[u]$ as

$$\mathcal{K}[u](x) \coloneqq \int_{f_1(x)}^{f_2(x)} [\, u(x+r) - \bar{u} \,]\, \Omega(r)\, \mathrm{d}r. \tag{4.43}$$

Note that this definition does not change the definition of the non-local term far away from the boundary (i.e. when x is at least a distance of R from the boundary) since there $\mathcal{K}[\bar{u}] = 0$. It only changes the definition of the operator near the boundary. For a numerical example of how the operator defined in equation (4.43) acts on functions see Fig. 4.8.

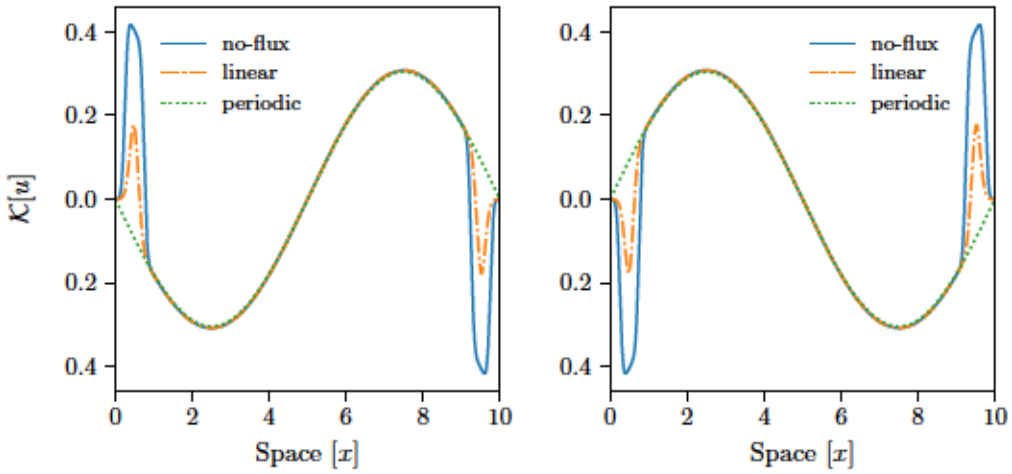

Figure 4.8: A comparison of the neutral non-local operator defined in equation (4.43) applied to the functions $u_1(x)$ and $u_2(x)$ as shown in Fig. 4.5. The non-flux term (equation (4.30)) applied to $u(x)$ is shown as the sharp solid line, the smooth solid line is the operator defined in Example 4.4 applied to $u(x)$, the periodic operator (defined in Chapter 3) applied to $u(x)$ is shown as a dotted line, and the naive operator (equation (4.14)) is shown as a separated line. Here we used Ω being normal (see Fig. 4.1).

4.1.4 Discussion of no-flux boundary operators

We recall from Chapter 3, that the periodic non-local term always points toward an increasing "mass" of $u(x)$. Or in the terminology of Chapter 2, the cell

polarization points in the direction in which the most new adhesion bonds were formed. However, when referring to the no-flux operator constructed in Example 4.3 and Example 4.4 this is no longer the case. Indeed, near the boundary the no-flux operators have opposite sign compared to the periodic non-local operator (see Fig. 4.6). For this reason, we refer to them as repellent. Using the terminology of Chapter 2, we can say that the polarization of a cell approaching the boundary reverses. This is consistent with biological observations of cells approaching solid boundaries [138].

The (neutral) non-local operator derived in Example 4.5 switches between a repulsive and attractive behaviour, depending on whether the population size is above or below the mass per unit length ($\bar{u}$). The neutral non-local operator has the important property that $\mathcal{K}[\bar{u}] = 0$ for all $x \in D$. For this reason, the bifurcation approach used in Chapter 3 could be applied. It is interesting to note, that only recently (2016) Watanabe et al. also used the comparison with the mass per unit length to obtain solutions of Burger's equation on a bounded domain with no-flux boundary conditions [171].

4.2 Mathematical properties of the non-local operator

In what follows we will concentrate on the non-local term defined in equation (4.30), see Example 4.3. For this section, we rewrite the non-local operator as an integral over the *sensing domain*, the boundary behaviour will be encoded using the choice of the sensing slice, which will be encoded using the indicator function of the sensing slice. That is, suppose that for $x \in D$ we have $E(x) \subset V$. Further, in the following discussion we concentrate on the changes due to the boundary requirements, and for that reason we do not consider a non-linear function under the integral.

Definition 4.6. Let X, Y be Banach spaces of functions, then we define the operator $\mathcal{K}: X \to Y$ by

$$\mathcal{K}[u(x)](x) = \int_{E(x)} u(x+r)\Omega(r)\,\mathrm{d}r. \tag{4.44}$$

The directionality function Ω is assumed to satisfy the following conditions

(A1) $\Omega(r) = \frac{r}{|r|}\omega(r)$, where $\omega(r) = \omega(-r)$,

(A2) $\omega(r) \geq 0$,

(A3) $\omega \in L^1(V) \cap L^\infty(V)$,

(A4) $\|\omega\|_{L^1(V)} = {}^1/_2$.

Further we assume that the set $E(x)$ has continuous boundary, and is defined as follows. The domain of integration of this function is very important. The domain of integration of this function is represented in Fig. 4.2. Rewriting equation (4.30) in terms of spatially dependent integration limits, allows us to rewrite the operator as

$$\mathcal{K}[u](x) = \int_{f_1(x)}^{f_2(x)} u(x+r)\Omega(r)\,\mathrm{d}r, \tag{4.45a}$$

where

$$f_1(x) = \begin{cases} R - 2x, & \text{if } x \in [0, R] \\ -R, & \text{if } x \in [R, L] \end{cases}, \tag{4.45b}$$

and

$$f_2(x) = \begin{cases} R, & \text{if } x \in [0, L-R] \\ 2L - 2x - R, & \text{if } x \in [L-R, L] \end{cases}. \tag{4.45c}$$

Using these two functions, we define a new sensing slice (see Definition 4.2)

$$E(x) = \{\, r \in V : f_1(x) \leq r \leq f_2(x) \,\}. \tag{4.46}$$

Later, we write the operator in equation (4.44) as

$$\mathcal{K}[u](x) = \int_V \chi_{E(x)}(r) u(x+r)\Omega(r)\,\mathrm{d}r, \tag{4.47}$$

using the indicator function $\chi_{E(x)}(r)$ of the sensing slice $E(x)$, as defined in equation (4.46).

4.2.1 Set Convergence

For the calculus of indicator functions we consider convergence in general metric spaces. Let $(V, \mathcal{A}, \mu)$ be a sigma-finite measure space. Then, let $A, B \in \mathcal{A}$ and we define the symmetric difference of A and B by

$$A \triangle B = (A \cup B) \setminus (A \cap B). \tag{4.48}$$

The function

$$d\colon \mathcal{A} \times \mathcal{A} \to \mathbb{R}, \tag{4.49}$$

defined by

$$d(A, B) = \mu(A \triangle B) \quad \text{for } A, B \in \mathcal{A}, \tag{4.50}$$

is a pseudometric and is called the Fréchet-Nikodym metric [17]. This allows us to view any sigma-finite measure space as a pseudometric space. We can turn this into a metric by introducing the following equivalence relation

$$X \sim Y \quad \Leftrightarrow \quad \mu(X \triangle Y) = 0. \tag{4.51}$$

It is easy to see that $A \sim B$ if and only if they differ by a set of measure zero. If we denote the set of equivalence classes of this relation by $\mathcal{A}/\mu$, then the function (4.49) is extended by setting $d(\tilde{A}, \tilde{B}) = d(A, B)$ where $\tilde{A}, \tilde{B} \in \mathcal{A}/\mu$. This turns $\mathcal{A}/\mu$ into a complete metric space [17 Theorem 1.12.6].

Now suppose that $V = [a, b]$, and that we have a spatial domain D given, and suppose that we have $f_{1,2}\colon D \to V$ continuous. Then we define the set

$$Y \coloneqq \{\, r \in V\colon f_1(x) \leq r \leq f_2(x) \,\} \subset V. \tag{4.52}$$

Then let $(x_n) \subset D$ such that $x_n \to x \in D$. We now define

$$Y_n \coloneqq \{\, r \in V\colon f_1(x_n) \leq r \leq f_2(x_n) \,\}. \tag{4.53}$$

Then the symmetric difference of Y and Y_n is

$$Y_n \triangle Y = \{\, r \in V\colon \min(f_1(x), f_1(x_n)) \leq r \leq \max(f_1(x), f_1(x_n)),$$

$$\min(f_2(x), f_2(x_n)) \leq r \leq \max(f_2(x), f_2(x_n))\,\}\,. \quad (4.54)$$

Then we can simply compute the measure of this set by

$$\mu(Y_n \,\triangle\, Y) = |f_1(x_n) - f_1(x)| + |f_2(x_n) - f_2(x)|. \quad (4.55)$$

As both $f_{1,2}$ are continuous, we have that

$$\mu(Y_n \,\triangle\, Y) \to 0 \quad \text{as } x_n \to x. \quad (4.56)$$

We summarize the finding in the following lemma.

Lemma 4.7. *Let $(V, \mathcal{A}, \mu)$ be a measure space, on this space we define the pseudometric* (4.49)*, which with the equivalence relation* (4.51) *becomes a metric. With this metric, $(V, \mathcal{A}, \mu)$ becomes a complete metric space. Suppose we have the set*

$$E(x) \coloneqq \{\, r \in V \colon f_1(x) \leq r \leq f_2(x)\,\}\,, \quad (4.57)$$

then $E(x)$ is continuous in the following sense, if $(x_n) \subset \mathbb{R}$ such that $x_n \to x$, then

$$E(x_n) \to E(x) \quad \Leftrightarrow \quad \mu(E(x_n) \,\triangle\, E(x)) \to 0. \quad (4.58)$$

Proof. See the above construction. □

Next we collect some properties of the indicator functions of symmetric differences. Suppose that $A, B \in \mathcal{A}$, then

$$\chi_A(r) = \begin{cases} 1 & \text{if } r \in A \\ 0 & \text{if } r \notin A. \end{cases} \quad (4.59)$$

Then from the definition of the symmetric product (4.48), we compute its characteristic function as,

$$\chi_{A \triangle B}(r) = \chi_A(r) + \chi_B(r) - 2\chi_{A \cap B}(r). \quad (4.60)$$

Next we note that

$$\chi_{A\cap B}(r) = \chi_A(r)\chi_B(r) = \min(\chi_A(r), \chi_B(r)). \tag{4.61}$$

Rewriting the minimum in terms of an absolute value, and substituting this into equation (4.60), we obtain

$$\chi_{A\triangle B}(r) = |\chi_A(r) - \chi_B(r)|. \tag{4.62}$$

4.2.2 Estimates for the no-flux non-local operator

In this section, we explore estimates for the no-flux non-local operator defined in equation (4.44). To distinguish between the norms over the sensing domain V and the spatial domain D, we introduce norm notation that indicates the set over which the norm is taken. That is given a domain X, the L^p norm over that set is denoted

$$|u|_{p,X} := \left(\int_X |u(x)|^p \, \mathrm{d}x\right)^{1/p}. \tag{4.63}$$

We first check that the function defined under the integral in equation (4.44) is integrable.

Lemma 4.8. *Let $p \geq 1$, $u \in L^p(D)$, and let $\Omega(\cdot)$ satisfy A1–A4. Further suppose that $E(x) \subset V, \forall x \in D$, then the function*

$$h(r; x) := \chi_{E(x)}(r)u(x + r)\Omega(r), \tag{4.64}$$

is in $L^1(V), \forall x \in D$.

Proof. Fix $x \in D$. Then

$$\int_V |\chi_{E(x)}(r)u(x + r)|^p \, \mathrm{d}r \leq \int_D |u(x)|^p \, \mathrm{d}x. \tag{4.65}$$

Thus, $\chi_{E(x)}(\cdot)u(x+\cdot) \in L^p(V)$. From assumption A3, we have that $\Omega \in L^\infty(V)$

then $\Omega \in L^q(V)$, $1 \leq q < \infty$. Thus, we apply Hölder's inequality and find that

$$\begin{aligned}\int_V |\chi_{E(x)}(r)u(x+r)\Omega(r)|\,\mathrm{d}r &\leq \left(\int_V |\chi_{E(x)}(r)u(x+r)|^p\,\mathrm{d}r\right)^{1/p}\left(\int_V |\Omega|^q\,\mathrm{d}r\right)^{1/q} \\ &\leq |u|_{p,D}|\Omega|_{\infty,V},\end{aligned} \tag{4.66}$$

where q is such that $1/p + 1/q = 1$. □

Next we investigate the range of $\mathcal{K}[u]$, in particular we prove the following lemma.

Lemma 4.9 (Non-local Regularity). *Let $D \subset \mathbb{R}$ bounded, let $p \geq 1$, and let $u \in L^p(D)$. Then we define the function*

$$x \to \mathcal{K}[u](x), \tag{4.67}$$

where $\mathcal{K}[u](x)$ is defined in equation (4.44), and A1 to A4 are satisfied. Then $\mathcal{K}[u] \in L^p(D)$, in particular the following holds

$$|\mathcal{K}[u]|_{p,D} < |u|_{p,D}|\Omega|_{\infty,V}. \tag{4.68}$$

Proof. Then by applying Theorem B.1 to equation (4.45a), we obtain

$$\begin{aligned}|\mathcal{K}[u](x)|_p &= \left|\int_{f_1(x)}^{f_2(x)} u(x+r)\Omega(r)\,\mathrm{d}r\right|_p \leq \int_V |u(x+r)\Omega(r)|_p\,\mathrm{d}r \\ &= \int_V \left\{\int_{g_1(r)}^{g_2(r)} |u(x+r)|^p\,\mathrm{d}x\right\}^{1/p} |\Omega(r)|\,\mathrm{d}r.\end{aligned} \tag{4.69}$$

Upon the application of Fubini's theorem the order of integration switches, and the new limits of integration are given by

$$g_1(r) = \frac{R-y}{2} \qquad g_2(r) = \frac{2L-y-R}{2}. \tag{4.70}$$

These functions describe the right and left vertical limits of the box in Fig. 4.2.

Note that $g_2(r) - g_1(r) = L - R$. We find, that

$$|\mathcal{K}[u](x)|_p \leq \int_{-R}^{R} \left\{ \int_{\frac{R-r}{2}}^{\frac{2L-r-R}{2}} |u(x+r)|^p \, \mathrm{d}x \right\}^{1/p} |\Omega(r)| \, \mathrm{d}r \tag{4.71}$$

$$< \int_{-R}^{R} |u|_p |\Omega(r)| \, \mathrm{d}r = |u|_{p,D} |\Omega|_{1,V} \leq |u|_{p,D}. \tag{4.72}$$

Note that $|\Omega|_{1,V} = 1$ from A4. □

Using the result of Lemma 4.9, we show that $\mathcal{K}$ is a continuous operator acting on $L^p(D)$.

Corollary 4.10. *The map $\mathcal{K}: L^p(D) \to L^p(D)$, defined by equation (4.44) is continuous.*

Proof. Let $(u_n) \subset L^p(D)$ such that $u_n \to u$ as $n \to \infty$, then

$$|\mathcal{K}[u_n] - \mathcal{K}[u]|_{p,D} = |K[u_n - u]|_{p,D} \leq |u_n - u|_{p,D}, \tag{4.73}$$

where the last inequality is by Lemma 4.9. □

Lemma 4.11. *Suppose in addition to the assumptions of Lemma 4.8, that $u \in \mathcal{C}^0(D)$, then the function defined by*

$$H(x) \coloneqq \int_V \chi_{E(x)}(r) u(x+r) \Omega(r) \, \mathrm{d}r, \tag{4.74}$$

is continuous.

Proof. Let $(x_n) \subset D$ such that $x_n \to x \in D$. Then,

$$\begin{aligned}
H(x) - H(x_n) &= \int_V \left\{ \chi_{E(x)}(r) u(x+r) - \chi_{E(x_n)} u(x_n + r) \right\} \Omega(r) \, \mathrm{d}r \\
&= \int_V \left\{ \chi_{E(x)}(r) u(x+r) - \chi_{E(x_n)} u(x_n + r) \right. \\
&\quad + \chi_{E(x)\cap E(x_n)}(r) u(x_n + r) - \chi_{E(x)\cap E(x_n)}(r) u(x_n + r) \\
&\quad \left. + \chi_{E(x)\cap E(x_n)}(r) u(x+r) - \chi_{E(x)\cap E(x_n)}(r) u(x+r) \right\} \Omega(r) \, \mathrm{d}r \\
&= \int_V \left\{ u(x+r) \chi_{E(x)}(r) \left(\chi_{E(x)}(r) - \chi_{E(x_n)}(r) \right) \right.
\end{aligned}$$

$$+ u(x_n + r)\chi_{E(x_n)}(r)\left(\chi_{E(x_n)}(r) - \chi_{E(x)}(r)\right)$$
$$+ \chi_{E(x)\cap E(x_n)}(r)\left(u(x+r) - u(x_n+r)\right)\Big\}\,\Omega(r)\,\mathrm{d}r.$$

Then we obtain

$$|H(x) - H(x_n)| \leq |u|_\infty |\Omega|_\infty \left[2\int_V \left|\chi_{E(x)}(r) - \chi_{E(x_n)}(r)\right| \mathrm{d}r \right.$$
$$\left. + \int_{E(x)\cap E(x_n)} |u(x+r) - u(x_n+r)|\,\mathrm{d}r \right].$$

For the integrals we obtain, that

$$\int_V |\chi_{E(x)}(r) - \chi_{E(x_n)}(r)|\,\mathrm{d}r = \int_{E(x)\triangle E(x_n)} \mathrm{d}r = \mu(E(x) \triangle E(x_n)).$$

By Lemma 4.7, we have that $\mu(E(x) \triangle E(x_n)) \to 0$ as $n \to \infty$. The second integral converges by the continuity of $u(\cdot)$. Hence, $H(\cdot)$ is continuous. □

Corollary 4.12. *Suppose that all the assumptions of Lemma 4.8 hold, then the function defined in equation* (4.44) *is continuous.*

Proof. Let $x_n \to x$ in D, and let $(u_m) \subset C^0(D)$ such that $u_m \to u$ in $L^p(D)$,

$$\begin{aligned}\mathcal{K}[u](x) - \mathcal{K}[u](x_n) &= \mathcal{K}[u](x) - \mathcal{K}[u_m](x) \\ &\quad + \mathcal{K}[u_m](x_n) - \mathcal{K}[u](x_n) + \mathcal{K}[u_m](x) - \mathcal{K}[u_m](x_n) \\ &\leq 2|u_m - u|_p |\Omega|_{\infty,V} + |\mathcal{K}[u_m](x) - \mathcal{K}[u_m](x_n)|.\end{aligned}$$

The first term vanished due to the density of the smooth functions in $L^p(D)$ and Lemma 4.9. The second terms vanished by Lemma 4.11. □

In summary we have shown that whenever $u \in L^p(D)$ and the sensing domain $E(x)$ is continuous in the sense of Lemma 4.7 we have that the no-flux non-local term in equation (4.11) is continuous.

4.2.3 Weak non-local derivative

Since in equation (4.1) we are taking the derivative of the non-local term $\mathcal{K}[u]$ and since due to the spatial dependence of the integration limits in (4.30), we

cannot simply interchange the derivative operator with the integration. The goal of this sub-section is to understand how we can interchange the order of differentiation and integration. The spatial dependence of the integration limits is equivalent to the occurrence of an indicator function of the sensing domain (see equation (4.44)) under the integral. Since the indicator function is not even continuous, we have to to employ the notion of generalized functions. For the following discussion, we denote the space of test functions by $\mathcal{D}(D)$, and the space of generalized function or distributions by $\mathcal{D}'(D)$. In the end, we are interested in the case in which $\mathcal{D}(D) = \mathcal{C}^\infty(D)$.

For the sake of clarity, we briefly introduce generalized functions. The definitions are based on Rudin [150], and Schwartz [155], and the discussion on weak differentiability [31].

Definition 4.13 (Generalized function [150]). Let $f: D \to \mathbb{R}$, such that $f \in L^1_{\text{loc}}(D)$, then f generates the following functional

$$f \to T_f \in \mathcal{D}'(D) \qquad \text{by} \quad \langle f, \phi \rangle = \langle T_f, \phi \rangle = \int_D f\phi \, \mathrm{d}x. \tag{4.75}$$

Note we can understand the space $\mathcal{D}'(D)$ using the weak star topology. We now extend the notion of a generalized function to a function, which takes an additional parameter, denoted by v.

Definition 4.14 (Generalized non-local function [31]). Let $f: D \times V \to \mathbb{R}$ be a generalized function in $x \in D$ for all $v \in V$, in the sense of Definition 4.13, such that

$$\int_V \left(\int_D f(x, v)\phi(x) \, \mathrm{d}x \right) \mathrm{d}v, \tag{4.76}$$

exists $\forall \phi \in \mathcal{D}(D)$. Then the function

$$g(x) = \int_V f(x, v) \, \mathrm{d}v, \tag{4.77}$$

generates the following functional

$$g \to T_g \in \mathcal{D}'(D) \quad \text{by} \quad \langle g, \phi \rangle = \langle T_g, \phi \rangle = \int_D g(x)\phi(x) \, \mathrm{d}x. \tag{4.78}$$

Remark 4.15. Note that condition (4.76) is easily satisfied for a function f that is integrable on $U \times V$. Further note that, if $\mathcal{D} = \mathcal{C}_c^\infty(U)$ then we only need local integrability in U just as in Definition 4.13. Since, if the function

$$x \to \int_V |f(x,v)|\,\mathrm{d}v, \tag{4.79}$$

is continuous, then it is bounded and achieves its extreme values on any compact set $K \subset\subset U$. Hence the function is locally integrable in x, and so satisfies the requirements of Definition 4.14.

From Lemma 4.11, we have that $\mathcal{K}[u]$ is continuous and then satisfies condition (4.76) in Definition 4.14 by Remark 4.15.

We find a condition that the functional T_g in Definition 4.14 is indeed continuous, in the subsequent lemma.

Lemma 4.16 ([31]). *The functional T_g defined in Definition 4.14, is continuous whenever*

$$\int_V \sup_n |\langle f, \phi_n \rangle|\,\mathrm{d}v < \infty, \tag{4.80}$$

for every convergence sequence ϕ_n of test functions in $\mathcal{D}(U)$.

For Lemma 4.16, we give a more detailed proof as the one in [31].

Proof. We are required to show that the function g does indeed generate a continuous linear functional on the $\mathcal{D}(U)$. Let $\phi_n \subset \mathcal{D}(U)$ such that $\phi_n \to \phi$ in $\mathcal{D}(U)$, further let the common compact support of ϕ_n be denoted by $K \subset\subset U$. For this proof, we define the following sequence

$$h_n(v) \coloneqq \langle f(\cdot, v), \phi_n \rangle\,. \tag{4.81}$$

We find, that

$$\begin{aligned}\langle f(\cdot,v), \phi_n - \phi\rangle &= \int_U f(x,v)\,(\phi_n - \phi)\,(x)\,\mathrm{d}x = \int_K f(x,v)\,(\phi_n - \phi)\,(x)\,\mathrm{d}x \\ &\leq \|\phi_n - \phi\|_\infty \int_K f(x,v)\,\mathrm{d}x.\end{aligned}$$

Then as long $f(\cdot, v) \in L^1_{\text{loc}}(U)$ for all $v \in V$, we have the integral in the previous line is finite and thus

$$\langle f(\cdot, v), \phi_n \rangle \to \langle f(\cdot, v), \phi \rangle \quad \forall v \in V. \tag{4.82}$$

Next we need to show that the sequence h_n is dominated by an integrable function

$$|h_n(v)| = \left| \int_U f(x, v)\phi_n(x)\,\mathrm{d}x \right| \leq \sup_n \left| \int_U f(x, v)\phi_n(x)\,\mathrm{d}x \right|. \tag{4.83}$$

Then for integrability we require that,

$$\int_V \left(\sup_n \left| \int_U f(x, v)\phi_n(x)\,\mathrm{d}x \right| \right) \mathrm{d}v < \infty. \tag{4.84}$$

This is exactly the condition we require in the lemma. Then by the Lebesgue dominated convergence theorem we conclude that,

$$\lim_n \int_V \langle f, \phi_n \rangle \,\mathrm{d}v = \int_V \langle f, \phi \rangle \,\mathrm{d}v. \tag{4.85}$$

Hence applying Fubini, we get

$$\langle g, \phi_n \rangle \to \langle g, \phi \rangle, \tag{4.86}$$

where the function $g(x)$ is defined in equation (4.77). □

Next we need a result on the conditions under which a linear operator on $\mathcal{D}'(D)$ and integration over V commute. This is a generalization of the result presented in [31]. One such operator is the differential operator. For this we have the following result.

Theorem 4.17 (Exchange of T with the integral). *Let $f(x, v)$ defined as above (Definition 4.14), and let $T: \mathcal{D}'(D) \to \mathcal{D}'(D)$ be continuous. Then,*

$$T\left(\int_V f(x, v)\,\mathrm{d}v \right) = \int_V Tf(x, v)\,\mathrm{d}v. \tag{4.87}$$

For the proof of Theorem 4.17 we require adjoint operators.

Theorem 4.18 (Theorem 4.10 from [150]). *Suppose X, Y are normed spaces and $T \in \mathcal{B}(X, Y)$, then we have unique $T' \in B(Y', X')$ such that,*

$$\begin{aligned} \langle Tx, y' \rangle &= \langle x, T'y' \rangle \quad \forall x \in X, \forall y' \in Y' \\ y'(Tx) &= (T'y')(x). \end{aligned} \tag{4.88}$$

Moreover $\|T\| = \|T'\|$.

We also need the following Lemma 4.19.

Lemma 4.19. *Suppose that for each $v \in V$, $f(x, v) \in \mathcal{D}'(U)$, and*

$$\int_V f(x, v) \, \mathrm{d}v, \tag{4.89}$$

exists. Further, suppose that $T : \mathcal{D}'(U) \to \mathcal{D}'(U)$ is continuous. Then we have, that

$$h(x) = \int_V Tf \, \mathrm{d}v, \tag{4.90}$$

defines a distribution in $\mathcal{D}'(U)$.

Remark 4.20. In the proof of Lemma 4.19 we make use of the adjoint of T. Since T is an operator on $\mathcal{D}'(U)$, its adjoint can be interpreted as the double adjoint of a linear operator acting on $\mathcal{D}(U)$. If we use $\mathcal{D}(U) = C_c^\infty(U)$, then $\mathcal{D}(U)$ is reflexive locally convex. Under these circumstances, the double adjoint of an operator is itself, i.e., suppose $S : \mathcal{D}(U) \to \mathcal{D}(U)$ then $S'' = S$.

Proof of Lemma 4.19. **Step 1:** The integral in equation (4.90) satisfies Definition 4.14. Let $\phi \in \mathcal{D}(U)$, then

$$\begin{aligned} \langle h(x), \phi \rangle &= \int_U \int_V Tf(x, v) \, \mathrm{d}v \; \phi(x) \, \mathrm{d}x \\ &= \int_V \langle Tf, \phi \rangle \, \mathrm{d}v = \int_V \langle f, T'\phi \rangle \, \mathrm{d}v. \end{aligned}$$

Then $T'\phi$ is just another test function, and since f is a generalized function as defined in Definition 4.14 the integral on the last line exists.

Step 2: $h(x)$ defines a continuous distribution. Since we want to apply Lemma 4.16 we compute,

$$\int_V \sup_n |\langle Tf, \phi_n \rangle| \, \mathrm{d}v = \int_V \sup_n |\langle f, T'\phi_n \rangle| \, \mathrm{d}v.$$

If $\phi_n \to \phi$, then $T'\phi_n \to T'\phi$, since T' is continuous. Then $T'\phi$ is another test function, and thus the integral on the right is finite. We then apply Lemma 4.16, to obtain the result.

□

Proof of Theorem 4.17. By Lemma 4.19, the integral on the right in equation (4.87) defines a distribution. Then let $\phi \in \mathcal{D}(U)$, and let $g(x)$ be defined as in equation (4.77).

$$\begin{aligned}\langle Tg, \phi \rangle = \langle g, T'\phi \rangle &= \int_U \left(\int_V f(x,v) \, \mathrm{d}v \right) T'\phi(x) \, \mathrm{d}x = \int_V \left(\int_U f(x,v) T'\phi(x) \, \mathrm{d}x \right) \mathrm{d}v \\ &= \int_V \langle f, T'\phi \rangle \, \mathrm{d}v = \int_V \langle Tf, \phi \rangle \, \mathrm{d}v = \left\langle \int_V Tf \, \mathrm{d}v, \phi \right\rangle.\end{aligned}$$

□

Remark 4.21. Note that in particular Theorem 4.17 applies to the case when $T = {}^{\partial}/_{\partial x}$, which means theorems such as the fundamental theorem of calculus or Leipniz integral formula follow from Theorem 4.17. For a discussion on these results and applications see [31].

We are now ready to use the theorems and lemmas of this section to compute the weak derivative of the non-local operator.

Lemma 4.22. *Suppose in addition to the assumptions of Lemma 4.8 that $u \in \mathcal{D}'(D)$, then the function*

$$H(x) = \int_V \chi_{E(x)}(r) u(x+r) \Omega(r) \, \mathrm{d}r, \tag{4.91}$$

where $E(x)$ is given in equation (4.46), is differentiable in $\mathcal{D}'(D)$ and its deriva-

tive is given by

$$H'(x) = \int_V u'(x+r)\chi_{E(x)}(r)\Omega(r)\,\mathrm{d}r + f_2'(x)u(x+f_2(x))\Omega(f_2(x)) - f_1'(x)u(x+f_1(x))\Omega(f_1(x)), \tag{4.92}$$

in $\mathcal{D}'(D)$.

Proof. First, we use interval notation to rewrite the indicator function as

$$\chi_{E(x)}(r) = \chi_{(\inf V, f_2(x))}(r)\chi_{(f_1(x),\sup V)}(r), \tag{4.93}$$

where $\chi_{(f_1(x),\sup V)}(r)$ is the indicator function of the set,

$$\{r \in V : f_1(x) \leq r\}. \tag{4.94}$$

Similarly, $\chi_{(\inf V, f_2(x))}(r)$ is the indicator function of the set

$$\{r \in V : r \leq f_2(x)\}. \tag{4.95}$$

Then in $\mathcal{D}'(D)$ we have

$$\begin{aligned}\frac{\partial}{\partial x}\chi_{E(x)}(r) &= \frac{\partial}{\partial x}\left\{\,\chi_{(\inf V, f_2(x))}(r)\chi_{(f_1(x),\sup V)}(r)\,\right\} \\ &= \frac{\partial}{\partial x}\left\{\,H(r-f_1(x))H(f_2(x)-r)\,\right\},\end{aligned}$$

where $H(\cdot)$ is the heaviside function. We find, that

$$\frac{\partial}{\partial x}\chi_{E(x)}(r) = H(r-f_1(x))\delta(f_2(x)-r)f_2'(x) - H(r-f_2(x))\delta(r-f_1(x))f_1'(x).$$

Then applying Theorem 4.17, and the product rule one more time, we obtain

$$\begin{aligned}\frac{\partial g(x)}{\partial x} &= \int_V \frac{\partial}{\partial x}\chi_{E(x)}u(x+r)\Omega(r)\,\mathrm{d}r + \int_V \chi_{E(x)}\frac{\partial}{\partial x}u(x+r)\Omega(r)\,\mathrm{d}r \\ &= \int_V H(r-f_1(x))\delta(f_2(x)-r)f_2'(x)u(x+r)\Omega(r)\,\mathrm{d}r \\ &\quad - \int_V H(r-f_2(x))\delta(r-f_1(x))f_1'(x)u(x+r)\Omega(r)\,\mathrm{d}r\end{aligned}$$

$$
\begin{aligned}
&\quad + \int_V \chi_{E(x)}(r) \frac{\partial}{\partial x} u(x+r)\Omega(r)\,\mathrm{d}r \\
&= \int_V \chi_{E(x)}(r) \frac{\partial}{\partial x} u(x+r)\Omega(r)\,\mathrm{d}r \\
&\quad + f_2'(x)u(x+f_2(x))\Omega(f_2(x)) - f_1'(x)u(x+f_1(x))\Omega(f_1(x)),
\end{aligned}
$$

where we use the fact that the distributional derivative of the Heaviside function is the δ distribution. □

We summarize the results of this section in the following lemma.

Lemma 4.23 (Properties of the non-local operator). *Let $u \in L^p(D)$, $p > 1$ and Ω satisfy A1–A4, then $\mathcal{K}$ defined in equation* (4.44)*, is*

1. *zero on ∂D,*

2. *continuous,*

3. *is weakly differentiable (in $\mathcal{D}'(D)$),*

4. *continuously differentiable if $\Omega(\cdot)\cdot\mathbf{n} = 0$ on ∂V.*

Proof. 1. We check, that if $x \in \partial D$, then $\mu(E(x)) = 0$. If $x = 0$ then $R - 2x = R$, hence $E(0) = \{0\}$. If $x = L$ then $2L - 2x - R = -R$ then $E(L) = \{L\}$.

2. By Corollary 4.12.

3. By Lemma 4.22.

4. The derivative of $\mathcal{K}[u](x)$ with respect to x is given by

$$\mathcal{K}[u]'(x) = \begin{cases} \displaystyle\int_{R-2x}^{R} u'(x+r)\Omega(r)\,\mathrm{d}r & \\ \qquad + 2u(R-x)\Omega(R-2x) & \text{if } x \in [0, R] \\ \displaystyle\int_{-R}^{R} u'(x+r)\Omega(r)\,\mathrm{d}r & \text{if } x \in [R, L-R] \\ \displaystyle\int_{-R}^{2L-2x-R} u'(x+r)\Omega(r)\,\mathrm{d}r & \\ \qquad - 2u(2L-R-x)\Omega(2L-2x-R) & \text{if } x \in [L-R, L] \end{cases}. \tag{4.96}$$

The only points, at which $\mathcal{K}[u]'$ may be discontinuous, are at the points $x = R, L-R$. Evaluating $\mathcal{K}[u]$ at $x = R$, gives

$$\lim_{x \to R^-} \mathcal{K}[u]'(x) = \int_{-R}^{R} u'(R+r)\Omega(r)\,\mathrm{d}r + 2u(0)\Omega(-R), \tag{4.97a}$$

and

$$\lim_{x \to R^+} \mathcal{K}[u]'(x) = \int_{-R}^{R} u'(R+r)\Omega(r)\,\mathrm{d}r. \tag{4.97b}$$

These match since, $\Omega(-R) = 0$.

Similarly, at $x = L - R$ we obtain that

$$\lim_{x \to (L-R)^-} \mathcal{K}[u]'(x) = \int_{-R}^{R} u'(L-R+r)\Omega(r)\,\mathrm{d}r, \tag{4.98a}$$

and

$$\lim_{x \to (L-R)^+} \mathcal{K}[u]'(x) = \int_{-R}^{R} u'(x+r)\Omega(r)\,\mathrm{d}r - 2u(L)\Omega(R). \tag{4.98b}$$

These match since, $\Omega(R) = 0$.

□

Finally using the weak non-local derivatives, we are able to formulate results when the no-flux non-local term are included in Sobolev spaces.

Lemma 4.24. *Let $D \subset \mathbb{R}$ bounded, let $p > 1$ and $u \in W^{1,p}(D)$, further let $V \subset \mathbb{R}$. Then we define,*

$$x \to \nabla_x \cdot \mathcal{K}[u](x) \tag{4.99}$$

where $\mathcal{K}[u]$ is defined in equation (4.44) and satisfies assumption A1 to A4. The function $\nabla_x \cdot \mathcal{K}[u](x)$ is computed in Lemma 4.22. Then $\mathcal{K}[u] \in W^{1,p}(D)$, in particular the following holds,

$$\|\mathcal{K}[u]\|_{1,p} < 6\|u\|_{1,p}|\Omega|_{\infty,V}. \tag{4.100}$$

Proof. Note, for this proof we will use the exact form of the functions $f_{1,2}(x)$ which are given in equations (4.45b), (4.45c).

$$\begin{aligned}
|\nabla \cdot \mathcal{K}[u](x)|_p &= \left| \int_{f_1(x)}^{f_2(x)} u'(x+r)\Omega(r)\,\mathrm{d}r + J_1(x) + J_2(x) \right|_p \\
&\leq \left| \int_{f_1(x)}^{f_2(x)} u'(x+r)\Omega(r)\,\mathrm{d}r \right|_p + |J_1(x)|_p + |J_2(x)|_p,
\end{aligned}$$

where

$$\begin{aligned}
J_1(x) &= f_1'(x)u(x+f_1(x))\Omega(f_1(x)) \\
J_2(x) &= f_2'(x)u(x+f_2(x))\Omega(f_2(x)).
\end{aligned}$$

Each of the J_i terms, is estimated by

$$|J_1(x)|_p^p = \int_D |f_1'(x)u(x+f_1(x))\Omega(f_1(x))|^p\,\mathrm{d}x \leq 2^p|u|_p^p|\Omega|_{\infty,V}^p, \tag{4.101}$$

and

$$|J_2(x)|_p^p = \int_D |f_2'(x)u(x+f_2(x))\Omega(f_2(x))|^p\,\mathrm{d}x \leq 2^p|u|_p^p|\Omega|_{\infty,V}^p. \tag{4.102}$$

For the first integral, we apply Lemma 4.9. Then combining the three terms, we obtain,

$$|\nabla \cdot \mathcal{K}[u](x)|_p \leq |u'|_p|\Omega|_{\infty,V} + 4|u|_p|\Omega|_{\infty,V} \leq 5\|u\|_{1,p}|\Omega|_{\infty,V}. \tag{4.103}$$

Then we compute the Sobolev norm of $\mathcal{K}[u](x)$

$$|\mathcal{K}[u]|_p^p + |\nabla_x \cdot \mathcal{K}[u]|_p^p \leq (1 + 5^p) \|u\|_{1,p}^p |\Omega|_{\infty,V}^p. \tag{4.104}$$

For $p \geq 1$, the function $g(p) = (1 + 5^p)^{1/p}$ achieves a maximum of 6. Hence we obtain the final result. □

Using the estimate in Lemma 4.24, we show that the operator $\mathcal{K}$ is $\mathcal{C}^1$.

Lemma 4.25. *The map $\mathcal{K}: L^p(D) \to L^p(D)$, defined by equation (4.11) is $\mathcal{C}^1$, and its derivative is given by*

$$\mathcal{D}_u \mathcal{K}[w](x) = \int_{E(x)} w(x + r)\Omega(r)\, \mathrm{d}r. \tag{4.105}$$

Proof. The proof is obvious, since $\mathcal{K}[u]$ is linear in $u(x)$. □

In the following, we make use of quotient Sobolev spaces. The significance of this space is that due to the no-flux boundary conditions, the steady-state solutions of equation (4.1) are in this quotient space. In particular, spaces of the form $W^{k,p}(D)/\mathbb{P}_{k-1}$, where $\mathbb{P}_{k-1}$ is the space of polynomials up to degree $k-1$, because in these spaces we have a simple equivalent norm $|u|_{k,p}$. Hence, giving us a Poincaré type inequality. This space is equipped with the norm

$$\|\hat{v}\|_{W^{k,p}(D)/\mathbb{P}_{k-1}} = \inf_{v \in \hat{v}} \|v\|_{W^{k,p}(D)}, \tag{4.106}$$

where $\hat{v}$ are the equivalent classes in the quotient $W^{k,p}(D)/\mathbb{P}_{k-1}$. The space $W^{k,p}(D)/\mathbb{P}_{k-1}$ has the following very useful norm equivalency.

Theorem 4.26 (Theorem 7.2 [127]). *Let $D \subset \mathbb{R}$ with a Lipschitz boundary, and let us assume that the identity mapping $\mathcal{I}: W^{1,p}(D) \to L^p(D)$ is compact. Then let $\hat{u} \in W^{k,p}(D)/\mathbb{P}_{k-1}$, then we have*

$$c_1 \|\hat{u}\|_{W^{k,p}(D)/\mathbb{P}_{k-1}} \leq \left[\sum_{|\alpha|=k} |D^\alpha u|_{L^p(D)}^p \right]^{1/p} \leq c_2 \|\hat{u}\|_{W^{k,p}(D)/\mathbb{P}_{k-1}}, \forall u \in \hat{u}. \tag{4.107}$$

when $p = 2$, $W^{k,2}(D)/\mathbb{P}_{k-1}$ is a Hilbert space with scalar product

$$(\hat{v}, \hat{u}) = \sum_{|\alpha|=k} \int_D D^\alpha v D^\alpha u \, \mathrm{d}x, \qquad \forall u \in \hat{u}, v \in \hat{v}. \tag{4.108}$$

Remark 4.27. In our case, we are interested in the case $k = 1$ i.e. the spaces $W^{1,p}(D)/\mathbb{R}$, where $D \subset \mathbb{R}$ bounded and with a Lipschitz boundary. This space is equipped with the norm

$$\|\hat{v}\|_{H^1(D)/\mathbb{R}} = \inf_{v \in \hat{v}} \|v\|_{1,D}. \tag{4.109}$$

It is easy to see, that Theorem 4.26 holds by the Sobolev embedding (see Theorem B.4) for $p \geq 1$.

For a further better understanding of this space, we will prove the following result.

Lemma 4.28. *The space $W^{1,p}(D)/\mathbb{R}$ is isomorphic to*

$$W := \left\{ u \in W^{1,p}(D) \colon \int_D u(x) \, \mathrm{d}x = 0 \right\}. \tag{4.110}$$

Proof. Define the operator $\mathcal{A} \colon L^p(D) \to \mathbb{R}$ by

$$\mathcal{A}[f] := \frac{1}{|D|} \int_D f(x) \, \mathrm{d}x. \tag{4.111}$$

Then it is easy to see, that $\|\mathcal{A}\| = 1$. On the other hand, the operator $Q := \mathcal{I} - \mathcal{A}$, gives

$$Qf(x) = f(x) - \frac{1}{|D|} \int_D f(x) \, \mathrm{d}x, \tag{4.112}$$

and we find that

$$\int_D Qf(x) \, \mathrm{d}x = 0. \tag{4.113}$$

Thus, $Qf \in W$. Hence, W and the set of constant functions are complements in $W^{1,p}$, i.e.,

$$W^{1,p}(D) = \{u \in W^{1,p} \colon u \equiv c \in \mathbb{R}\} \oplus W. \tag{4.114}$$

Thus applying [55 Proposition 4.4], we have that

$$W^{1,p}(D)/\mathbb{R} \cong W. \tag{4.115}$$

□

Lemma 4.29. *Let $D \subset \mathbb{R}$ bounded, let $p > 1$ and $u \in W^{1,p}(D)/\mathbb{R}$. Then we define,*

$$x \to \nabla_x \cdot \mathcal{K}[u](x) \tag{4.116}$$

where $\mathcal{K}[u]$ is defined in equation (4.44) and assumptions A1 to A4 are satisfied, and $\nabla_x \cdot \mathcal{K}[u](x)$ is computed in Lemma 4.23. Then $\mathcal{K}[u] \in W^{1,p}(D)$, in particular the following holds,

$$\|\mathcal{K}[u]\|_{1,p} \leq (4C+1)\,|\Omega|_\infty \|u\|_{1,p}. \tag{4.117}$$

Proof. The proof is very similar to the proof of Lemma 4.24. □

Finally we derive a simple estimate, that shows that the non-local term $\mathcal{K}[u]$ is bounded by the average of the function $u(x)$.

Lemma 4.30. *Let the operator $\mathcal{K}[u](x)$ be defined as in equation (4.11), and suppose that $u(x) \geq 0$, with $|u|_{1,D} = \mathcal{A}[u] < \infty$. Then*

$$-\sup_{r\in[0,1]} \omega(r)\,\mathcal{A}[u] \leq \mathcal{K}[u](x) \leq \sup_{r\in[0,1]} \omega(r)\,\mathcal{A}[u]. \tag{4.118}$$

Proof. Let $u(x) \geq 0$ such that $\mathcal{A}[u] < \infty$. Then we compute

$$\begin{aligned}\mathcal{K}[u](x) &= \int_{-1}^{1} \chi_{E(x)}(r)u(x+r)\Omega(r)\,\mathrm{d}r \\ &= \int_{0}^{1} \chi_{E(x)}(r)u(x+r)\omega(r)\,\mathrm{d}r - \int_{-1}^{0} \chi_{E(x)}(r)u(x+r)\omega(r)\,\mathrm{d}r.\end{aligned} \tag{4.119}$$

It is easy to see, that both integrals are non-negative as $u(x) \geq 0$ and $\omega(r) \geq 0$.

Hence it follows, that

$$\mathcal{K}[u](x) \leq \int_0^1 \chi_{E(x)}(r) u(x+r)\omega(r)\,\mathrm{d}r \leq \sup_{r\in[0,1]} \omega(r)\,\mathcal{A}[u]. \tag{4.120}$$

In the same spirit, we find

$$\mathcal{K}[u](x) \geq -\int_{-1}^0 \chi_{E(x)}(r) u(x+r)\omega(r)\,\mathrm{d}r \geq -\sup_{r\in[0,1]} \omega(r)\,\mathcal{A}[u]. \tag{4.121}$$

□

4.3 Steady States

In this section, we consider the steady-states of equation (4.1) using the different non-local operators that were constructed in Section 4.1.

4.3.1 Steady states for neutral non-local term

The steady states of equation (4.1) subject to the neutral non-local term constructed in Example 4.5, are given by the solutions of the following equation.

$$u_{xx}(x,t) - \alpha\left(u(x,t)\int_{E(x)} [\,u(x+r) - \bar{u}\,]\,\Omega(r)\,\mathrm{d}r\right)_x = 0, \tag{4.122a}$$

where $E(x)$ is defined in equation (4.46). As equation (4.1) exhibits mass conservation we impose the following mass constraint on the solutions of equation (4.122a).

$$\mathcal{A}[u] = \bar{u}, \tag{4.122b}$$

where $\mathbb{R} \ni \bar{u} > 0$, is the mass per unit length of population $u(x)$ in D. Then since $\mathcal{K}[\bar{u}] = 0$ for all $x \in D$, it is easy to see that $u(x) = \bar{u}$ is a solution for all $\alpha \in \mathbb{R}$.

If we want to extend the results of Chapter 3 to equation (4.122a), we have to show that if $u(x)$ is a solution so is $u(L-x)$. Once again the non-local term is critical.

Lemma 4.31. *Let $u(x) \in \mathcal{C}^1_{\mathcal{B}}$ be a positive function, and consider $w(x) = u(L-x)$. Then for the non-local term defined in equation (4.43), we have that*

$$\mathcal{K}[w](x) = -\mathcal{K}[u](L-x). \tag{4.123}$$

Proof. We only have to consider the boundary region, i.e., $[0, R] \cup [L-R, L]$, since for the interior the result follows from Lemma 3.82. Thus we are left with checking the four intervals $[0, R/2], [R/2, R], [L-R, L-R/2], [L-R/2, L]$.

Let $x \in [0, R/2]$, then since $R - 2x > 0$ we have that,

$$\mathcal{K}[w](x) = \int_{R-2x}^{R} [\, w(x+r) - \bar{u}\,]\, \omega(r)\, \mathrm{d}r = \int_{R-2x}^{R} [\, u(L-x-r) - \bar{u}\,]\, \omega(r)\, \mathrm{d}r.$$

Replacing W with u, letting $y = L - x$, and switching the sign of the integration variable we obtain,

$$\mathcal{K}[w](x) = \int_{-R}^{2L-2y-R} [\, u(y+r) - \bar{u}\,]\, \omega(r)\, \mathrm{d}r. \tag{4.124}$$

Since $y \in [L - R/2, L]$ we have that $2L - 2y - R \leq 0$, thus we obtain,

$$\mathcal{K}[w](x) = -\int_{-R}^{2L-2y-R} [\, u(y+r) - \bar{u}\,]\, \Omega(r)\, \mathrm{d}r = \mathcal{K}[u](y) = \mathcal{K}[u](L-x). \tag{4.125}$$

Let $x \in [R/2, R]$, and consider

$$\begin{aligned} \mathcal{K}[w](x) &= \int_{R-2x}^{R} [\, w(x+r) - \bar{u}\,]\, \Omega(r)\, \mathrm{d}r \\ &= \underbrace{\int_{0}^{R} [\, w(x+r) - \bar{u}\,]\, \omega(r)\, \mathrm{d}r}_{\mathrm{I}} - \underbrace{\int_{R-2x}^{0} [\, w(x+r) - \bar{u}\,]\, \omega(r)\, \mathrm{d}r}_{\mathrm{II}}. \end{aligned}$$

Then we switch the sign of the integration variable in II, to obtain

$$\mathcal{K}[w](x) = \int_{0}^{R} [\, u(L-x-r) - \bar{u}\,]\, \omega(r)\, \mathrm{d}r - \int_{0}^{2x-R} [\, u(L-x+r) - \bar{u}\,]\, \omega(r)\, \mathrm{d}r. \tag{4.126}$$

Finally, we set $y = L - x$ to obtain

$$\begin{aligned}\mathcal{K}[w](y) &= \int_0^R [\,u(y-r) - \bar{u}\,]\,\omega(r)\,\mathrm{d}r - \int_0^{2L-2y-R} [\,u(y+r) - \bar{u}\,]\,\omega(r)\,\mathrm{d}r \\ &= \int_{-R}^{2L-2y-R} [\,u(y+r) - \bar{u}\,]\,\Omega(r)\,\mathrm{d}r = -\mathcal{K}[u](y) = -\mathcal{K}[u](L-x).\end{aligned} \tag{4.127}$$

For the intervals $[L-R, L-R/2]$ and $[L-R/2, L]$ we simply revert the above arguments. □

Corollary 4.32. *Let $u(x)$ be a solution of equation (4.122a), then $w(x) = u(L-x)$ is also a solution.*

Proof. Let $w(x) = u(L-x)$, which we substitute into equation (4.122a) to obtain

$$\underbrace{w''(x)}_{\mathrm{I}} - \underbrace{\alpha w(x)\,(\mathcal{K}[w](x))_x}_{\mathrm{II}} - \underbrace{\alpha w'(x)\,\mathcal{K}[w](x)}_{\mathrm{III}}. \tag{4.128}$$

Then, we obtain

$$\begin{aligned}\mathrm{I} &= u''(L-x), \\ \mathrm{II} &= \alpha u(L-x)\,(-\mathcal{K}[u](L-x)) = \alpha u(L-x)\,(\mathcal{K}[u])'\,(L-x), \\ \mathrm{III} &= \alpha u'(L-x)\,\mathcal{K}[u](L-x).\end{aligned}$$

Hence $w(x)$ satisfies equation (4.122a). □

Corollary 4.32 shows that equation (4.122a) satisfies the basic reflection as the equation in Chapter 3. However, the stronger symmetry property we build into the space H_P^2 is not satisfied until we prove that $u(L-x) = u(x)$. In Chapter 3, this property implied that the flux at $x = 0, L$ is zero. Nevertheless, this suggests that the solutions obtained in Chapter 3 may be related to the solutions of equation (4.122a).

4.3.2 Steady states for repellent non-local term

The steady states of equation (4.1) with repellent non-local term $\mathcal{K}[u]$ (see Example 4.3), are given by the solutions of the following equation.

$$u_{xx}(x,t) - \alpha \left(u(x,t) \int_{E(x)} h(u(x+r))\Omega(r)\,\mathrm{d}r \right)_x = 0, \tag{4.129a}$$

where $E(x)$ is defined in equation (4.46). As equation (4.1) exhibits mass conservation we impose the following mass constraint on the solutions of equation (4.129a).

$$\mathcal{A}[u] = \bar{u}, \tag{4.129b}$$

where $\mathbb{R} \ni \bar{u} > 0$, is the mass per unit length of population $u(x)$ in D. To be able to easily carry out the subsequent asymptotic expansion, we assume that the function $h(\cdot)$ under the integral in equation (4.129a) is linear (i.e. $h(u) = u$.)

When $\alpha = 0$ the boundary conditions are given by the classical Neumann boundary conditions (4.7). It is then easy to see, that equation (4.1) admits a constant steady state solution $u(x) \equiv \bar{u}$. When $\alpha \neq 0$, the situation is much more complicated. In this section, we approximate the ground steady state of equation (4.129a) by using an asymptotic expansion for small values of α. In this section, we assume that $R = 1$. In the following, we assume that $\alpha = \epsilon$. Then we consider the following asymptotic expansion,

$$u(x) = u_0(x) + \epsilon u_1(x) + \epsilon^2 u_2(x) + \mathcal{O}(\epsilon^3). \tag{4.130}$$

Substituting this into equation (4.129a), we obtain

$$\begin{aligned} 0 = &\left(u_0(x) + \epsilon u_1(x) + \epsilon^2 u_2(x)\right)_{xx} \\ &- \epsilon \left((u_0 + \epsilon u_1) \int_{-1}^{1} \left(u_0 + \epsilon u_1 + \epsilon^2 u_2\right)(x+r)\chi_{E(x)}(r)\Omega(r)\,\mathrm{d}r \right)_x . \end{aligned} \tag{4.131}$$

Separating the scales of ϵ, we obtain for the zeroth order equation.

$$(u_0)_{xx} = 0, \tag{4.132}$$

and for the first order equation

$$(u_1)_{xx} - \left(u_0 \int_{-1}^{1} u_0(x+r)\chi_{E(x)}(r)\Omega(r)\,\mathrm{d}r \right)_x = 0. \tag{4.133}$$

Finally, the second order equation is given by

$$(u_2)_{xx} - \left(u_1 \int_{-1}^{1} u_0(x+r)\chi_{E(x)}(r)\Omega(r)\,\mathrm{d}r \right)_x \tag{4.134}$$

$$- \left(u_0(x) \int_{-1}^{1} u_1(x+r)\chi_{E(x)}(r)\Omega(r)\,\mathrm{d}r \right)_x = 0.$$

The zeroth order equation (4.132) is easily solved.

$$u_0(x) = ax + b, \tag{4.135}$$

where $a, b \in \mathbb{R}$ have to be chosen. Due to the Neumann boundary conditions (4.5), we find that $a = 0$, and thus $u_0 \equiv b$. Due to constraint (4.129b), we find that $b = \bar{u}$. The first order equation is solved by considering the following system

$$(u_1)_{xx} - b^2 \left(\int_{-1}^{1} \chi_{E(x)}(r)\Omega(r)\,\mathrm{d}r \right)_x = 0, \tag{4.136}$$

subject to

$$\frac{\partial u_1}{\partial n} = 0 \qquad \text{on } \partial D, \tag{4.137}$$

where n is the unit outward normal of ∂D. This boundary condition is obtained from an expansion of the flux condition (4.4) in ϵ. To ensure that equation (4.136) has a solution, we impose the constraint that

$$\int_D u_1(x)\,\mathrm{d}x = 0. \tag{4.138}$$

Using the properties of the function Ω, we rewrite equation (4.136) as

$$(u_1)_{xx} = b^2 \begin{cases} 2\omega(1-2x) & \text{for } x \in [0, 1/2] \\ -2\omega(1-2x) & \text{for } x \in [1/2, 1] \\ 0 & \text{for } x \in [1, L-1] \\ -2\omega(2L-2x-1) & \text{for } x \in [L-1, L-1/2] \\ 2\omega(2L-2x-1) & \text{for } x \in [L-1/2, L] \end{cases} . \tag{4.139}$$

We solve this differential equation by integrating, and impose that the solution $u_1(x)$ be C^2 and condition (4.138). After much algebra we obtain, the following expression for the function $u_1(x)$

$$u_1(x) = \begin{cases} u(0) + b^2 \int_0^x \int_{1-2s}^1 \omega(r)\,\mathrm{d}r\,\mathrm{d}s & \text{for } x \in [0, 1/2] \\ A - b^2 \int_x^1 \int_{-1}^{1-2s} \omega(r)\,\mathrm{d}r\,\mathrm{d}s & \text{for } x \in [1/2, 1] \\ A & \text{for } x \in [1, L-1] \\ A - b^2 \int_{L-1}^x \int_{2L-2s-1}^1 \omega(r)\,\mathrm{d}r\,\mathrm{d}s & \text{for } x \in [L-1, L-1/2] \\ u(L) + b^2 \int_x^L \int_{-1}^{2L-2s-1} \omega(r)\,\mathrm{d}r\,\mathrm{d}s & \text{for } x \in [L-1/2, L] \end{cases} , \tag{4.140}$$

where

$$A = \frac{b^2}{L} \int_0^1 r\omega(r)\,\mathrm{d}r, \tag{4.141}$$

and

$$u(0) = u(L) = b^2 \left[\frac{1-L}{L} \right] \int_0^1 r\omega(r)\,\mathrm{d}r. \tag{4.142}$$

The second order equation (4.134) is complicated, and we do not solve it here. For a visual depiction of the asymptotic expansion (4.130), see Fig. 4.9.

Note that this implies, that if we compare $u = u_0 + \epsilon u_1$ to the constant steady state solution that we would expect in the case of periodic boundary

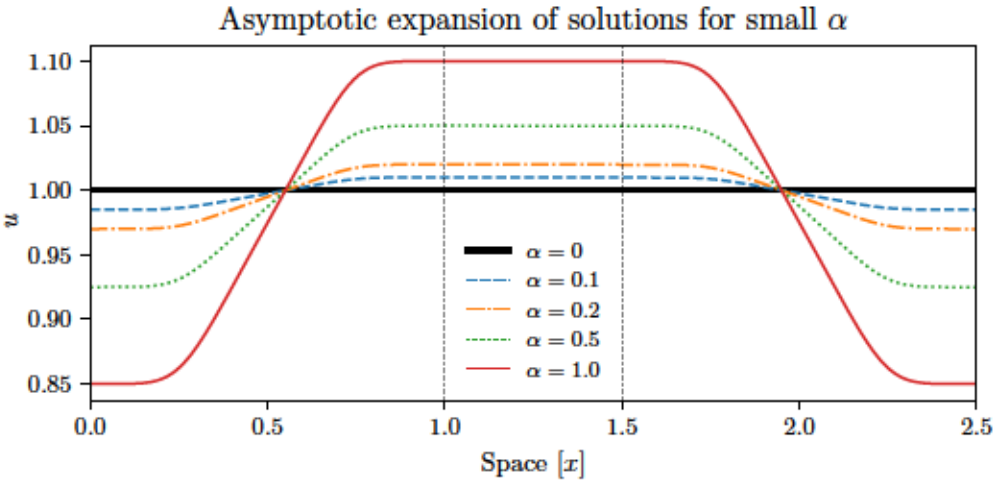

Figure 4.9: The solution $u(x)$ given in equation (4.130) for various values of $\alpha \sim \epsilon$. The black dotted lines denote the boundaries of the areas that are within one sensing radius of the domain boundary. The dotted lines denote R and $L - R$ respectively.

conditions in the following denoted by $\bar{u}$, we observe that $u(x,t) > \bar{u}$ for $x \in D_0$, and $u(x,t) < \bar{u}$ for $x \in D \setminus D_0$. It is of note that the point at which $u(x) = \bar{u}$ remains constant for changing values of ϵ.

4.4 Future Outlook

In the previous section, we discussed the steady states of equation (4.1) subject to the repellent and neutral non-local term which were constructed in Section 4.1. In the case of the repellent non-local operator, we were only able to asymptotically approximate the steady states for small values of adhesion strength α. A more detailed exploration of the steady-states of these equations is hindered by the fact that there is no constant steady-state that exists for all values of α. This means that the approach pionereed by Rabinowitz [144] (used in Chapter 3) cannot be applied. In the following, we briefly outline approaches frequently used in the literature to address nonlinear steady-state equations, and discuss their challenges when applied to the non-local equations (4.129a).

A common approach to show the existence of solutions of nonlinear steady-state equations is the construction of a monotone bounded sequence of solutions

[5]. For this approach, one first develops weak solutions for a linear eigenvalue problem that is related to the nonlinear equation. The solution operator of this eigenvalue problem is then shown to be compact (elliptic regularity) and positive (the equation's structure). These properties allow the application of the Krein-Ruthmann theorem to the solution operator. Thus, showing that there exists a unique positive eigenfunction [6, 112]. The existence of solutions of the nonlinear equation is then shown using a monotone iteration [5], which originates either at a sub or super solution constructed from the eigenfunction. Applications of this technique include a non-local model of Ohmic heating [110] and the construction of solutions of a non-local equation resulting from a birth-jump process [44].

A different approach is to rewrite equation (4.129a) as an abstract fixed point equation. Then topological degree (e.g. Leray-Schauder degree) arguments can be used to show the existence of solutions. Bifucation points are those at which the index (degree for isolated solutions of the fixed point equation) changes sign. Applications of the Leray-Schauder include the work by Crandall, Rabinowitz [34] who classified the solutions of nonlinear Sturm-Liouville equations. Indeed the theorem of Rabinowitz [144] (and its extensions [113, 158] which are used in Chapter 3) provide easy to check conditions, which identify bifurcation points (index changes). In combination with the Krein-Ruthmann theorem the Leray-Schauder degree is a popular tool to show the existence of positive solutions of equations contained a non-local term of the form,

$$\bar{u} = \int_X u(x)\,\mathrm{d}x \tag{4.143}$$

either as perturbation of the Laplacian or in the reaction term [19, 40, 41, 42, 60, 61, 62]. In our case of equation (4.129a) the challenge of this approach is that we cannot apply Krein-Ruthmann.

The so-called Mawhin coincidence degree is also sometimes used to prove the existence of non-trivial solutions [57]. Using a Lyapunov-Schmidt reduction, one obtains the so-called bifurcation equation (a mapping between the kernel and co-kernel of the operator equation). From this equation, the Mawhin degree is computed. While a Lyapunov-Schmidt reduction and subsequently the Mawhin

degree can be computed for equation (4.129a), it does not yield a useful result.

In the case of equation (4.129a), this leaves an application of the Leray-Schauder degree to its abstract fixed point equation as the only viable option. The challenge here is that a detailed understanding of the equation's structure (i.e., non-local term behaviour). Further, to ensure progresses a thorough numerical study of the equation's steady states should be done. This however requires fast numerical methods to compute the modified non-local terms, i.e., extensions of the methods developed by Gerisch [66].

4.5 Discussion

In this chapter, we considered the non-local cell adhesion model (4.1) on a bounded domain with no-flux boundary conditions. The presence of the boundary meant that the definition of the non-local operator in the boundary region (within one sensing radius of the boundary) had to be revisited. In three steps, we constructed non-local operators that are (1) well-defined, (2) satisfy the boundary condition (4.6), and (3) have different behaviours in the boundary region. There are many different ways to construct non-local operators that satisfy conditions (2) and (3). In particular, the behaviour in the boundary region can be chosen freely. In theory, the behaviour in the boundary region (condition (3)) could be chosen independent from condition (2). Here however, we considered only non-local operators $\mathcal{K}[u]$ that are continuous in the boundary region, so that some boundary effects are always felt within the boundary region.

In Example 4.3, we modified the limits of integration so that $\mathcal{K}[u]$ satisfies the boundary condition and is continuous. In Example 4.4, the correction terms n_b were continuously decreased to zero through the boundary region. Finally, in Example 4.5, we introduced an additional correction term to ensure that the constant $\bar{u}$ is always a solution of equation (4.1).

Using two functions, one with a peak and the other with a trough on the boundary, we compared the behaviour of the newly constructed non-local terms to the periodic non-local operator used in Chapter 3, which always points in the direction of increasing cell mass. Depending on whether this property

is retained by the newly constructed non-local operators, we classified them as either repulsive or attractive. The non-local operators from Example 4.3 and Example 4.4 are repellent, while the operator from Example 4.5 is either depending on the size of $u(x)$ compared to $\bar{u}$.

Mathematically novel is the non-local operator in which the integration limits are spatially dependent (see Example 4.3), whose mathematical properties we investigated further. The spatial dependence of the integration limits posed a particular challenge, since properties such as continuity require a notion of convergence of sets (integration domain). For this reason, we make use of the Fréchet-Nikodym metric (see Section 4.2.1). Using this metric, we extended the estimates of Chapter 3, to the non-local operator with spatially dependent limits of integration. Differentiation of this non-local operator was equally made more challenging by the spatially dependent integration limits. Using the theory of distributions, we computed the non-local term's weak derivative, which coincides with the classical derivative if the integration kernel $\Omega(\cdot)$ is zero on the boundary of the sensing domain (∂V).

We explored the steady states of equation (4.1) with the non-local terms constructed in Example 4.3 and Example 4.5. In the case of Example 4.5, there exists a constant steady state $u \equiv \bar{u}$ for all α. Further, we showed that equation (4.122a) is equi-variant under reflections through the centre of the domain. Hence, a sub-set of solutions of equation (4.122a) seem to be related to the periodic steady state solutions found in Chapter 3. At the same time, however, we expect the set of solutions of equation (4.122a) to be richer. An exploration of the set of non-trivial solutions of equation (4.122a) using the techniques employed in Chapter 3 is a worthwhile future research project.

In the case of the non-local operator constructed in Example 4.3, however, the constant function is a solution if and only if $\alpha = 0$. Using an asymptotic expansion, we study the steady states in a zero neighbourhood (i.e. $\alpha \sim \mathcal{O}(\epsilon)$). We found that, near the boundary, the steady-states have values below $\bar{u}$ while far away from the boundary values above $\bar{u}$. This supports our earlier classification of the non-local term constructed in Example 4.3 as repellent. Since the constant solution exists only for $\alpha = 0$, it is impossible to use the approach taken in Chapter 3. This leaves the direct application of topological degree the-

ory as the only viable option. This is however challenging and almost certainly requires the guidance by detailed numerical studies.

The required numerical methods to further explore the steady states and time-dependent solutions of the non-local cell adhesion model subject to no-flux boundary conditions need developing. For the time-dependent equation, the methods developed by Gerisch for the periodic case are a good starting point [66]. Equally important would be the development of methods to solve the steady-state problem directly. This would allow the use of numerical continuation techniques to explore the set of steady-state solutions directly.

The experimental results by Paksa et al. motivated the development of the boundary dependent non-local operators [138], who studied the positioning of progenitor cells during organogenesis. They found that cell-cell adhesions and the presence of repulsive boundaries were critical to the correct positioning of the final organ. In an analysis of cell polarization at the individual cell level, they showed that when cells encounter a repulsive boundary their polarization reverses [138]. In the derivation of equation (4.1), we assumed that the non-local term represents each cell's polarization. This behaviour seems to be included in the non-local operator constructed in Example 4.3 (see Fig. 4.6), where the non-local operator reverses near the boundary. It is however clear that the cell's polarization is a result of the sub-cellular signalling networks. Hence, it would be a worthwhile future project to identify the central regulatory sub-units of this network that control cell polarization, and cell polarization reversal upon encountering solid boundaries. The final goal would be to obtain the behaviour of the non-local term in the boundary region from a realistic intra-cellular signalling model.

Chapter 5

Discussion

In the *Introduction*, we formulated the aims of this thesis. These were:

1. Can non-local models be derived from an underlying individual description of cell movement?

2. What are the steady-states of the non-local cell adhesion model (i.e., equation (1.1)) in the absence of boundary effects?

3. How to model and include boundary effects in the non-local term of the cell adhesion model (i.e., equation (1.1))?

In Chapter 2, starting from the master equation of a space-jump process, we showed how a cell's polarization vector is naturally included in the process' transition rates. All that remained was to develop models of cell polarization. We developed models for adhesion and chemotaxis. For cellular adhesion, we developed a cell polarization model based on biological insights of individual cell movement. We assumed that the cells "sample" their surrounding environment using filopodia, which are thin cylindrical cell membrane protrusions. The filopodia attach to other cells using cellular adhesion molecules. Once the adhesion bonds are formed, the cells utilize them to pull themselves forward.

Filopodia are however only one type of membrane extension cells commonly use. Others include lamellipodia, a sheet like structure used during the migration on flat surfaces, or cell blebs used during migration through three-dimensional extracellular matrix [147]. Models of cell polarization for these

types of structures would be great. Equally important would be the validation of the filopodia-based polarization model against biological data. The selection of the particular reaction kinetics of the cellular adhesion molecules is of particular interest. The original Armstrong model (1.1) assumed law of mass action kinetics. However, cellular adhesion molecules are confined to the cell's membrane, i.e., a two-dimensional surface. This should change the reaction kinetics. However, without biological data this remains pure speculation. If detailed cell-tracking data would be available, including velocity data, a more detailed individual model based on a velocity-jump process would be more suitable.

Most significant would be identification of the critical sub-units of the intracellular signalling network of genes and proteins that control cell polarization (e.g., Rho-Rac GTPase [94, 95]) in combination with cellular adhesion molecules. Our definition of the polarization vector, and its inclusion in the population level model, provides us with a natural method to build multi-scale models of cell migration in the presence of cell-cell adhesion.

In Chapter 3, we focused on the steady states of the non-local cell adhesion model in the absence of boundary effects. Since the constant solution is always a steady state, we used global bifurcation results pioneered by Rabinowitz to identify points along the constant solution branch at which branches containing non-trivial solutions are spawned. We classified the solutions in the newly spawned branches using their symmetries, which they inherit from the eigenfunction of the linearization at the bifurcation point. Further, using the particular structure of the non-local operator and of the cell adhesion equation (1.1), we showed that the locations of the solution's extrema are fixed. We characterized the solutions by showing that they are elements in a particular subspace of C^2, whose functions have derivatives of alternating sign on a fixed tiling. Finally, we proved that the first bifurcation branch is unbounded and has one peak, and that the bifurcation is of pitch-fork type. The integral kernel in the non-local term determines the bifurcation's direction and whether a switch of stability occurs at the bifurcation point. Finally, using numerics, we presented some the steady-states and observe the formation of rotating waves in the long-time limit.

A major limitation of Theorem 3.97 is that it is only valid for the first bifurcation branch and only for linear $h(u)$. However, as discussed in Chapter 3, an extension to all bifurcation branches seems imminent with nonlinear $h(u)$ satisfying the assumptions outlined in Definition 3.1. Even with this result we cannot exclude the possibility of secondary bifurcations occurring along the branches of non-trivial solutions. These bifurcations may lead to further symmetry breaking. However, the identification of points of secondary bifurcations is a challenging mathematical problem, since no result equivalent to the global bifurcation theorems exists. This leaves a direct application of topological degree theory in combination with numerical solutions as the only viable option. A first result describing the set of possible points of secondary bifurcation could be obtained by an application of the analytic bifurcation theory developed by Dancer [37, 38]. However, secondary bifurcations are only truly identifiable by discovering points at which the index changes.

The next step in the analysis of equation (1.1) is to study time-dependent solutions. There are several interesting questions such as can formed cell aggregates merge? Do there exist meta-stable solutions? Such studies have two goals (1) the characterization of the global attractor of equation (1.1), and (2) develop the mathematical insights to study extensions of the cell adhesion model. A similar extension would be the inclusion of temporally and spatially varying adhesion coefficients. Such varying coefficients have been used to obtain realistic biological solutions describing cancerous tissues [47]. Such varying adhesion coefficients have wide applications in biological phenomena in which the transition of stationary cells to motile cells is critical. These include wound-healing, cancer cell invasion and normal tissue development.

Both biologically and mathematically relevant would be extensions of model (1.1) to include several cell populations, to study the steady-states of cell-sorting using the global bifurcation approach. An extension to higher spatial dimensions would allow us to study wound-healing and tissue formation more realistically.

In Chapter 4, we considered the non-local cell adhesion model on a bounded domain, with no-flux boundary conditions. Without modification, the non-local term used in Chapter 3 would neither satisfy the no-flux boundary nor be well-defined. In a three step process, we ensured that the non-local term is (1)

well-defined, (2) satisfied the no-flux boundary conditions, and (3) proposed how it behaves in the boundary region. Intuitively, depending on the adhesive properties of the boundary, cells would be either repelled or attracted by the boundary. We constructed a repellent and one that is both repellent and attractant (neutral) depending on the population level.

The cell adhesion model, including the neutral non-local boundary conditions, admits a constant steady state for all values of α. In addition, the equation is equi-variant with respect to reflection through the domain's centre. The existence of the constant solution for all α implies that the bifurcation theorems used in Chapter 4 are admissible to this problem. Further, similar symmetry properties suggest that some parts of the arguments from Chapter 3 may be applicable. In the case of the cell adhesion model including the repellent non-local model, the constant function is a solution if and only if $\alpha = 0$. We used an asymptotic expansion to study the first steady-state of this model for small α. This analysis demonstrated that the solution is depressed near the boundary, with the replaced mass being added in the middle.

In the construction of the non-local operators that include the no-flux boundary conditions, we had freedom to choose their behaviour in the boundary region (within one sensing radius of the boundary). From biological experiments, it is known that the cell polarization adapts when cells encounter physical boundaries [138]. Responsible for this adaptation are the intra-cellular signalling networks. In Chapter 2, we argued that the non-local operator is a model of cell polarization. Thus a natural extension would be to include the involved intra-cellular processes in a multi-scale model of cell adhesion.

In conclusion, in this thesis we made significant progress in understanding of non-local models of cell adhesion. We proposed a framework to derive such models from an underlying stochastic random walk, studied the steady states spawning through bifurcations from the constant solution, and finally considered the non-local cell adhesion model on a bounded domain with no-flux boundary conditions. Finally, perhaps one of the most important outcomes of this thesis are the new possible directions of research that have been identified. The main questions are: identification of secondary bifurcations, analysis of the time-dependent solutions of equation (1.1), several cell populations, higher

space dimensions, and multi-scale modelling including intra-cellular signalling networks.

Bibliography

[1] M. Adioui, O. Arino, N. El Saadi (2005) A nonlocal model of phytoplankton aggregation. *Nonlinear Analysis: Real World Applications* **6**(4): 593–607

[2] B. Alberts (2008) *Molecular Biology of the Cell: Reference edition.* Garland Science, New York

[3] W. Alt (1985) Degenerate diffusion equations with drift functionals modelling aggregation. *Nonlinear Analysis: Theory, Methods & Applications* **9**(8): 811–836

[4] W. Alt (1985) Models for mutual attraction and aggregation of motile individuals. in: V. Capasso, E. Grosso, S. L. Paveri-Fontana (Eds.) *Mathematics in Biology and Medicine. Lecture Notes in Biomathematics*, vol. 57. Springer, Berlin, Heidelberg, pp. 33–38

[5] H. Amann (1976) Fixed point equations and nonlinear eigenvalue problems in ordered Banach spaces. *SIAM review* **18**(4): 620–709

[6] H. Amann (1976) Supersolutions, monotone iterations, and stability. *Journal of Differential Equations* **21**(2): 363–377

[7] V. Andasari, M. A. J. Chaplain (2012) Intracellular Modelling of Cell-Matrix Adhesion during Cancer Cell Invasion. *Mathematical Modelling of Natural Phenomena* **7**(1): 29–48

[8] V. Andasari, A. Gerisch, G. Lolas, A. P. South, M. A. J. Chaplain (2011) Mathematical modeling of cancer cell invasion of tissue: biological insight from mathematical analysis and computational simulation. *Journal of mathematical biology* **63**(1): 141–71

[9] A. R. A. Anderson (2005) A hybrid mathematical model of solid tumour invasion: the importance of cell adhesion. *Mathematical medicine and biology* **22**(2): 163–86

[10] N. J. Armstrong, K. J. Painter, J. A. Sherratt (2006) A continuum approach to modelling cell-cell adhesion. *Journal of theoretical biology* **243**(1): 98–113

[11] N. J. Armstrong, K. J. Painter, J. A. Sherratt (2009) Adding adhesion to a chemical signaling model for somite formation. *Bulletin of mathematical biology* **71**(1): 1–24

[12] P. B. Armstrong (1971) Light and electron microscope studies of cell sorting in combinations of chick embryo neural retina and retinal pigment epithelium. *Wilhelm Roux' Archiv für Entwicklungsmechanik der Organismen* **168**(2): 125–141

[13] G. Bell (1978) Models for the specific adhesion of cells to cells. *Science* **200**(4342): 618–627

[14] H. Berestycki, A. Zilio (2017) Predators-prey models with competition: existence, bifurcation and qualitative properties. *submitted*: 1–33

[15] D. A. Beysens, G. Forgacs, J. A. Glazier (2000) Cell sorting is analogous to phase ordering in fluids. *Proceedings of the National Academy of Sciences* **97**(17): 9467–9471

[16] V. Bitsouni, M. A. J. Chaplain, R. Eftimie (2017) Mathematical modelling of cancer invasion: The multiple roles of TGF-β pathway on tumour proliferation and cell adhesion. *Mathematical Models and Methods in Applied Sciences* **27**(10): 1929–1962

[17] V. I. Bogachev (2007) *Measure Theory*. Springer, Berlin, Heidelberg

[18] I. Borsi, A. Fasano, M. Primicerio, T. Hillen (2017) A non-local model for cancer stem cells and the tumour growth paradox. *Mathematical Medicine and Biology* **34**(1): 59–75

[19] B. Brandolini, P. Freitas, C. Nitsch, C. Trombetti (2011) Sharp estimates and saturation phenomena for a nonlocal eigenvalue problem. *Advances in Mathematics* **228**(4): 2352–2365

[20] G. W. Brodland (2002) The Differential Interfacial Tension Hypothesis (DITH): A Comprehensive Theory for the Self-Rearrangement of Embryonic Cells and Tissues. *Journal of Biomechanical Engineering* **124**(2): 188

[21] G. W. Brodland, H. H. Chen (2000) The mechanics of cell sorting and envelopment. *Journal of biomechanics* **33**(7): 845–51

[22] B. Buffoni, J. Toland (2003) *Analytic Theory of Global Bifurcation: An Introduction*. Princeton series in applied mathematics. Princeton University Press, Princeton, Oxford

[23] P. L. Buono, R. Eftimie (2015) Symmetries and pattern formation in hyperbolic versus parabolic models of self-organised aggregation. *Journal of Mathematical Biology* **71**(4): 847–881

[24] A. Buttenschön, T. Hillen, A. Gerisch, K. J. Painter (2017) A space-jump derivation for non-local models of cell-cell adhesion and non-local chemotaxis. *Journal of Mathematical Biology*. doi: 10.1007/s00285-017-1144-3

[25] H. M. Byrne, M. A. J. Chaplain (1996) Modelling the role of cell-cell adhesion in the growth and development of carcinomas. *Mathematical and Computer Modelling* **24**(12): 1–17

[26] H. M. Byrne, D. Drasdo (2009) Individual-based and continuum models of growing cell populations: A comparison. *Journal of Mathematical Biology* **58**: 657–687

[27] J. Calvo, J. Campos, V. Caselles, O. Sánchez, J. Soler (2015) Flux-saturated porous media equations and applications. *EMS Surveys in Mathematical Sciences* **2**(1): 131–218

[28] M. A. J. Chaplain, M. Lachowicz, Z. Szymanska, D. Wrzosek (2011) Mathematical Modelling of Cancer Invasion: the Importance of Cell-Cell Adhesion and Cell-Matrix Adhesion. *Mathematical Models and Methods in Applied Sciences* **21**(04): 719–743

[29] G. Charras, E. Sahai (2014) Physical influences of the extracellular environment on cell migration. *Nature Reviews Molecular Cell Biology* **15**(12): 813–824

[30] H. H. Chen, G. W. Brodland (2000) Cell-level finite element studies of viscous cells in planar aggregates. *Journal of biomechanical engineering* **122**(4): 394–401

[31] S. Cheng (2010) *Differentiation Under the Integral Sign with Weak Derivatives*. `http://www.gold-saucer.org/math/diff-int/diff-int.pdf`. Accessed 8 October 2015

[32] A. Coddington, N. Levinson (1955) *Theory of ordinary differential equations*. International series in pure and applied mathematics. McGraw-Hill

[33] R. Courant (1923) Ein allgemeiner Satz zur Theorie der Eigenfunktione selbstadjungierter Differentialausdrücke. *Nachrichten von der Gesellschaft der Wissenschaften zu Göttingen Mathematisch-Physikalische Klasse*: 81–84

[34] M. G. Crandall, P. H. Rabinowitz (1970) Nonlinear Sturm-Liouville Eigenvalue Problems and Topological Degree. *J. Math. Mech.* **19**(12): 1083–1102

[35] M. G. Crandall, P. H. Rabinowitz (1971) Bifurcation from simple eigenvalues. *Journal of Functional Analysis* **8**: 321–340

[36] M. G. Crandall, P. H. Rabinowitz (1973) Bifurcation, Perturbation of Simple Eigenvalues, and Linearized Stability. *Archive for Rational Mechanics and Analysis* **52**(2): 161–180

[37] E. N. Dancer (1971) Bifurcation Theory in Real Banach Space. *Proceedings of the London Mathematical Society* **3**(23): 699–734

[38] E. N. Dancer (1973) Bifurcation Theory for Analytic Operators. *Proceedings of the London Mathematical Society* **3**(26): 359–384

[39] G. Danuser, J. Allard, A. Mogilner (2013) Mathematical modeling of eukaryotic cell migration: insights beyond experiments. *Annual review of cell and developmental biology* **29**: 501–28

[40] F. A. Davidson, N. Dodds (2006) Spectral properties of non-local differential operators. *Applicable Analysis* **85**(6-7): 717–734

[41] F. A. Davidson, N. Dodds (2006) Spectral properties of non-local uniformly-elliptic operators. *Electronic Journal of Differential Equations* **126**: 1–15

[42] F. A. Davidson, N. Dodds (2007) Existence of positive solutions due to non-local interactions in a class of nonlinear boundary value problems. *Methods and Applications of Analysis* **14**(1): 15–28

[43] J. A. Davies (2013) *Mechanisms of morphogenesis.* Academic Press, Amsterdam

[44] M. Delgado, I. B. M. Duarte, A. Suarez (2017) Nonlocal Problem Arising From the Birth-Jump Processes. *submitted*

[45] J. S. Desgrosellier, D. A. Cheresh (2010) Integrins in cancer: biological implications and therapeutic opportunities. *Nature Reviews Cancer* **10**(1): 9–22

[46] Y. Dolak (2004) *Advection dominated models for chemotaxis.* Dissertation, University of Vienna

[47] P. Domschke, D. Trucu, A. Gerisch, M. A. J. Chaplain (2014) Mathematical modelling of cancer invasion: Implications of cell adhesion variability for tumour infiltrative growth patterns. *Journal of theoretical biology* **361C**: 41–60

[48] D. Dormann, C. J. Weijer (2001) Propagating chemoattractant waves coordinate periodic cell movement in Dictyostelium slugs. *Development* **128**(22): 4535–4543

[49] D. Drasdo, S. Höhme (2005) A single-cell-based model of tumor growth in vitro: monolayers and spheroids. *Physical biology* **2**(3): 133–47

[50] J. Dyson, S. A. Gourley, R. Villella-Bressan, G. F. Webb (2010) Existence and Asymptotic Properties of Solutions of a Nonlocal Evolution Equation Modeling Cell-Cell Adhesion. *SIAM Journal on Mathematical Analysis* **42**(4): 1784–1804

[51] R. Eftimie, G. De Vries, M. A. Lewis, F. Lutscher (2007) Modeling group formation and activity patterns in self-organizing collectives of individuals. *Bulletin of Mathematical Biology* **69**(5): 1537–1565

[52] R. Eftimie, G. de Vries, M. A. Lewis (2007) Complex spatial group patterns result from different animal communication mechanisms. *Proceedings of the National Academy of Sciences of the United States of America* **104**(17): 6974–6979

[53] R. Erban, J. S. Chapman, P. K. Maini (2007) A practical guide to stochastic simulations of reaction-diffusion processes. *arXiv:0704.1908*: 24–29

[54] R. Estrada, R. P. Kanwal (1993) *Asymptotic Analysis: A Distributional Approach*. Birkhäuser, Boston

[55] M. Fabian, P. Habala, P. Hájek, V. Montesinos, V. Zizler (2011) *Banach Space Theory*. CMS Books in Mathematics. Springer, New York, NY

[56] M. Fabian, P. Habala, P. Hájek, V. M. Santalucía, J. Pelant, V. Zizler (2001) *Functional Analysis and Infinite-Dimensional Geometry*. Springer, New York, NY

[57] G. Feltrin, F. Zanolin (2015) Existence of positive solutions in the superlinear case via coincidence degree: the Neumann and the periodic boundary value problems. *Advances in Differential Equations* **20**(9): 937–982

[58] G. B. Folland (1999) *Real Analysis: Modern Techniques and Their Applications*. Wiley, New York

[59] R. A. Foty, M. Steinberg (2004) Cadherin-mediated cell-cell adhesion and tissue segregation in relation to malignancy. *The International journal of developmental biology* **48**(5-6): 397–409

[60] P. Freitas (1994) A nonlocal Sturm–Liouville eigenvalue problem. *Proceedings of the Royal Society of Edinburgh: Section A Mathematics* **124**(01): 169–188

[61] P. Freitas (1994) Bifurcation and stability of stationary solutions of nonlocal scalar reaction-diffusion equations. *Journal of Dynamics and Differential Equations* **6**(4): 613–629

[62] P. Freitas, M. Vishnevskii (2000) Stability of stationary solutions of nonlocal reaction-diffusion equations in m-dimensional space. *Differential and Integral Equations* **13**(1-3): 265–288

[63] P. Friedl, S. Alexander (2011) Cancer invasion and the microenvironment: plasticity and reciprocity. *Cell* **147**(5): 992–1009

[64] B. Geiger, J. P. Spatz, A. D. Bershadsky (2009) Environmental sensing through focal adhesions. *Nature reviews. Molecular cell biology* **10**(1): 21–33

[65] A. Gerisch (2001) *Numerical Methods for the Simulation of Taxis Diffusion Reaction Systems*. Dissertation, Martin-Luther-Universitat Halle-Wittenberg

[66] A. Gerisch (2010) On the approximation and efficient evaluation of integral terms in PDE models of cell adhesion. *IMA Journal of Numerical Analysis* **30**(1): 173–194

[67] A. Gerisch, M. A. J. Chaplain (2008) Mathematical modelling of cancer cell invasion of tissue: local and non-local models and the effect of adhesion. *Journal of theoretical biology* **250**(4): 684–704

[68] A. Gerisch, K. J. Painter (2010) Mathematical modeling of cell adhesion and its applications to developmental biology and cancer invasion in: A. Chauvière, L. Preziosi, C. Verdier (Eds.) *Cell Mechanics: From Single Scale-Based Models to Multiscale Modelling*,. CRC Press, pp. 319–350

[69] D. Gilbarg, N. S. Trudinger (1983) *Elliptic Partial Differential Equations of Second Order*. Classics in Mathematics. Springer Berlin Heidelberg, Berlin, Heidelberg

[70] D. T. Gillespie (2007) Stochastic simulation of chemical kinetics. *Annual review of physical chemistry* **58**: 35–55

[71] J. A. Glazier, F. Graner (1993) Simulation of the differential adhesion driven rearrangement of biological cells. *Physical Review E* **47**(3): 2128–2154

[72] I. Gohberg, S. Goldberg, M. A. Kaashoek (1990) *Classes of Linear Operators Vol. I*. Vol. 49. Birkhäuser, Basel

[73] M. Golubitsky, I. Stewart (2002) *The Symmetry Perspective*. Progress in Mathematics. Birkhäuser, Basel

[74] F. Graner (1993) Can Surface Adhesion Drive Cell-rearrangement? Part I: Biological Cell-sorting. *Journal of Theoretical Biology* **164**(4): 455–476

[75] F. Graner, J. A. Glazier (1992) Simulation of biological cell sorting using a two-dimensional extended Potts model. *Physical Review Letters* **69**(13): 2013–2016

[76] F. Graner, Y. Sawada (1993) Can Surface Adhesion Drive Cell Rearrangement? Part II: A Geometrical Model. *Journal of Theoretical Biology* **164**(4): 477–506

[77] M. L. Graves, J. A. Cipollone, P. Austin, E. M. Bell, J. S. Nielsen, C. B. Gilks, K. M. McNagny, C. D. Roskelley (2016) The cell surface mucin podocalyxin regulates collective breast tumor budding. *Breast Cancer Research* **18**(1): 11

[78] J. M. Halbleib, W. J. Nelson (2006) Cadherins in development: Cell adhesion, sorting, and tissue morphogenesis. *Genes and Development* **20**(23): 3199–3214

[79] D. Hanahan, R. A. Weinberg (2000) The hallmarks of cancer. *Cell* **100**(1): 57–70

[80] D. Hanahan, R. A. Weinberg (2011) Hallmarks of cancer: the next generation. *Cell* **144**(5): 646–74

[81] H. Hanche-Olsen, H. Holden (2010) The Kolmogorov-Riesz compactness theorem. *Expositiones Mathematicae* **28**(4): 385–394

[82] A. K. Harris (1976) Is Cell sorting caused by differences in the work of intercellular adhesion? A critique of the Steinberg hypothesis. *Journal of theoretical biology* **61**(2): 267–85

[83] T. J. Healey (1988) Global Bifurcations and Continuation in the Presence of Symmetry with an Application to Solid Mechanics. *SIAM Journal on Mathematical Analysis* **19**(4): 824–840

[84] T. J. Healey, H. Kielhöfer (1991) Symmetry and nodal properties in the global bifurcation analysis of quasi-linear elliptic equations. *Archive for Rational Mechanics and Analysis* **113**(4): 299–311

[85] T. J. Healey, H. Kielhöfer (1993) Preservation of Nodal Structure on Global Bifurcating Solution Branches of Elliptic Equations with Symmetry. *Journal of Differential Equations* **106**(1): 70–89

[86] T. Hillen (2002) Hyperbolic Models for Chemosensitive Movement. *Mathematical Models and Methods in Applied Sciences* **12**(07): 1007–1034

[87] T. Hillen (2005) On the L2-Moment Closure of Transport Equations: the General Case. *Discrete and Continuous Dynamical Systems* **5**(2): 299–318

[88] T. Hillen, B. Greese, J. Martin, G. de Vries (2015) Birth-jump processes and application to forest fire spotting. *Journal of Biological Dynamics* **9**(sup1): 104–127

[89] T. Hillen, K. J. Painter (2009) A user's guide to PDE models for chemotaxis. *Journal of Mathematical Biology* **58**(1-2): 183–217

[90] T. Hillen, K. J. Painter (2013) Transport and anisotropic diffusion models for movement in oriented habitats in: M. A. Lewis, P. Maini, S. Petrovskii (Eds.) *Dispersal, individual movement and spatial ecology: A mathematical perspective*, vol. 2071. Springer, Heidelberg, pp. 177–222

[91] T. Hillen, K. J. Painter, C. Schmeiser (2006) Global existence for chemotaxis with finite sampling radius. *Discrete and Continuous Dynamical Systems - Series B* **7**(1): 125–144

[92] T. Hillen, K. J. Painter, M. Winkler (2017) Global solvability and explicit bounds for a non-local adhesion model. *submitted*

[93] S. Hoehme, D. Drasdo (2010) Biomechanical and Nutrient Controls in the Growth of Mammalian Cell Populations. *Mathematical Population Studies* **17**(3): 166–187

[94] W. R. Holmes, A. E. Golding, W. M. Bement, L. Edelstein-Keshet (2016) A mathematical model of GTPase pattern formation during single-cell wound repair. *Interface Focus* **6**(5): 1–10

[95] W. R. Holmes, J. Park, A. Levchenko, L. Edelstein-Keshet (2017) A mathematical model coupling polarity signaling to cell adhesion explains diverse cell migration patterns. *PLOS Computational Biology* **13**(5): 1–22

[96] D. Horstmann (2003) From 1970 until present : the Keller-Segel model in chemotaxis and its consequences. *Jahresbericht der Deutschen Mathematiker-Vereinigung* **105**(3): 103–165

[97] S. B. Hsu, J. López-Gómez, L. Mei, M. Molina-Meyer (2014) A Nonlocal Problem from Conservation Biology. *SIAM Journal on Mathematical Analysis* **46**(6): 4035–4059

[98] B. D. Hughes (1995) *Random Walks and Random Environments: Random walks.* Oxford science publications v. 1. Clarendon Press, Oxford

[99] T. Ikeda (1985) Standing pulse-like solutions of a spatially aggregating population model. *Japan Journal of Applied Mathematics* **2**(1): 111–149

[100] T. Ikeda, T. Nagai (1987) Stability of localized stationary solutions. *Japan Journal of Applied Mathematics* **4**(1): 73–97

[101] D. Iron, M. J. Ward (2000) A Metastable Spike Solution for a Nonlocal Reaction-Diffusion Model. *SIAM Journal on Applied Mathematics* **60**(3): 778–802

[102] A. Jilkine, L. Edelstein-Keshet (2011) A comparison of mathematical models for polarization of single eukaryotic cells in response to guided cues. *PLoS computational biology* **7**(4): e1001121

[103] K. L. Johnson, K. Kendall, A. D. Roberts (1971) Surface Energy and the Contact of Elastic Solids. *Proceedings of the Royal Society A: Mathematical, Physical and Engineering Sciences* **324**(1558): 301–313

[104] S. T. Johnston, M. J. Simpson, R. E. Baker (2012) Mean-field descriptions of collective migration with strong adhesion. *Physical Review E* **85**(5): 051922

[105] H. Knútsdóttir, E. Pálsson, L. Edelstein-Keshet (2014) Mathematical model of macrophage-facilitated breast cancer cells invasion. *Journal of theoretical biology* **357**: 184–99

[106] D. Lauffenburger (1989) A simple model for the effects of receptor-mediated cell-substratum adhesion on cell migration. *Chemical Engineering Science* **44**(9)

[107] D. A. Lauffenburger, A. F. Horwitz (1996) Cell Migration: A Physically Integrated Molecular Process. *Cell* **84**(3): 359–369

[108] D. Leckband (2010) Design rules for biomolecular adhesion: lessons from force measurements. *Annual review of chemical and biomolecular engineering* **1**: 365–89

[109] L. Li, S. F. Nørrelykke, E. C. Cox (2008) Persistent Cell Motion in the Absence of External Signals: A Search Strategy for Eukaryotic Cells. *PLoS ONE* **3**(5): e2093

[110] J. López-Gómez (1998) On the Structure and Stability of the Set of Solutions of a Nonlocal Problem Modeling Ohmic Heating **10**(4): 537–566

[111] J. López-Gómez (2001) *Spectral Theory and Nonlinear Functional Analysis*. Chapman & Hall/CRC Research Notes in Mathematics Series. Taylor & Francis, Boca Raton, FL

[112] J. López-Gómez (2013) *Linear Second Order Elliptic Operators*. World Scientific Publishing Company, Singapore

[113] J. López-Gómez (2016) Global bifurcation for Fredholm operators. *Rendiconti dell'Istituto di matematica dell'Università di Trieste: an International Journal of Mathematics* **48**: 539–564

[114] J. López-Gómez, C. Mora-Corral (2007) *Algebraic multiplicity of eigenvalues of linear operators*. Vol. 177. Operator Theory: Advances and Applications. Birkhäuser, Basel

[115] J. S. Lowengrub, H. B. Frieboes, F. Jin, Y.-L. Chuang, X. Li, P. Macklin, S. M. Wise, V. Cristini (2010) Nonlinear modelling of cancer: bridging the gap between cells and tumours. *Nonlinearity* **23**(1): R1–R91

[116] P. Macklin, S. McDougall, A. R. A. Anderson, M. A. J. Chaplain, V. Cristini, J. S. Lowengrub (2009) Multiscale modelling and nonlinear simulation of vascular tumour growth. *Journal of mathematical biology* **58**(4-5): 765–98

[117] J. Martin, T. Hillen (2016) The spotting distribution of wildfires. *Applied Sciences* **6**(6): 177

[118] H. Matano (1988) Asymptotic behavior of solutions of semilinear heat equations on S 1 in: *Nonlinear Diffusion Equations and their Equilibrium States II,*. Springer, pp. 139–162

[119] P. McMillen, S. A. Holley (2015) Integration of cell-cell and cell-ECM adhesion in vertebrate morphogenesis. *Current Opinion in Cell Biology* **36**: 48–53

[120] A. M. Middleton, C. Fleck, R. Grima (2014) A continuum approximation to an off-lattice individual-cell based model of cell migration and adhesion. *Journal of Theoretical Biology* **359**: 220–232

[121] A. Mogilner, L. Edelstein-Keshet (1999) A non-local model for a swarm. *Journal of Mathematical Biology* **38**(6): 534–570

[122] J. C. M. Mombach, J. A. Glazier, R. C. Raphael, M. Zajac (1995) Quantitative comparison between differential adhesion models and cell sorting in the presence and absence of fluctuations. *Physical Review Letters* **75**(11): 2244–2247

[123] H. Murakawa, H. Togashi (2015) Continuous models for cell-cell adhesion. *Journal of Theoretical Biology* **374**: 1–12

[124] T. Nagai (1983) Some nonlinear degenerate diffusion equations with a nonlocally convective term in ecology. *Hiroshima Mathematical Journal* **13**(1): 165–202

[125] T. Nagai, M. Mimura (1983) Asymptotic Behavior for a Nonlinear Degenerate Diffusion Equation in Population Dynamics. *SIAM Journal on Applied Mathematics* **43**(3): 449–464

[126] T. Nagai, M. Mimura (1983) Some nonlinear degenerate diffusion equations related to population dynamics. *Journal of the Mathematical Society of Japan* **35**(3): 539–562

[127] J. Nečas (2012) *Direct Methods in the Theory of Elliptic Equations.* Springer Monographs in Mathematics. Springer, Berlin, Heidelberg

[128] M. G. Neubert, H. Caswell (2000) Demography and dispersal: Calculation and sensitivity analysis of invasion speed for structured populations. *Ecology* **81**(6): 1613–1628

[129] M. A. Nieto (2011) The ins and outs of the epithelial to mesenchymal transition in health and disease. *Annual review of cell and developmental biology* **27**: 347–76

[130] N. Nishiya, W. B. Kiosses, J. Han, M. H. Ginsberg (2005) An alpha4 integrin-paxillin-Arf-GAP complex restricts Rac activation to the leading edge of migrating cells. *Nature cell biology* **7**(4): 343–352

[131] H. G. Othmer, S. R. Dunbar, W. Alt (1988) Models of dispersal in biological systems. *Journal of mathematical biology* **26**(3): 263–98

[132] H. G. Othmer, T. Hillen (2002) The Diffusion Limit of Transport Equations II: Chemotaxis Equations. *SIAM Journal on Applied Mathematics* **62**: 1222–1250

[133] C. Ou, Y. Zhang (2013) Traveling Wavefronts of nonlocal Reaction-diffusion Models for Adhesion in Cell Aggregation and Cancer Invasion. *Canadian Applied Mathematics Quarterly* **21**(1): 21–62

[134] K. J. Painter (2009) Continuous models for cell migration in tissues and applications to cell sorting via differential chemotaxis. *Bulletin of mathematical biology* **71**(5): 1117–47

[135] K. J. Painter, N. J. Armstrong, J. A. Sherratt (2010) The impact of adhesion on cellular invasion processes in cancer and development. *Journal of theoretical biology* **264**(3): 1057–67

[136] K. J. Painter, J. M. Bloomfield, J. A. Sherratt, A. Gerisch (2015) A Nonlocal Model for Contact Attraction and Repulsion in Heterogeneous Cell Populations. *Bulletin of Mathematical Biology* **77**(6): 1132–1165

[137] K. J. Painter, T. Hillen (2002) Volume-filling and quorum-sensing in models for chemosensitive movement. *Canadian Applied Mathematics Quarterly* **10**(4): 501–543

[138] A. Paksa, J. Bandemer, B. Hoeckendorf, N. Razin, K. Tarbashevich, S. Minina, D. Meyen, A. Biundo, S. A. Leidel, N. Peyriéras, N. S. Gov, P. J. Keller, E. Raz (2016) Repulsive cues combined with physical barriers and cell-cell adhesion determine progenitor cell positioning during organogenesis. *Nature communications* **7**: 1–14

[139] E. Palsson (2008) A 3-D model used to explore how cell adhesion and stiffness affect cell sorting and movement in multicellular systems. *Journal of theoretical biology* **254**(1): 1–13

[140] E. Palsson, H. G. Othmer (2000) A model for individual and collective cell movement in Dictyostelium discoideum. *Proceedings of the National Academy of Sciences of the United States of America* **97**(19): 10448–10453

[141] A. J. Perumpanani, J. A. Sherratt, J. Norbury, H. M. Byrne (1996) Biological inferences from a mathematical model for malignant invasion. *Invasion & metastasis* **16**(4-5): 209–21

[142] A. Puliafito, L. Hufnagel, P. Neveu, S. Streichan, A. Sigal, D. K. Fygenson, B. I. Shraiman (2012) Collective and single cell behavior in epithelial contact inhibition. *Proceedings of the National Academy of Sciences of the United States of America* **109**(3): 739–44

[143] P. H. Rabinowitz (1970) Nonlinear Sturm-Liouville problems for second order ordinary differential equations. *Comm. Pure Appl. Math.* **23**(1 970): 939–961

[144] P. H. Rabinowitz (1971) Some Global Results for Nonlinear Eigenvalue Problems. *Journal of Functional Analysis* **513**: 487–513

[145] I. Ramis-Conde, M. A. J. Chaplain, A. R. A. Anderson (2008) Mathematical modelling of cancer cell invasion of tissue. *Mathematical and Computer Modelling* **47**(5-6): 533–545

[146] I. Ramis-Conde, D. Drasdo, A. R. A. Anderson, M. A. J. Chaplain (2008) Modeling the influence of the E-cadherin-beta-catenin pathway in cancer cell invasion: a multiscale approach. *Biophysical journal* **95**(1): 155–165

[147] A. J. Ridley (2011) Life at the leading edge. *Cell* **145**(7): 1012–22

[148] A. J. Ridley, M. A. Schwartz, K. Burridge, R. A. Firtel, M. H. Ginsberg, G. Borisy, J. T. Parsons, A. R. Horwitz (2003) Cell migration: integrating signals from front to back. *Science* **302**(5651): 1704–1709

[149] E. T. Roussos, J. S. Condeelis, A. Patsialou (2011) Chemotaxis in cancer. *Nature reviews. Cancer* **11**(8): 573–87

[150] W. Rudin (1991) *Functional Analysis*. International series in pure and applied mathematics. McGraw-Hill, New York

[151] R. Schaaf (1985) Stationary solutions of chemotaxis systems. *Transactions of the American Mathematical Society* **292**(2): 531–531

[152] M. Schienbein, K. Franke, H. Gruler (1994) Random walk and directed movement: Comparison between inert particles and self-organized molecular machines. *Physical Review E* **49**(6): 5462–5471

[153] D. K. Schlüter, I. Ramis-Conde, M. A. J. Chaplain (2012) Computational modeling of single-cell migration: the leading role of extracellular matrix fibers. *Biophysical journal* **103**(6): 1141–51

[154] D. K. Schlüter, I. Ramis-Conde, M. A. J. Chaplain (2015) Multi-scale modelling of the dynamics of cell colonies: insights into cell-adhesion forces and cancer invasion from in silico simulations. *Journal of the Royal Society, Interface* **12**(103): 20141080

[155] L. Schwartz (1957) *Théorie des distributions*. Actualités scientifiques et industrielles: Publications de l'Institut de Mathématique de l'Université de Strasbourg. Hermann, Paris

[156] M. Scianna, L. Preziosi (2013) *Cellular Potts Models: Multiscale Extensions and Biological Applications*. Chapman & Hall/CRC Mathematical and Computational Biology. Taylor & Francis, Boca Raton, FL

[157] J. A. Sherratt, S. A. Gourley, N. J. Armstrong, K. J. Painter (2008) Boundedness of solutions of a non-local reaction-diffusion model for adhesion in cell aggregation and cancer invasion. *European Journal of Applied Mathematics* **20**(01): 123

[158] J. Shi, X. Wang (2009) On global bifurcation for quasilinear elliptic systems on bounded domains. *Journal of Differential Equations* **246**(7): 2788–2812

[159] L. Shi, Z. Yu, Z. Mao, A. Xiao (2014) A Directed Continuous Time Random Walk Model with Jump Length Depending on Waiting Time. *The Scientific World Journal* **2014**: 1–4

[160] M. Steinberg (1963) Reconstruction of tissues by dissociated cells. *Science* **141**(3579): 401–408

[161] M. Steinberg (1970) Does differential adhesion govern self-assembly processes in histogenesis? Equilibrium configurations and the emergence of a hierarchy among populations of embryonic cells. *The Journal of experimental zoology* **173**(4): 395–433

[162] M. Steinberg (2007) Differential adhesion in morphogenesis: a modern view. *Current opinion in genetics & development* **17**(4): 281–6

[163] A. Stevens, H. G. Othmer (1997) Aggregation, Blowup, and Collapse: The ABC's of Taxis in Reinforced Random Walks. *SIAM Journal on Applied Mathematics* **57**(4): 1044–1081

[164] G. Sweers (2000) *Lecture notes on Maximum Principles*

[165] M. Théry, V. Racine, M. Piel, A. Pépin, A. Dimitrov, Y. Chen, J.-b. Sibarita, M. Bornens (2006) Anisotropy of cell adhesive microenvironment governs cell internal organization and orientation of polarity. *Proceedings of the National Academy of Sciences of the United States of America* **103**(52): 19771–6

[166] C. M. Topaz, A. L. Bertozzi, M. A. Lewis (2006) A nonlocal continuum model for biological aggregation. *Bulletin of Mathematical Biology* **68**(7): 1601–1623

[167] S. Turner, J. A. Sherratt (2002) Intercellular adhesion and cancer invasion: a discrete simulation using the extended Potts model. *Journal of theoretical biology* **216**(1): 85–100

[168] S. Turner, J. A. Sherratt, K. J. Painter, N. Savill (2004) From a discrete to a continuous model of biological cell movement. *Physical Review E* **69**(2): 021910

[169] N. G. Van Kampen (2007) *Stochastic Processes in Physics and Chemistry*. North-Holland Personal Library. Elsevier Science, Amsterdam

[170] X. Wang, Q. Xu (2013) Spiky and transition layer steady states of chemotaxis systems via global bifurcation and Helly's compactness theorem. *Journal of Mathematical Biology* **66**: 1241–1266

[171] S. Watanabe, S. Matsumoto, T. Higurashi, N. Ono (2016) Burgers equation with no-flux boundary conditions and its application for complete fluid separation. *Physica D: Nonlinear Phenomena* **331**: 1–12

[172] O. D. Weiner (2002) Regulation of cell polarity during eukaryotic chemotaxis: The chemotactic compass. *Current Opinion in Cell Biology* **14**(2): 196–202

[173] O. D. Weiner, G. Servant, C. A. Parent, P. N. Devreotes, H. R. Bourne (2000) Cell polarity in response to chemoattractants in: D. G. Drubin (Ed.) *Cell Polarity*, 1st. Oxford University Press, Oxford, pp. 201–239

[174] R. Weiner, B. A. Schmitt, H. Podhaisky (1997) ROWMAP–a ROW-code with Krylov techniques for large stiff ODEs. *Applied Numerical Mathematics* **25**: 303–319

[175] M. D. White, N. Plachta (2015) How Adhesion Forms the Early Mammalian Embryo in: *Current Topics in Developmental Biology*, 1st ed. vol. 112. Elsevier Inc., pp. 1–17

[176] T. Xiang (2013) A study on the positive nonconstant steady states of nonlocal chemotaxis systems. *Discrete and Continuous Dynamical Systems - Series B* **18**(9): 2457–2485

[177] V. Y. Zaburdaev (2006) Random walk model with waiting times depending on the preceding jump length. *Journal of Statistical Physics* **123**(4): 871–881

[178] X. Zhang, L. Mei (2011) On a nonlocal reaction-diffusion-advection system modeling phytoplankton growth with light and nutrients. *Discrete and Continuous Dynamical Systems - Series B* **17**(1): 221–243

[179] A. Zygmund (2002) *Trigonometric Series*. Cambridge Mathematical Library. Cambridge University Press, Cambridge

Appendix A

Non-dimensionalization of non-local cell-cell adhesion model

Note that this non-dimensionalization is only for the case when $h(u) = u$ for other nonlinear functions we may want to change the scaling of u. In one dimension equation (3.211) reads,

$$\frac{\partial u}{\partial t} = D\frac{\partial^2 u}{\partial x^2} - \alpha\frac{\partial}{\partial x}\left(u\frac{\phi}{R}\int_{-R}^{R} h(u(x+r))\Omega(r)\,\mathrm{d}r\right) \tag{A.1}$$

which will be non-dimensionalized by introducing the following variables,

$$x^* = \frac{x}{R} \qquad t^* = t\frac{D}{R^2} \qquad u^* = \frac{u}{\hat{u}} \qquad \alpha^* = \frac{\alpha}{\hat{\alpha}}. \tag{A.2}$$

Then,

$$\mathrm{d}x^* = \mathrm{d}x\frac{1}{R} \qquad \mathrm{d}t^* = \mathrm{d}t\frac{D}{R^2} \qquad \mathrm{d}u^* = \mathrm{d}u\frac{1}{\hat{u}} \tag{A.3}$$

Then we get that,

$$\frac{\partial u^*}{\partial x^*} = \frac{\hat{u}}{R}\frac{\partial u}{\partial x} \qquad \frac{\partial^2 u^*}{\partial x^{*2}} = \frac{R^2}{\hat{u}}\frac{\partial^2 u}{\partial x^2}. \tag{A.4}$$

$$\begin{aligned}\frac{\partial u^*}{\partial t^*} &= \frac{R^2}{D\hat{u}}\left[D\frac{\partial^2 u}{\partial x^2} - \frac{\partial}{\partial x}\left(u\frac{\phi}{R}\int_{-R}^{R}\alpha h(u(x+r))\Omega(r)\,\mathrm{d}r\right)\right] \\ &= \frac{\partial^2 u^*}{\partial x^{*2}} - \frac{1}{D}\frac{\partial}{\partial x^*}\left(u^*\phi\int_{-R}^{R}\alpha h(u(x^*R+r))\Omega(r)\,\mathrm{d}r\right)\end{aligned}$$

We introduce the following change of variables in the integral $y = {}^{r}/_{R}$. Then,

$$\frac{\partial u^*}{\partial t^*} = \frac{\partial^2 u^*}{\partial (x^*)^2} - \frac{1}{D}\frac{\partial}{\partial x^*}\left(u^*\phi R \int_{-1}^{1} \alpha h(u\left(R\left(x^* + y\right)\right))\,\Omega(yR)\,\mathrm{d}y\right)$$

Then we introduce,

$$\Omega^*(y) = \Omega(yR) \qquad y \in [-1, 1], \tag{A.5}$$

and we introduce

$$\tilde{h}(u^*) = \frac{1}{\hat{u}} h(\hat{u}u^*). \tag{A.6}$$

Finally, we note that $u(R\left(x^* + y\right)) = u^*(x^* + y)/\hat{u}$.

$$\frac{\partial u^*}{\partial t^*} = \frac{\partial^2 u^*}{\partial (x^*)^2} - \frac{R\phi\hat{u}\hat{\alpha}}{D}\frac{\partial}{\partial x^*}\left(u^* \int_{-1}^{1} \alpha^* h(u^*\left(x^* + y\right))\Omega^*(y)\,\mathrm{d}y\right)$$

Then we let,

$$\hat{\alpha} = \frac{D}{R\phi\hat{u}}. \tag{A.7}$$

Then the non-dimensionalized equation is given by,

$$\frac{\partial u^*}{\partial t^*} = \frac{\partial^2 u^*}{\partial x^{*2}} - \frac{\partial}{\partial x^*}\left(u^* \int_{-1}^{1} \alpha^* h(u^*\left(x^* + y\right))\Omega^*(y)\,\mathrm{d}y\right). \tag{A.8}$$

For simplicity in the notion we will drop all the stars from this equation in the subsequent discussions.

Appendix B

Essential mathematical results

Theorem B.1 (Minkowski's integral inequality [58]). *Suppose that (X, M, μ) and (Y, N, ν) are σ-finite measure spaces, and let f be an $M \times N$ measurable function on $X \times Y$.*

- *If $f \geq 0$ and $q \leq p < \infty$, then*

$$\left[\int \left(\int f(x,y)\,\mathrm{d}\nu(y)\right)^p \mathrm{d}\mu(x)\right]^{1/p} \leq \int \left[\int f(x,y)^p\,\mathrm{d}\mu(x)\right]^{1/p} \mathrm{d}\nu(y). \tag{B.1}$$

- *If $1 \leq p \leq \infty$, $f(\cdot, y) \in L^p(\mu)$ for a.e. y, and the function $y \to \|f(\cdot,y)\|_p$ is in $L^1(\nu)$, then $f(x,\cdot) \in L^1(\nu)$ for a.e. x, the function $x \to \int f(x,y)\,\mathrm{d}\nu(y)$ is in $L^p(\mu)$, and*

$$\left\|\int f(\cdot,y)\,\mathrm{d}\nu(y)\right\|_p \leq \int \|f(\cdot,y)\|_p\,\mathrm{d}\nu(y). \tag{B.2}$$

In the following let $\Omega \subset \mathbb{R}^n$.

Theorem B.2. *Let $\Omega \in \mathcal{R}^{0,1}$, $p \geq 1$, $kp = n$. Then $W^{k,p}(D) \subset L^q(D)$ algebraically and topologically for any q, $1 \leq q < \infty$.*

Theorem B.3 (Sobolev). *Let $\Omega \in \mathcal{R}^{0,1}$, $p \geq 1$, $kp > n$, and denote*

$$\mu \begin{cases} = k - (n/p) & \text{if } k - (n/p) < 1 \\ < 1 & \text{if } k - (n/p) = 1 \\ = 1 & \text{if } k - (n/p) > 1 \end{cases}. \tag{B.3}$$

Then $W^{k,p}(D) \subset C^{0,\mu}(\bar{D})$ algebraically and topologically.

Theorem B.4 (Sobolev). *Let $D \subset \mathbb{R}^n$ bounded with Lipschitz boundary ∂D, and let $k \geq 1$, $1 \leq p \leq \infty$.*

- *If $kp < n$, then $W^{k,p}(D) \hookrightarrow L^q(D)$ for all $q \leq q \leq np/(n-kp)$; the embedding is compact provided $1 \leq p < np/(n-kp)$.*
- *If $kp = n$, then $W^{k,p}(D) \hookrightarrow L^q(D)$ for all $1 \leq q < \infty$, and the embedding is compact.*
- *If $kp > n$, then $W^{k,p}(D) \hookrightarrow C^{k-j,\alpha}$ is compact, where $j = [N/p] + 1$ and $\alpha < j - N/p$.*

Theorem B.5 (Kolmogorov-Riesz [81]). *Let $1 \leq p < \infty$. A subset $\mathcal{F}$ of $L^p(\mathbb{R}^n)$ is totally bounded if and only if*

1. *$\mathcal{F}$ is pointwise bounded,*
2. *for every $\epsilon > 0$ there is some R so that, for every $f \in \mathcal{F}$,*

$$\int_{|x|>R} |f(x)|^p \, \mathrm{d}x < \epsilon^p, \tag{B.4}$$

3. *for every $\epsilon > 0$ there is some $\rho > 0$ so that, for every $f \in \mathcal{F}$ and $y \in \mathbb{R}^n$ with $|y| < \rho$,*

$$\int_{\mathbb{R}^n} |f(x+y) - f(x)|^p \, \mathrm{d}x < \epsilon^p. \tag{B.5}$$

Theorem B.6 (Poincaré-Wirtinger). *Suppose $1 \leq p < \infty$ and let $D \subset \mathbb{R}^n$ such that D has a Lipschitz boundary. Then for every $u \in W^{1,p}(D)$ there exists a constant C such that*

$$\|u - u_D\|_p \leq C \|\nabla u\|_p, \tag{B.6}$$

where

$$u_D = \frac{1}{|D|} \int_D u(x) \, \mathrm{d}x. \tag{B.7}$$

Theorem B.7 (Gagliardo-Nirenberg). *Let $D \subset \mathbb{R}$ be bounded and let $1 \leq r \leq \infty$, $1 \leq q \leq p \leq \infty$. Then, there exists a constant C such that*

$$\|u\|_p \leq C \|u\|_q^{1-a} \|u\|_{1,r}^a \qquad \forall u \in W^{1,r}(D), \tag{B.8}$$

where $0 \leq a \leq 1$ is defined by $a\,(1/q - 1/r + 1) = 1/q - 1/p$.

Theorem B.8. *Suppose $T: X \to X$ is a continuous and compact mapping. Assume further that the set*

$$\{ u \in X : u = \lambda A[u] \text{for some } 0 \leq \lambda \leq 1 \} \tag{B.9}$$

is bounded. Then T has a fixed point.

Theorem B.9. *Let $a, b \in \mathbb{R}, \epsilon \in \mathbb{R}$ such that $a, b, \epsilon > 0$. Then,*

$$ab < \epsilon a^2 + \frac{b^2}{4\epsilon}. \tag{B.10}$$

Lemma B.10. *[85] Let $\Omega \subset \mathbb{R}^n$ be a bounded domain. If $u \in H^1(D) \cap C(\bar{D})$ and $u = 0$ on ∂D then $u \in H_0^1(D)$.*

Lemma B.11. *If (X, d) is a metric space. Then the following are equivalent*

1. *$U \subset X$ is open in (X, d),*
2. *$\forall x \in U$ and for all (x_n) such that $x_n \to x$ there exists $N \in \mathbb{N}$ such that $\forall n \geq N$ we have that $x_n \in U$.*

Lemma B.12. *Let $L^2_{\text{per}}(0, L)$ be the set of periodic functions in $L^2(0, L)$. Then*

$$\mathcal{E} = \left\{ 1, \cos\left(\frac{2\pi n x}{L}\right), \sin\left(\frac{2\pi n x}{L}\right) \right\} \tag{B.11}$$

forms an orthonormal basis for $L^2_{\text{per}}(0, L)$.

Proof. We solve the following operator equation

$$\begin{cases} \phi''(x) + \lambda \phi(x) = 0 \quad \text{in } [0, L] \\ \mathcal{B}[\phi, \phi'] = 0. \end{cases} \tag{B.12}$$

1. $\lambda = 0$. Then $\phi(x) = ax + b$, applying the boundary conditions we get $\phi(x) = 1$ and $\lambda = 0$ is an eigenvalue.
2. $\lambda < 0$. Then $\phi(x) = c_1 \exp(\sqrt{\lambda} x) + c_2 \exp(-\sqrt{\lambda} x)$, but then the boundary conditions imply that $\phi \equiv 0$.
3. $\mu^2 = \lambda > 0$. Then $\phi(x) = c_1 \sin(\mu x) + c_2 \sin(\mu x)$. Applying the boundary conditions we obtain the system.

$$\begin{bmatrix} 1 - \cos \mu L & -\sin \mu L \\ \sin \mu L & 1 - \cos \mu L \end{bmatrix} \begin{bmatrix} c_1 \\ c_2 \end{bmatrix} = 0. \tag{B.13}$$

We have a non-trivial solution whenever the determinant is zero that is when $4\sin^2\left(\frac{\mu L}{2}\right) = 0$. Solving for λ respectively μ we obtain that

$$\lambda_n = \mu_n^2 = \left(\frac{2n\pi}{L}\right)^2. \tag{B.14}$$

Finally as we can find a Green's function for this problem, we have that the inverse of this equation is compact and self-adjoint and so we can apply the spectral result [56 Theorem 7.46] to conclude that its eigenfunctions form a basis of L^2. □

Appendix C

Maximum principles for elliptic equations

Let $D \subset \mathbb{R}^n$ be an open and connected subset with boundary ∂D. Let L be the following second order differential operator

$$L = \sum_{i,j=1}^{n} a_{ij}(x) D_{ij} + \sum_{i=1}^{n} b_i(x) D_i + c(x), \tag{C.1}$$

where $a_{ij} \in L^{\infty}_{\text{loc}}(D)$, and $b_i, c \in L^{\infty}(D)$, and $D_{ij} = \frac{\partial}{\partial x_i}\frac{\partial}{\partial x_j}$, and $D_i = \frac{\partial}{\partial x_i}$, and we assume $a_{ij} = a_{ji}$.

In the following we will denote $u^+(x) = \max(u(x), 0)$ and $u^-(x) = \min(-u(x), 0)$.

Theorem C.1 (Strong Maximum principle [69]). *Suppose that L is strictly elliptic and that $c(x) \leq 0$. If $u \in C^2(D) \cap C(\bar{D})$ and $Lu \geq 0$ in D, then either*

1. *$u \equiv \sup_D u$,*
2. *u does not attain a non-negative maximum in D.*

Theorem C.2 (Strong Maximum principle [69]). *Suppose that L is strictly elliptic and that $c(x) \leq 0$. If $u \in C^2(D) \cap C(\bar{D})$ and $Lu \leq 0$ in D, then either*

1. *$u \equiv \inf Du$,*
2. *u does not attain a non-positive minimum in D.*

To weaken the assumptions on the sign of the function $c(x)$ we can impose strong sign conditions on u. Then we can prove.

Theorem C.3 (Maximum principle for nonpositive functions [164]). *Let D be bounded. Suppose that L is strictly elliptic. If $u \in C^2(D) \cap C(\bar{D})$ satisfies $Lu \geq 0$ and $u \leq 0$ in D, then either*

1. $u \equiv 0$,

2. $u(x) < 0$ *for all* $x \in D$.

Theorem C.4 (Maximum principle for nonnegative functions [164]). *Let D be bounded. Suppose that L is strictly elliptic. If $u \in C^2(D) \cap C(\bar{D})$ satisfies $Lu \leq 0$ and $u \geq 0$ in D, then either*

1. $u \equiv 0$,

2. $u(x) > 0$ *for all* $x \in D$.

Proof. Decompose $c(x) = c^+(x) - c^-(x)$. Then, we note that

$$\left(L - c^+\right) u \leq -c^+ u \leq 0, \tag{C.2}$$

using both the non-negativity of c^+ and u. Further, note that the c component in $L - c^+$ is non-positive. Hence, we can apply Theorem C.2, from which the conclusions follow. □